Mirabela MARIN

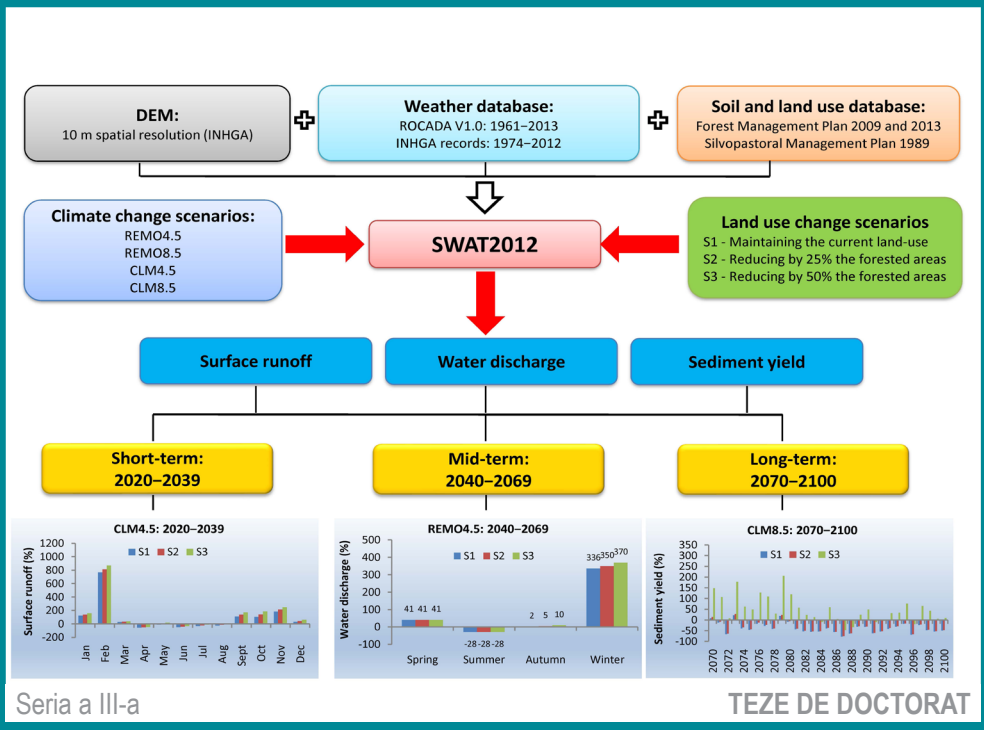

Seria a III-a

TEZE DE DOCTORAT

HYDROLOGICAL IMPACT OF CLIMATE CHANGE AND FORESTED AREA REDUCTION IN SMALL, FORESTED WATERSHEDS

Case study: Upper Tarlung watershed

editura SILVICĂ

PUBLICATĂ DE INSTITUTUL NAȚIONAL DE CERCETARE-DEZVOLTARE
ÎN SILVICULTURĂ „MARIN DRĂCEA” - INCDS

Adresa: Bd. Eroilor nr. 128
Voluntari, 077190, Ilfov
Tel./Fax: 021 350 32 40 / 021 350 32 45
E-mail: comunicare@icas.ro.
Site: www.editurasilvică.ro; www.icas.ro.

Referenți științifici:
CS I dr. Habil. Sorin CHEVAL Director Meteorologie Aplicată, Administrația Națională de Meteorologie, București, România
CS II dr. Viorel CHENDEȘ Director Științific, Institutul Național de Hidrologie și Gospodărire a Apelor, București, România
Conf. dr. ing. Victor Dan PĂCURAR Universitatea Transilvania din Brașov, Facultatea de Silvicultură și Exploatări forestiere, Brașov, România

The present research benefits from funding from the project Climate Services for Water–Energy–Land–Food Nexus (CLISWELN) funded by ERA4CS. ERA4CS is an ERA-NET initiated by JPI Climate, and CLISWELN is funded by Bundesministerium für Bildung und Forschung (BMBF-Germany), Executive Agency for Higher Education, Research, Development, and Innovation Funding (UEFISCDI -Romania), Bundesministerium für Bildung, Wissenschaft und Forschung and ¨Osterreichische Forschungsf¨orderungsges ellschaft (BMBWF and FFG Austria), and Ministerio de Economía y Competitividad (MINECO Spain), with co-funding from the European Union’s Horizon 2020 under Grant Agreement No 690462. This project was also financed by PN 23090203–Contribuții științifice noi pentru un management sustenabil al bazinelor hidrografice torențiale, terenurilor degradate, perdelelor forestiere și al altor sisteme agrosilvice în contextul schimbărilor climatice.

Editare inDesign: Magdalena Popa
Grafic copertă: Mirabela Marin

HYDROLOGICAL IMPACT OF CLIMATE CHANGE AND FORESTED AREA REDUCTION IN SMALL, FORESTED WATERSHEDS

Case study: Upper Tarlung watershed

-carte electronică online-

Seria III TEZE DE DOCTORAT

Mirabela MARIN

HYDROLOGICAL IMPACT OF CLIMATE CHANGE AND FORESTED AREA REDUCTION IN SMALL, FORESTED WATERSHEDS.
Case study: Upper Tarlung watershed

editura SILVICĂ
Voluntari | 2023

ISBN 978-606-8020-84-6

ABSTRACT

The simulations performed with the SWAT hydrological model under four climate and land use change scenarios allowed us to foreseen the evolution of three hydrological processes (surface runoff, water discharge, and sediment yield) in the Upper Tarlung watershed, at monthly, seasonal, annual and multi-annual level for 2020–2100 divided into three periods. Compared to the baseline (1979-1988), at the monthly level, the projections regarding the evolution of the surface runoff, water discharge, and sediment yield are either increasing or decreasing in all time periods. At the seasonal level, the projections show variations from season to season. At the annual level, the projected tendency is alternative, increasing or decreasing, depending on the climate change scenario and time interval. The multiannual average shows an exclusive increasing trend for surface runoff and water discharge in all climate and land use change scenarios, while for sediment yield an alternative trend is projected consisting of increments in all climate change scenarios coupled with land use scenario S3 and decreases in scenarios S1 and S2. Finally, the annual projections of surface runoff and water discharge frequency shows a prevalent increasing trend, highlighted also by the prevalence factor value, while for sediment yield a prevalent decreasing trend is projected, regardless of climate and use change scenario.

Contents

LIST OF NOTATIONS

GHG–greenhouse gasses emissions

ppm–parts per million

B.H–bazin hidrografic

u.a.–compartment level unit

ha–hectares

HRU–Hydrologic Response Units

LIST OF ABBREVIATIONS

IPCC–Intergovernmental Panel on Climate Change

WMO–World Meteorological Organization

UNEP–United Nations Environment Programme

RCPs–Representative Concentrations Pathways

ECPs–Extended Concentration Pathways

SSP–Shared Socioeconomic Pathways

SRES–Special Report on Emissions Scenarios

GAESC–Guidelines on Adaptation to the Effects of Climate Change

ANM–National Meteorological Agency

CREAMS–Chemicals, Runoff and Erosion from Agricultural Mangement Systems)

GLEAMS–Groundwater Loading Effects on Agricultural Management Systems

EPIC–Erosion-Productivity Impact Calculator

DEM–Digital Elevation Model

SWAT–Soil and Water Assessment Tool

USDA–ARS–United States Department of Agriculture–Agricultural Research Service

USDA–United States Department of Agriculture

SPAW–SOIL-PLANT-ATMOSPHERE-WATER-FIELD & POND HYDROLOGY

SCS–Soil Conservation System

MIKE-SHE–European Hydrological System Model

DHSVM–Distributed Hydrology Soil Vegetation Model

MODFLOW–Modular Finite Difference Groundwater Flow Model

CLISWELN–Climate Services for the Water–Energy–Land–Food Nexus

INCDS–National Institute of Research and Development in Forestry "Marin Drăcea"

ROCADA–ROmanian ClimAtic Dataset

INHGA–National Institute of Hydrology and Water Management

SWAT-CUP–SWAT Calibration and Uncertainty Programs

NSE–Nash-Sutcliffe Efficiency

INTRODUCTION

Knowing the impact of climate change has become a global preoccupation given that these changes, by increasing GHG emissions but also through the implications for technological and socio-economic development (IPCC 2000, 2014), are affecting the living standards of humans by influencing the availability of water and energy, food security, land use and agricultural production (Cai et al., 2016; Reed et al., 2013; Lehmann et al., 2013; Pandey et al., 2017).

Because natural resources are limited, many studies focused on assessing climate change impact on natural resources and the adoption of appropriate solutions for achieving the sustainability of the resources in the following years.

Since 1988, the World Meteorological Organization (WMO) and the United Nations Environment Program (UNEP) founded the Intergovernmental Panel on Climate Change (IPCC). Currently, IPCC include 195 member states and has the role to periodically assess global warming risks through special reports. Based on the information presented in these scientific papers, the IPCC supports Member States' governments to adopt the most appropriate climate change mitigation and adaptation strategies.

A first step in this direction was taken in 1992, when, at Rio de Janeiro, the United Nations Framework Convention on Climate Change (UNFCC) was signed, and subsequently, in 1997, the Kyoto Protocol (Japan), an international agreement by which 194 developed countries engaged to adopt policies and strategies for maintain a constant level of GHG emissions so that their effect on ecosystems to be diminished (***, 2013).

For investigating how climate will evolve and also to make harmonized forecasts about the dynamics of technological and socio-economic development, the scientific research must use a common set of scenarios (Wayne, 2013)

Globally, the reports published by IPCC since 1990 estimate, especially for the last decades of the 21st century, an increase in air temperatures p to 5 °C, but also the changes of precipitations, intensification of GHG emissions, rising sea and ocean levels, as well as intensification of extreme weather events (e.g., droughts and floods) (IPCC, 1992; 2000; 2014; 2018). For the Europe, the IPCC estimates that by the end of the 21st century there will be an increase in temperature up to 6.4 °C, while for the precipitation regime, the changes will be differentiated according to altitude (the southern part of the continent will be prone to more frequent and prolonged droughts, compared to northern regions that will be affected by floods) (Kovats et al., 2014).

1. STATE OF THE ART REGARDING THE HYDROLOGICAL IMPACT OF CLIMATE CHANGE IN SMALL, FORESTED WATERSHEDS

1.1. A brief history of the climate change scenarios evolution

1.1.1. SA90 scenarios

The first set of climate scenarios developed since 1990 and called SA90 (A, B, C, and D), estimated for the 1990–2100 period an increase in the global average temperature of 1 °C by 2025 and 3 °C by 2100 in scenario A, while in scenario B, the estimated increases were 0.2 °C per decade (Houghton et al., 1990). For scenarios C and D, was estimated an increase of 0.1 °C per decade (Houghton et al., 1990). For the 2025–2050 period, it was assumed that the amount of CO_2 released into the atmosphere it will double, the sea level will increase by 0.3–0.5 m until 2050 and by around 1 m until 2100, while the global population will reach 11 billion inhabitants by the end of 21st century (Tegart et al., 1990).

1.1.2. IS92 scenarios

In 1992, as a result of the adoption of new policies but also the increase of the development degree, the initial SA90 scenarios were improved. The six new types of alternative scenarios (IS92a-f) were presented in the Supplementary Climate Change Assessment Report. The report examines socio-economic and environmental development features in the absence of mitigation measures to reduce the negative effects of climate change, as is shown in Table 1.1 (IPCC, 1992). The new scenarios consider two periods, 1990-2025 and 1990-2100 respectively, and describes a world in which incomes and the global population are growing while the consumption of fossil fuels becomes intensive.

Table 1.1. Projections of IS92 climate change scenarios for 1990–2100 (IPCC, 1992).

Scenario	Population growth (billion inhabitants)	CO_2 emissions (GtC)		Economic growth (%)	
		2025	2100	1990–2025	1990–2100
IS92a	11,3	12,2	20,3	2,9	2,3
IS92b	11,3	11,8	19,0	2,9	2,3
IS92c	6,4	8,8	4,6	2,0	1,2
IS92d	6,4	9,3	10,3	2,7	2,0
IS92e	11,3	15,1	35,0	3,5	3,0
IS92f	17,6	14,4	26,6	2,9	2,3

1.1.3. SRES scenarios

Subsequently, the IS92 scenarios were also improved. The team of over 50 members from 18 countries, with the participation of non-governmental organizations, designed the new so-called "SRES scenario families" (A1, A2, B1, B2). From these SRES families, six types of scenarios (A1B, A1T, AIFI, A2, B1 and B2) were differentiated (IPCC, 2000).

Used in several researches as well as in the Three and Four Assessment Reports these scenarios are differentiated in relation to population growth, socio-economic and technological development, as is shown in Table 1.2 (IPCC, 2000; Wayne, 2013).

Table 1.2. The main characteristics of SRES scenario families (Arnell et al., 2004 from the IPCC, 2000).

Criteria	A1	A2	B1	B2
Population growth	Around 7 billion inhabitants	Around 15 billion inhabitants	Around 7 billion inhabitants	Around 10 billion inhabitants
Energy use	Very high and high	High	Low	Medium
Energy type	Fossil / Mixed / Renewable	Regional diversity	Efficient	Dynamic
Technological development	Faster	Reduced	Reduced	Medium

1.1.4. RCP scenarios

The new scenarios, called Representative Concentration Pathways (RCP), were designed in 2007 when IPCC, together with the 130-member Integrated Assessment Model Consortium research community, non-governmental and governmental organizations and users, initiated the RCPs development process (Wayne, 2013) These scenarios describe four new variations way, uniquely determined for each RCP, GHG emissions and other air pollutants, in relation to future assumptions on population growth, economic and technological development and energy consumption (IPCC, 2014). The global average temperatures (Table 1.3) were projected to increase by 1–3.7 °C, with a 0.4–4.8 °C range of variation (IPCC, 2014).

Table 1.3. Global average temperature increment projected in the RCPs scenarios for 2046–2065 and 2081–2100 period (IPCC, 2014).

Scenario	Period			
	2046-2065		2081-2100	
	Average value (°C)	Variation interval (°C)	Average value (°C)	Variation interval (°C)
RCP2.6	1.0	0.4–1.6	1.0	0.3–1.7
RCP4.5	1.4	0.9–2.0	1.8	1.1–2.6
RCP6.0	1.3	0.8–1.8	2.2	1.4–3.1
RCP8.5	2.0	1.4–2.6	3.7	2.6–4.8

Moreover, Rogelj et al. (2012) present projections of global air temperature until 2300, as is shown in the following table (Table 1.4). The sharpest increase in global temperature, of 10 °C were projected in the RCP8.5, scenario in which measures for adaptation and mitigation of the negative effects of climate change are missing.

Table 1.4. Global air temperature dynamics in the RCPs scenarios until 2300 (Rogelj et al., 2012).

Scenario	Period	
	Average value (°C)	
	2100	2300
RCP2.6	1.5	1.1
RCP4.5	2.4	2.8
RCP6.0	3.0	4.1
RCP8.5	4.9	10.0

Regarding the precipitation regime, non-uniform changes are expected. This tendency is similar to those from SRES scenarios, namely: a very high probability (over 90%) of increase in the annual average precipitation in the areas located at high altitudes, while, with a probability higher than 66%, there will be a decrease of the annual quantities in the areas located at low altitudes but also in the subtropical ones (IPCC, 2014). At the same time, is estimated that the extreme events (e.g., droughts, floods) will become frequent and intense (IPCC, 2014). The air temperature and precipitation projected changes are shown in the Figure 1.1.

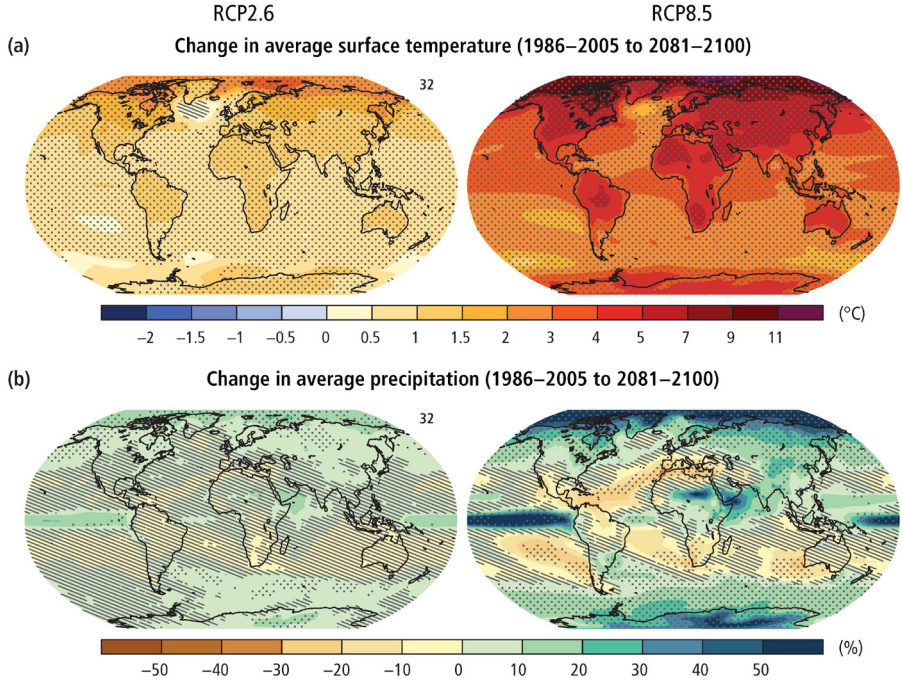

Figure 1.1. Change in average surface temperature (a) and change in average precipitation (b) based on multi-model mean projections for 2081–2100 relative to 1986–2005 under the RCP2.6 (left) and RCP8.5 (right) scenarios. The number of models used to calculate the multi-model mean is indicated in the upper right corner of each panel. Stippling (i.e., dots) shows regions where the projected change is large compared to natural internal variability and where at least 90% of models agree on the sign of change. Hatching (i.e., diagonal lines) shows regions where the projected change is less than one standard deviation of the natural internal variability. (from IPCC, 2014).

In October 2018, the IPCC published the Special Report on the negative effects that a global warming of 1.5 °C above pre-industrial levels could have on natural ecosystems and human wellbeing, including the extinction of certain aquatic, plant or animal ecosystems. For the 2030–2052 period it is estimated, with a very high probability, a global warming of 1.5–2 °C (IPCC, 2018). The authors also pointed out that the effects are more pronounced at a global warming of 2 °C compared to 1.5 °C. Therefore, it is very likely to be recorded increases in extreme temperatures between 3−6 °C, increased precipitation and flooding occurrence in high altitude areas of the northern hemisphere and an increase in the frequency and intensity of droughts in other regions, rising sea and ocean levels as well as the conversion of plant and terrestrial ecosystems (IPCC, 2018). Humans are also affected by global warming, which can influence their living

standards through altering food production, water availability and the economic development of regions (IPCC, 2018). The same report states that maintaining global warming at 1.5 °C can reduce the range of these projections up to 50% compared to global warming of 2 °C. At the same time, GHG (CO2) emissions could be reduced by 20% until 2030 compared to 2010 and could even reach the 0 value if global warming does not exceed 1.5 °C by the middle of the 21st century. At the same time, fewer adaptation measures will be needed at global warming of 1.5 °C compared to 2 °C (IPCC, 2018).

1.2. Climate change scenarios for Romania

Romania has a unique diversity in Europe, both in terms of geographical conditions and due to the specific flora and fauna. Thus, understanding the climate change impact is an essential prerequisite not only for this unique diversity but also for the future sustainability of forest ecosystems (Barbu et al., 2016).

Since 1901, our country has been recorded an increase in average annual temperatures by 0.6 °C (Busuioc et al., 2007), while summers are characterized by higher temperatures and lower precipitations. The summer of the 2007 is noted as the warmest due to the recorded temperatures above 40 °C (Anders et al., 2014), while for the summers of 2000 and 2003 was reported a precipitations deficit of 49% and 48% respectively (Busuioc et al., 2007). In addition, for our country were estimated increases in air temperature between 0.5–2 °C by the end of the 21st century (Barbu et al., 2016). These projections are also confirmed by Dumitrescu et al. (2014) who, in a study that analyses the evolution of climate parameters in 1961–2013 period, observed an obvious increasing trend of temperatures, especially during spring and summer, and a varied dynamic of the precipitations.

In 2008 was published the Climate Change Adaptation Guide, which presents the main changes in temperature and precipitation for our country. Thus, for the 1901−2000 period, the annual average temperatures increased by 0.3 °C and by 0.5 °C for the 1901−2006 period. These changes are more pronounced for the southeast part of the country and less significant in the intra-Carpathian area, as is shown in Figure 1.2. Starting with 1980, due to the increased temperatures and reduced precipitations, a period with dry years can be noticed. At the same time, the winter of 2007 is mentioned as the warmest winter in the history (GAESC, 2008).

Regarding the precipitation, a reduction in annual average values recorded between the 1900−2000 period was observed (Figure 1.3). Additionally, since 1960 was recorded an increase in drought events for the southern part of the country, while for the west and southwest part an increasing trend of periods without rains were observed (GAESC, 2008).

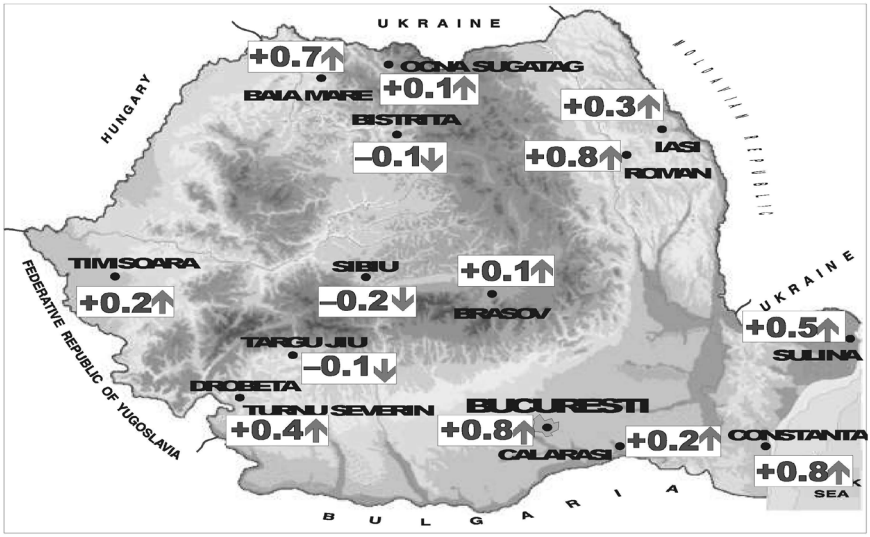

Figure 1.2. Average annual temperature dynamics in the 1901–2000 period (GAESC, 2008).

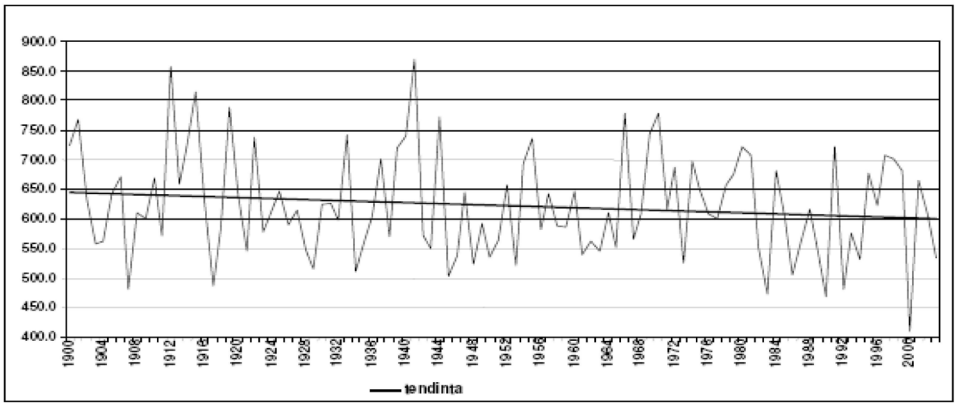

Figure 1.3. The evolution of average annual precipitations in the 1900–2000 period (NMA, 2007 quoted by GAESC, 2008).

Related to the climate scenarios developed for our country, the GAESC confirms the projections of the Fourth Assessment Report of the IPCC (IPCC, 2007). For the 2020–2029 period was estimated increases of temperatures by 0.5–1.5 °C. Towards the end of the 21st century (2070–2099 compared to 1961–1990), the average minimum temperature during winter would increase by 4–6 °C in the intra-Carpathian area and by 3–4 °C in other regions (GAESC, 2008). In summer, the maximum temperature will increase by 4–5 °C in the north of the country and by 5–6 °C in the south. Regarding the precipitations, in

the 2070–2099 period, an increase of 30–40 mm in the western and southwestern parts of the country is projected during winters. In addition, summers will be characterized by severe droughts in the south and southeast regions during the 2090–2099 period (GAESC, 2008).

The National Environmental Protection Agency publishes the Report on the State of the Environment in Romania (RSMR, 2009) that estimates that, in our country, during the 2020-2099 period compared to 1980-1990, the average annual temperatures are projected to increase by 0.5 (1.5)–5 °C. For precipitations, the same source predicts that average annual precipitations will be reduced especially in the south-east part of the country during the middle of the 21st century, while towards its end severe droughts are projected (RSER, 2009).

Other studies estimated increases of temperature up to 3.3 °C for the 2021–2100 period as is shown in Table 1.5 (Busuioc et al., 2010).

Table 1.5. Inter-annual variation of average air temperature projected for Romania (Busuioc et al., 2010).

Season	Period			
	2021–2050		2070–2100	
	Average value (°C)	Variation interval (°C)	Average value (°C)	Variation interval (°C)
Spring	1.0	±0.4	2.3	±0.4
Summer	1.6	±0.3	3.3	±0.6
Autumn	1.4	±0.4	2.8	±0.9
Winter	1.0	±0.5	2.6	±0.7

Instead, the precipitations projected for the 2021–2050 period, shows a decrease of 12% of the average monthly values within the southern part of the country compared to the northern and north-eastern area, for which an increase of 14% are estimated (Busuioc et al., 2010). Similar findings are obtained for the 2070–2100 period, but with different patterns at seasonal level, e.g., annual precipitations increase by 50% during autumn in the north and north-eastern part, and decreases by 16% in spring and summer for the south-eastern and southwest part (Busuioc et al., 2010).

In this context, National Institute of Hydrology and Water Management (INHGA, 2009), projects a decrease by 20–30% of average annual surface runoff by the middle of the 21st century and by 30–40% towards its end, as well as a higher probability of extreme events occurrence, especially for spring and autumn. In addition, Corbuș et al. (2017) estimates for the 2021−2050 period a varied trend of the average monthly water discharge that is expected either to increase by 6.2% or to decrease by a maximum of 24.6%.

1.3. Land and forest ecosystems vulnerability to climate change

Climate change influences both biodiversity (Marcu, 2005; Vasile et al., 2015) and the surface occupied by tree species such as the expansion or reduction of the natural area of trees (Giurgiu, 2005; Păcurar, 2008a). In addition, climate change also affects land degradation processes, favouring the intensification of erosion generated by wind (especially in Oltenia) (Păcurar, 2007). Environmental conditions also influence the trees growth processes (e.g., stomatal conductance, respiration, transpiration, photosynthesis) (Blujdea, 2005).

In our country, an increase by 2 °C of temperatures will increase the vulnerability of the forests (especially of the oak trees), but also of the mixtures of beech, ash, or hornbeam, which will be confronted with ecological imbalances generated by various disturbing factors (Giurgiu, 2005). In addition, certain ecological, auxological and economic changes in forest ecosystems will be favoured by increased number of harmful insects, reduced biodiversity and biomass accumulation, intensification of the frequency and intensity of fires, droughts and floods, the accentuation of the thermal stress, and so forth (Cuculeanu and Bălteanu, 2004 quoted by Giurgiu, 2005; Blujdea, 2005). Implications for climate change on natural ecosystems include also the intensification of desertification, the change in vegetation layers due to increased temperatures, and the intensification of floods and especially of flash floods mainly in small watersheds due to changed patterns of precipitations (Cuculeanu and Bălteanu, 2005). In addition, the forest monitoring carried out for our country between the 1990−1994 period, showed a decline in the health of forests, especially of those located in forest-steppe, due to the increased number of heavily damaged trees as a result of intensification, in terms of frequency and intensity, of the drought events recorded in the 1981-1994 period (Pătrășcoiu et al., 1995 quoted by Cuculeanu et al., 2005).

Badea et al. (2005) in their study regarding the possible correlations between the phytosanitary status of forests and climate change emphasize the interconnectivity between climatic parameters and the development of forest ecosystems. The authors stated that, due to temperature increments and increased water stress, the health of deciduous species (especially oak from the southern and southeast parts of the country) is poor compared to coniferous species. Forest ecosystems will be affected by all these changes because they have long production cycles and are permanently exposed to the climate change effects (Barbu et al., 2016).

1.4. Knowledge of climate change hydrological impact at watershed level

Climate change generate modification of many variables (increments in air temperature, intensification of evapotranspiration, changes the hydrological cycle, influence the dynamics of soil moisture and precipitation, favour increments in flood frequency and intensity). Hence, assessing the possible consequences of climate change on watershed behaviour has become today a prerequisite especially for the management of torrential watershed.

In other words, considering that these changes influence the hydrological processes which controls the water availability (its quality and quantity respectively), the next question arises: how should be adapted the management of mainly forested torrential watershed to the climate changes context?

It is true that, if we refer to the investigation of hydrological behaviour of watersheds, especially of those mainly forested, we state that this concern is not a novelty today. Processes as runoff, erosion, sediment yield were investigated, by simple visual observation, since antiquity and subsequently by experimental studies organized in the early 20th century (Switzerland–1900; USA–1906; Japan–1908, etc.), when were provided the first quantitative evidence on how the forest influences those processes within watersheds.

Although, at the beginning, the watershed response was investigated mainly by assessing the influence of some triggering factors (e.g., precipitations), in the last decades were taken into account other different variables such as climate factors (e.g., air temperature, wind direction and wind speed), or soil moisture, land use and management, nature and structure of vegetation, and so forth.

Currently, the hydrological studies within watersheds, regardless of their size, have acquired a novelty due to the increasing orientation to the climate change context that modifies the patterns of hydrological processes.

Researchers pledge for assessing the hydrological impact of climate change at the river basins scale, the necessity and urgency of this activity being advocated with priority in the case of small watersheds (Gautam et al., 2018), as is the case of our research.

Thus, the influence of precipitation on water discharge has been observed since 1966 by Lull and Sopper, who consider latitude, altitude and afforestation percentage as factors that influence both hydrological and physiological processes. Studies conducted by Guo and Ying (1997) and Fekete et al. (2004) pointed out that the influence of precipitation on runoff is greater compared to temperatures. However, this issue remains a scientifically controversial one since, about a decade later, the study of Joh et al. (2011) outlined the opposite situation. Vertessy (2000) and Zhang et al. (2020) states that the watersheds deforestation

leads to decreases of evapotranspiration and groundwater level and increases of surface runoff and water discharge. Alongside the soil and water protection functions or balancing climatic extremes, the forest ensures the retention of important amounts of precipitation in the canopy, reduces soil moisture and the speed of surface runoff on slopes and riverbeds, increases the groundwater runoff for the surface runoff detriment (Gaspar, 2004; Miță, 2019), thus leading to the water discharge regularization and a reduced risk of flash floods occurrence (Nicolescu, 2006).

The findings of Huang and Zhang (2004) and Stonefelt et al. (2007) highlights the significant influences of precipitation on the surface runoff, while the temperatures influence the timing of streamflow. Streamflow occurrence is influenced also by extreme events (e.g., droughts and floods) (Brooks, 2009). Additionally, any change in the forest vegetation structure and land use alter the physiological and hydrological processes and consequently the water availability (Marin et al., 2020c). In addition, other authors states that significant increases in surface runoff occur mainly due to changes in land use that favours the onset and intensification of flash floods (Costache et al., 2020; Zhang et al., 2020). This is the reason of many recommendations regarding the amplification of the studies conducted in different watershed for quantifying the climate and land use change impact on hydrological processes (Jones et al., 2009).

For sustainable management of land use and especially for securing the water resources, is necessary to ensure a balance between the existing land use (Briones et al., 2016). This equilibrium is a prerequisite both for integrated management of natural resources as well as for the sustainable management of watersheds. Moreover, is mandatory to consider also the changes in the forested areas, and to include forest vegetation in the assessment of the hydrological impact of climate change (Wei et al., 2018).

1.5. Hydrological models applied for assessing the climate change impact in small, forested watersheds

1.5.1. Hydrological modelling, a tool for projecting the hydrological impact of climte change

Given the importance of water and soil in securing the food resources, but also in socio-economic and technological development (Schewe et al., 2013), hydrological modelling represents both the necessary support for integrated management of soil and water resources and the tool which allows projecting the hydrological impact of climate change.

The aim of hydrological modelling is to accurately represent the future evolution of hydrological processes within watersheds, regardless of their size (Gayathri et al., 2015).

The hydrological models enables both predictions of climate change impact on the hydrological response of watersheds (Dwarakish and Ganasri, 2015) as well as providing an overview of these changes' effects on water resources (Praskievicz and Chang, 2009 quoted by Bajracharya et al., 2018). At the same time, the human component can be also included the simulation process to investigate the influence of human activities on water resources and land management (Chong, 2002).

Although the first attempts in hydrological modelling date back to 1674, the actual development of modelling activities took place in 1930, when the concept of unit hydrograph and the Hortonian infiltration theory appeared (Džubáková, 2010). However, the reference period for the development of hydrological models is the middle of the 20th century, when physically distributed and stochastic and conceptual models were designed (Chong, 2002; Džubáková, 2010). Through their continuous improvement, around 1980, the models developed were characterized by a high spatial resolution and the ability to simulate not only the runoff but also the land use influence on hydrological processes (Chong, 2002; Džubáková, 2010).

1.5.2. Hydrological models classification

A wide range of hydrological model types currently exist. A first classification of hydrological models was made in 1988 (Singh, 1988 quoted by Chong, 2002). The hydrological models were divided in two main categories, symbolic and material as is presented in Figure 1.4, adapted from (Singh, 1988 quoted by Chong, 2002). In the material category are included the laboratory and analog models, while in the symbolic are framed the non-mathematical and mathematical models. The mathematical ones comprise the empirical, conceptual and theoretical models (Chong, 2002).

Empirical or 'black box' models are characterized by high predictive ability even if they do not take into account information about the watershed's behaviour or runoff processes (Džubáková, 2010). However, empirical models have the disadvantage that they do not allow the assessment of different impacts (Chong, 2002), or the impossibility of generalizing the model to other basins, forests or altitudes (Džubáková, 2010). Nevertheless, empirical models are easy to use and describe the connection between the input and the output parameters (Adams et al., 2010).

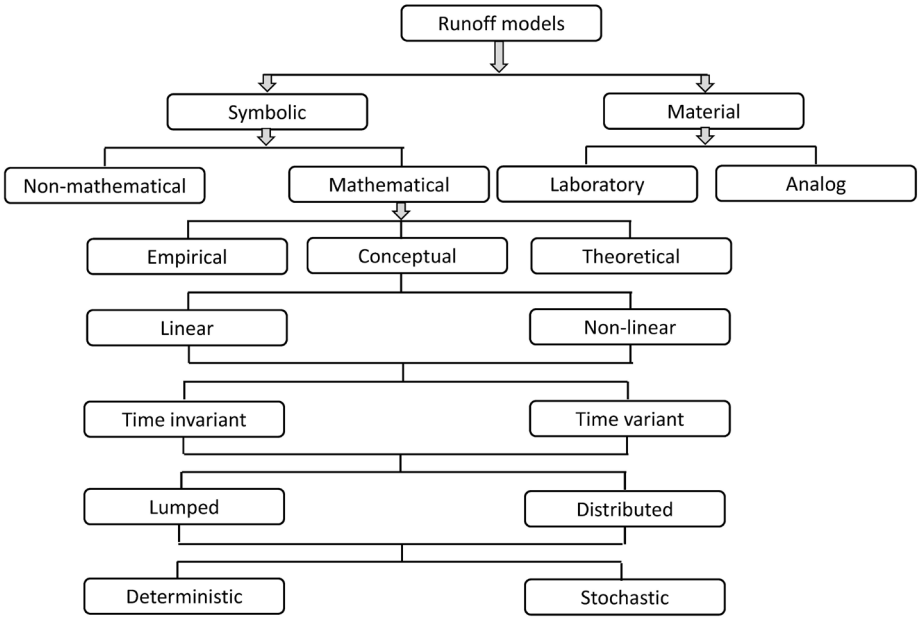

Figure 1.4. Classification of hydrological models (from Singh, 1988 quoted by Chong, 2002).

Theoretical or 'white box' models are characterized by a structure that allows accurate representation of the watersheds, thus improving the process of understanding the hydrological system as a whole (Chong, 2002). However, these models request a large number of input data and a long time for data processing (Adams et al., 2010).

Conceptual or 'gray box' models are intermediate models between the two categories mentioned above and include the majority of the hydrological models (Chong, 2002). These models are complex and use as input data a large number of parameters for describing the hydrological processes within the watersheds (Gayathri et al., 2015). However, the structure of these models relies on time series that must be defined before using the models (Džubáková, 2010).

1.5.3. A brief presentation of some hydrological model

SWAT is a semi-distributed hydrological model that operates at daily basis (Arnold et al., 1998). The model allows both the assessment of different impacts as well as the simulation of hydrological processes within different size watersheds, that are divided into sub-basins and subsequently into hydrological responses units (HRU), homogeneous in terms of soil and land use properties (Beckers et al., 2009). As input data, SWAT requires the digital elevation model

(DEM), weather data (e.g., minimum and maximum temperature, precipitation, relative humidity, wind speed and solar radiation) soil properties and land use data (Neitsch et al., 2005).

MIKE-SHE is a distributed physical model which can be applied not only for different size watersheds but also for reservoirs (Beckers et al., 2009). The watersheds area is divided into homogeneous polygons in terms of soil type, land use and precipitation (Golmohammadi et al., 2014). The disadvantage of the model is the large volume of measured data required to set up and ran the model (Golmohammadi et al., 2014).

BROOK90 is a physical model that operates at daily time steps and can be used only in small river basins for modelling the hydrological processes from both rain and snow events (Beckers et al., 2009). The model requires a large number of mandatory parameters to ran (30–40 parameters) and does not take into account the path followed by surface runoff (Beckers et al., 2009).

DHSVM is a fully distributed physical model that can be applied in river basins up to 10,000 km^2 (Wigmosta et al., 1994, Wigmosta et al., 2002 quoted by Beckers et al., 2009) whose surface is divided into small grid cells characterized by unique values of soil, vegetation or climate parameters (Gupta et al., 2015). The model does not capture the groundwater flow (Beckers et al., 2009).

MODFLOW it is also a physical completely distributed model, very often applied in studies focused on two-dimensional, three-dimensional or quasi-dimensional simulations of groundwater flow dynamics (Beckers et al., 2009; ***, 2018b). The model can simulate not only the hydrological processes that occur in rivers, riverbeds or reservoirs but also of those that take place in drains or wells (***, 2018b).

1.6. Results of hydrological models applied for assessing the hydrological impact of climate change in small, forested watersheds

After consulting various international databases, we selected particularly those studies that were carried out in mainly forested watersheds, with an area up to 100 km^2 as is the case of our watershed (Marin et al., 2020c). Out of the total of 27 studies retained, 22 are conducted in watersheds with an area less than 100 km^2 and forested in a proportion of 30−100% (in most cases over 60–70%).

In relation to the surface, the analysed watersheds are divided as follows: 14 watersheds have an area less than 10 km^2, 6 watersheds with an area between 10−40 km^2, 2 watersheds with an area between 50−60 km^2, and 5 watersheds with an area between 200−300 km^2. In relation to the geographical region, most

studies have been developed in Europe and America (North and South).

However, the effects of climate change on hydrological parameters vary depending not only on the hydrological model used, the scenario adopted, or the period considered in simulations but also across geographic gradient (Marin et al., 2020c). Future changes in runoff processes are more pronounced in scenarios that involves changes both in temperature and precipitation (Kalogeropoulos and Chalkias, 2013). A similar situation can be seen in studies that considers also land use change (Peraza-Castro et al., 2018), CO_2 emission (Chambers et al., 2017; Lee et al., 2018) or solar radiation scenarios (Leta et al., 2018).

Many studies reported that during the 21st century, significant changes in temperature and precipitations are expected, changes that will significantly influence hydrological processes (e.g., surface runoff, water discharge, sediment yield, evapotranspiration, and so forth) within small forested watersheds (Marin et al., 2020c).

Thus, for air temperature are projected increases of up to 2.6 °C with the MODFLOW model (Beaulieu et al., 2016), up to 4.3 °C with the SWAT model (Joh et al., 2011) and up to 7 °C with the DHSVM model (Alvarenga et al., 2016).

Instead, for precipitation, the results reported showed different dynamics as follows: the SWAT model predicts both a decrease in precipitation amounts by up to 32% (Senent-Aparicio et al., 2017), as well as their increase by up to 20% (Ahn et al., 2013). The BROOK model simulations predict an increase in precipitation amounts by up to 11% (Im et al., 2007), while the MODFLOW and DHSVM models simulations show a decrease of precipitation by 4.5% (Beaulieu et al., 2016) and 35% respectively (Alvarenga et al., 2016).

For evapotranspiration, it is observed that regardless of scenario adopted, the period considered or the hydrological model used, an overall increase tendency of this parameter is projected: up to 4% with MODFLOW (Beaulieu et al., 2016), by 16% with MIKE SHE (Thompson, 2012), by 62% with SWAT (Joh et al., 2011), and by 70% with BROOK model (Im et al., 2007).

Regarding the dynamics of runoff processes, the SWAT model predicts a reduction of between 8% (Leta et al., 2018) and 14% approximately (Kalogeropoulos and Chalkias, 2013). Surface runoff could decrease up to 18% (Serpa et al., 2015) and 54% (Senent-Aparicio et al., 2017), or could increases up to 16% (Ahn et al., 2013) and 50% (Lee et al., 2018).

The projected discharges show both a reduction between 25–39% (Leta et al., 2018) and an increase up to 71% (Chambers et al., 2017). The changes in extreme peak flow are also projected and those could either increase up to 22% or decrease up to 60% (Leta et al., 2018). The MIKE-SHE model estimates that

discharges can both decrease up to 49% and increase up to 51% (Thompson, 2012). The MODFLOW model predicts that discharges can decrease up to 26%, while the DHSVM model estimates decreases between 56–69% (Alvarenga et al., 2016) and up to 80% until 2099 (Alvarenga et al., 2018).

For sediment yield, Zabaleta et al. (2014) foresaw a decrease up to 55% and an increase up to 285%. Similar results are reported by Serpa et al. (2015), that foresaw increases up to 257% and decreases up to 29% in sediment yield. Rodriguez-Blanco et al. (2016) predict both increases of up to 10% and decreases of up to 42% for sediment yield.

1.7. Main conclusions of the state-of-the art analysis

1) Climate change influences: biodiversity and productivity of forests, the spatial distribution of forest ecosystems, the phytosanitary status of stands, forest composition and structure, fundamental physiological processes (e.g., stomatal conductance, transpiration, respiration or photosynthesis), land degradation processes.

2) At the international level, an increase in air temperature of 2.6–7 °C is projected, while precipitations can either increase by up to 20% or decrease by up to 35%.

3) At the national level, it is estimated temperatures increases up to 3.3 °C, while precipitations can either decreases up to 12% or increase by 14%.

4) The assessment of the risks induced by climate change is necessary for emphasizing how these are influencing the availability of natural resources over time.

5) Modelling processes allows the assessment of climate change impact on watersheds and provide the necessary support towards integrated management of water resources.

6) Studies conducted so far, have considered different periods (either short term, medium, and long term) and have been used different hydrological models developed since 1960 for assessing various impacts.

7) Many authors have shown that precipitation is the main parameter that influence the runoff processes, while other authors claims that the influence of precipitations on hydrological processes is less important compared to temperatures.

8) Some authors argue that more accentuated changes in runoff processes are expected in scenarios that include not only temperature and precipitation scenarios but also land use change scenarios.

7) Many authors pointed that the climate change effects will be felt not only on hydrological processes, but also on the composition and structure of the forest

ecosystems. Therefore, the forest health, productivity and area are significantly influenced by climate change.

8) Regarding the future dynamics of surface runoff, water discharge and sediment yield, the study's findings cannot be aligned to a single trend.

9) Therefore, we believe that for scientific substantiation of the solutions for diminishing the climate change hydrological impact, the first step is to assess the dimensions of this impact through case studies conducted at small watersheds scale.

2. RESEARCH AIM, OBJECTIVES AND STUDY AREA LOCATION

2.1. Aim and objectives

According to the findings presented in the previous chapter, climate change has become a reality today. Those changes have implications both on a global and local scale, and the hydrological effects of these events are becoming increasingly visible. Climate change modify and/or restrict the availability and access to three of the most important natural resources, namely forest, water, and soil.

After reviewing many studies focused on assessing the hydrological impact of climate change, we noticed that the results obtained are difficult to align (even for one and same model). Therefore, as we have already mentioned, the pathway toward scientific substantiation of solutions that pursue diminishing the negative effects of the climate change is an advanced knowledge of these effects through case studies conducted at the local level, particularly in small forested watersheds.

Hence, the aim and objective of this research were developed starting precisely from the above premise, as follows:

The research aim: forecasting, on three periods (2020–2039; 2040–2069; 2070–2100), the hydrological impact of climate change in a small forested watershed, representative in terms of forest and water supply, in order to substantiate the future adaptation measures of forest and water resources management plans.

The main objective: to evaluate the monthly, seasonal, annual and multiannual variation of three hydrological processes (e.g., surface runoff, water discharge and sediment yield) for the 2020–2100 period in four local climate change scenarios (REMO4.5; REMO8.5; CLM4.5; CLM8.5) and three land use change scenarios (maintaining the current forested areas; reducing the forested areas by 25%; reducing the forested areas by 50%).

For achieving the main objective, we have established the following specific objectives:

(1) The SWAT hydrological model adaptation to the local specificity of the studied watershed;

(2) Forecasting trends in the evolution of precipitation and air temperature;

(3) Forecasting trends in surface runoff dynamics;

(4) Forecasting trends in water discharge dynamics;

(5) Forecasting trends in sediment yield dynamics;

(6) Analysis of the frequency of projections regarding the annual surface runoff, water discharge, and sediment yield.

Additionally, it will be highlighted the hydrological role of the forests under the possible land use scenarios and the consequences on hydrological processes. Thus, will be emphasized the importance of preserving the forests both for balancing the water flow regime in the studied region and to ensure the water resources quality in the coming years.

2.2. Study area location

The current research was performed under the Climate Services for Water–Energy–Land–Food Nexus project (CLISWELN [1]) conducted between 2017 and 2020. Within this project, the Tarlung river basin upstream Sacele reservoir was chosen as a case study. The river basin covers 184 km^2 and has great socio-economic and industrial importance, being the main sources of water used for drinking and industrial purposes of the Brașov metropolitan area.

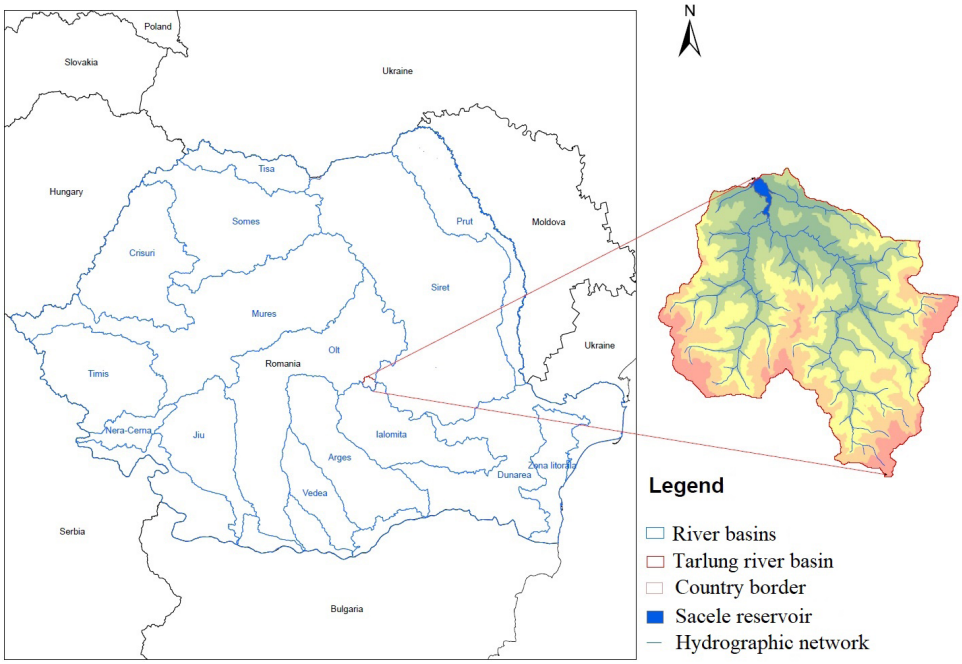

Figure 2.1. Location of the Tarlung watershed

More than 90% of the water demands of this area are provided by Tărlung basin and the Săcele reservoir (Compania Apa, 2020). The watershed is located in the central part of Romania, in Brașov County, at around 20 km from the

[1] CLISWELN is a European research project funded by ERA4CS. ERA4CS is an ERA-NET initiated by JPI Climate, and CLISWELN is funded by Bundesministerium für Bildung und Forschung (BMBF-Germany), Executive Agency for Higher Education, Research, Development and Innovation Funding (UEFISCDI-Romania), Bundesministerium für Bildung, Wissenschaft und Forschung and Österreichische Forschungsförderungsgesellschaft (BMBWF and FFG-Austria), and Ministerio de Economía y Competitividad (MINECO-Spain), with co-funding from the European Union's Horizon 2020 under Grant Agreement No 690462.

Brașov city (Figure 2.1). The climate is temperate-continental, with 600–700 mm annual precipitation and 7–8° C average annual temperature (www.vremea.ro/gt/clima-brasov/).

This present research was carried out in the upper sector of the Tărlung watershed, highlighted in Figure 2.2 by the black border (Marin et al., 2020b).

The Upper Tărlung watershed covers 7169.53 ha and the computing section is bounded by 45°52” East latitude and 25°84” North latitude. The watershed has a length of the hydrographic network of 216.49 km and a length of the main stream length of 14.95 km. The elevation ranges between 874 and 1,842 m a.s.l. and was divided into 11 elevation classes differentiated at a 100 m interval as is highlighted in Figure 2.3 (Marin et al., 2019).

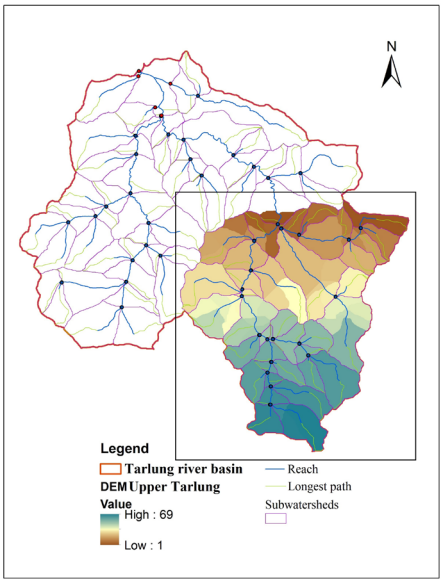

Figure 2.2. Upper Tărlung watershed, located upstream of Tărlungul Mare and Tărlungul Mic confluence

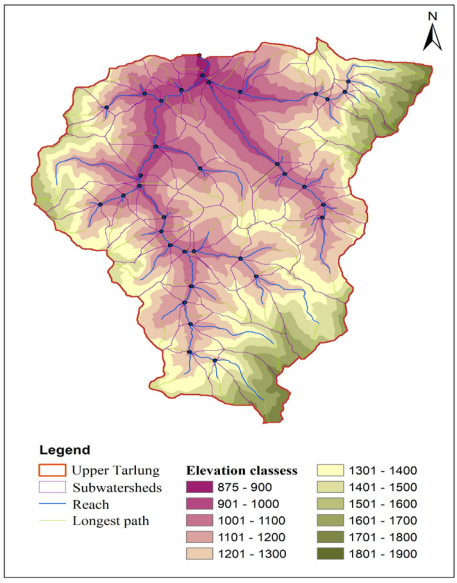

Figure 2.3 Distribution of the studied watershed surface into altitudinal classes

The average slope within the Upper Tarlung watershed is 37%, and the main riverbed slope is 6%. The watershed surface was split into five slope classes, divided by a 15% interval. The area covered by each class is presented in Table 2.1, and the slope classes’ distribution is highlighted in Figure 2.4. It can be noticed that the dominant slope classes are class 2 (15–30%) and class 3 (30–45%), which covers 66% of the studied watershed area (Figure 2.5).

Table 2.1. Distribution of the Upper Tărlung watershed surface into slope classes.

Slope class	Slope interval (%)	Area covered	
		ha	%
1	0–15	329.41	5
2	15–30	2227.97	31
3	30–45	2516.15	35
4	45–60	1363.62	19
5	> 60	732.39	10
Total		**7169.53**	**100**

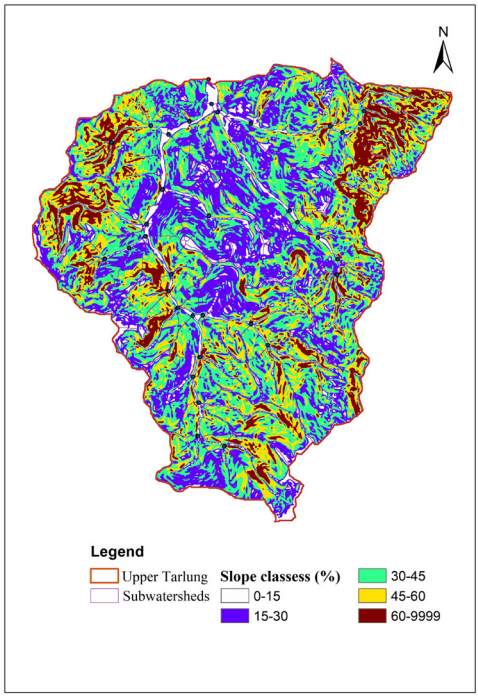

Figure 2.4. Distribution of the Upper Tărlung watershed surface into slope classes.

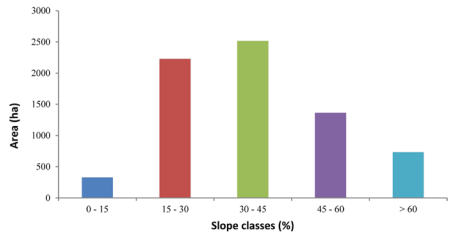

Figure 2.5. Histogram of the surface occupied by each slope class within the studied watershed.

The land use categories were identified after consulting the management database in geospatial format (GIS) developed by the National Institute of Research and Development in Forestry 'Marin Dracea' (INCDS) and is presented in Table 2.2. The spatial distribution of each land use category can be seen in Figure 2.6.

Table 2.2. The land use categories and the surface covered by them within the studied watershed.

No.	Land use	S W A T code	Area covered	
			ha	%
1	Forest evergreen	FRSE	2176.92	30
2	Forest deciduous	FRSD	3557.23	50
3	Pastures	PAST	1352.49	19
4	Forest nursery	AGRL	0.62	0.01
5	Pasture with scattered trees	RNGB	30.3	0.42
6	Meadows	RNGE	24.59	0.34
7	Water bodies	WATR	5.74	0.08
8	Build-up area	URML	0.02	0.00
9	Rocky lands (waste lands)	SWRN	3.27	0.05
10	Public roads	UTRN	18.35	0.26
		Total	**7169.53**	**100**

The watershed is mainly forested with forests in which prevails deciduous species found on 50% of the surface (3557.23 ha) and with forests in which prevails evergreen species extend over 30% of the area (2176.92 ha) (Figure 2.6). The next dominant land use is pastures, founded on 19% of the area (1352.49 ha).

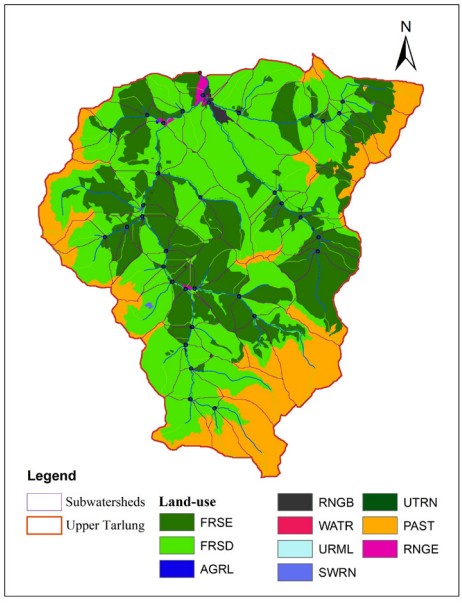

Figure 2.6. Spatial distribution of the land-use categories within the studied watershed.

Regarding the soil types within the Upper Tarlung watershed, according to the forest and forest-pastoral management plans developed by INCDS for the 2009–2013 period, four soil classes were identified, namely: Cambisols class on 5674.13 ha (78%), Spodisols class on 1136.34 ha (16%), Protisols class on 265.45 ha (5%) and Cernisols class on 93.61 ha (1%) (Table 2.3).

Table 2.3. Soil types identified within the studied watershed.

No.	Soil class	Soil type	Soil subtype	Area covered	
				ha	%
1	Cambisols	Eutric Cambisols	Typic	966.07	13
2			Mollic	78.90	1
3			Lithic	5.62	0
4			Gleyic	22.58	0
5			Stagnic	69.38	1
6		Dystric Cambosols	Typic	3070.56	43
7			Umbric	555.09	8
8			Prespodic	95.61	1
9			Lithic	810.31	11
10	Spodisols	Prepodzols	Lithic	1096.08	15
11			Histic	40.26	1
12	Protisols	Litosols	Rendzic	178.56	3
13		Aluviosols	Dystric	51.26	1
14			Gleyic	35.63	1
15	Cernisols	Rendolls	Eutric	93.61	1
			TOTAL	**7169.53**	**100**

The main types of soil within the studied watershed are: Dystric Cambosols (4531.58 ha–63%), Prepodzols (1136.34 ha–16%) and Eutric Cambisols (1142.55 ha–15%). Litosols, Aluviosols and Rendolls occupy a small area, being found on only 359.06 ha (6%).

3. RESEARCH METHODOLOGY

3.1. Adaptation of the SWAT model

As we previously specified, some input data are required to operate the SWAT model: digital elevation model (DEM), weather database, land use database and soil database. The adaptation to the local specificity of each component is detailed below (Marin et al., 2019).

3.1.1. Digital elevation model

Foreseen with an ArcSWAT interface of the ArcGIS program, the SWAT model enables users to make graphically and vectorially edits of watersheds regardless their size (Arnold et al., 1998). Therefore, the first component required is the DEM. In this study, we used the DEM for the entire Tărlung river basin available at a 10 m spatial resolution and taken from the CLISWELN project (Tudose et al., 2018).

From the entire Tărlung watershed DEM was chosen its upper sector as is highlighted in Figure 3.1 by a different colour ramp of DEM, and also through the yellow square. Only for this area was compiled the physiographic data characteristics that describe the watershed under study.

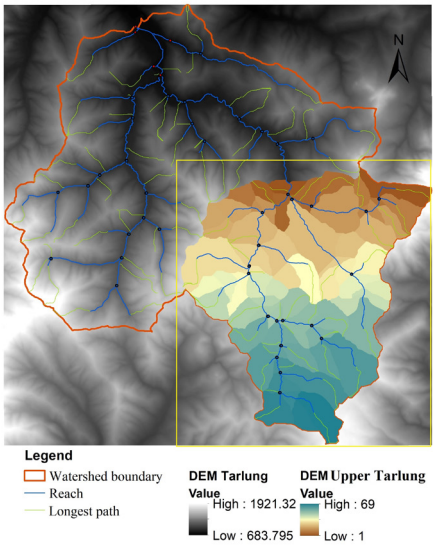

Figure 3.1. DEM of the entire Tărlung watershed related to Săcele reservoir and the delineation within it of the Upper Tărlung watershed.

Considering that the management unit boundaries were different from the "hydrographic" boundary of the watershed, we used the Reshape command in ArcGIS 10.3 (Figure 3.2) to reposition the watershed boundaries at the compartment level. Using the Topology command an overlap verification of the watershed boundary was performed.

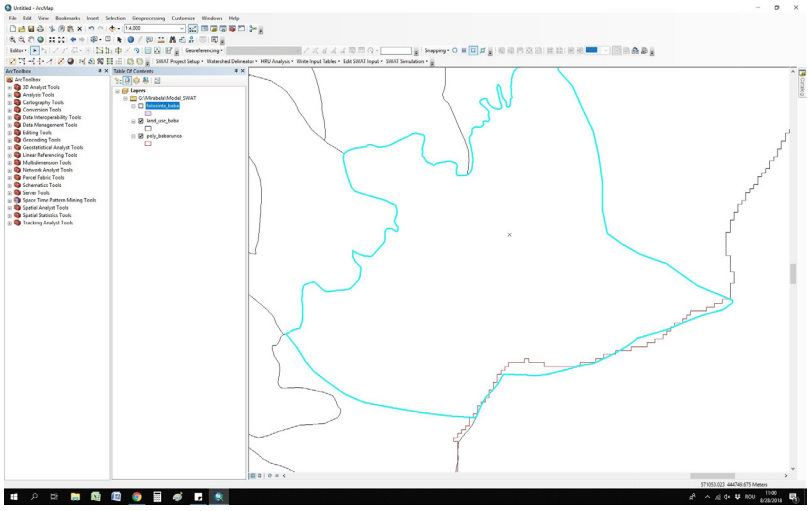

Figure 3.2. Relocation of the studied watershed boundaries through the Reshape command.

Afterwards, using Watershed Delineator command (Figure 3.3) the watershed boundary, streams and flow directions were defined, while the computing section was manually positioned (Figure 3.4) and the hydrological parameters were determined at sub-watershed level.

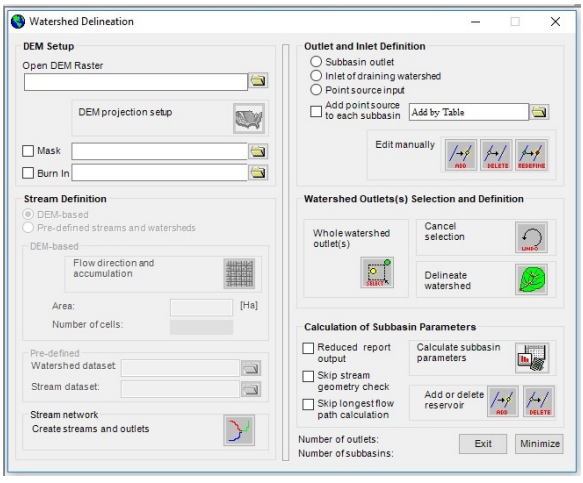

Figure 3.3. The interface of Watershed Delineator command that allows watershed, streams and flow directions definition.

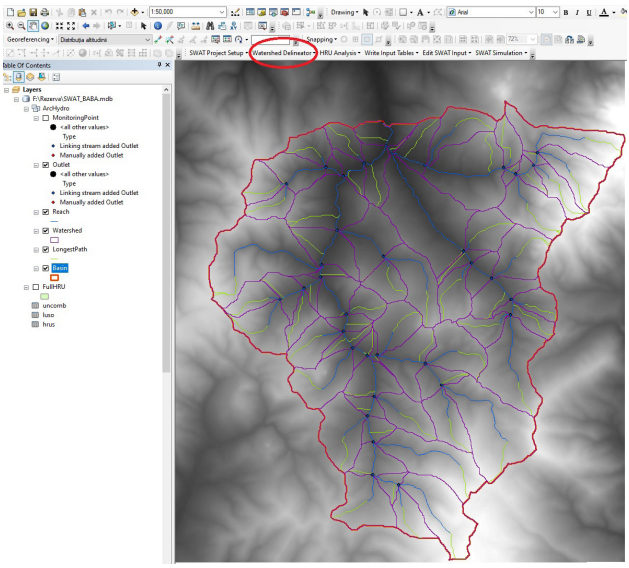

Figure 3.4. DEM, streams and flow directions defined for Upper Tărlung watershed, after performing the Watershed Delineator command.

Subsequently, the streams and flow directions were obtained and the watershed was divided into 69 sub-watersheds and 1001 HRUs (Figure 3.5). With green is represented the study area corresponding to the computing section manually positioned in the sub-watershed number 5 (highlighted by the yellow colour) and represents the area for which the calibration and validation were performed.

HRUs were defined through the HRU Analysis command that allows loading into ArcGIS the databases on land use, soil properties, characteristics, and slopes. Finally, was obtained the distribution of soils and land use at the watershed level (Figure 3.6). For each parameter's (land use, soil and slope), the model allows setting a threshold representing a certain percentage of its surface; this threshold enables the SWAT model to remove and redistribute land use with lowest area at the sub-watersheds level (Winchell et al., 2013). For this study, we adopted a 5% threshold (Figure 3.7).

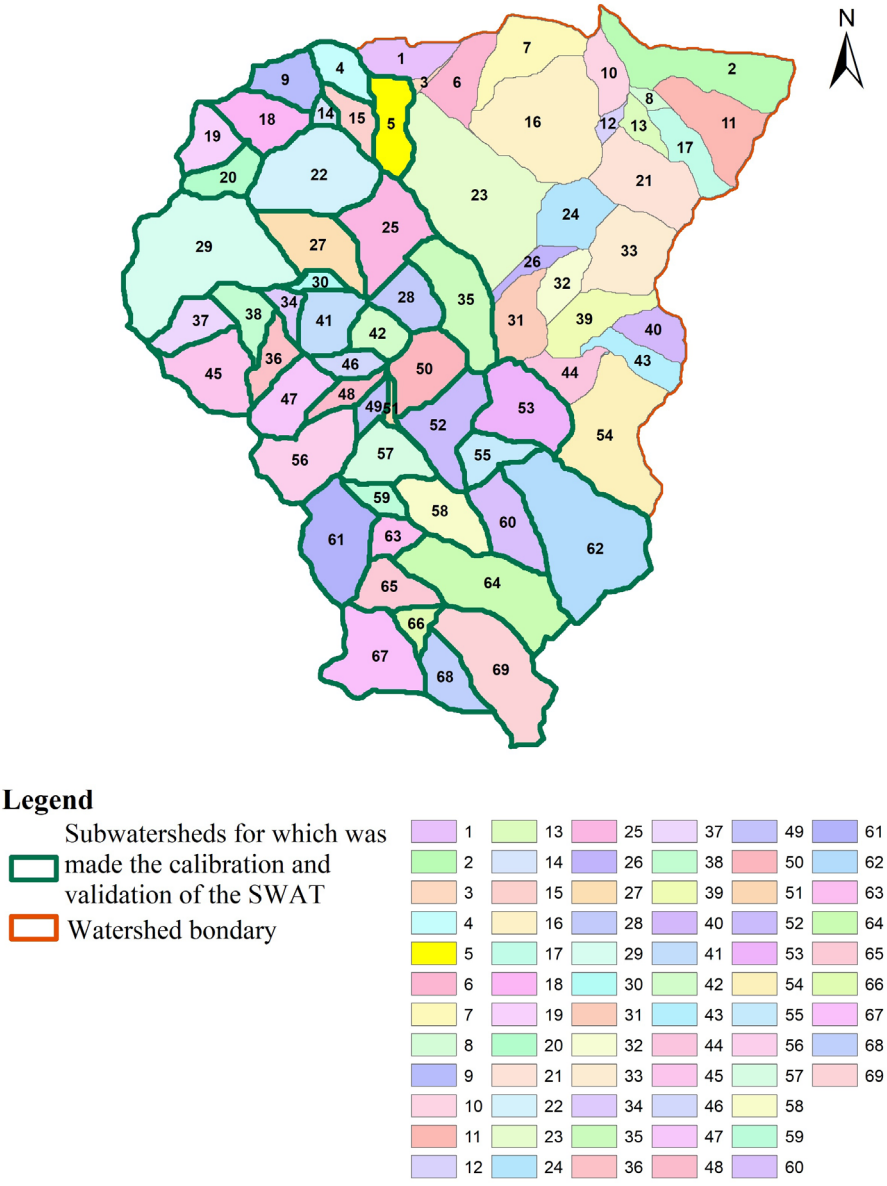

Figure 3.5. Watershed delineation into sub-watersheds, after performing the Watershed Delineator command.

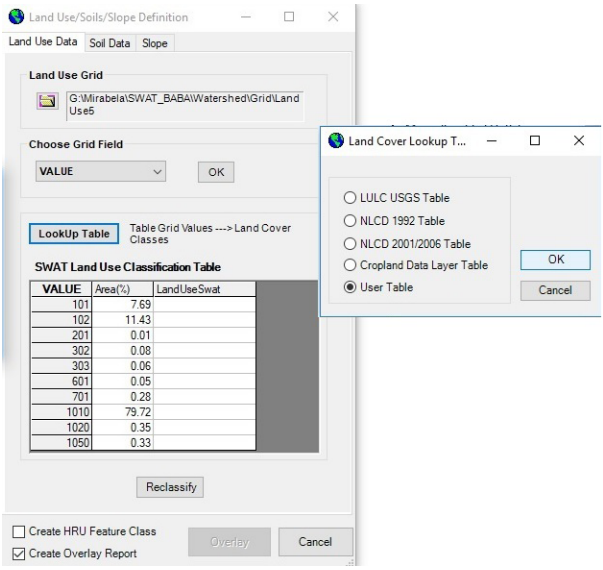

Figure 3.6. HRU Analysis command that allows the watershed definition according to land use, soil, and slope categories.

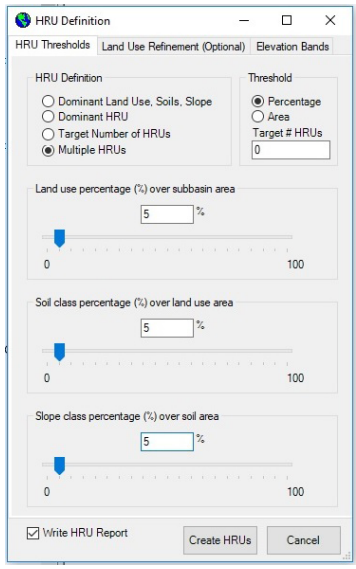

Figure 3.7. Definition by HRU Analysis command of the threshold for land use, soil and slope categories.

The ArcSWAT database regarding the sub-watersheds properties and characteristics is presented in the following figure (Figure 3.8).

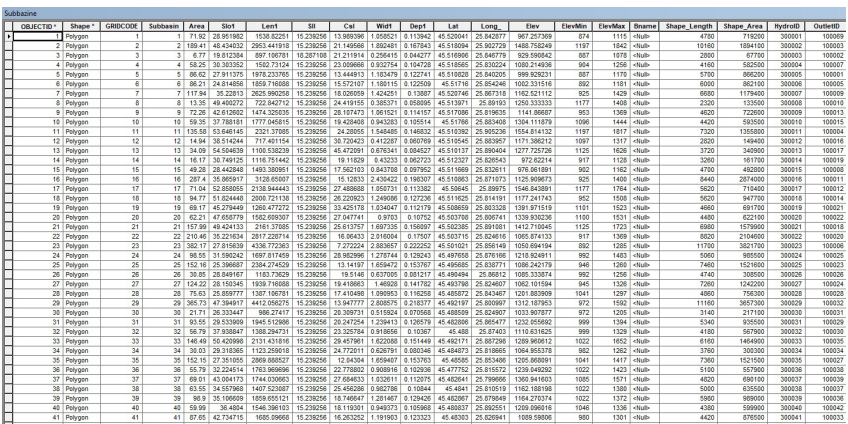

Figure 3.8. Geomorphological characteristics database of the sub-watersheds delineated within studied watershed.

3.1.2. Weather database

For building the weather database were used two points spatially distributed at the watershed level namely ROCADA for air temperature, precipitations, wind speed, solar radiation and relative humidity and INHGA for air temperature and precipitation. These data were uptake from the CLISWELN project (Tudose et al., 2018). The climate datasets from ROCADA V1.0 are available for the 1961–2013 period and are provided at 0.1° spatial resolution (Dumitrescu and Bîrsan, 2015). The climate datasets provided by INHGA cover the 1988–2010 period but the recorded data were inconsistent. Alongside climate data, records of water discharge provided by INHGA were also used. These data were recorded at two hydrometric stations surrounding the case study area (namely Babarunca and Săcele reservoir) and are available for the 1974–2015 period.

After creating the weather databases for each parameter (Figure 3.9) these were individually fed into ArcGIS, and used into simulations. For exemplification, the process of uploading the precipitation and solar radiation databases is presented in Figures 3.10 and 3.11.

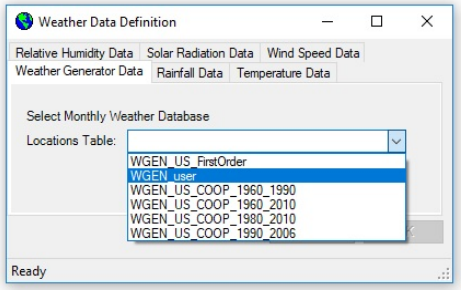

Figure 3.9. Uploading the weather database (WGEN_user).

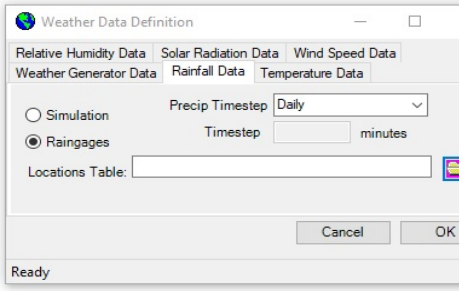

Figure 3.10. Uploading the precipitation database.

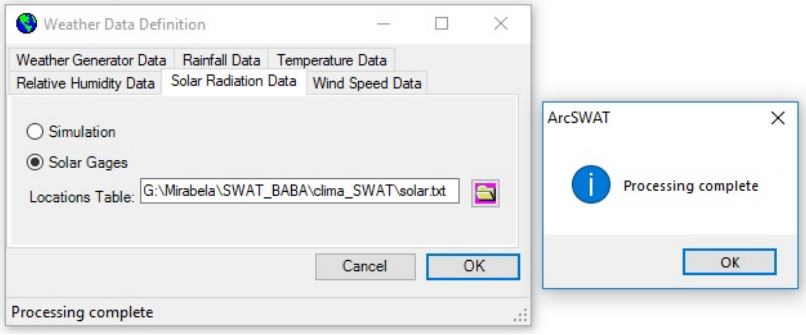

Figure 3.11. Uploading the solar radiation database and the process success confirmation.

3.1.3. Soil database

As alluded above, for developing the soil database, the Forest management plan and Forest-pastoral management plan developed by INCDS for the 1989–2013 period were used. Data regarding the properties and characteristics of soils (e.g., organic matter, clay, dust, sand, etc.), available at compartment level unit were uptake from the soil profile analysis of the aforementioned management plans.

However, the soil database request also some parameters (such as bulk density–SOL_BD, hydraulic conductivity–SOL_K, water content–SOL_AWC) for which data from measurements or analysis bulletins are not available. Therefore, we proceeded similarly to the CLISWELN project (Tudose et al., 2018), and we use open-source SPAW software, downloaded from the official USDA website (https://www.nrcs.usda.gov/wps/portal/nrcs/ detailfull/national/?&cid=stelprdb1045331).

Therefore, the first step was setting the measurement unit (Figure 3.12) and the soil equation (Figure 3.13), actions highlighted by the red border.

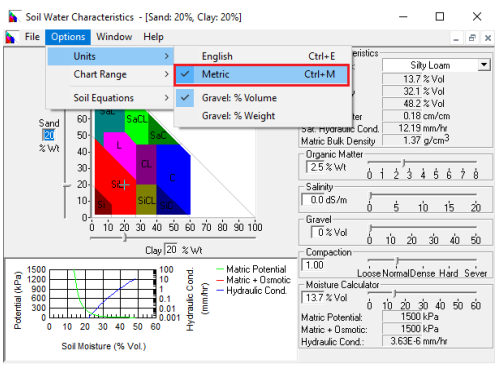

Figure 3.12. Defining the measurement unit in the SPAW program interface.

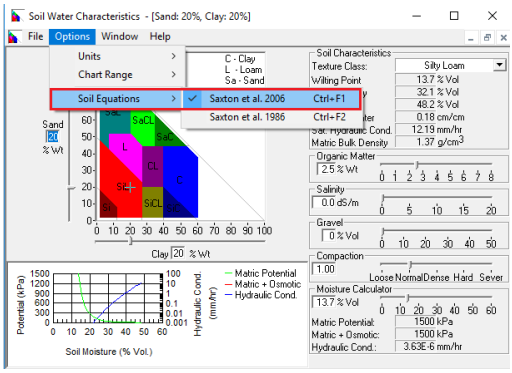

Figure 3.13. Defining the soil equation in the SPAW program interface.

Second, we introduced both the organic matter content and the percentage of sand and clay (Figure 3.14), for computing the bulk density, hydraulic conductivity and water content; the values corresponding to each parameter are delivered automatically as is highlighted in Figure 3.15 by the red border.

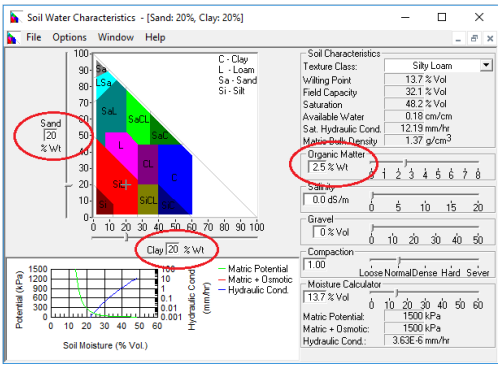

Figure 3.14. Defining the sand, clay and organic matter percentage in the SPAW program interface.

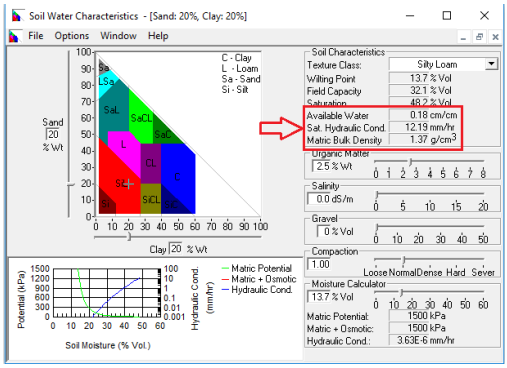

Figure 3.15. Parameters determined using the SPAW program.

Additionally, were requested other parameters such as soil albedo (SOL_ALB), soil erodibility factor (K_USLE) and hydrological group (HYDGRP), which were computed using the equations recommended by Williams (1995) in Neitsch et al., 2011.

Thus, the soil albedo was computed for each soil layer, according to certain coefficients as is presented in the following equation. The value of the soil layer colour was extracted from the Soil manual (Late, 1997; Spârchez et al., 2011):

$$Sol_{Alb} = 0.069 * (soil\ layer\ value) - 0.114$$

Next, the soil erodibility factor was determined also at soil layer level using the next equation:

$$K_{USLE} = f_{csand} * f_{cl\text{-}si} * f_{orgc} * f_{hisand}$$

where:

f_{csand} = factor that give low soil erodibility value for soils with high coarse sand amount

$f_{(cl\text{-}si)}$ = factor that give soil erodibility value for soils with high clay to silt amount

f_{orgc} = factor that reduces the soil erodibility for soil with high organic carbon amount

f_{hisand} = factor that reduces the soil erodibility for soil with extremely high sand amount

These parameters were computed using the following equations:

$$f_{csand} = (0.2 + 0.3 * \exp(-0.256 * m_s * \left(1 - \frac{m_{silt}}{100}\right)$$

$$f_{cl-si} = \left(\frac{m_{silt}}{m_c + m_{silt}}\right)^{0.3}$$

$$f_{orgc} = \left(1 - \frac{0.0256 * orgC}{orgC + \exp\left(-5.51 + 22.9 * \left(1 - \frac{m_s}{100}\right)\right)}\right)$$

$$f_{hisand} = \left(1 - \frac{0.7 * \left(1 - \frac{m_s}{100}\right)}{\left(1 - \frac{m_s}{100}\right) + \exp\left[-5.51 + 22.9 * \left(1 - \frac{m_s}{100}\right)\right]}\right)$$

where: m_s = sand percentage from the total amount; m_{silt} = silt percentage from the total amount; m_c = clay percentage from the total; org_C = organic matter percentage for each soil layers from the total amount.

The soil hydrologic group was obtained based on certain parameters such as soil layer depth, percentage of sand, clay and dust for each soil type. Framing in a certain hydrological group (A, B, C or D) was made based on the values of the parameters mentioned above. Finally, the soil types within the watershed were classified into hydrological groups B and C, differentiated according to the drainage and infiltration capacity of the soils. Hydrological group B comprises approximately 91% of existing soils (6,524.27 ha) and has a medium infiltration capacity, with light or medium soil texture (Clinciu, 2001). Hydrological group C, comprising 9% (645.26 ha) of existing soils, is characterized by shallow soils with a low infiltration capacity (Clinciu, 2001). In doing so, the soil database was completed (Figure 3.16), and was obtained the soil types distribution within the Upper Tărlung watershed (Figure 3.17).

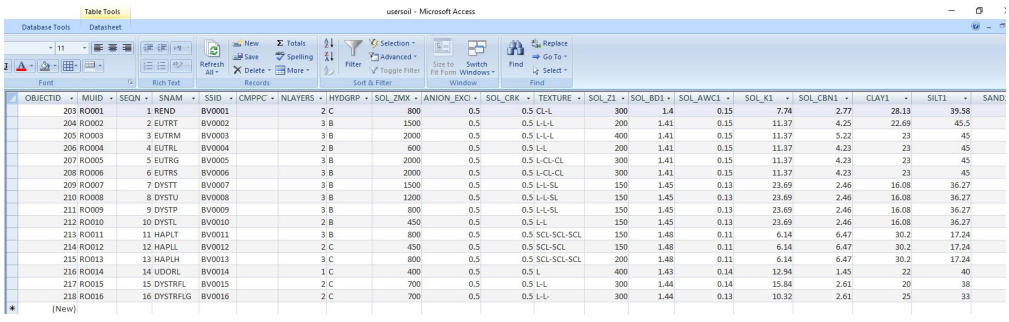

OBJECTID	MUID	SEQN	SNAM	SSID	CMPPC	NLAYERS	HYDGRP	SOL_ZMX	ANION_EXCL	SOL_CRK	TEXTURE	SOL_Z1	SOL_BD1	SOL_AWC1	SOL_K1	SOL_CBN1	CLAY1	SILT1	SAND
203	RO001	1	REND	BV0001		2	C	800	0.5	0.5	CL-L	300	1.4	0.15	7.74	2.77	28.13	39.58	
204	RO002	2	EUTRT	BV0002		3	B	1500	0.5	0.5	L-L	200	1.41	0.15	11.37	4.25	22.69	45.5	
205	RO003	3	EUTRM	BV0003		3	B	2000	0.5	0.5	L-L	400	1.41	0.15	11.37	5.22	23	45	
206	RO004	4	EUTRL	BV0004		2	B	600	0.5	0.5	L-L	200	1.41	0.15	11.37	4.23	23	45	
207	RO005	5	EUTRG	BV0005		3	B	2000	0.5	0.5	L-CL-CL	300	1.41	0.15	11.37	4.23	23	45	
208	RO006	6	EUTRS	BV0006		3	B	2000	0.5	0.5	L-CL-CL	300	1.41	0.15	11.37	4.23	23	45	
209	RO007	7	DYSTT	BV0007		3	B	1500	0.5	0.5	L-L-SL	150	1.45	0.13	23.69	2.46	16.08	36.27	
210	RO008	8	DYSTU	BV0008		3	B	1200	0.5	0.5	L-L-SL	150	1.45	0.13	23.69	2.46	16.08	36.27	
211	RO009	9	DYSTP	BV0009		3	B	800	0.5	0.5	L-L-SL	150	1.45	0.13	23.69	2.46	16.08	36.27	
212	RO010	10	DYSTL	BV0010		2	B	450	0.5	0.5	L-L	150	1.45	0.13	23.69	2.46	16.08	36.27	
213	RO011	11	HAPLT	BV0011		3	B	800	0.5	0.5	SCL-SCL-SCL	150	1.48	0.11	6.14	6.47	30.2	17.24	
214	RO012	12	HAPLL	BV0012		2	C	450	0.5	0.5	SCL-SCL	150	1.48	0.11	6.14	6.47	30.2	17.24	
215	RO013	13	HAPLH	BV0013		3	C	800	0.5	0.5	SCL-SCL-SCL	200	1.48	0.11	6.14	6.47	30.2	17.24	
216	RO014	14	UDORL	BV0014		1	C	400	0.5	0.5	L	400	1.43	0.14	12.94	1.45	22	40	
217	RO015	15	DYSTRFL	BV0015		2	C	700	0.5	0.5	L-L	300	1.44	0.14	15.84	2.61	20	38	
218	RO016	16	DYSTRFLG	BV0016		2	C	700	0.5	0.5	L-L-	300	1.44	0.13	10.32	2.61	25	33	
*	(New)																		

Figure 3.16. Soil database for the Upper Tărlung watershed.

The main soil types identified in the watershed, the corresponding SWAT codes and the area covered by each soil type are given in Table 3.1.

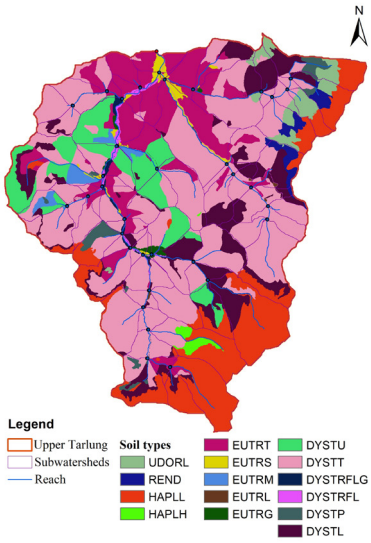

Figure 3.17. Spatial distribution of soil types within the studied watershed.

Table 3.1. Soil types, SWAT codes and the area covered by each soil type in the studied watershed.

Soil type	Soil name	SWAT code	Area covered	
			ha	%
REND	Rendolls	RO001	89.80	1
EUTRT	Eutric Cambisols typic	RO002	1005.97	14
EUTRM	Eutric Cambisols mollic	RO003	80.69	1
EUTRL	Eutric Cambisols lithic	RO004	1.51	0
EUTRG	Eutric Cambisols gleyc	RO005	8.15	0
EUTRS	Eutric Cambisols stagnic	RO006	34.94	1
DYSTT	Dystric Cambosols typic	RO007	3128.14	44
DYSTU	Dystric Cambosols umbric	RO008	576.17	8
DYSTP	Dystric Cambosols prespodic	RO009	87.54	1
DYSTL	Dystric Cambosols lithic	RO010	810.60	11
HAPLL	Prepodzol lithic	RO012	1095.04	15
HAPLH	Prepodzol histic	RO013	40.37	1
UDORL	Litosol	RO014	165.68	2
DYSTRFL	Aluviosol dystric	RO015	29.00	1
DYSTRFLG	Aluviosol gleyc	RO016	15.91	0
	Total		**7169.53**	**100**

Most of the soil types identified are included in the Cambisols class, respectively Eutric Cambisols and Dystric Cambosols with different subtypes founded on 80% of the watershed area. The next dominant soil class are the Spodisols (Prepodzol occupy 16%, Protisols and Cernisols classes founded on 3% and 1% respectively from the watershed area (Figure 3.18).

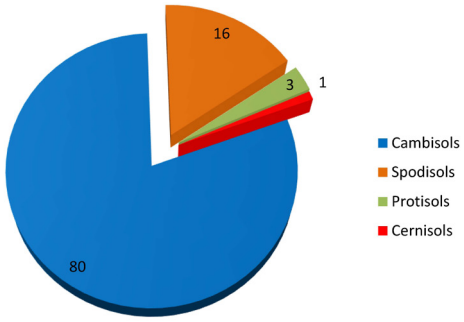

Figure 3.18. The proportion of soil classes (%) identified within the Upper Tărlung watershed.

3.1.4. Land use database

For building the land use database, the necessary data were extracted from the same management plans used for the soil database. In addition, were analysed satellite images of the region for completing the database with new layers for roads and buildings. Subsequently, the correspondence between the land use types identified and the specific types defined in ArcSWAT was made. In doing so, we obtained the distribution of the land use at the compartment level, for each sub-watershed and also for the entire watershed (Table 3.2, Figure 3.19).

Table 3.2. Land use categories, SWAT code and the proportion covered by each land use within the watershed.

No.	Land use code	Name	SWAT code	Area covered	
				ha	%
1	FRSE	Forest evergreen	101	2178.59	31
2	FRSD	Forest deciduous	102	3619.25	50
3	PAST	Pastures	1010	1333.76	19
5	RNGB	Pasture with scattered trees	1020	13.40	0
6	RNGE	Meadows	1050	24.53	0
		Total		**7169.53**	**100**

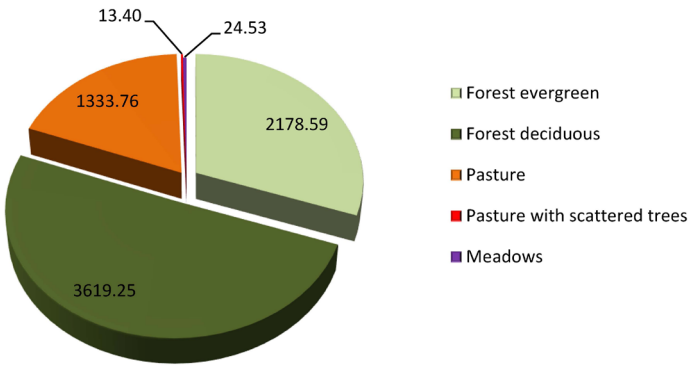

Figure 3.19. The proportion of land use categories (ha) in the studied watershed.

3.2. Run the SWAT model

After filling the required databases, the model was run for 10 years (1979–1988) at monthly basis. Previously, we set a 5-year threshold (1974–1788) necessary for 'warm-up' the model. This interval was not taken into account when running the model but is necessary for stabilizing the calibration process (Figure 3.20). The SWAT model was run for the entire area of the watershed under study.

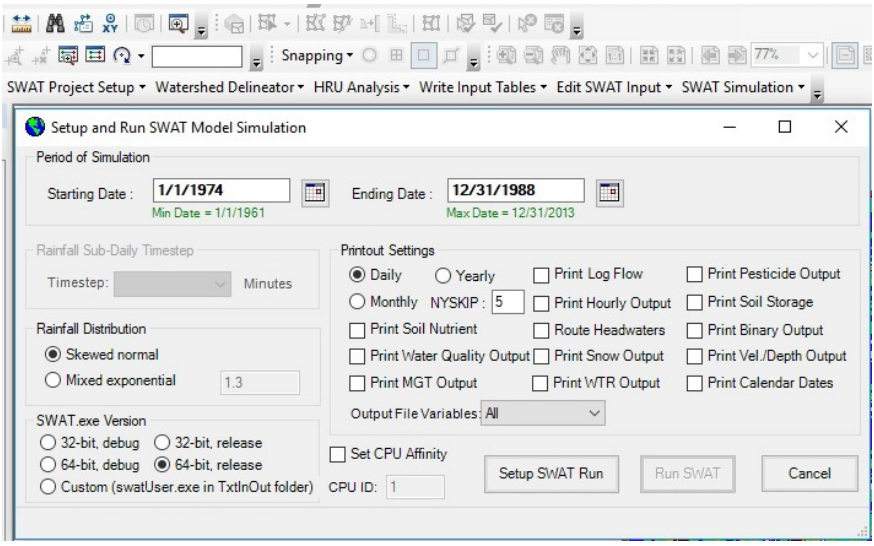

Figure 3.20. SWAT Model Simulation command interface that allows setting the simulations interval, the time step and the 'warm-up' period.

Consequently, the water discharge and other parameters were determined at the sub-watershed level (Figure 3.21).

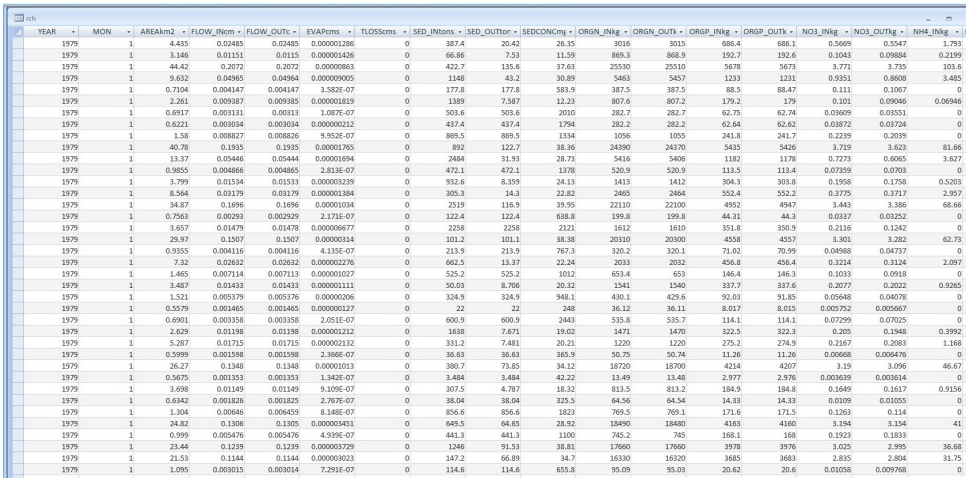

YEAR	MON	AREAkm2	FLOW_INcm	FLOW_OUTc	EVAPcms	TLOSScms	SED_INtons	SED_OUTtor	SEDCONCmg	ORGN_INkg	ORGN_OUTk	ORGP_INkg	ORGP_OUTk	NO3_INkg	NO3_OUTkg	NH4_INkg
1979	1	4.435	0.02485	0.02485	0.000001286	0	387.4	20.42	26.35	3016	3015	686.4	686.1	0.5669	0.5547	1.793
1979	1	3.146	0.01151	0.0115	0.000001426	0	66.86	7.53	11.59	869.3	868.9	192.7	192.6	0.1043	0.09884	0.2199
1979	1	44.42	0.2072	0.2072	0.00000863	0	422.7	135.6	37.63	25530	25510	5678	5673	3.771	3.735	103.6
1979	1	9.632	0.04965	0.04964	0.000009005	0	1148	43.2	30.89	5463	5457	1233	1231	0.9351	0.8608	3.485
1979	1	0.7104	0.004147	0.004147	3.582E-07	0	177.8	177.8	583.9	387.5	387.5	88.5	88.47	0.111	0.1067	0
1979	1	2.261	0.009387	0.009385	0.000001819	0	1389	7.587	12.23	807.6	807.2	179.2	179	0.101	0.09046	0.06946
1979	1	0.6917	0.003131	0.00313	1.087E-07	0	503.6	503.6	2010	282.7	282.7	62.75	62.74	0.03609	0.03551	0
1979	1	0.6221	0.003034	0.003034	0.000000212	0	437.4	437.4	1794	282.2	282.2	62.64	62.62	0.03872	0.03724	0
1979	1	1.58	0.008827	0.008826	9.952E-07	0	869.5	869.5	1334	1056	1055	241.8	241.7	0.2239	0.2039	0
1979	1	40.78	0.1935	0.1935	0.00001765	0	892	122.7	38.36	24390	24370	5435	5426	3.719	3.623	81.66
1979	1	13.37	0.05446	0.05444	0.00001694	0	2484	31.93	28.73	5416	5406	1182	1178	0.7273	0.6065	3.627
1979	1	0.9855	0.004866	0.004865	2.813E-07	0	472.1	472.1	1378	520.9	520.9	113.5	113.4	0.07359	0.0703	0
1979	1	3.799	0.01534	0.01533	0.000003239	0	932.6	8.359	24.13	1413	1412	304.3	303.8	0.1958	0.1758	0.5203
1979	1	8.564	0.03179	0.03179	0.000001384	0	305.3	14.3	22.82	2465	2464	552.4	552.2	0.3775	0.3717	2.957
1979	1	34.87	0.1696	0.1696	0.00001034	0	2519	116.9	39.95	22110	22100	4952	4947	3.443	3.386	68.66
1979	1	0.7563	0.00293	0.002929	2.171E-07	0	122.4	122.4	638.8	199.8	199.8	44.31	44.3	0.0337	0.03252	0
1979	1	3.657	0.01479	0.01478	0.000006677	0	2258	2258	2121	1612	1610	351.8	350.9	0.2116	0.1242	0
1979	1	29.97	0.1507	0.1507	0.00000314	0	101.2	101.1	38.38	20310	20300	4558	4557	3.301	3.282	62.73
1979	1	0.9355	0.004116	0.004116	4.135E-07	0	213.9	213.9	767.3	320.2	320.1	71.02	70.99	0.04988	0.04737	0
1979	1	7.32	0.02632	0.02632	0.000002276	0	662.5	13.37	22.24	2033	2032	456.8	456.4	0.3214	0.3124	2.097
1979	1	1.465	0.007114	0.007113	0.000001027	0	525.2	525.2	1012	653.4	653	146.4	146.3	0.1033	0.0918	0
1979	1	3.487	0.01433	0.01433	0.000001111	0	50.03	8.706	20.32	1541	1540	337.7	337.6	0.2077	0.2022	0.9265
1979	1	1.521	0.005379	0.005376	0.00000206	0	324.9	324.9	948.1	430.1	429.6	92.03	91.85	0.05648	0.04078	0
1979	1	0.5579	0.001465	0.001465	0.000000127	0	22	22	248	36.12	36.11	8.017	8.015	0.005752	0.005667	0
1979	1	0.6901	0.003358	0.003358	2.051E-07	0	600.9	600.9	2443	535.8	535.7	114.1	114.1	0.07299	0.07025	0
1979	1	2.629	0.01198	0.01198	0.000001212	0	1638	7.671	19.02	1471	1470	322.5	322.3	0.205	0.1948	0.3992
1979	1	5.287	0.01715	0.01715	0.000002132	0	331.2	7.481	20.21	1220	1220	275.2	274.9	0.2167	0.2083	1.168
1979	1	0.5999	0.001598	0.001598	2.366E-07	0	36.63	36.63	365.9	50.75	50.74	11.26	11.26	0.00668	0.006476	0
1979	1	26.27	0.1348	0.1348	0.00001013	0	380.7	73.85	34.12	18720	18700	4214	4207	3.19	3.096	46.67
1979	1	0.5675	0.001353	0.001353	1.342E-07	0	3.484	3.484	42.22	13.49	13.48	2.977	2.976	0.003639	0.003614	0
1979	1	3.698	0.01149	0.01149	9.109E-07	0	307.5	4.787	18.32	813.5	813.2	184.9	184.8	0.1649	0.1617	0.9156
1979	1	0.6342	0.001826	0.001825	2.767E-07	0	38.04	38.04	325.5	64.56	64.54	14.33	14.33	0.0109	0.01055	0
1979	1	1.304	0.00646	0.006459	8.148E-07	0	856.6	856.6	1823	769.5	769.1	171.6	171.5	0.1263	0.114	0
1979	1	24.82	0.1306	0.1305	0.000003451	0	649.5	64.65	28.92	18490	18480	4163	4160	3.194	3.154	41
1979	1	0.999	0.005476	0.005476	4.939E-07	0	441.3	441.3	1100	745.2	745	168.1	168	0.1923	0.1833	0
1979	1	23.44	0.1239	0.1239	0.000003729	0	1246	91.53	38.81	17660	17660	3978	3976	3.025	2.995	36.68
1979	1	21.53	0.1144	0.1144	0.000003023	0	147.2	66.89	34.7	16330	16320	3685	3683	2.835	2.804	31.75
1979	1	1.095	0.003015	0.003014	7.291E-07	0	114.6	114.6	655.8	95.09	95.03	20.62	20.6	0.01058	0.009768	0

Figure 3.21. The database obtained after running the model for the 1979–1988 period.

Besides, the measured and simulated water discharge for the 1979–1988 period and the average amounts of precipitation are represented in Figure 3.22 (Marin et al., 2019). It can be noticed that, as other authors states (Arnold et al., 1998; Qiu et al., 2012; Arias et al., 2014; Meaurio et al., 2015; Leta el al., 2016; Briones et al., 2016; Benti Tolera et al., 2018), the SWAT model has certain deficiencies in capturing the water discharge after heavy rainfall events (for example May 1980 and May 1984 when the simulated values were much lower compared with those measured). At the same time, was also noticed that, in some cases, the simulated values were higher than those measured (for example, March 1982, March 1986). Considering that in those months, were recorded low quantities of rainfalls, the higher water discharge values can be attributed to the snowmelt process (Bîrsan et al., 2012), situation that was also mentioned by Abbas et al. (2016).

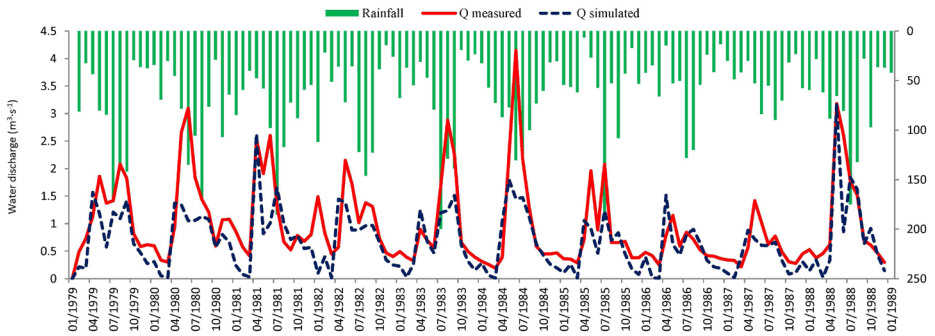

Figure 3.22. Water discharge hydrographs (measured and simulated) and precipitation hietogram for the1979–1988 period.

3.3. SWAT model calibration and validation

After running SWAT, the next step was to perform the sensitivity of analysis. This procedure role is to identify and prioritize the most sensitive parameters in accordance with their influence on hydrological processes (Abbaspour et al., 2017). Similar to the CLISWELN project (Tudose et al., 2018), we used the SWAT–CUP version 2012 program downloaded from the official page of the SWAT model (https://swat.tamu.edu/software/swat- cup /).

SWAT–CUP is open-source software, developed by Abbaspour et al. (2007), which allow users to automatic perform the sensitivity analysis, the calibration-validation stages, and the uncertainty analysis of the model outputs (Abbaspour, 2015). The program is made available for users, along with the ArcSWAT and QGis interface (https://swat.tamu.edu/).

For this procedure were considered 12 parameters (Figure 3.23). The sensitivity degree is highlighted by high values of the t-test and low p-values, where p indicates the degree of sensitivity of the parameters (Emam et al., 2016). After applying the t-test we noticed that the hydrological processes are mostly influenced by parameters that describe the groundwater and lateral flow properties, but also those related to watershed and soil characteristics (GWQMN, ALFA_BF, CN2, LAT_TIME, ESCO, SOL_BD, GW_REVAP, HRU_SLP, SOL_K, SOL_AWC).

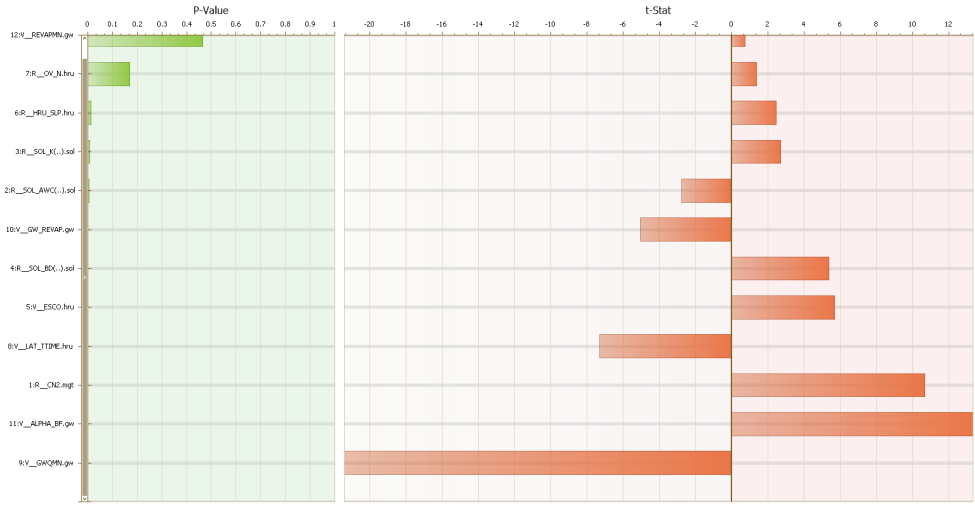

Figure 3.23. Graphical result of sensitivity analysis.

After identifying the parameters with the largest influence on hydrological processes, we proceeded to SWAT model calibration and validation. Both stages were performed in sub-watershed no. 5 (highlighted in Figure 3.5 by yellow colour), which provided the water discharge measurements. The area corresponding to the computing section (manually positioned in sub-watershed no. 5) is 4,586.41 ha, both procedures (calibration, validation) being performed for this area. Calibration and validation of the SWAT model for the entire surface of the studied watershed (7,169.53 ha) could not be performed because the measured data were inconsistent for the computing section related to the Small Branch watershed and no successive period with dry, medium and average rainy years, as is the recommended for the success of the process (Gan et al., 1997; Abbaspour et al., 2007; Moriasi et al., 2007).

Calibration and validation were also carried out using the SWAT–CUP program. To perform these stages, the SWAT–CUP program is foreseen with five different procedures, namely SUFI–2 (Sequential Uncertainty Fitting version 2), PSO (Particle Swarm Optimization), GLUE (Generalized Likelihood Uncertainty Estimation), ParaSol (Parameter Solution) and MCMC (Markov Chain Monte Carlo) (Abbaspour, 2015). For our research, the SUFI–2 procedure was chosen. SUFI-2 is foreseen with different techniques that allow a fast identification (applying a small number of iterations) of the parameters with a large influence on hydrological processes (Yang et al., 2008). Calibration stage aims to minimize the differences between the measured and simulated values (Abbaspour, 2015).

For our research, this stage was performed for ten years (1974–1988), period that included also the 'warm-up' interval (1974–1788) which was not included in the calibration. To obtain the performance level recommended by Moriasi et al. (2007) were performed six iterations with 500 simulations each. The considered parameters for model calibration are presented in Table 3.3. Moreover, to obtain the new parameter values, two methods were applied, namely 'V'-method that consists in replacing the initial value of the existing parameter with a certain value from a default range and 'R'-method in which the initial value of the existing parameter is multiplied by 1+ a certain value from the default range (Abbaspour, 2015).

Table 3.3. Parameters considered for performing the calibration stage, name, range of variation and their fitted value.

No.	Parameter	Definition	Default range		Calibrated value
			minimum	maximum	
1	V__REVAPMN.gw	Threshold depth of water in the shallow aquifer for revap or percolation	0.000000	500.000000	134.500000
2	R__OV_N.hru	Manning's "n" value for overland flow	-0.200000	0.000000	-0.128600
3	R__HRU_SLP.hru	Average slope steepness	0.000000	1.000000	0.613000
4	R__SOL_K(..).sol	Saturated hydraulic conductivity	-0.800000	0.800000	-0.776000
5	R__SOL_AWC(..).sol	Available water capacity of the soil layer	-0.200000	0.100000	-0.119900
6	V__GW_REVAP.gw	Groundwater "revap" coefficient	0.020000	0.200000	0.025580
7	R__SOL_BD(..).sol	Moist bulk density	-0.500000	0.600000	0.312900
8	V__ESCO.hru	Soil evaporation compensation factor	0.000000	1.000000	0.699000
9	V__LAT_TTIME.hru	Lateral flow travel time	0.000000	180.000000	5.940000
10	R__CN2.mgt	SCS runoff curve number	-0.200000	0.200000	-0.016400
11	V__ALPHA_BF.gw	Baseflow alpha factor	0.000000	1.000000	0.931000
12	V__GWQMN.gw	Threshold depth of water in the shallow aquifer for return flow	0.000000	5000.000000	75.000000

Figure 3.24 shows the SWAT–CUP program interfaces when above actions were carried out, while Figure 3.25 presents the SWAT–CUP program during the calibration process.

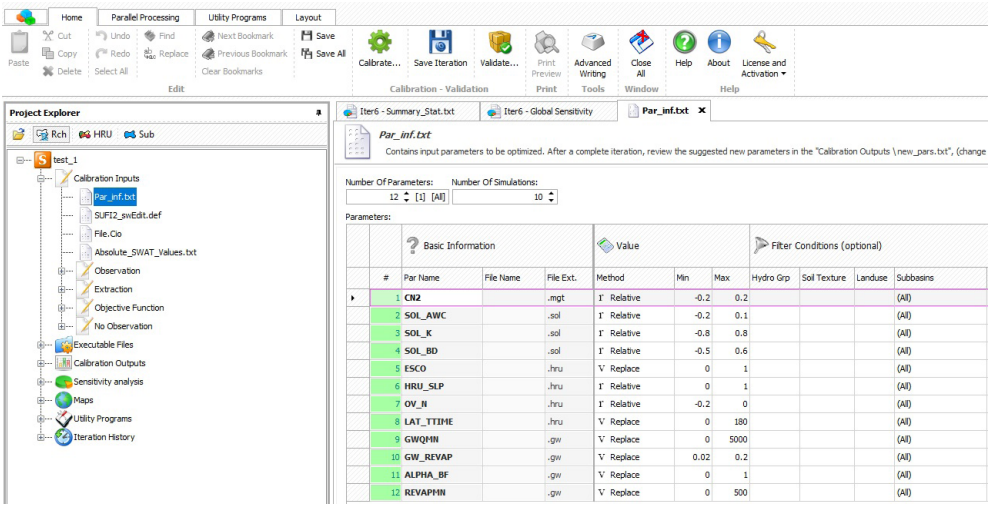

Figure 3.24. SWAT – CUP program interface for selecting and defining parameters considered in the calibration.

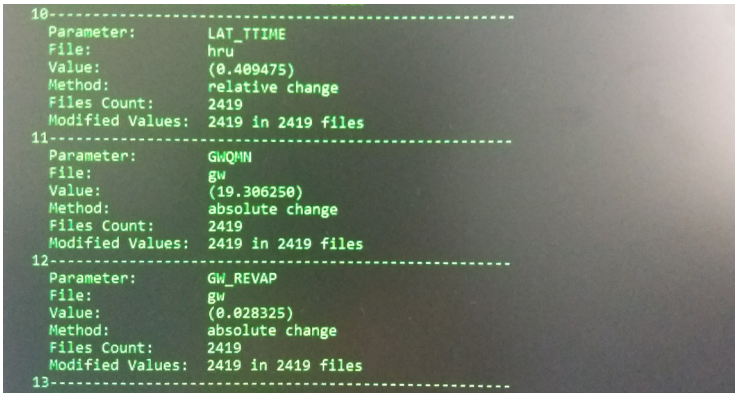

Figure 3.25. SWAT – CUP interface during the calibration process.

For assessing the model performance, the NSE statistical function (Nash and Sutcliffe, 1970) was chosen. This function is frequently used to assess the accuracy of hydrological models in replicating the measured flow values (Moriasi et al., 2007; Jain and Sudheer, 2008). The NSE statistical function can take values from 0 to 1, the closeness of 1 indicating a very good performance of the model (Moriasi et al., 2007). According to the statistical indices related to this function, the model obtained a good performance level (Table 3.4) (Marin et al., 2019).

Table 3.4. The SWAT model performance after performing the calibration-validation stages assessed according to Moriasi et al. (2007).

Stage	Values obtained for the statistical function adopted in the SUFI–2 algorithm					
	NSE	**R^2**	**RSR**	**PBIAS (%)**	***p*- factor**	***r*-factor**
●Calibration (1979-1988)	0.67	0.79	0.57	26.4	0.72	0.91
Performance	Good	Good	Good	Unsatisfactory	Model accepted	
●Validation (2009-2012)	0.65	0.66	0.59	2.1	0.75	1.46
Performance	Good	Good	Good	Very good	Model accepted	

The uncertainty of the model outputs was assessed through p–factor and r–factor and appraised according to Abbaspour (2015). For water discharge, the value of the p–factor is recommended to be higher or equal with 0.7 and the value of r–factor should be less than 1.5 (Abbaspour 2015). The p–factor shows the percentage of measured data enveloped by the 95PPU confidence interval (which can take values between 0 and 1), while the r–factor represents the width of this interval (r <1.5) and shows the dispersion of the measured data around a values considered average value (standard deviation) (Abbaspour, 2015). The values obtained in our research indicate a low degree of uncertainty of the model results. The 95PPU confidence interval obtained after performing the calibration process is represented in Figure 3.26. According to the value obtained for p-factor, 72% of the data are included in this interval, which means that the model is accepted.

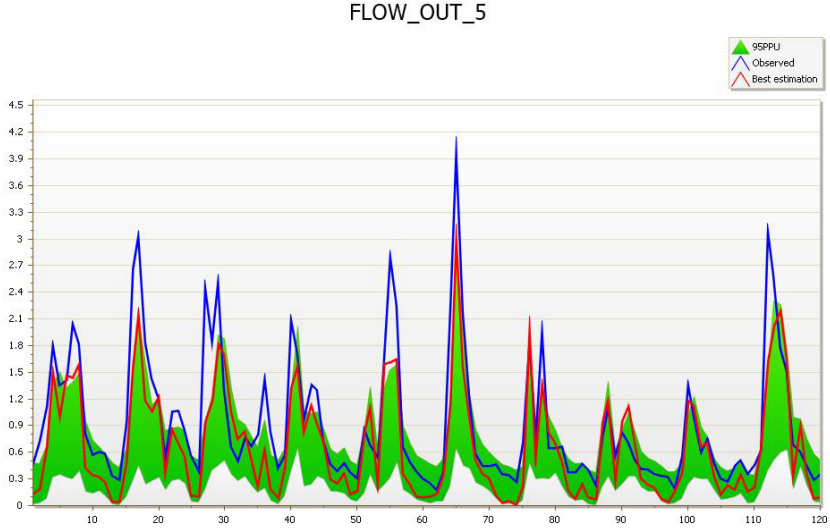

Figure 3.26. The 95PPU confidence interval, measured water discharges and those obtained after calibration stage using the SUFI2 algorithm from the SWAT-CUP program.

Figure 3.27 shows the standard deviation of the parameters considered in calibration. The higher closeness of the values shows a higher sensitivity degree of the parameters (Giurgiu, 1972; Drobot, 1996).

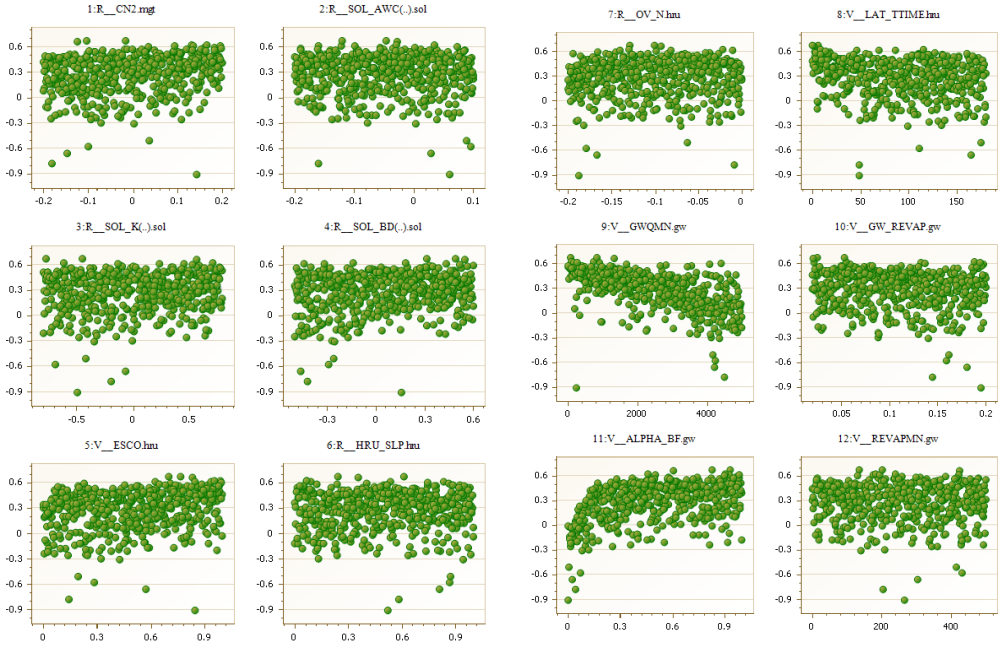

Figure 3.27. The standard deviation obtained for parameters considered in the calibration stage.

The graphical representation of the measured and simulated water discharge after calibration stage for the 1979–1988 period is given in Figure 3.28.

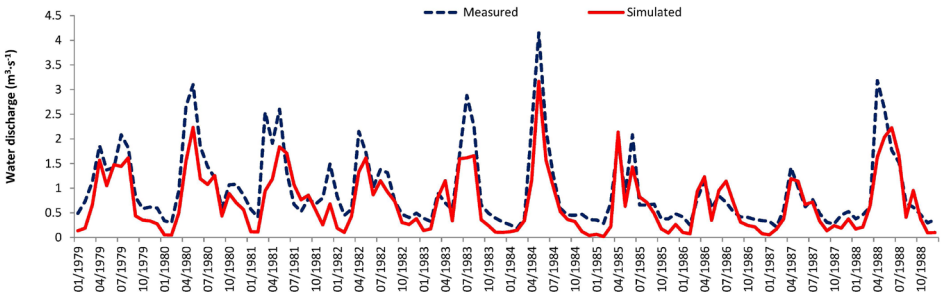

Figure 3.28. Measured and calibrated water discharge hydrograph for the 1979–1988 period.

Validation has the role to certify the results obtained during calibration (Abbaspour, 2015). For this procedure, we have chosen the 2007–2012 period that includes also a two-year interval for model warm-up (2007–2008). A single iteration of 500 simulations was performed. Repeating this step is not recommended because will increase the uncertainty degree of the considered parameters (Abbaspour, 2015; Abbaspour et al., 2017). The results obtained after validation are presented in Table 3.4, and according to Moriasi et al. (2007), those indicate a good model performance in simulating water discharge compared with the measured values which are represented in the next figure (Figure 3.29).

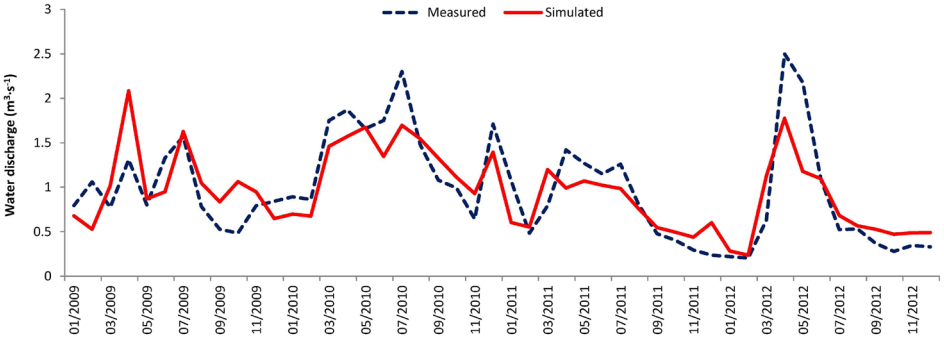

Figure 3.29. The hydrograph of the measured and simulated water discharges after performing the validation stage.

The value dispersion of the considered parameters during validation is represented in Figure 3.30.

The 95PPU confidence interval obtained after the SWAT validation suggests that 75% of the data are within this range, which means that the model can be accepted (Figure 3.31).

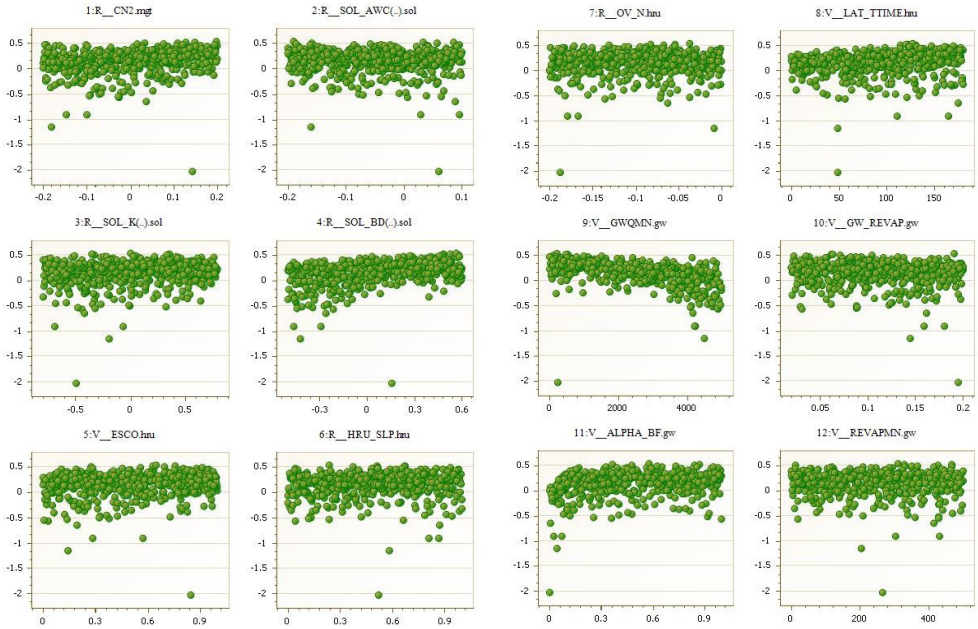

Figure 3.30. The standard deviation obtained for parameters considered in the validation stage.

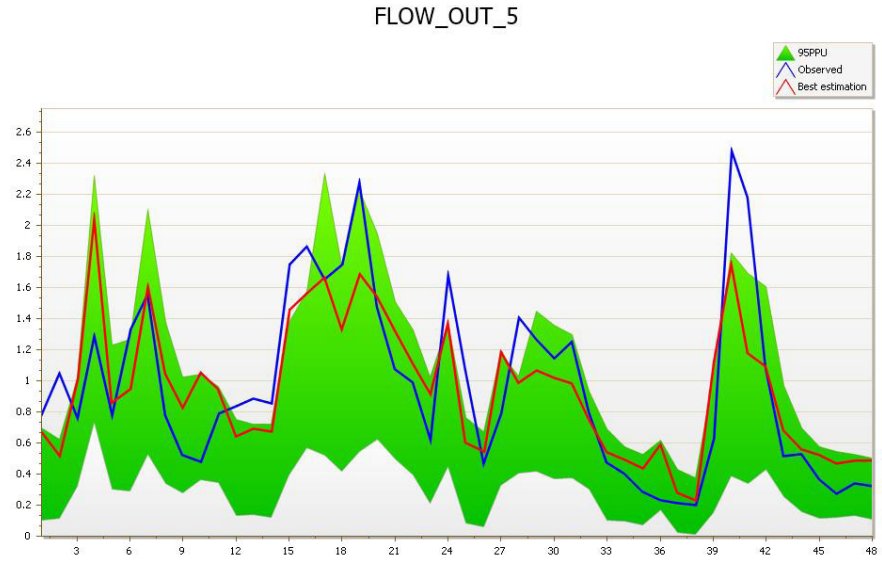

Figure 3.31. The 95PPU confidence interval, measured water discharges and those obtained after validation stage.

3.4. Regional climate scenarios tailored to the local conditions of the study area

According to the above, the assessment of climate change dynamics can be done for different time periods, using the Global Climate Models–GCMs (Flato et al., 2013). The spatial resolution of these models varies between 250–600 km (Benestad et al., 2017) and is too coarse when it used in studies focused on assessing climate change at regional or local level (Busuioc et al., 2010; Benestad et. al., 2017). For accurate assessments, it is necessary to use Regional Climate Models–RCMs, which are derived from the global ones and downscaled at regional or even local scales (Feser et al., 2011; Benestad et al., 2017). Given that RCMs are characterized by spatial resolution between 10 and 50 km (Benestad et al., 2017,) the climate change can be reproduced with higher accuracy (Jacob et al., 2014).

For this research, two GCMs were used (ICHEC-ECEARTH and MPI-ESM-LR), in which the projections of the RCP4.5 and RCP8.5 global climate change scenarios regarding temperature and precipitation were embedded. Subsequently, to obtain a finer spatial resolution that captures with a high accuracy the local conditions of the watershed under study (particularly since it is located in a mountainous area) two RCMs, CCLM4-8-17 and REMO (version 2009), were also used:

• **CCLM4-8-17** is a regional atmospheric model developed by the Climate Limited-Area Modeling Community (CCLMcom) (***, 2019a) and is characterized by a spatial resolution of 12 km (***, 2019b). The model was uptake and improved by Rossy Center, Swedish Meteorological and Hydrological (SHIM)–Sweden;

• **REMO** is a three-dimensional atmosphere model (Gao et al., 2015) characterized by a spatial resolution of 12.5 km (0.11 °) (Jacob et al., 2014; Kotlarski et al., 2014) and used in various research in Europe, America, Africa, etc. (Jacob et al., 2012). The model was uptake by the Max Planck Institute for Meteorology and improved by the Climate Service Center Germany (GERICS).

In choosing these two regional climate models we pursued that the average values of climatic parameters (precipitation) that characterize the models to be as close as possible to the baseline values of the studied region (1961–2013) and uptake from the ROCADA V1.0 project. Further, in order to obtain more accurate climate datasets, the climate parameters were downscaled and bias-corrected at the local level in accordance with the precipitation regime that characterizes the region. The downscales and bias-corrections were made using the Linear Scaling Method (Michelangeli et al., 2009; Gudmundsson et al, 2012; Luo et al.,

2018). Subsequently, we used the climate datasets uptake by the EURO–CORDEX[2], and we considered also the data recorded at surrounding weather stations (e.g., Predeal, Întorsura Buzăului and Ghimbav). Finally, we obtained four regional climate scenarios adjusted at the local level (Table 3.5), which were subsequently adopted in present research (Marin et al., 2020a).

Table 3.5. Regional climate scenarios downscaled at the local level and used in SWAT simulations.

Global climate model	Spatial resolution	Global climate change scenario	Regional climate model	Institution	Regional climate scenarios downscaled at the local level	Period used in simulations
MPI-ESM-LR	0,11°	RCP4.5	REMO2009	Max Planck Institute for Meteorology	REMO4.5 REMO8.5	2011–2100
ICHEC-EC-EARTH	0,11°	RCP8.5	CCLM4-8-17	Climate Limited-Area Modelling Community	CLM4.5 CLM8.5	

The future climate projections of the four local climate change scenarios were obtained by accessing the Earth System Grid Federation – ESGF server, hosted by the German Climate Computing Centre – DKRZ (https://esgfdata.dkrz.de/search/cordex-dkrz/). The work steps followed are presented in Figure 3.32, while the simplified scheme of the methodology is shown in Figure 3.33 (Marin et al., 2020a).

2 EURO-CORDEX is part of the CORDEX (Coordinated Regional Climate Downscaling Experiment) international program, that characterizes the region of Europe (***, 2019d). Designed in 2009 by the World Climate Research Program (WCRP), CORDEX comprises 14 regions of the globe, including Europe (EURO-CORDEX) (***, 2019c).

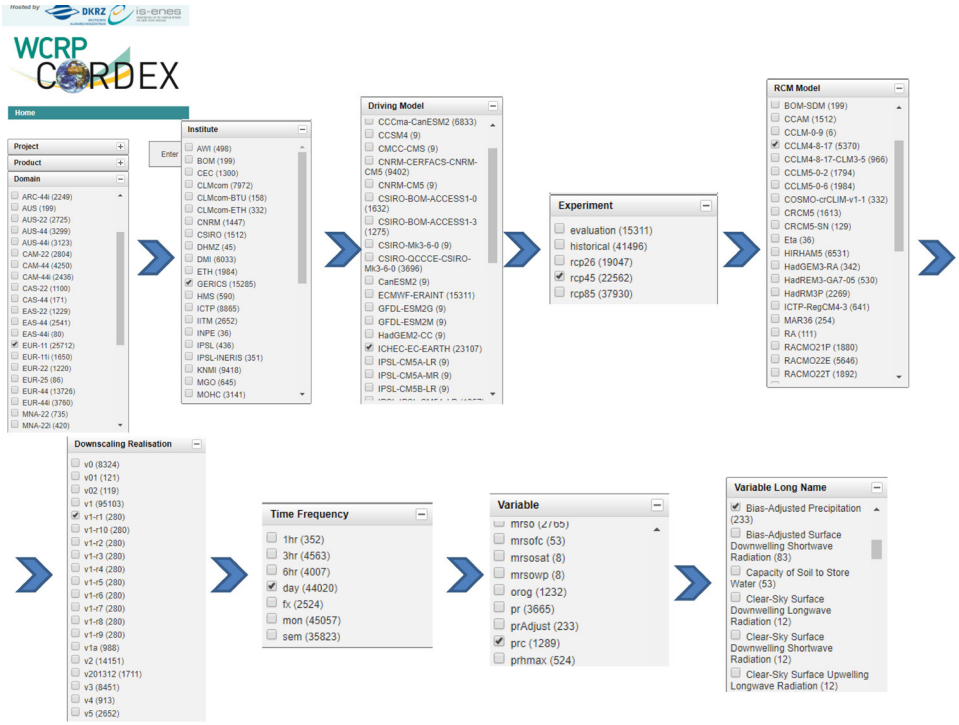

Figure 3.32. Selecting the climate variables of interest (precipitation) according to different climate change scenarios and models.

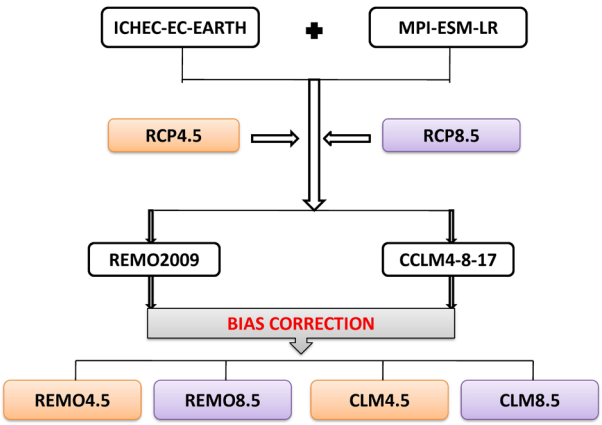

Figure 3.33. The process diagram of conceiving the local climate scenarios.

The average values of the climate parameters that characterize the four local climate change scenarios adopted for performing the simulations are close to the average values uptake from ROCADA (1961–2013). The distribution of the annual precipitation amounts for the aforementioned period is shown in the figure below (Figure 3.34). The multiannual average of precipitation estimated in ROCADA is 881.85 mm. The maximum average annual precipitation value of 1,226.68 mm was recorded in 2005, while the minimum value of 559.13 mm corresponds to the 2000 year. For the present study, the 1979–1988 period was chosen as baseline. For this period, besides the fact that there were recorded continuous measurements of water discharge at Babarunca station (located upstream of the confluence with Ramura Mică), were identified dry, wet and average rainy, an essential condition recommended by Gan et al. (1997) for obtaining accurate simulation results. The average annual precipitation for the 1979–1988 period was 823.5 mm.

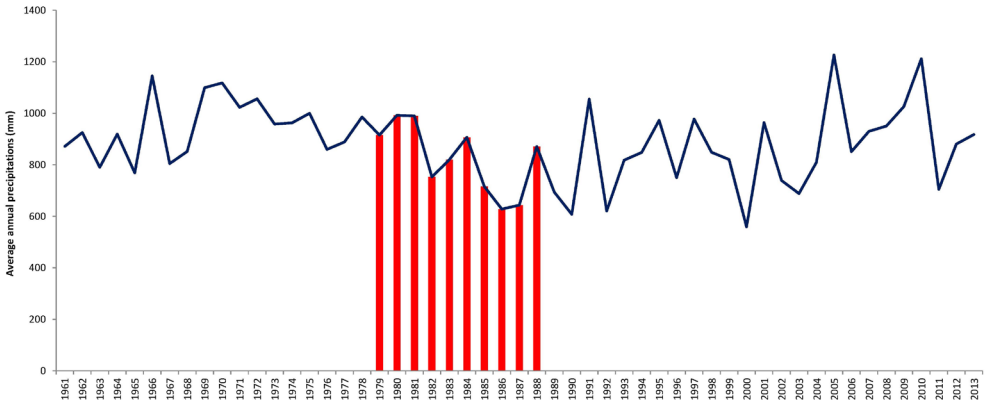

Figure 3.34. The average annual precipitations retrieved from ROCADA dataset for the 1961–2013 period.

The average monthly temperatures for the entire period considered are presented in the following table (Table 3.6). The average temperature for the 1961–2013 period is 2.8 °C.

Table 3.6. The average monthly air temperatures (°C) in ROCADA during the 1961–2013 period

Year	January	February	March	April	May	June	July	August	September	October	November	December
1961	-7.3	-6.0	-1.8	4.6	4.6	10.5	10.6	10.8	7.6	3.9	1.5	-4.6
1962	-4.2	-7.8	-4.1	2.3	7.0	8.7	11.1	13.1	7.5	4.4	2.4	-6.5
1963	-1.5	-62	-5.4	1.4	7.0	10.2	12.8	13.2	9.3	3.4	3.2	-5.1
1964	-8.5	-8.7	-3.9	2.0	4.6	12.1	11.1	10.0	7.1	5.7	-0.7	-1.6
1965	-4.2	-12.0	-2.5	-0.7	5.4	9.7	11.5	9.4	9.4	2.8	-0.6	-2.7
1966	-7.5	-0.7	-3.0	3.6	5.9	7.9	11.6	11.6	7.3	7.9	0.8	-5.0
1967	-9.1	-7.7	-2.7	1.6	6.9	8.6	12.0	11.7	8.7	6.4	0.3	-5.4
1968	-9.2	-3.7	-4.0	4.9	9.4	10.8	10.2	9.9	7.7	3.3	2.0	-5.3
1969	-8.4	-6.0	-5.1	0.0	8.9	8.7	9.5	11.3	7.9	3.7	2.4	-4.5
1970	-5.1	-6.5	-3.4	2.5	4.4	9.2	12.1	10.6	6.7	2.1	1.3	-4.6
1971	-2.3	-6.4	-4.6	1.4	7.7	8.9	10.3	11.9	5.8	2.0	-1.2	-4.3
1972	-7.7	-4.2	-1.2	4.4	6.7	10.7	12.0	10.8	5.4	1.4	-0.5	-3.1
1973	-6.0	-4.9	-5.2	1.7	7.0	9.0	11.1	10.0	9.0	3.5	-4.1	-5.2
1974	-7.2	-3.1	-1.5	-1.0	4.9	8.3	10.5	11.8	8.2	3.5	-1.0	-3.7
1975	-3.9	-8.1	0.4	2.3	7.6	10.6	11.1	10.5	9.2	2.9	-2.5	-4.5
1976	-7.2	-8.0	-5.4	2.2	5.4	7.6	10.6	7.7	6.3	4.5	0.3	-4.9
1977	-4.3	-2.1	-0.3	1.1	6.5	8.6	11.1	10.6	5.4	4.3	0.7	-6.0
1978	-7.0	-4.7	-1.7	0.9	4.4	8.9	9.8	9.1	5.8	3.6	1.1	-4.2
1979	-5.9	-6.0	-0.6	0.5	7.4	11.9	9.3	10.4	8.6	2.5	-0.2	-2.3
1980	-8.8	-6.6	-3.9	0.0	4.5	8.9	10.8	10.0	6.0	5.0	0.2	-4.7
1981	-8.1	-7.1	-0.6	0.3	5.5	11.7	10.4	10.3	8.3	5.4	-3.9	-4.2
1982	-5.9	-8.7	-3.9	-0.5	7.7	9.9	10.0	11.6	10.7	4.9	1.0	-1.9
1983	-4.9	-8.4	-1.5	4.3	7.8	8.8	11.6	10.3	8.2	3.4	-3.2	-3.9
1984	-4.9	-7.3	-5.1	-0.9	7.0	7.9	9.4	9.1	8.6	6.2	-0.3	-5.2
1985	-9.0	-13.4	-3.5	2.3	8.6	8.1	10.7	11.6	6.5	2.3	-1.6	-2.2
1986	-5.9	-8.2	-2.7	4.7	8.3	9.8	10.3	12.7	8.7	3.0	-0.7	-5.4
1987	-8.4	-5.1	-8.7	0.1	5.1	10.4	14.0	9.6	10.1	2.1	-0.2	-4.6
1988	-3.1	-5.4	-3.9	0.4	6.7	9.2	13.8	12.4	7.7	2.5	-5.9	-5.4
1989	-5.2	-3.8	-0.4	5.6	5.4	8.4	11.2	12.3	7.1	3.7	-2.7	-4.1
1990	-5.2	-2.7	1.2	1.7	6.1	9.2	11.6	11.6	5.8	51	1.4	-4.3
1991	-5.7	-8.5	-1.6	0.4	3.4	10.5	12.6	10.6	8.0	3.2	0.9	-7.9
1992	-6.0	-8.0	-3.6	2.4	5.1	9.5	11.3	14.8	6.4	4.0	-1.0	-5.9
1993	-5.8	-9.5	-4.6	0.6	7.3	9.8	11.0	12.0	7.2	6.8	-3.9	-2.6
1994	-2.6	-4.8	-0.9	3.4	6.9	10.0	12.5	12.2	12.0	4.1	-1.2	-4.9
1995	-7.2	-2.5	-2.8	0.8	5.5	10.7	13.0	10.8	6.5	4.7	-3.9	-4.6
1996	-7.4	-7.1	-8.0	0.5	9.2	11.4	11.1	10.9	4.5	3.0	2.4	-3.7
1997	-3.3	-5.9	-4.9	-2.8	7.4	10.5	10.8	10.1	5.9	0.9	0.3	-3.8
1998	-4.6	-3.3	-6.1	3.9	6.0	10.9	12.7	12.4	6.8	5.0	-3.0	-7.4
1999	-3.4	-6.8	-2.5	2.5	6.1	11.6	13.7	12.1	9.0	3.6	-1.1	-3.3
2000	-10.0	-6.1	-3.7	4.0	7.9	10.9	12.4	13.0	7.0	5.5	4.3	-1.2
2001	-4.2	-5.3	0.8	2.2	6.9	8.9	13.4	13.3	7.9	6.3	-2.5	-9.6
2002	-5.3	-1.0	-0.5	1.0	8.5	11.1	13.9	11.1	7.1	4.1	2.4	-6.5
2003	-5.3	-11.0	-5.0	-0.2	11.1	12.1	12.0	13.3	6.8	1.7	1.9	-3.4
2004	-8.2	-6.3	-2.5	2.7	5.4	9.6	12.2	11.4	8.0	5.7	0.3	-2.9
2005	-6.0	-8.2	-5.4	1.9	7.6	8.9	12.0	12.0	8.5	3.4	-1.3	-4.6
2006	-8.3	-7.4	-3.2	2.8	6.4	10.0	12.3	12.0	8.1	5.8	0.3	-2.0
2007	-2.5	-4.1	-0.8	1.8	9.4	12.2	14.9	13.3	6.8	4.5	-2.3	-4.5
2008	-5.3	-4.9	-1.4	2.9	6.8	11.3	12.0	13.7	6.8	5.4	0.7	-3.7
2009	-4.8	-6.3	-3.3	3.6	7.4	11.3	13.0	12.3	8.5	4.6	1.8	-3.2
2010	-7.2	-4.8	-3.0	2.3	7.5	11.4	13.0	14.6	7.8	1.4	4.6	-4.7
2011	-5.5	-6.2	-2.1	1.2	6.7	10.6	13.1	12.7	10.6	2.5	-1.6	-2.8
2012	-8.0	-9.9	-3.0	3.9	8.0	13.2	16.4	13.8	11.2	7.0	2.7	-5.2
2013	-5.6	-4.3	-3.1	4.4	9.3	11.4	12.4	13.6	6.1	5.8	2.5	-2.9

To highlight the seasonal dynamics of average annual temperatures in ROCADA, the data were grouped at ten-year intervals (Figure 3.35). As can be seen, starting with the 1981 year the average annual temperatures during the summer and autumn months are characterized by an increased trend.

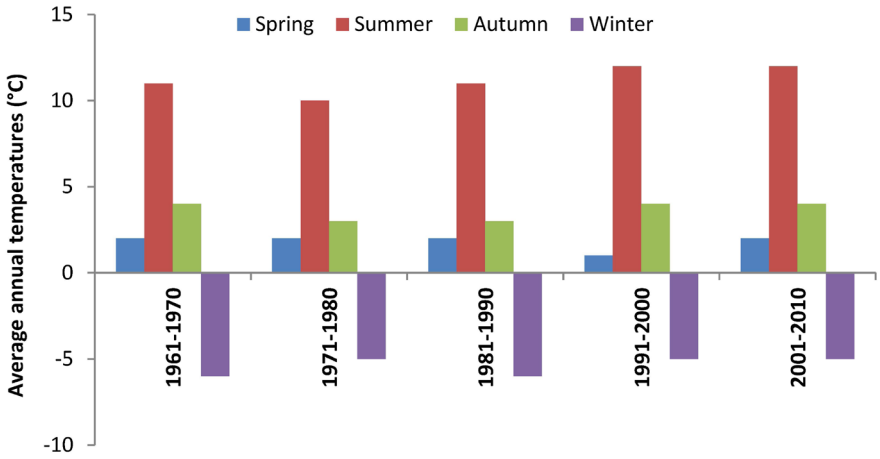

Figure 3.35. Seasonal variation of average annual air temperatures recorded in ROCADA.

From the aforementioned local climate change scenarios, the following parameters were extracted for the region of interest: air temperature, precipitation, solar radiation, relative humidity and wind speed. The datasets were adjusted according to the baseline values (1961–2013). Subsequently, these data were fed into the SWAT database to run the model and perform simulations for the 2011–2100 period. However, in the analysis of climatic conditions, we excluded the 2011–2019 period and we focused only on the future interval, namely 2020–2100 period. In Subchapter 3.1 is given a detailed description of how were built the databases needed to run the SWAT model.

3.5. Precipitation and air temperature projections using local climate change scenarios for the 2020–2100 period

3.5.1. Projections regarding the annual precipitation

The distribution of the average annual precipitation projected within the climate change scenarios compared with the baseline value (ROCADA) is shown in Figure 3.36 (Marin et al., 2020a). It can be seen that, for the following years, the precipitation regime will show both increases and decreases trends (Marin et al., 2020a).

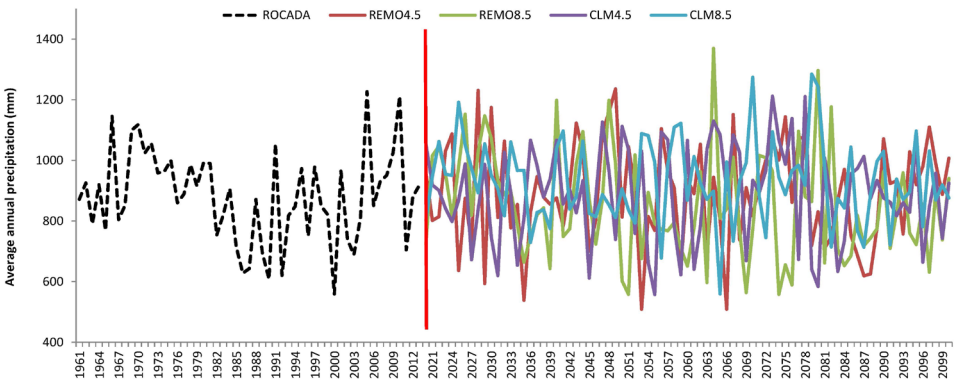

Figure 3.36. Annual precipitation in ROCADA and those projected within the local climate change scenarios considered for the 2020–2100 period.

The multiannual averages of precipitation projected in the climate change scenarios, and those from the baseline period (1961–2013) are given in the following table (Table 3.7).

Table 3.7. The average multiannual precipitation evolution for the 2020–2100 period compared to baseline.

	Average annual precipitation (mm)				
	1961–2013	**2020–2039**	**2040–2069**	**2070–2100**	**2020–2100**
ROCADA	881,85	-	-	-	-
REMO4.5	-	874.30	894.36	899.32	891.30
REMO8.5	-	898.95	846.43	827.34	852.09
CLM4.5	-	874.18	901.83	895.13	892.44
CLM8.5	-	935.97	916.46	937.88	929.47

Data climate dataset from the baseline period (1961–2013) and those projected within the climate change scenarios (2020–2100) was statistically analysed (Table 3.8). If are recorded insignificant differences between the values, then the datasets have small variation (Giurgiu, 1972; Drobot, 1996). The values of the coefficient of variation obtained both for the projected and baseline datasets indicate a small variation between climate change scenarios, due to the fact that the data from each model were previously adjusted in relation to the data from ROCADA.

Table 3.8. Statistical indices of precipitation datasets from the baseline compared to those obtained after downscaling the regional climate scenarios at the local level.

	Precipitation (mm)			Variance	Standard deviation	Coefficient of variation	Standard error
	Medium value	Minimum value	Maximum value				
ROCADA	881.85	559.13	1226.68	23152.92	152.16	17.25	20.90
REMO4.5	889.66	508.73	1235.69	28444.49	168.65	18.92	18.74
REMO8.5	849.33	557.93	1369.65	31653.90	177.92	20.88	19.77
CLM4.5	891.22	557.41	1211.87	25662.71	160.20	17.95	17.80
CLM8.5	934.46	559.16	1284.57	18432.91	135.77	14.61	15.09

The average multiannual precipitation dynamics projected at the seasonal level, both for the baseline and future period, are given in Table 3.9 (Marin et al., 2020a). The '+' and '-' symbols were used to highlighted the modification trend compared with baseline. To emphasize the modification trend, we chose four different colours for each season, namely: red for spring, blue for summer, black for autumn and green for winter.

Table 3.9. Seasonal multiannual average precipitation for the 2020–2100 period compared to the baseline (1961–2013).

	Season	Average multiannual precipitation (mm)				
		1961–2013	2020–2039	2040–2069	2070–2100	2020–2100
ROCADA	Spring	213.5	-	-	-	-
	Summer	351.5	-	-	-	-
	Autumn	164.0	-	-	-	-
	Winter	152.9	-	-	-	-
REMO4.5	Spring	-	209.1 (-)	278.5 (+)	283.9 (+)	263.4 (+)
	Summer	-	206.2 (-)	199.6 (-)	195.2 (-)	199.6 (-)
	Autumn	-	228.8 (+)	185.9 (+)	194.0 (+)	199.6 (+)
	Winter	-	230.2 (+)	230.3 (+)	226.2 (+)	228.7 (+)
REMO8.5	Spring	-	296.4 (+)	264.2 (+)	273.9 (+)	275.9 (+)
	Summer	-	188.5 (-)	187.3 (-)	168.5 (-)	180.4 (-)
	Autumn	-	168.7 (+)	160.5 (-)	174.0 (+)	167.7 (+)
	Winter	-	245.3 (+)	234.5 (+)	211.0 (+)	228.1 (+)
CLM4.5	Spring	-	210.7 (-)	246.2 (+)	239.0 (+)	234.7 (+)
	Summer	-	285.5 (-)	265.1 (-)	255.3 (-)	266.4 (-)
	Autumn	-	171.8 (+)	175.4 (+)	169.8 (+)	172.4 (+)
	Winter	-	206.2 (+)	215.2 (+)	231.0 (+)	219.0 (+)
CLM8.5	Spring	-	231.8 (+)	237.4 (+)	244.9 (+)	238.9 (+)
	Summer	-	290.7 (-)	263.9 (-)	262.2 (-)	269.9 (-)
	Autumn	-	187.5 (+)	158.7 (-)	193.1 (+)	179.0 (+)
	Winter	-	226.0 (+)	256.5 (+)	237.8 (+)	241.8 (+)

3.5.2. Projections regarding air temperature

As is highlighted in Figure 3.37, the baseline (ROCADA) is the 1961–2013 period, while the 2020–2100 period was considered in the local climate change scenarios (Marin et al., 2020a). The multiannual average air temperature of the baseline period is 2.8 °C, while the multiannual average air temperature projected for the 2020–2100 period is 4.8 °C in REMO4.5 and 5.7 °C in REMO8.5. For the CLM4.5 and CLM8.5 scenarios, is projected a multiannual average air temperature of 5.2 °C and 6 °C respectively. Compared to the baseline, we notice a clear increased trend, particularly toward the end of the considered period (Figure 3.37).

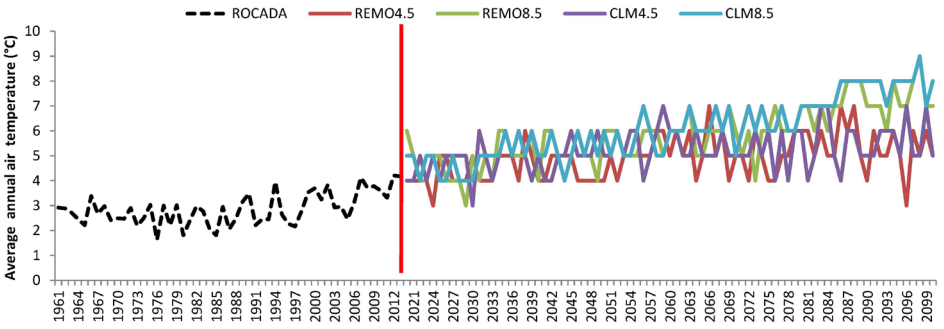

Figure 3.37. Average annual air temperatures recorded in ROCADA and those projected within the local climate change scenarios considered for the 2020−2100 period.

Table 3.10 shows the multiannual average air temperature values for each climate change scenarios divided into three periods compared to the baseline temperatures.

Table 3.10. Multiannual average air temperature (° C) projected for the 2020–2100 period compared to the baseline

	Multiannual average air temperature (°C)				
	1961–2013	**2020–2039**	**2040–2069**	**2070–2100**	**2020–2100**
ROCADA	2.8	-	-	-	-
REMO4.5	-	4.3	4.9	5.2	4.8
REMO8.5	-	4.6	5.4	6.6	5.7
CLM4.5	-	4.9	5.3	5.3	5.2
CLM8.5	-	4.8	5.7	7.1	6.0

The seasonal multiannual averages, both for baseline and future period, are given in Table 3.11 (Marin et al., 2020a). Similar to seasonal multiannual average precipitation, the increased trend was highlighted with '+' symbol while decreased trend with '-' symbol. The same colour palette as for precipitation was used. Hence, it can be seen that three seasons (spring, summer and autumn) are exclusively on the upward trend of air temperature, while one season (winter) is on the downward trend.

Table 3.11. Multiannual seasonal averages (° C) projected for the 2020–2100 period compared to the baseline

		Average multiannual air temperature (°C)				
		1961–2013	**2020–2039**	**2040–2069**	**2070–2100**	**2020–2100**
ROCADA	Spring	1.9	-	-	-	
	Summer	11.1	-	-	-	
	Autumn	3.9	-	-	-	
	Winter	-5.6	-	-	-	
REMO4.5	Spring	-	3.9 (+)	4.0 (+)	4.6 (+)	4.2 (+)
	Summer	-	13.2 (+)	13.8 (+)	13.8 (+)	13.7 (+)
	Autumn	-	4.6 (+)	5.7 (+)	6.0 (+)	5.6 (+)
	Winter	-	-4.5 (-)	-4.1 (-)	-3.7 (-)	-4.0 (-)
REMO8.5	Spring	-	3.7 (+)	4.8 (+)	5.5 (+)	4.8 (+)
	Summer	-	13.5 (+)	14.4 (+)	15.8 (+)	14.7 (+)
	Autumn	-	5.4 (+)	6.3 (+)	7.4 (+)	6.5 (+)
	Winter	-	-4.1 (-)	-3.7 (-)	-2.1 (-)	-3.2 (-)
CLM4.5	Spring	-	3.9 (+)	4.4 (+)	4.7 (+)	4.4 (+)
	Summer	-	12.8 (+)	13.7 (+)	13.8 (+)	13.5 (+)
	Autumn	-	6.2 (+)	6.2 (+)	6.9 (+)	6.5 (+)
	Winter	-	-4.1 (-)	-3.0 (-)	-3.4 (-)	-3.4 (-)
CLM8.5	Spring	-	4.4 (+)	5.1 (+)	6.2 (+)	5.3 (+)
	Summer	-	13.1 (+)	14.2 (+)	15.8 (+)	14.6 (+)
	Autumn	-	5.8 (+)	7.0 (+)	8.1 (+)	7.1 (+)
	Winter	-	-4.2 (-)	-3.4 (-)	-1.6 (-)	-2.9 (-)

The results of statistical analysis performed for both datasets are given in Table 3.12. Similar to precipitation, small differences between coefficients of variation are obtained and this is justified by the fact that the data within each scenario have been adjusted in relation to the data from ROCADA.

Table 3.12 Statistical indices of air temperature data set from the baseline compared to those obtained in the downscaled climate change scenario

	Annual air temperature (°C)						
	Medium value	Minimum value	Maximum value	Variance	Standard deviation	Coefficient of variation	Standard error
ROCADA	2.8	1.6	4.2	0.41	0.64	22.31	0.09
REMO4.5	4.8	3.0	7.0	0.75	0.87	17.68	0.10
REMO8.5	5.6	3.0	9.0	1.41	1.19	20.47	0.13
CLM4.5	5.1	3.0	7.0	0.70	0.84	16.02	0.09
CLM8.5	5.8	3.0	9.0	1.53	1.24	20.43	0.14

3.6. Land use change scenarios

Under the climate change scenarios considered, we pursued to assess the hydrological impact resulted from the application of three land use change scenarios, as follows:

- **Scenario 1**: maintaining the current forested areas (Figure 3.38);
- **Scenario 2**: reducing the forested areas (FRSD and FRSE) by 25% and converting those into the pasture (PAST) (Figure 3.39);
- **Scenario 3**: reducing the forested areas (FRSD and FRSE) by 50% and converting those into the pasture (PAST) (Figure 3.40).

Noteworthy mention that the reduction of forested areas was not made uniformly on the entire surface of the basin, but only for certain forest management compartment and without considering their spatial distribution. The land use change from FRDS and FRSE to PAST has been stopped when the percentages considered in the two hypothetical scenarios were reached. The distribution of land use categories after running the three hypothetical scenarios is presented in Table 3.13.

Table 3.13. Current land use surface and those obtained after applying the forested areas reduction scenarios.

Land use	SWAT code	Initial surface		Reducing the forested areas by 25%		Reducing the forested areas by 50%	
		ha	%	ha	%	ha	%
FRSD	101	3619.25	50	1630.63	23	1098.94	15
FRSE	102	2178.59	31	2703.99	38	1763.01	25
PAST	1010	1333.76	19	2802.07	39	4274.63	60
RNGB	1020	13.40	0	13.28	0	13.28	0
RNGE	1050	24.53	0	19.56	0	19.67	0
TOTAL		**7169.53**	**100**	**7169.53**	**100**	**7169.53**	**100**

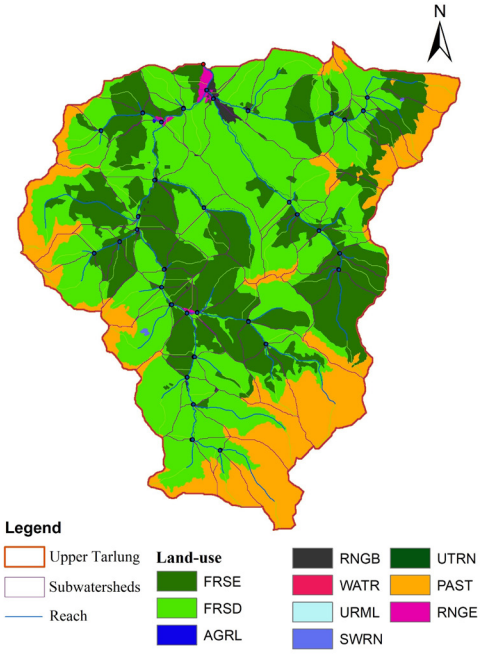

Figure 3.38. Current land use categories in Upper Tărlung watershed (Scenario S1).

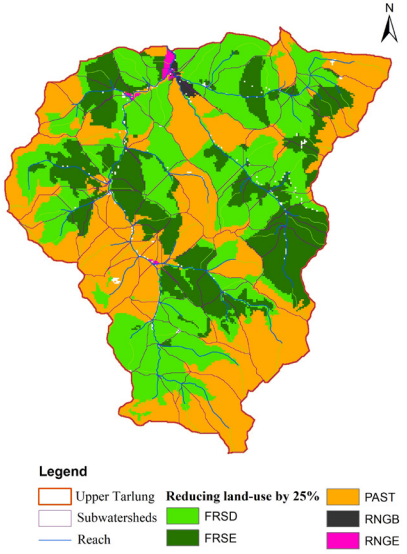

Figure 3.39. The land use categories distribution after reducing forested areas by 25% and converting them into pasture
(Scenario S2).

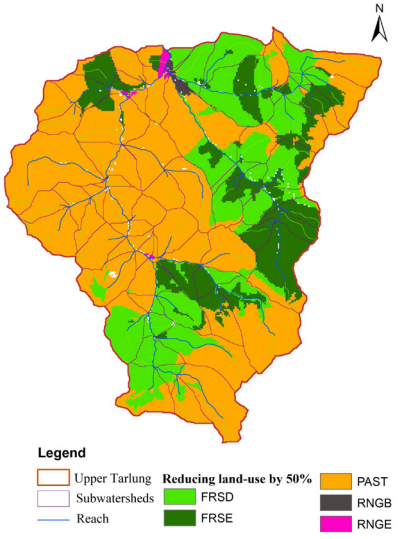

Figure 3.40. The land use categories distribution after reducing forested areas by 50% and converting them into pasture
(Scenario S3)

3.7. Brief summary and conclusions derived from the precipitation and air temperature projections

3.7.1. Predicted trend in precipitation evolution

After applying the local climate change scenarios for the 2020–2100 period, we did not observe major differences in the precipitation dynamics compared with baseline (1961–2013). Analysing the multiannual average of the entire interval we obtain a percentage difference of ±3–5% between projected and baseline value. The most significant precipitation increases and decreases are estimated in scenarios developed from RCP8.5.

In the short term (2020–2039) the multiannual average of precipitation can register both a slight decrease (by 1%) in the scenarios derived from RCP4.5, and an increase by 2%, respectively 6% in the scenarios derived from RCP8.5. At the annual level, is projected that the annual precipitation can record an increase between 20–40%, and also a decrease by 17–39%. The sharpest increases are projected in REMO4.5 and CLM8.5 scenarios, while significant reductions are projected in scenarios derived from RCP4.5. Regarding the seasonal dynamics, is estimated that during spring, precipitation amounts may be reduced by 1–2% in scenarios derived from RCP4.5, or may increase by 9–39% in scenarios derived from RCP8.5. During the summer, precipitation will decrease in all climate change scenarios by 17–46%. The sharpest reductions are projected in REMO4.5 and REMO8.5. In the autumn, compared to the baseline value, the precipitation will increase by 3–40%. During the winter season, the overall trend of precipitation is to increase by up to 60%, particularly in REMO scenarios.

In the medium term (2040–2069) the multiannual average of precipitation will record both increases and decreases by 4%, both trends being projected in the scenarios derived from RCP8.5. At the annual level, average precipitation can increase by up to 55% or can decrease by up to 37%. The precipitation increases will be recorded particularly in REMO scenarios, while the decreases will be more accentuated in scenarios derived from RCP8.5. Regarding seasonal dynamics, during the spring, precipitation can increase by 11–30%, more significant being obtained under REMO scenarios. In the summer season, precipitation will be reduced by up to 47% (REMO8.5) compared to the baseline. In autumn, it is estimated both a slight decrease of precipitation by 2–3% in scenarios derived from RCP8.5, and an increase of 7–13% in those derived from RCP4.5. During the winter, precipitation can intensify by 41–68%, particularly in REMO8.5 and CLM8.5.

In the long term (2070–2100) the multiannual average of precipitation shows a decrease by 6% in REMO8.5, and an increase by 2–6%, the maximum values being projected in CLM8.5. At the annual level, compared with the baseline value, is projected is both an increases by 30–47% and decreases by up to 37% of precipitation. The higher increases were obtained in the scenarios derived from RCP8.5, while the decreases are more significant in CLM4.5 and REMO8.5. At the seasonal level, we noticed an increase by 12–33% of the precipitation projected in the springs, more pronounced values being projected in REMO4.5 and REMO8.5. During summer, precipitation can decrease up to 52%, more pronounced decreases being projected in REMO scenarios. For autumn, a precipitation increases by 4–18% is projected, particularly in REMO4.5 and CLM8.5, while during winter precipitation can increase by 38–55%, the more pronounced values being obtained in CLM scenarios.

3.7.2. Predicted trend in air temperature evolution

In the studied period, the air temperature will be characterized exclusively by an increases trend in all scenarios and period analysed. Compared to the baseline, for the 2020–2100 period, is projected an increase in air temperature between 2–3.2 °C, particularly in scenarios derived from RCP8.5.

In the short term (2020–2039) is projected an increase in the multiannual average air temperature between 1.5–2 °C, particularly in CLM scenarios. The seasonal temperature can increase during spring by 1.8–2.5 °C, the highest values being projected under CLM8.5. In summer, the multiannual average air temperature can increase by 1.7–2.4 °C, maximum values being projected in REMO scenarios. In the autumn months, the temperature can increase up to 2.3 °C, especially in CLM4.5 and CLM8.5. During winter, the multiannual air temperature will increase up to 1.5 °C in CLM4.5 and REMO8.5.

In the medium term (2040–2069) the multiannual average air temperature will increase up to 3 °C compared to the baseline. The sharpest increases are projected in scenarios derived from RCP8.5. At the seasonal level, the air temperature may increase up to 3.2 °C during spring. In summer, increases up to 3.3 °C of are projected. For the autumn months, the projected air temperature show increases between 1.8–3.1 °C. During the winter, the air temperature can increase up to 1.5–2.6 °C compared to the baseline, the maximum values being projected in CLM4.5 and CLM8.5.

In the long term (2070–2100) increases between 2.4–4.3°C of the air temperature are projected, particularly in REMO8.5 and CLM8.5. In spring, the air temperature can increase up to 4.3 °C, while, for the summer months, the increase is between 2.7–4.7 °C. In autumn, a temperature increases of 2.1–4.2 °C is projected. During winter, the average air temperature can increase between 2 °C–4 °C.

4. PROJECTED IMPACT OF CLIMATE CHANGE AND FORESTED AREA REDUCTION SCENARIOS ON HYDROLOGICAL PROCESSES WITHIN THE UPPER TĂRLUNG WATERSHED

4.1. Preliminary aspects

The state-of-art analysis highlights that climate and land use change scenarios influences the hydrological processes within watersheds.

The hydrological impact can be quantitatively evaluated by predicting the short-, medium-, and long-term dynamics of the main hydrological parameters, such as surface runoff, water discharge and sediment yield. The first two parameters define the quantitative aspect of water resources, while the third is important for the qualitative aspect (Marin et al., 2020c).

Using the SWAT hydrological model, we were able to make projections regarding the dynamics of these three hydrological parameters for 2020–2100 (divided into three period). We considered four levels of analysis (monthly, seasonal, annual and multiannual), four climate change scenarios tailored to the local condition, and three land use change scenarios.

As baseline, a 10 years period (1979–1988) was adopted for comparison. The simulated values of hydrological parameters for the 2020–2100 period was structured and analysed compared with the baseline values at monthly, monthly–seasonal and annual level.

The abbreviations used in the subsequent tables have the following meanings:

- **S1–scenario 1:** run the model under preserving current land use and considering only the four climate change scenarios;
- **S2–scenario 2:** run the model under the four climate change scenarios coupled with the reduction by 25% of the forested areas;
- **S3–scenario 3:** run the model under the four climate change scenarios coupled with the reduction by 50% of the forested areas.

It worth mentioning that although for the future torrent control works within the Upper Tărlung watershed the current analysis does not seem to have immediate usefulness, however, this study provides guidance for adapting the future forest and water management plans due to the multiple levels of assessment.

4.2. Surface runoff projected for the 2020–2100 period

4.2.1. Surface runoff in the short term (2020–2039)

4.2.1.1. Monthly surface runoff

Compared to the baseline values, the monthly surface runoff projected for the 2020-2039 period (Table 4.1, Annex 1) shows different trends, both in relation to the climate and land use change scenarios. The monthly projected values show that the largest increases will be recorded in October–February. The surface runoff volume projected for February can increase from 193 thousand cm to 1872 thousand cm, which means a percentage difference of 8.7 times higher compared to the baseline. We believe that this is mainly due to the precipitation and temperature increments by 35–60% and up to 1.5 °C respectively. This favours the occurrence of liquid (and not solid) precipitation, faster snowmelt and more consistent surface runoff. This aspect was also mentioned in other nationwide studies (Diaconu, 1971; Busuioc et al., 2010; Bîrsan et al., 2012). On the other hand, for June–August, there is projected a general decreasing trend of surface runoff, particularly for REMO4.5 and REMO8.5. The larger decreases in surface runoff are projected under the climate change scenarios, while in the land use scenarios the reductions are not so significant. In contrast, the increase in monthly surface runoff is projected to be recorded mainly due to the forested area reduction, particularly under S3 scenario.

Figure 4.1a−d (Annex 1) illustrate the projected monthly surface runoff compared to the baseline, the difference amongst them being expressed in percentage. The results are presented both for climate and land use change scenarios. It can be noticed that the projected monthly surface runoff varies in relation to the scenario applied. The larger increases are projected mainly under land use change scenarios and less due to the changes in climate conditions. The influence of afforestation degree in the surface runoff was also observed by Weber et al. (2001), which states that the conversion of forested areas into pasture will generate increases in surface runoff. The sharpest increases in monthly surface runoff are projected for February in all climate and land use change scenarios. The most pronounced increases, of approximately 9-fold compared with baseline, are projected particularly in CLM4.5 compounded with scenario S3 (Figure 4.1-b, Annex 1). Overall, all climate change scenarios follow the same trend in all land use scenarios considered. However, a different trend can be observed in CLM8.5 (Figure 4.1-d, Annex 1), were for January, unlike the

others scenarios, are projected decreases of this parameter (by 22%, in scenario S1). The same situation was noticed in April–May, when unlike the others scenarios that estimate increases in monthly surface runoff almost 3.4 times higher compared with baseline, in CLM4.5 is projected a decrease by 11–53% of this parameter (Figure 4.1-c, Annex 1).

4.2.1.2. Seasonal surface runoff

During spring months (Table 4.2, Annex 1), compared with baseline, the seasonal surface runoff will increase in all climate change scenarios, particularly in REMO8.5, where the value projected for seasonal surface runoff can reach a maximum of 3278 thousand cm. A different trend was obtained in CLM4.5 compounded with scenario S1, where is estimated both a slight decrease and increases of this parameter. In the summer season, the surface runoff is projected to decrease in all scenarios applied, particularly in REMO4.5 and REMO8.5. Here, the surface runoff can reach a maximum of 211 thousand cm, lower by 49% compared with the baseline value (414 thousand cm). This may be due to the temperatures increases up to 2.5 °C as well as the reduction of precipitation amounts up to 46% estimated for the spring season. During autumn, the surface runoff is projected to increase by 2.5 times fold compared to the baseline. The most significant increases of surface runoff are projected for the winter season, particularly in REMO4.5 and CLM4.5, when seasonal surface runoff can reach a maximum of 1126 thousand cm and 1057 thousand cm respectively.

The seasonal surface runoff dynamics on considered scenarios are highlighted in Figure 4.2a−d (Annex 1). In spring, surface runoff can decrease by 2% (S1) or can increase up to 86% (S3) (Figure 4.2c, Annex 1). In summer, the surface runoff will decrease particularly in REMO8.5/S1, when values lower by 69% are projected (Figure 4.2-c, Annex 1). During autumn, are projected increases between 69% (CLM8.5/S1) and 244% (REMO4.5/S3) (Figure 4.2-d and a, Annex 1). This trend is maintained also in the winter season, where increases of almost 3.2 times fold compared to the baseline are projected especially in scenario S3 (Figure 4.2-b, Annex 1). This situation may be due to the temperature and precipitation increases up to 1.5 °C and 35–60% respectively. It can be noticed that the most important increases of surface runoff are projected in scenario S3, while the decreases are projected particularly in scenario S1. Thus, the land use change has a much greater influence on surface runoff compared to changes in climate conditions.

4.2.1.3. Annual surface runoff

Regarding the annual variation of surface runoff, the values projected for the first analysed period (2020–2039) are given in Table 4.3 (Annex 1). Compared to the baseline, both decreases up to 58% and increases of up to 2.3-fold are projected for surface runoff. If in the scenario S1 the changes are less significant, the scenario S3 instead can generate the most pronounced changes of this parameter. Hence, the surface runoff can increase from 7782 thousand cm to 25357 thousand cm (year 2024/REMO4.5/S3), or it can be reduced up to 3285 thousand cm (year 2035/REMO4.5/S1).

Figure 4.3a-d (Annex 1), shows that the sharpest decrease in this parameter is projected for 2035 (Figure 4.3-a, Annex 1), mainly due to changes in climatic parameters (scenario S1), while the influence of land use scenarios is slightly lower. Instead, the reduction of forested areas (by 25% and 50%, respectively) generates the annual surface runoff increments between 4–226% in all climate change scenarios. The sharpest increases are estimated for 2024 in REMO4.5 (Figure 4.3-a, Annex 1) when, in scenario S1, an increment of surface runoff by 195% is projected. Conversely, in scenarios S2 and S3, the annual surface runoff can increase by 209% and 226% respectively (year 2024). The lowest impact on annual surface runoff is projected in CLM4.5 (Figure 4.3-b, Annex 1), when the surface runoff can increase up to 109% (year 2029/S3) or can decrease up to 43% (year 2030/S1).

On the other hand, if we analyse the multiannual average of the surface runoff for the entire period considered, we notice an overall increment trend of this parameter (Figure 4.4). The most pronounced increases (by 42–87%) are projected in REMO4.5 and REMO8.5. The surface runoff increases are mainly due to land use change (scenarios S2 and S3), and less due to climate change (scenario S1).

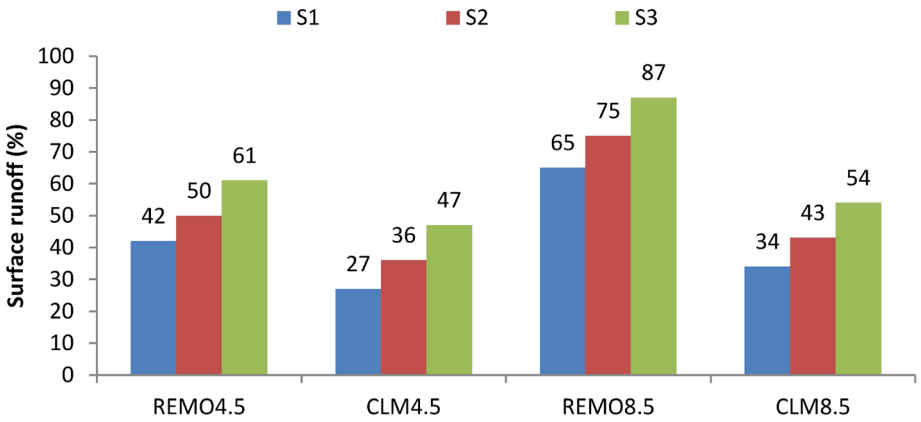

Figure 4.4. Multiannual average of surface runoff (expressed in percentage) projected in all climate and land use change scenarios for the 2020–2039 period.

4.2.2. Surface runoff in the medium term (2040–2069)

4.2.2.1. Monthly surface runoff

The monthly surface runoff projected for the 2040–2069 period is given in Table 4.4 (Annex 1) and compared to the baseline both increases and decreases of this parameter are projected. The largest increases are estimated for December–February, particularly in the land use change scenarios. In February the surface runoff is expected to increase from 193 thousand cm to about 2120 thousand cm, which means a 10-fold increase compared to the baseline. This situation can occur due to the temperatures and precipitation increments up to 1–3 °C and 19–46% respectively which generates faster snowmelt. In June–August, a reduction in surface runoff is expected in all scenarios considered, when the projected monthly values are decreasing up to 65% compared to the baseline. For July on the other hand, is projected a different trend, characterized both by a decrease from a baseline value of 305 thousand cm (baseline value) to 67 thousand cm (REMO4.5/S1) as well as by an increase to 384 thousand cm (CLM8.5/S3). The most pronounced decreases occur in the climate change scenarios and less due to the land use change, while the influence of land use scenarios generates increases of this parameter in all climate change scenarios applied. The surface runoff will decrease also in April, but only in the CLM scenarios when the monthly values can decrease up to 68% compared to the baseline. Scenario S2 generates a more pronounced decrease of surface runoff compared with scenario S3.

Figure 4.5a−d (Annex 1), shows the projected monthly surface runoff compared to the baseline. The decreasing trend is generated mainly due to climate change, while the increases generally occur due to the reduction of forested areas, with a slightly more pronounced trend in scenario S3 compared to scenario S2.

4.2.2.2. Seasonal surface runoff

The data given in Table 4.5 (Annex 1) shows that, in the spring months, the surface runoff can increase from approximately 1800 thousand cm to 2500 thousand cm, the most pronounced increases being estimated in REMO4.5 and REMO8.5. For the summer months, is projected an overall decreases trend. Here, the surface runoff can decrease from 414 thousand cm (baseline value) to 179 thousand cm, particularly in REMO scenarios. In autumn, an increase in surface runoff is projected, trend that will be intensified during winter when this parameter can be 2.5–4.6 times higher than baseline due to the temperatures and precipitation increments up to 1.5–2.6 °C and 70% respectively.

Figure 4.6a−d (Annex 1) show that for the spring, is projected either a slight decrease of 1% in CLM4.5/S1 (Figure 4.6-b, Annex 1) or an increase of up to 37% in REMO8.5/S3 (Figure 4.6-c, Annex 1). During the summer months, the surface runoff is expected to decrease by 14–57%, particularly in REMO4.5 and REMO8.5 coupled with scenario S1. In autumn, the surface runoff presents an increasing trend, especially in the scenario S3 and REMO4.5 and CLM4.5, situation that can be noticed also for the winter. The graphs below shows that both the most pronounced decreases (Figure 4.6-a, Annex 1) and increases (Figure 4.6-b, Annex 1) are projected in REMO4.5 and CLM4.5.

4.2.2.3. Annual surface runoff

Table 4.6 (Annex 1) shows that the increases of annual surface runoff occur mainly due to the reduction of the forest areas by 50% (scenario S3) when the surface runoff can increase from 7782 thousand cm (baseline value) up to 24964 thousand cm (year 2062/REMO8.5). The most pronounced decreases are projected in scenario S1 when the surface runoff can reach a maximum value of 3286 thousand cm (year 2059/CLM4.5). Overall, in the analysed period, it is estimated that annual surface runoff can be reduced up to 58% or intensified up to 221% compared to the baseline value.

The projected values of the annual surface runoff (Figure 4.7a−d, Annex 1), show similar trends between the land use scenarios, but with different results for the climate change scenarios. It can be noticed that after applying the land use

change scenarios the trends obtained for annual surface runoff are quite similar and present more pronounced increases particularly in scenario S3. Conversely, the surface runoff decreases mainly in scenario S1 and less in scenario S2 and S3.

Figure 4.8 illustrate an overall increasing trend the projected for multiannual average of surface runoff compared with the baseline. The most pronounced increases are projected in REMO4.5 and CLM4.5. In scenario S1, it can be noticed that the surface runoff is slightly lower, while in scenarios S2 and S3, can reach values up to 45–77% higher compared to the baseline.

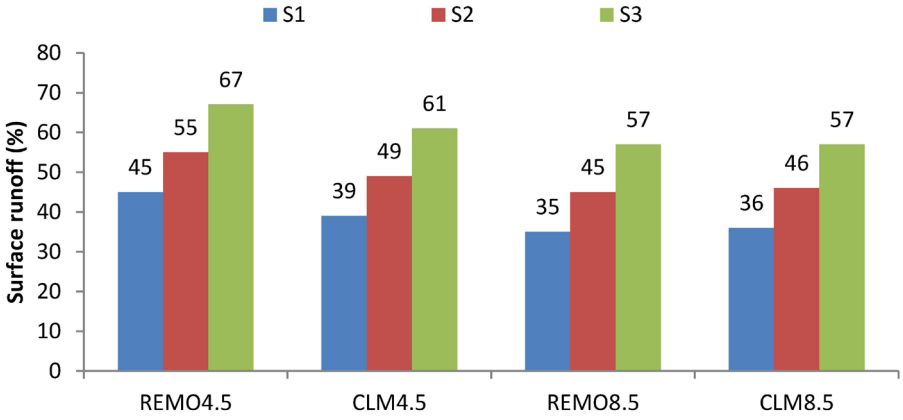

Figure 4.8. Multiannual average of surface runoff (expressed in percentage) projected in all climate and land use change scenarios for 2040–2069 period.

4.2.3. Surface runoff in the long term (2070–2100)

4.2.3.1. Monthly surface runoff

In the last analysed period, the projected values for the monthly surface runoff indicate a decrease between 1–69% compared to the baseline. The most pronounced decreases are projected for June-August under REMO4.5 and REMO8.5 and also for April in REMO8.5 and CLM8.5. The decreasing trend (Table 4.7, Annex 1) is more pronounced in scenario S1 when the surface runoff can be reduced, in August, from 285 thousand cm (baseline value) to 88 thousand cm (REMO4.5/S1). The surface runoff increases are more pronounced particularly in February, when from 193 thousand cm (baseline value), it reaches 2398 thousand cm projected in CLM4.5/S3 (Table 4.7, Annex 1). This means an 8–10-fold increase compared to the baseline.

The monthly surface runoff projected for the 2070–2100 period is highlighted in Figure 4.9a−d (Annex 1), where slight differences can be noticed between the applied scenarios. An increasing trend of surface runoff is observed starting with September in REMO4.5, CLM4.5, CLM8.5 models (Figure 4.9-a,b and d, Annex 1), and less in REMO8.5 (Figure 4.9=c, Annex 1) for which the surface runoff may decrease up to 28%. The decrease of surface runoff is projected also for June–August in all scenarios applied, and also for March in REMO8.5 and CLM8.5 (Figures 4.9-c and d, Annex 1). A different trend for surface runoff in relation to the applied scenario is noticeable for July (Figure 4.9-b and d, Annex 1). Thus, if in CLM4.5 and CLM8.5 is projected a decrease up to 13% in scenario S1, the scenario S3 predicts an increase by up to 21% of surface runoff. The same situation is noticed for September (Figure 4.9-c, Annex 1) when in the scenario S1 is projected a decrease by 28% compared to the baseline, while in the scenario S3 an increase of 14% of surface runoff is projected.

4.2.3.2. Seasonal surface runoff

Table 4.8 (Annex 1), shows that, in spring, the surface runoff is projected to increase from approximately 1800 thousand cm (baseline value) to approximately 2021 thousand cm (REMO4.5/S3), or can decrease to 1267 thousand cm (CLM8.5/S1). For summer, is projected an overall trend for surface runoff, particularly under REMO4.5 and REMO8.5 coupled with scenario S1. Starting with the autumn, the surface runoff is on an upward trend and it can reach values twice as high compared to the baseline. However, the most pronounced increases are projected for the winter months, when the surface runoff can increase from 269 thousand cm (baseline value) to 1523 thousand cm. This situation is mainly due to the increments in temperature and precipitation by 2–4 °C and 55% respectively.

The surface runoff projected at the seasonal level is presented in Figure 4.10a−d (Annex 1). For spring two trends can be noticed: increases up to 15% in REMO4.5 and CLM4.5 (Figure 4.10-a and b, Annex 1), and decreases up to 18–28% in REMO8.5 and CLM8.5 coupled with scenario S1 (Figure 4.10-b and c, Annex 1). For the summer, the surface runoff is projected to decrease between 13–60%, while in autumn, this parameter can increase particularly in the REMO4.5 and CLM4.5 (Figure 4.10-a and b, Annex 1). During the winter, are projected the most pronounced increases in surface runoff, more than four times higher than the baseline value (Figure 4.10-d, Annex 1). Figure 4.10a−d (Annex 1), shows that the decreasing trend of seasonal surface runoff is mainly projected in scenario S1, while the increments arise particularly in scenarios S2 and S3.

4.2.3.3. Annual surface runoff

The values given in Table 4.9 (Annex 1) presents different trends for the annual surface runoff, both in relation to the climate and land use change scenario. Thus, it is projected that the annual surface runoff can decrease from 7782 thousand cm (baseline value) to 3646 thousand cm in 2087 (CLM8.5/S1) or can increase to 22739 thousand cm in 2075 (REMO4.5/S3). The most pronounced decreases of annual surface runoff are mainly projected in scenario S1, while the increments arise particularly in scenarios S2 and S3.

The dynamics of the annual surface runoff projected for the 2070–2100 period is illustrated in Figure 4.11a–d (Annex 1). After applying the land use change scenarios, similar trends of annual surface runoff can be noticed. Conversely, on climate scenarios, we can observe two trends, respectively: increases especially in REMO4.5 and CLM4.5 (Figure 4.11-a and b, Annex 1), and decreases in REMO8.5 and CLM8.5 (Figure 4.11-c and d, Annex 1).

Finally, the multiannual average for the last period analysed (Figure 4.12) highlights the increasing trends of this parameter, particularly in REMO4.5 and CLM4.5. Increments are also projected in REMO 8.5 and CLM8.5, particularly in scenario S3, while in scenarios S2 and S3 the increases are not so pronounced.

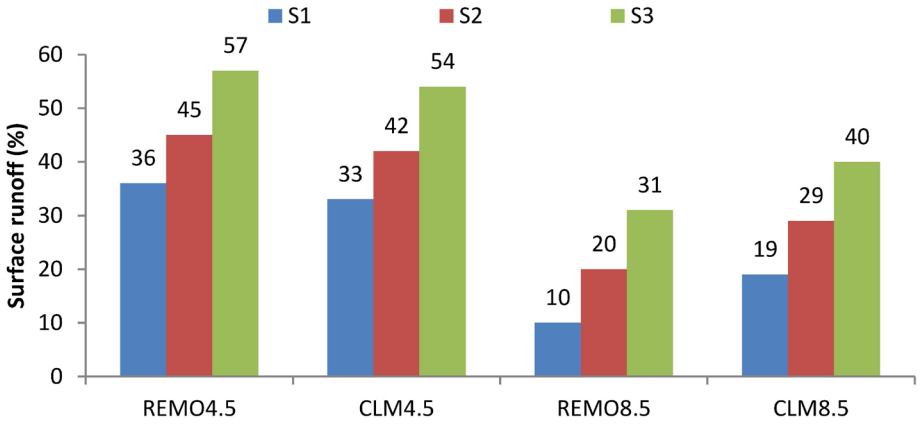

Figure 4.12. Multiannual average of surface runoff (expressed in percentage) projected in all climate and land use scenarios for the 2070–2100 period.

4.3. Water discharge projected for the 2020–2100 period

4.3.1. Water discharge in the short term (2020–2039)

4.3.1.1. Monthly water discharge

The monthly water discharge projected for the 2020–2039 period is given in Table 4.10 (Annex 2). During this period, it can be noticed that, the monthly water discharge has a decreasing trend in June-September (except September in REMO4.5 coupled with scenario S3) in all climate and land use change scenarios, as well as in April – May, but only in CLM4.5. Starting with October is projected an increasing trend of this parameter, the highest values being projected for winter when the monthly water discharge can be up to eight times higher compared to the baseline particularly in CLM4.5.

The projected monthly water discharge is illustrated in Figure 4.13a−d (Annex 2) compared with the baseline values. For the analysed period, decreases of this parameter is projected especially in June-August under REMO4.5 and REMO8.5. The increasing trend is outlined starting with March in all climate change scenarios. Starting with September the increases are more pronounced, the highest values being projected for February, particularly in scenario S3.

4.3.1.2. Seasonal water discharge

The projected seasonal water discharge for the 2020–2039 period is given in Table 4.11 (Annex 2). For spring, the water discharge is projected to increase from 1.12·m^3 s^{-1} to 1.95 m^3 s^{-1}, the highest values being obtained in REMO8.5 and CLM8.5. For the summer months, an overall decreasing trend of water discharge is projected, the sharpest decreases being noticed in REMO scenarios. In autumn, the water discharge is projected to increase from 0.40· m^3 s^{-1} to 0.69·m^3 s^{-1}, particularly in scenario S3. However, the most significant increases are projected for the winter months, especially in REMO4.5 and CLM4.5 when the water discharge increases from 0.15·m^3 s^{-1} (baseline) to 0.50–0.65·m^3 s^{-1}. This aspect was also reported by Chendeș et al. (2010), who mentions a predisposition of mountainous watersheds to record significant increases in water discharge during the winter months.

The seasonal water discharge is illustrated in Figure 4.14 a−d (Annex 2) and shows that, in spring, this parameter can increase by 8–75%, particularly in REMO8.5 and CLM8.5 (Figure 4.14-c and d, Annex 2). In summer, the water discharge is projected to decrease between 14% (Figure 4.14-d, Annex 2) and

44% (Figure 4.14-a, Annex 2). In autumn, the water discharge may decrease by 3% in scenario S1 (Figure 4.14-c, Annex 2) or may increase up to 73% (Figure 4.14-a, Annex 2), the highest values being projected in scenario S3. For winter, the water discharge is projected up to 3.4-fold increase compared to the baseline values.

4.3.1.3. Annual water discharge

The data given in Table 4.12 (Annex 2), shows both increases in annual water discharge from 0.67 m3·s-1 (baseline) to 1.44 m^3 s^{-1} (year 2029, scenarios S2 and S3), as well as decreases of water discharge up to 0.43 m^3 s^{-1} (year 2035, scenario S1). The highest increases are projected in scenario S3, while the water discharge decreases mainly in scenario S1.

Figure 4.15 a–d (Annex 2) illustrates the projected water discharge compared to the baseline values. The increases trend of water discharge is more pronounced in REMO8.5 and CLM8.5 (Figure 4.15-c and d, Annex 2). Conversely, REMO4.5 and CLM4.5 present a higher frequency of years with a decreasing trend projected for water discharge Figure 4.15-a and b, Annex 2).

The multiannual average of water discharge (Figure 4.16) shows that the most accentuated increases, up to 33%, are projected in REMO8.5 and CLM8.5. The lowest increases are projected in CLM4.5 when the water discharge increases by 13–15% compared to the baseline.

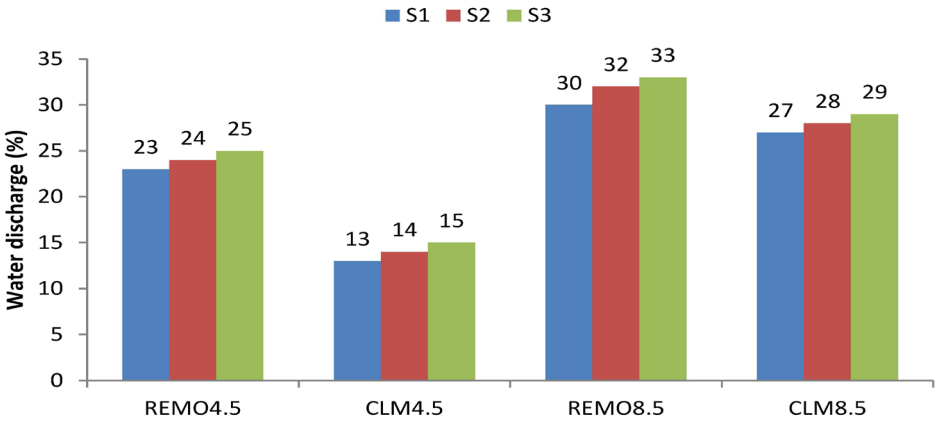

Figure 4.16. The multiannual average of water discharges (expressed in percentage) projected in all climate and land use change scenarios for the 2020–2039 period.

4.3.2. Water discharge in the medium term (2040–2069)

4.3.2.1. Monthly water discharge

The monthly water discharge projected under climate and land use change scenarios for the 2040–2069 period, are given in Table 4.13 (Annex 2) and illustrated in Figure 4.17 a−d (Annex 2) as percentage differences. Compared to the baseline, increases of the monthly water discharge are projected particularly for the winter months in CLM8.5 scenarios. An overall decreases trend of this parameter is projected for June–September, mainly in REMO4.5 and REMO8.5.

Compared to the baseline, monthly water discharge is projected to increase starting with November, the highest values being forecasted for February, especially in CLM8.5 (Figure 4.17-d, Annex 2). For April, the monthly water discharge is projected to decrease only under CLM scenarios, the lowest values being obtained in scenario S3 (Figure 4.17-b and d, Annex 2). Conversely, for the same month, in REMO scenarios, increases in the monthly water discharge are projected (Figure 4.17-a and c, Annex 2). The most pronounced increases in monthly water discharge are projected in scenarios S2 and S3, while scenario S1 have a slightly lower influence on the values projected for 2040–2069 period.

4.3.2.2. Seasonal water discharge

According to the data given in Table 4.14 (Annex 2) it can be noticed that, in spring, the seasonal water discharge is projected to increase from $1.12 \cdot m^3\ s^{-1}$ (baseline value) to approximately $1.58 \cdot m^3\ s^{-1}$. For the summer months, the seasonal water discharge is projected decrease from $1.04 \cdot m^3\ s^{-1}$ to approximately $0.64\ m^3\ s^{-1}$, particularly in REMO scenarios. In autumn, a slightly increase compared to the baseline values is projected (but only in REMO4.5 and CLM4.5). During winter, compared to the baseline, a 3–4-fold increase is projected especially in REMO4.5 and CLM4.5.

The projected seasonal water discharge and illustrated compared to the baseline values are given Figure 4.18 a−d (Annex 2). For spring, an increase of 14–41% in seasonal water discharge is projected, particularly in REMO scenarios (Figure 4.18-a and c, Annex 2) but also in CLM8.5 scenario (Figure 4.18-d, Annex 2). During summer, the water discharge is projected to decrease by up to 38% (Figure 4.18-c, Annex 2). For autumn, was projected decreases trends in REMO8.5 and CLM8.5 (Figure 4.18-c and d, Annex 2) as well as increases in REMO4.5 and CLM4.5 (Figure 4.18-a and b, Annex 2). The most noticeable differences compared to the baseline are obtained for winter. The seasonal water discharge increases are more pronounced in REMO4.5 and CLM4.5 (Figure

4.18-a and b, Annex 2). The increase in seasonal water discharge occurs mainly in scenarios S2 and S3, while the scenario S1 has a slightly lower influence.

4.3.2.3. Annual water discharge

The projected annual water discharge for 2040–2069 period, are presented in Table 4.15 (Annex 2). Compared to the baseline, the annual water discharge can increase from 0.67 $m^3 s^{-1}$ to 1.37 $m^3 s^{-1}$ (year 2048/REMO8.5/S3), the most pronounced increases being projected in scenario S3. For this time interval, are projected also decreases annual water discharge between 0.34–0.66 $m^3 s^{-1}$.

Analysing Figure 4.19 a–d (Annex 2), it can be noticed that a higher frequency of years with increases of the annual water discharge. The most pronounced decreases and increases of this parameter are projected in REMO8.5. The decreasing trend is more pronounced in scenario S1 scenario, while the increases are projected particularly in scenario S3.

The multiannual average of water discharge projected for 2040–2069 period (Figure 4.20) highlights the fact that the most pronounced increases, between 21–29% are projected in REMO4.5 and CLM8.5. Conversely, the lowest increases are projected in REMO8.5 (14–17%) and CLM4.5 (18–21%).

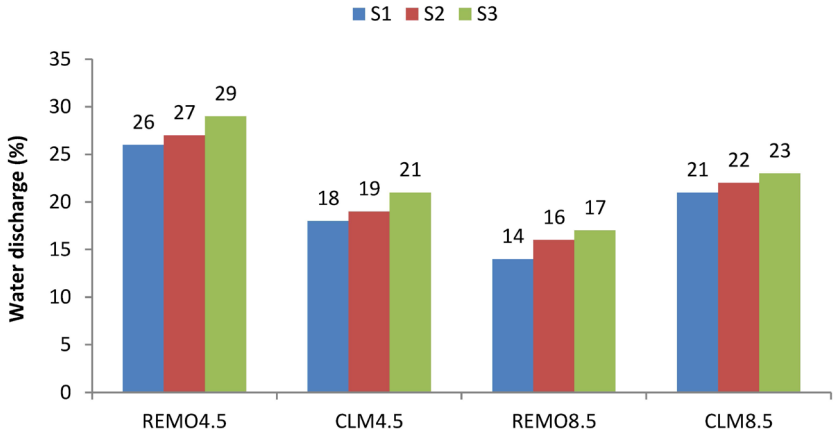

Figure 4.20. Multiannual average of discharges (expressed in percentage) projected in all climate and land use change scenarios for the 2040–2069 period.

4.3.3. Water discharge in the long term (2070–2100)

4.3.3.1. Monthly water discharge

The projected monthly water discharge given in Table 4.16 (Annex 2), highlight that, starting with November, is projected an overall increasing trend of this parameter, which can be two times fold compared with that baseline. In December the monthly water discharge can increase from 0.19 $m^3 \cdot s^{-1}$ (baseline value) to 0.73 $m^3 \cdot s^{-1}$ in CLM8.5/S1 model, while in January they can increase up to about three times fold. However, the most significant increases are projected for February, when the monthly water discharge can increase from 0.10 $m^3 \cdot s^{-1}$ to 1.20 $m^3 \cdot s^{-1}$. The monthly water discharge is projected to decrease not only for June-July (as in previous periods), but also for April (in CLM4.5 and CLM8.5), September (in all scenarios applied) and October (in CLM4.5 and REMO8.5).

Figure 4.21 a−d (Annex 2), shows a decreasing trend of monthly water discharge starting with April in both CLM scenarios (Figure 4.21-b and d, Annex 2), and for June-September (Figure 4.21-a and d, Annex 2) in REMO scenarios. Increases of this parameter are projected starting with October (Figure 4.21-d, Annex 2), trend that will be intensified in the following months and will reach, in February, values up to 12 times folds compared to the baseline value (Figure 4.21-b and d, Annex 2).

4.3.3.2. Seasonal water discharge

The seasonal water discharge projected for 2070–2100 is given in Table 4.17 (Annex 2). In spring, this parameter can increase from 1.12·m3 s-1 (baseline value) to 1.47· $m^3 \cdot s^{-1}$ (in REMO4.5), while in the summer, the water discharge can decrease from 1.04 $m^3 \cdot s^{-1}$ to 0.59–0.79·$m^3 \cdot s^{-1}$, in REMO8.5 and CLM8.5. In autumn, the water discharge can decrease up to 0.34· $m^3 \cdot s^{-1}$ or can increase up to 0.49· $m^3 \cdot s^{-1}$. The most pronounced increases are projected for the winter, when the water discharge can increase from 0.15·$m^3 \cdot s^{-1}$ to 0.85· $m^3 \cdot s^{-1}$in CLM8.5.

The seasonal water discharge illustrated compared to the baseline are presented in Figure 4.22 a−d (Annex 2). In the spring months, the water discharge is projected to increase between up to 32%, particularly in REMO4.5 and CLM4.5 (Figure 4.22-a and b, Annex 2). For summer, is projected an overall decreasing trend of this parameter, which can be reduced up to 43% (Figure 4.22-c, Annex 2). In autumn, the water discharge can decrease up to 15% (Figure 4.22-c, Annex 2) or can increase up to 23%, particularly in scenario S3 (Figure 4.22-a, Annex 2). In winter, are projected the most pronounced, which can reach values of 3–5 times fold compared to the baseline.

4.3.3.3. Annual water discharge

Compared to the baseline, the projected annual water discharge (Table 4.18, Annex 2) can be reduced by 53%, from 0.67 $m^3 \cdot s^{-1}$ to 0.31$\cdot m^3 \cdot s^{-1}$ (year 2088/ REMO4.5/S1). In the same time, an increase between 0.68–1.35$\cdot m^3 \cdot s^{-1}$ in annual water discharge is projected, which means an increase of 101% compared to the baseline. The maximum value (1.35$\cdot m^3 \cdot s^{-1}$) corresponds to 2080 and is projected in REMO8.5 coupled with scenario S3.

Analysing Figure 4.23 a–d (Annex 2), it can be seen that the highest increases of water discharge are projected especially in REMO4.5 and REMO8.5 coupled with scenario S3 (Figure 4.23-a and c, Annex 2), while scenario S1 generates the most pronounced decreases of annual water discharge particularly in REMO4.5 (Figure 4.23-a, Annex 2).

The multiannual average of the analysed period (Figure 4.24) shows an increase of the water discharge in all climate change scenarios, but with the lowest values in REMO8.5 and highest in REMO4.5. Analysing the impact of land use change scenarios, we noticed that the largest increases of water discharge (from 9% to 26%) occur in scenario S3, while scenario S1 generates the water discharge increases between 5–23%.

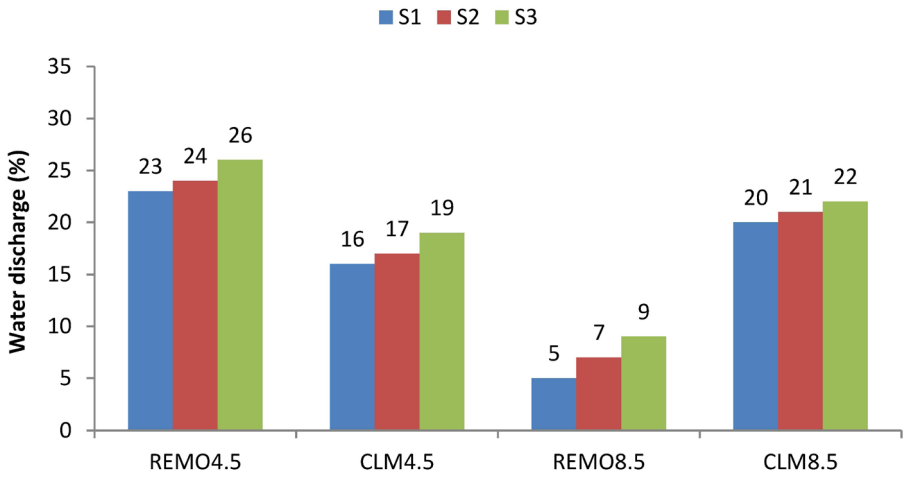

Figure 4.24. Multiannual average of water discharges (expressed in percentage) projected in all climate and land use change scenarios for the 2070–2100 period.

4.4. Sediment yield projected for the 2020–2100 period

4.4.1. Sediment yield in the short term (2020–2039)

4.4.1.1. Monthly sediment yield

In the 2020–2039 period, the monthly sediment yield is projected to record both increases and decreases in all climate and land use change scenarios considered (Table 4.19, Annex 3). The most accentuated increases are generated under the land use change scenarios, particularly in scenarios that assume a reduction of forested areas by 50% (scenario S3), while CLM climate scenarios can generate higher amounts of sediment yield compared to REMO. The largest increases are projected for February, when sediment yield can increase from 160 tons (baseline) to about 1800 tons in the CLM4.5 coupled with the scenario S3. The monthly sediment yield is projected to decreases particularly in August, when from 408 tons (baseline), it reaches up to approximately 130 tons (REMO4.5/S1).

The monthly averages obtained for sediment yield and represented as percentage difference to the baseline, are illustrated in Figure 4.25a−d (Annex 3). Here is highlighted the different influence of land use change, with a more pronounced trend in scenarios S3, while scenarios S1 shows the lowest influences.

4.4.1.2. Seasonal sediment yield

According to the data from Table 4.20 (Annex 3), in the spring, the sediment yield is projected to decrease from about 1700 tonnes (baseline value) to 1094 tonnes (CLM4.5/S1), or can increase to about 3800 tonnes (REMO8.5/S3). Different trends obtained for sediment yield are also noticeable for the summer and autumn. For winter instead, is projected an increasing trend, this parameter can increase from 249 tons (baseline value) to 1118 tonnes (REMO4. 5/S3).

Figure 4.26a−d (Annex 3), shows that compared to the baseline, the sediment yield can decrease in spring months by up to 37% (Figure 4.26-b, Annex 3) or can increase by up to 120% (Figure 4.26-c, Annex 3). In summer, sediment yield is projected decrease in all climate and land use change scenarios applied, with the exception of scenario S3 coupled with CLM4.5 and CLM8.5 (Figure 4.26-b and c, Annex 3). In autumn, sediment yield can register either an increase between 13–201% or a decrease of up to 16% (Figure 4.26-c, Annex 3). Conversely, for the winter season, an accentuated increase of sediment yield is projected, particularly in scenario S3.

4.4.1.3. Annual sediment yield

Compared to the baseline value, namely 8253 tonnes (Table 4.21, Annex 3), the sediment yield is projected to reach a maximum increase of up to 26047 tonnes (in 2023/CLM8.5/S3). The most pronounced increases are projected in scenario S3 for all climate change scenarios. However, the annual sediment yield can also decrease by up to 2493 tonnes, particularly in scenarios S2 and S3.

Figure 4.27a−d (Annex 3) illustrates the sediment yield dynamics projected for the 2020–2039 period in all climate and land use change scenarios. We can observe that in REMO4.5 and CLM4.5 (Figure 4.27-a and b, Annex 3), the annual sediment yield can decrease by up to 70% in scenarios S1 and S2 (with a more pronounced trend in scenario S1), while scenario S3 highlights a sharp increase of this parameter due to the reduction of forested areas by 50%. However, the most accentuated increases of sediment yield are projected in REMO8.5 and CLM8.5 (Figure 4.27-c and d, Annex 3) when this parameter reaches values of three times -fold compared to the baseline (Figure 4.27-c, Annex 3).

The multiannual average of sediment yield (Figure 4.28) shows that the most pronounced decreases (up to 24%) are obtained in scenario S1, while scenario S2 can lead to a sediment yield decrease by up to 17%, as well as a slight increase of 7%. However, the most pronounced increases (from 70% to 105%) are projected in REMO8.5 and CLM8.5 coupled with scenario S3.

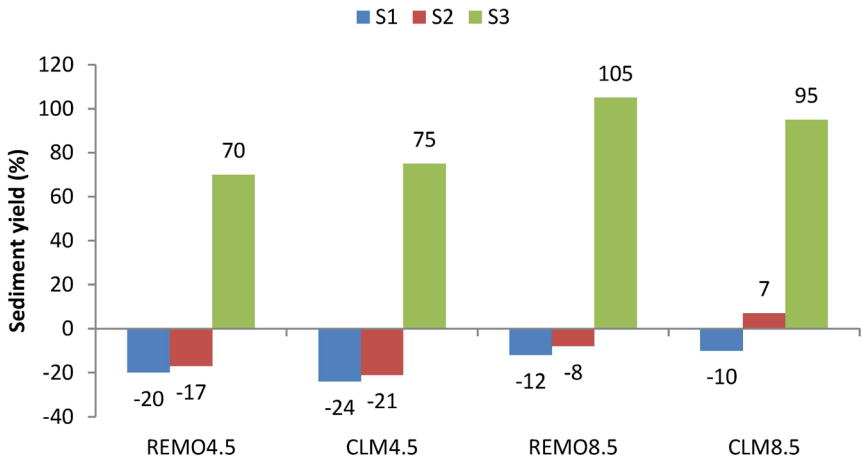

Figure 4.28. The multiannual average of sediment yield (expressed in percentage) projected in all climate and land use change scenarios for the 2020–2039 period.

4.4.2. Sediment yield in the medium term (2040–2069)

4.4.2.1. Monthly sediment yield

Compared to the baseline, the monthly sediment yield is projected to register both increases and decreases in the 2040–2069 period (Table 4.22, Annex 3). Similar to the previous period (2020–2039), the increases trends are more pronounced in scenario S3 coupled with REMO4.5 and CLM8.5. For instance, in February, the monthly sediment yield is projected to increase from 160 tonnes (baseline value) to about 1700–2100 tonnes. On the other hand, a pronounced decrease of this parameter is projected for August when from 408 tonnes (baseline value) the sediment yield can register only 121 tonnes in the REMO8.5/S1.

Figure 4.29a−d (Annex 3), shows that in all climate change scenarios, an accentuated increases trend of sediment yield is projected in scenario S3, particularly in REMO4.5 and CLM8.5 (Figure 4.29-a and d, Annex 3). For July–September we observe a decreasing trend of sediment yield (8–48%) projected in scenario S3 coupled with REMO4.5 and REMO8.5. The decrease of sediment yield is projected especially in scenarios S1 and S2 coupled with REMO8.5 and CLM8.5 (Figure 4.29-c and d, Annex 3).

4.4.2.2. Seasonal sediment yield

The seasonal averages of sediment yield projected for the 2040–2069 period (Table 4.23, Annex 3), show that, in spring, this parameter can either increase from about 1700 tonnes (baseline value) to about 2900 tonnes projected in REMO4.5/S3, or can decrease to about 950 tonnes (CLM4.5/S1). In summer, sediment yield is projected to decrease in all climate and land use change scenarios, with the exception of CLM4.5 and CLM8.5 coupled with scenario S3, which predicts an increase of sediment yield from 570 tonnes (baseline value) to 600 and 732 tonnes respectively. In autumn, the sediment yield can increase from 201 tonnes (baseline value) to 440 tonnes (REMO4.5/S3) or can decrease to 138 tonnes (CLM8.5/S1). For winter, is projected an overall increasing trend, when sediment yield can reach a maximum value of 1435 tonnes in the analysed period (REMO4.5/S3).

Figure 4.30a−d (Annex 3), shows that in scenario S3 an increase of sediment yield is projected in all seasons and climate change scenarios, with more pronounced values in the winter season. Here, the sediment yield can increase 3–4 times fold increase compared to the baseline. In scenarios S1 and S2 are projected an overall decreasing trend, except for the CLM4.5 when in the autumn and winter season the sediment yield is projected to increase compared to the baseline value.

4.4.2.3. Annual sediment yield

Compared to the baseline value, the annual sediment yield (Table 4.24, Annex 3) may decrease from 8253 tonnes to 2466 tonnes (year 2053 / REMO4.5 / S1), particularly in REMO8.5 coupled with scenario S1 and scenario S2. The most pronounced increases are projected in the CLM4.5 and CLM8.5 coupled with scenario S3 when sediment yield is projected to reach a maximum value of 28186 tonnes.

Figure 4.31a–d (Annex 3), highlights the decreasing trend of annual sediment yield in scenarios S1 and S2, when this parameter is projected to decrease by 2–82%, particularly in REMO4.5 and CLM4.5 (Figure 4.31-a and b, Annex 3). In contrast, scenario S3 shows pronounced increases in all climate change scenarios, the sediment yield is projected to reach values up to about three times higher compared to the baseline, especially in REMO4.5 and CLM8.5 (Figure 4.31-c and d, Annex 3).

The multiannual average of the analysed period (Figure 4.32) highlights even more clearly these two trends described above: decreases by 17–32%, particularly in CLM4.5 and REMO8.5 coupled with scenario S1, and increases by 64–94%, values projected in all climate change scenarios coupled scenario S3.

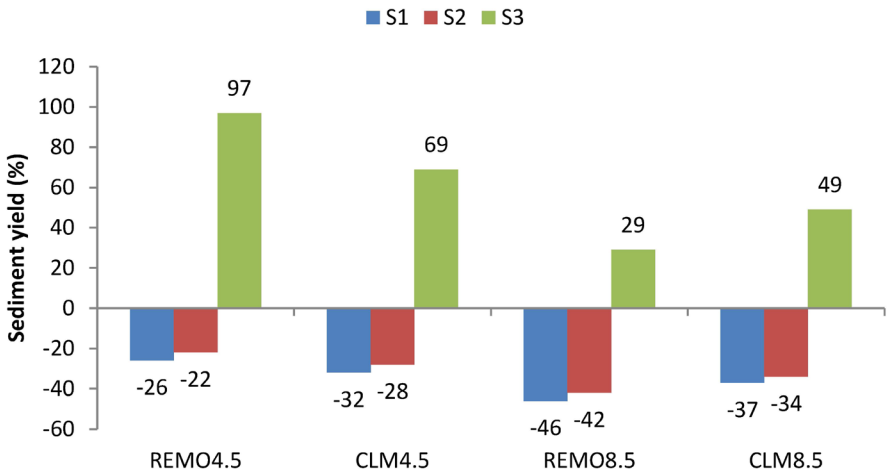

Figure 4.32. The multiannual average of sediment yield (expressed in percentage) projected in all climate and land use change scenarios for the 2040–2069 period.

4.4.3. Sediment yield on the long term (2070–2100)

4.4.3.1. Monthly sediment yield

The projected monthly sediment yield given in Table 4.25 (Annex 3), shows decreases in April – May and also in June – November, with two exceptions: October – REMO4.5 and CLM8.5 in which are projected increases of sediment yield; a similar situation is observed in November, but only in REMO4.5. Instead, for the winter months, the sediment yield is projected to increase, the most pronounced increases being forecast for February, when from 160 tonnes it can reach up to about 2200 tonnes, particularly in CLM4.5 and CLM8.5 coupled with scenario S3.

Figure 4.33a−d (Annex 3), shows the decreasing trends of monthly sediment yield particularly in scenarios S1 and S2, with the exception of October and November in REMO4.5 (Figure 4.33-a, Annex 3) and October in CLM8.5 (Figure 4.33-d, Annex 3), for which are projected an increasing trend. For December–February sediment yield is projected to increase in all climate change scenarios under the scenario S3. The most pronounced increases are projected in February, for CLM4.5 and CLM8.5 coupled with scenario S3, when sediment yield can reach values of 10–14 times fold compared to the baseline value (Figure 4.33-b and d, Annex 3).

4.4.3.2. Seasonal sediment yield

According to the data given in Table 4.26 (Annex 3), in the spring season, the sediment yield is projected to decrease from 1732 tonnes (baseline value) to 725 tonnes (CLM8.5/S1) or can increase to approximately 1700 tonnes (CLM8.5/S3). For the summer months, sediment yield can decrease to 294 tonnes (REMO4.5/S1) or increase to around 680 tonnes (CLM8.5/S3). In autumn, is projected an increase from 201 tonnes (baseline value) to a maximum value of 621 tonnes (REMO4.5/S3), and also a decrease to 135 tonnes (REMO8.5/S1). In winter, the sediment yield is projected to increase compared to the baseline value (249 tons) and can reach a maximum value of 1533 tonnes.

The averages of projected seasonal sediment yield (Figure 4.34a−d (Annex 3), shows that in spring, this parameter can decrease by up to 59% in scenarios S1 and S2 (Figure 4.34-c, Annex 3) or can increase by 30–58% in scenario S3 (Figure 4.34-a and b, Annex 3). In summer, sediment yield is projected to decrease between 8–60%, particularly in REMO8.5 coupled with scenario S1 (Figure 4.34-c, Annex 3), or can increase by 19% (Figure 4.34-d, Annex 3). In autumn, the increases in sediment yield can be up to twice fold compared to

the baseline (Figure 4.34-a, Annex 3), while the decreases can reach 33% (Figure 4.34-c, Annex 3). In winter, the sediment yield is projected to increase by 62–516% in all scenarios applied (Figure 4.34-c and a, Annex 3).

4.4.3.3. Annual sediment yield

At annual level (Table 4.27, Annex 3), compared to the baseline values (8253 tonnes), the sediment yield is projected to decrease to about 1600 tonnes (year 2088/REMO4.5/S1) and to increase to the maximum value of 32038 tonnes (year 2075/REMO4.5/S3). The decreasing trend is projected mainly in REMO4.5 and REMO8.5 coupled especially with scenario S1, while the sediment yield increases occur particularly in REMO4.5 and CLM4.5 coupled with scenario S3.

The annual averages of sediment yield projected for the 2070–2100 period is illustrated in Figure 4.35a−d (Annex 3). Here, is highlighted the decreasing trend, particularly in REMO4.5 coupled with scenarios S1 and S2 (Figure 4.35-c, Annex 3), when the sediment yield can be reduced by 80% (scenario S1) and 77% (scenario S2). The increasing trend of this parameter is projected in all climate change scenarios coupled with scenario S3, the maximum values being obtained in REMO4.5 and CLM4.5 (Figure 4.35-a and b, Annex 3) when the increase can reach 288% (REMO4.5).

Finally, the multiannual average computed for the 2070–2100 period (Figure 4.36) shows decrease in sediment yield between 22–46%, particularly in REMO8.5 and CLM8.5, while the increases of this parameter are projected especially in REMO4.5 and CLM4.5. Noteworthy, the differentiation of the land use change scenarios, which shows only decreases in scenarios S1 and S2, while scenario S3 presents only increases.

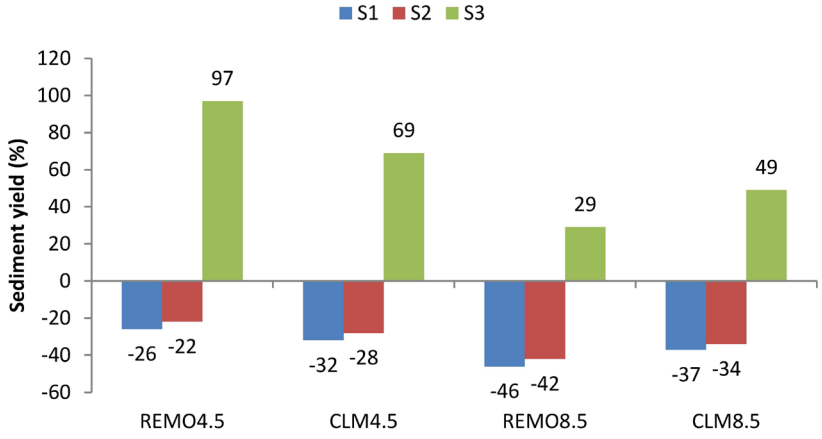

Figure 4.36. The multiannual average of sediment yield (expressed in percentage) projected in all climate and land use change scenarios for the 2070–2100 period.

4.5. Statistical analysis of the influence of climate and land use change scenarios on surface runoff, water discharge and sediment yield

4.5.1. Statistical analysis for surface runoff

Using the STATISTICA13.5.0.17 was performed a statistical analysis of the values projected for surface runoff in the 2020–2100 period. The analysis of variances was performed using the ANOVA test. The monthly averages of surface runoff were analysed in terms of data homogeneity in relation to climate and land use change scenarios. Applying Levene's test for homogeneity of variances (Table 4.28) it was found that the assumption is not met (Petrițan, 2008).

Table 4.28. Testing the surface runoff datasets homogeneity.

Depend.:	Levene's Test for Homogeneity of Variance Effect: "Clim"*"Land use" Degree of freedom for all F's = 11, 11652			
	MS Effect	MS Error	F	P
Surface runoff	3852660	1860548	2.070713	0.019077

Subsequently, the Kruskal-Wallis non-parametric test was applied and the influence of climate and land use change scenarios on surface runoff was tested. Table 4.29 shows that among climate change scenarios significant differences in surface runoff appear only in REMO8.5. The differences in surface runoff between the other climate change scenarios applied are insignificant. Moreover, REMO4.5, CLM4.5 and CLM8.5 did not show significant influences on the surface runoff variation.

Table 4.29. Testing the influence of climate change scenarios on surface runoff.

Depend.: Surface runoff	Multiple Comparisons p values (2-tailed); Surface runoff Independent (grouping) variable: Clim Kruskal-Wallis test: H (3, N= 11664) =15.82106 p =.0012			
	REMO4.5	REMO8.5	CLM4.5	CLM8.5
REMO4.5	-	0.473808	0.277271	1.000000
REMO8.5	0.473808	-	0.001060	0.023342
CLM4.5	0.277271	0.001060	-	1.000000
CLM8.5	1.000000	0.023342	1.000000	-

Assessing the influence of land use scenarios (S1–S3), from Table 4.30 we observe that, for 2020–2100 period, significant differences of the surface runoff appear only in scenario S1 compared to scenario S3. The differences between scenarios S1 and S2 are insignificant.

Table 4.30. Testing the influence of land use change scenarios on surface runoff.

Depend.: Surface runoff	Multiple Comparisons p values (2-tailed); Surface runoff Independent (grouping) variable: Land Kruskal-Wallis test: H (2, N= 11664) =11.57920 p =.0031		
	S1	S2	S3
S1	-	0.618954	0.002339
S2	0.618954	-	0.108203
S3	0.002339	0.108203	-

Figure 4.37 shows the variation of the average monthly surface runoff under the cumulative influence of climate and land use change scenarios within the Upper Tarlung watershed. The surface runoff averages register the largest increases in REMO4.5 coupled with scenarios S1 and S3. The lowest averages of surface runoff were obtained in CLM8.5 under all land use change scenarios.

The average surface runoff at seasonal level for the 2020-2100 period is represented in Figure 4.38, considering the cumulative influence of climate and land use change scenarios. The highest averages are projected in spring, particularly in REMO4.5 and REMO8.5. In winter, the increasing trend of this parameter is maintained, with the highest values in REMO4.5 and CLM4.5.

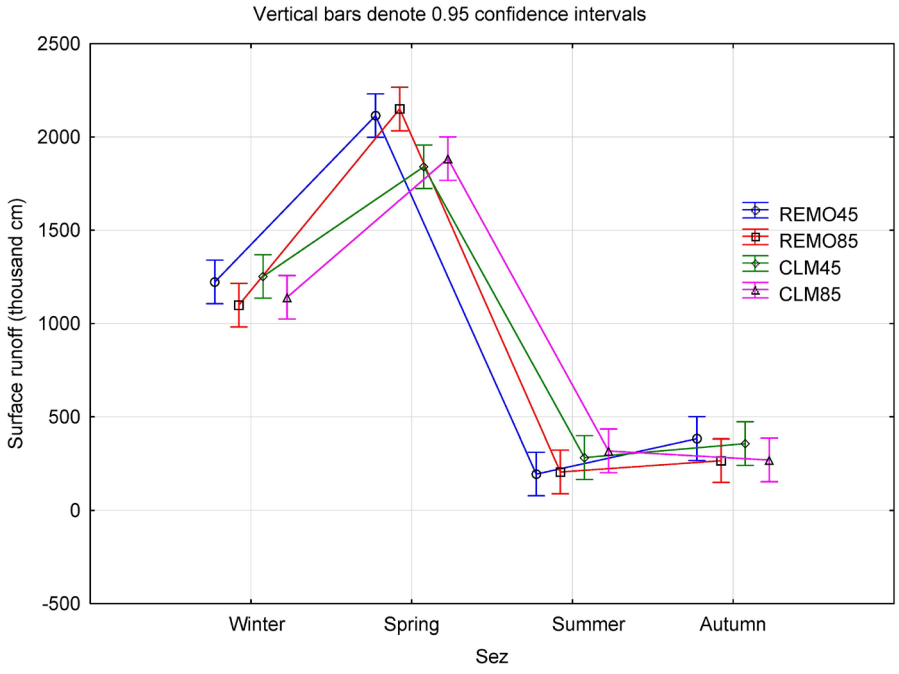

Figure 4.38. Average seasonal surface runoff (thousand cm) tendency projected for the 2020–2100 period in all climate and land use change scenarios.

4.5.2. Statistical analysis for water discharge

The water discharge projected in all climate and land use change scenarios were statistically analysed for testing the homogeneity of variances and the normality of the distribution. Applying Factorial ANOVA – LEVENE's test, it was observed that, as for the previous parameter, that the assumption is not fulfilled (Table 4.31).

Table 4.31. Testing the water discharges datasets homogeneity.

Depend.:	Multiple Comparisons p values (2-tailed); Surface runoff Independent (grouping) variable: Land Kruskal-Wallis test: H (2, N= 11664) =11.57920 p =.0031			
	MS Effect	MS Error	F	P
Water discharge	1.041283	0.301908	3.449013	0.000082

Next, the Kruskal-Wallis non-parametric test was applied, to analyse the link between water discharge, climate and land use change scenarios. Testing the influence of climate change scenarios on water discharge we observed that significant differences on this parameter are obtained only in REMO8.5 (Table 4.32).

Table 4.32. Testing the influence of climate change scenarios on water discharge.

Depend.: Water discharge	Multiple Comparisons p values (2-tailed); Water discharge Independent (grouping) variable: Clim Kruskal-Wallis test: H (3, N= 11664) =38.56643 p =.0000			
	REMO4.5	REMO8.5	CLM4.5	CLM8.5
REMO4.5	-	0.000003	1.000000	1.000000
REMO8.5	0.000003	-	0.000520	0.000000
CLM4.5	1.000000	0.000520	-	0.506616
CLM8.5	1.000000	0.000000	0.506616	-

Regarding the land use change scenarios, from Table 4.33 we observe that between all scenarios considered there are insignificant differences in the variation of water discharge for the 2020-2100 period.

Table 4.33. Testing the influence of land use change scenarios on water discharges.

Depend.: Water discharge	Multiple Comparisons p values (2-tailed); Water discharge Independent (grouping) variable: Land Kruskal-Wallis test: H (2, N= 11664) =.4752943 p =.7885		
	S1	S2	S3
S1	-	1.000000	1.000000
S2	1.000000	-	1.000000
S3	1.000000	1.000000	-

Figure 4.39 shows the cumulated influence of climate and land use change scenarios on the monthly water discharge. Significant variations on this parameter are generated only under climate change scenarios. The highest values of the water discharge are obtained in REMO4.5, while the lowest values are attributed to REMO8.5.

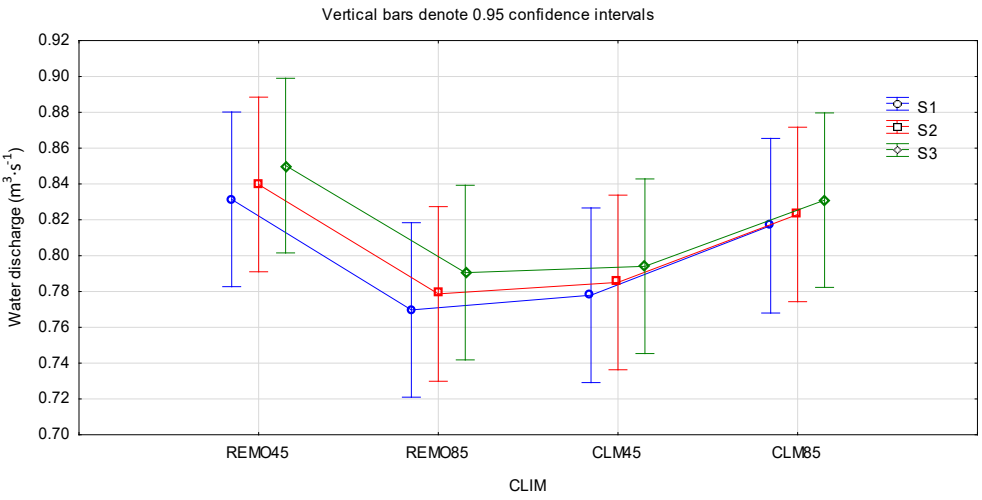

Figure 4.39. Average monthly water discharges ($m^3 \cdot s^{-1}$) tendency projected for the 2020–2100 period in all climate and land use change scenarios.

Figure 4.40 illustrates water discharge trend at seasonal level for the 2020–2100 period. We observe that the most accentuated values are projected in spring, particularly in REMO scenarios. Starting with the summer months, is projected an overall decreasing trend of water discharge; the same situation is observed in the winter months and especially in autumn, when the lowest water discharges are projected in REMO8.5.

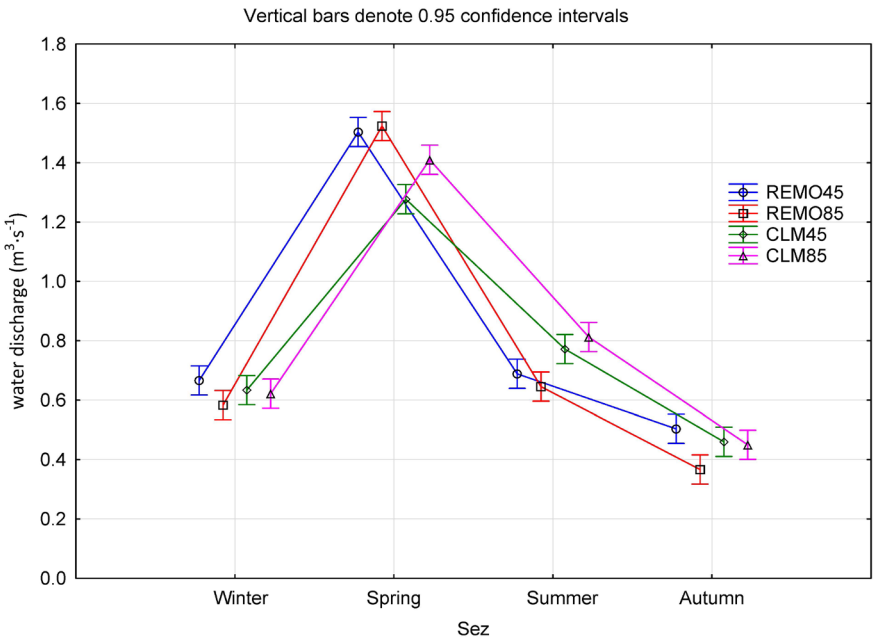

Figure 4.40. Average seasonal water discharges ($m^3 \cdot s^{-1}$) projected for 2020–2100 period in all climate and land use change scenarios.

4.5.3. Statistical analysis for sediment yield

The statistical analysis of sediment yield variance using the ANOVA Factorial test, highlights that, even in this case, the homogeneity condition of the variance is not fulfilled (Table 4.34). Therefore, the non-parametric Kruskal-Wallis test was further used to test the cumulative influence of climate and land use change scenarios on sediment yield.

Table 4.34. Testing the sediment yield datasets homogeneity.

Depend.:	Levene's Test for Homogeneity of Variance Effect: "Clim"*"Land use" Degree of freedom for all F's = 11, 11652			
	MS Effect	MS Error	F	P
Sediment yield	140917692	1112616	126.6544	0.00

Testing the influence of climate change scenarios, we noticed that sediment yield is influenced only by REMO8.5 (Table 4.35), while in the case of land use change scenarios, significant influences were obtained only in scenario S3 compared to scenario S1. The differences between scenarios S1 and S2 are insignificant (Table 4.36).

Table 4.35. Testing the influence of climate change scenarios on sediment yield.

Depend.: Sediment yield	Multiple Comparisons p values (2-tailed); Sediment yield Independent (grouping) variable: Clim Kruskal-Wallis test: H (3, N= 11664) =36.85951 p =.0000			
	REMO4.5	REMO8.5	CLM4.5	CLM8.5
REMO4.5	-	0.000006	1.000000	1.000000
REMO8.5	0.000006	-	0.000010	0.000001
CLM4.5	1.000000	0.000010	-	1.000000
CLM8.5	1.000000	0.000001	1.000000	-

Table 4.36. Testing the influence of land use change scenarios on sediment yield.

Depend.: Sediment yield	Multiple Comparisons p values (2-tailed); Sediment yield Independent (grouping) variable: Land Kruskal-Wallis test: H (2, N= 11664) =277.9100 p =0.000		
	S1	S2	S3
S1	-	0.948707	0.00
S2	0.948707	-	0.00
S3	0.000000	0.000000	-

Figure 4.41, shows the influence of climate and land use change scenarios on the average monthly sediment yield. It can be noticed that the most important increases of this parameter occur in scenario S3, for all climate change scenarios used, but with the highest values in REMO4.5.

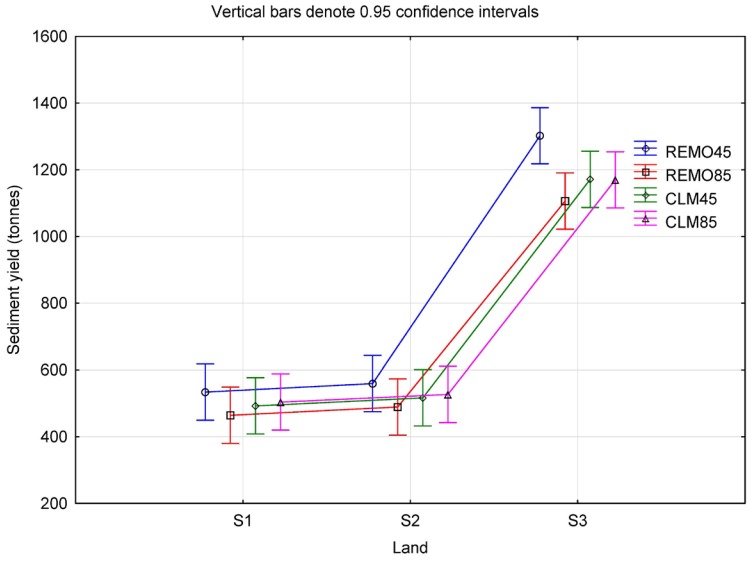

Figure 4.41. Monthly sediment yield (tonnes) projected for the 2020–2100 period in all climate and land use change scenarios.

At the seasonal level, for the entire period (2020–2100) we can see that the sediment yield dynamics are similar to one obtained for water discharge (Figure 4.42). The highest values were projected in spring, particularly under REMO scenarios. In winter, sediment yield also shows significant increases, slightly pronounced in REMO4.5 and CLM4.5. Starting with the summer season, the sediment yield is projected to decrease, while in autumn, this parameter shows the lowest values (Figure 4.43).

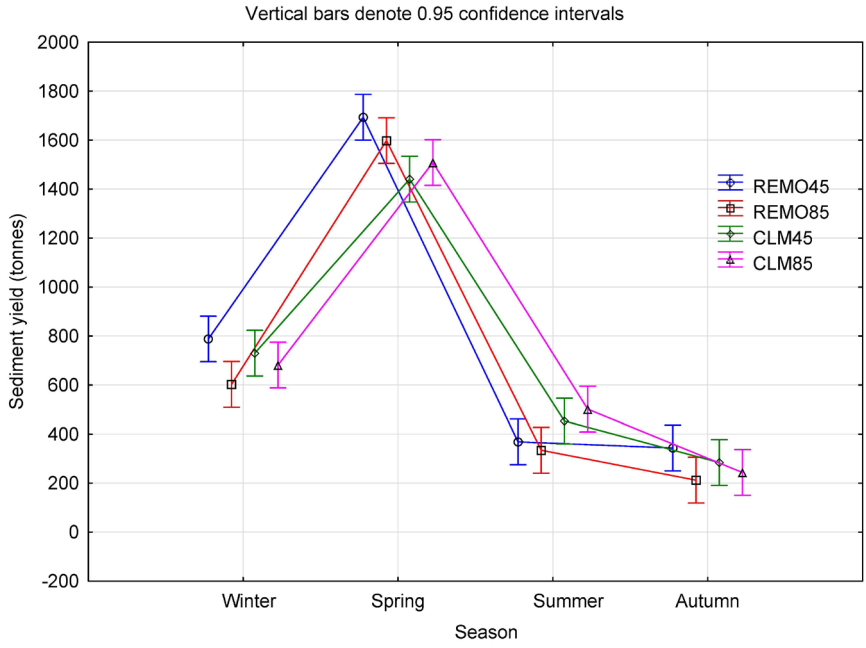

Figure 4.42. Average seasonal sediment yield (tonnes) projected for the 2020–2100 period in all climate and land use change scenarios.

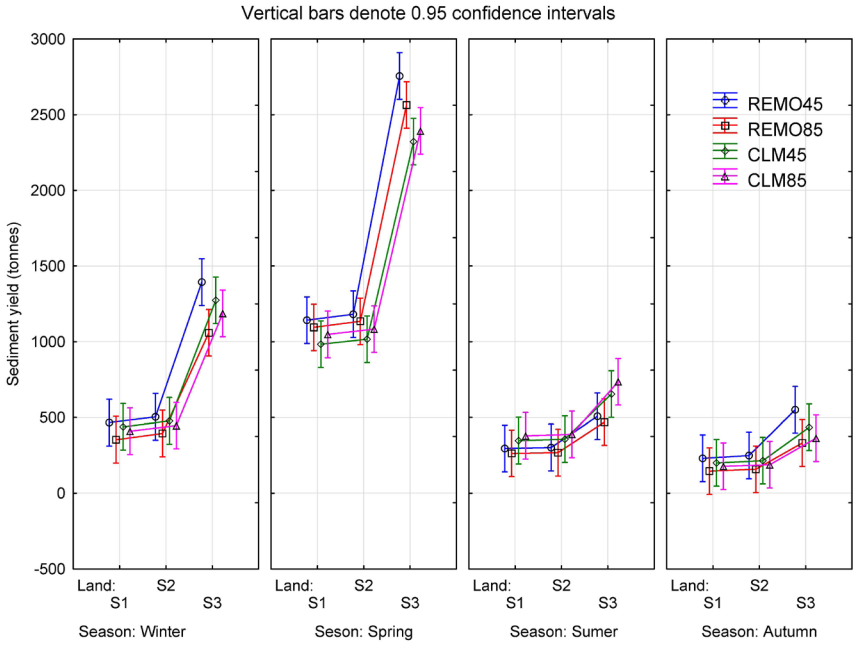

Figure 4.43. Average seasonal sediment yield (tonnes) projected for the 2020–2100 period in all climate and land use change scenarios.

4.6. Analysis of the frequency of the projections in the evolution of the annual surface runoff, water discharge and sediment yield

4.6.1. Methodological notes

Given that the detailed analysis undertaken in chapters 4.2–4.5 provided a wide range of the projected results, the question still remains justified: what is the overall trend of surface runoff, water discharge and sediment yield evolution for the next eight decades (2020-2021)?

To find this answer, we proceeded to design a "frequency matrix" considering the annual values of the three parameters analysed, for each considered period: 2020–2039, 2040–2069 and 2070–2100.

As is shown in the graphs that will be presented in Annex 4 (Figures 4.44, 4.45, 4.46), such a "matrix" consists of a network of cells with the number of lines equal to the number of years for each period (20, 30, 31 years), and the number of columns being equal to 12, number that results from the four climate change scenarios each of them coupled with the three land use change scenarios.

The three colours used in the matrix field show the trend of the analysed parameter, compared to the baseline: red is used to highlight the increasing trend (when the simulated value is higher than the value from the baseline), colour blue highlights the decreasing trend (when the simulated value is lower than the baseline value), while the yellow colour was used to highlight the same trend, namely for the cases when projected values are equal to the baseline value.

On the vertical column from the right side of each matrix and on the two horizontal columns positioned at the base of the matrix field, are inscribed, as ratio, two digits, both next to each year and each studied climate and land use change scenario. The first digit (entered in the ratio numerator) is equivalent to the number of cells coloured in red and quantifies the frequency of increasing trend of the analysed parameter; the second digit (entered in the ratio denominator), is equivalent to the number of cells coloured in blue and shows the frequency of decreasing trend of the same parameter.

4.6.2. Assessing the frequency matrices developed on considered periods

4.6.2.1. Surface runoff matrix

The frequency matrix of the projected surface runoff for the 2020–2039 period (Figure 4.44-a, Annex 4) highlights the following (Marin et al., 2020b):

- the frequency ratio of the projected surface runoff shows an obvious increasing trend of this parameter (208/32);
- for half of the total number of years of this period (10 out of 20), the surface runoff is characterized only by an increasing trend; in addition, for all the constituent years of the analysed period we notice and overall increasing trend;
- a balanced situation between the increasing and decreasing trends is recorded for 2035, when the frequency ratio obtained is quite similarly (7/5);
- no significant differences in the surface runoff dynamics were noticed in the land use change scenarios; however, a slightly more pronounced decreasing trend was observed in scenario S1, while the increasing trend is more pronounced in scenario S3;
- clear prevalence of the increasing trend can be observed in all climate change scenarios; the lowest values of surface runoff are projected in CLM8.5, while the highest increases of this parameter are projected in REMO8.5.

Analysing the frequency matrix designed for the second period considered (2040–2069) we notice the following (figure 4.44-b, Annex 4):

- the frequency ratio of the increasing and decreasing trend is quite similar

to the one obtained for the previous period, but with slightly more pronounced values for both trends (297/63);

- for 27 of the 30 years of the analysed period can be noticed that the increasing trend prevails; for 10 of the total of 30 years is projected only an increasing trend of surface runoff; a quite balanced situation of the frequency ratio between the increasing and decreasing trend is obtained for 2052 (7/5), while for 2053 an equal frequency ratio was obtained (6/6); instead, for 2056 seven values of out 12 indicate a decreasing trend of surface runoff;
- the most pronounced decreases in surface runoff are projected in scenario S1, while for scenarios S2 and S3 the situation is quite similar; conversely, scenario S3 generates the highest increases of surface runoff;
- the sharpest decreasing trend of surface runoff is projected in CLM4.5 and REMO8.5, while the higher increases of this parameter are projected in REMO4.5 and CLM8.5.

For the third period (2070–2100), the surface runoff frequency matrix highlights the following aspects (Figure 4.44-c, Annex 4):

- the frequency ratio (263/109) shows that, unlike the previous periods, the decreasing trend of surface runoff is more pronounced, while the increasing trend is lower compared to the second period and more pronounced compared to the first;
- for 19 of the total of 31 years of the third period prevails the increasing trend; instead, the prevalence of the decreasing trend is projected for a single year (2092), when 10 of the 12 values indicate the surface runoff decrease; an equal trend of the frequency ratio (6/6) is noticed for five of the total of 31 years of the analysed period;
- on land use change scenarios, the frequency matrix indicates a similar trend as in the previous periods, respectively a more pronounced decreasing trend in scenario S1, while the increases are projected particularly in scenario S3;
- on climate change scenarios, we distinguish that the sharpest decreases in surface runoff are projected in REMO8.5 and CLM8.5, while the largest increases are projected in REMO4.5 and CLM4.5.

4.6.2.2. Water discharge matrix

For the 2020–2039 period (Figure 4.45-a, Annex 4), the frequency matrix designed shows the following (Marin et al., 2020b):

- the frequency ratio of water discharge reveals a clear prevalence of the increasing trend (171/69);
- for 15 of the total of 20 years of the analysed period prevails the increas-

ing trend, while for four of the 20 years, is forecasted only an increasing trend; instead, the prevalence of the decreasing trend is projected only for two years from the total number of years of the analysed period; a balanced situation (6/6) of the frequency ratio between the increasing and decreasing trend is projected for three of the total of 20 years of the period;

- on land use change scenarios, no significant differences are observed for none of the two trends, the projections being relatively similar in all scenarios applied;
- the frequency matrix developed on climate models highlights a more pronounced decreasing trend in REMO4.5 and CLM4.5; conversely, REMO8.5 and CLM8.5 show a more accentuated increasing trend.

For the second period (2040-2069), the water discharge frequency matrix (figure 4.45-b, Annex 4) highlights the following aspects:

- the frequency ratio (258/99), reveals an obvious increasing trend, much more accentuated compared to the previous periods;
- the prevalence of the increasing trend is highlighted in 22 of the total of 30 years, while for six of the 30 years, is projected only an increasing trend; instead, the decreasing trend prevails for two years of the total of 30 years; a balanced situation of the frequency ratio (6/6) is projected for five years; for 2043, we distinguish relatively equal trends when 6 value indicate the increases and 5 value indicates decreases; the opposite situation (six values indicate the decrease of the water discharge while its increase is indicated by five of the total 12 values) can be noticed for 2045; for three years (2043, 2045, 2061) we observe that the projected values are equal to the baseline values;
- on the land use change scenarios, there were no significant differences in the variation trend; however, a slightly more pronounced decreasing trend was obtained for scenario S1 coupled with REMO4.5 and CLM4.5;
- on climate change scenarios, a more pronounced decreasing trend is observed in REMO8.5 and CLM4.5 models, while the increasing one is more accentuated in REMO4.5 and CLM8.5.

The analysis of the water discharge frequency matrix for 2070–2100 period (figure 4.45-c, Annex 4) shows that:

- an obvious prevalence of the increasing trend (240/128);
- for 17 of the 31 years prevails the increasing trend, while the decreasing trend prevails for five of the total of 31 years of the period; an equal frequency ratio can be observed for seven years (2070, 2079, 2081, 2084, 2091, 2092, 2099); as in the previous period, we encounter the situation in which the simulated values are equal to the baseline (in four cases out of the total of the 372 possible);

- in the context of REMO models coupled with land use scenarios, we do not distinguish different trends of water discharge variation, while for CLM model the trends of water discharge variation are very little differentiated;
- on climate change scenarios, the sharpest water discharge decrease is projected for the REMO8.5, while the increasing trend is more pronounced in CLM8.5.

4.6.2.3. Sediment yield matrix

The configuration of the frequency matrix designed for the 2020–2039 period (Figure 4.46-a, Annex 4), highlights the following (Marin et al., 2020b):

- overall, the frequency ratio is quite balanced (123/117), a clear prevalence of a certain trend cannot be sustained;
- for almost half of the number of years of the considered period (respectively in nine out of 20) prevails the increasing trend, while for six years the prevalence is reversed; the frequency ratio shows an equal trend for five years;
- year 2022 reveals that nine out of the 12 projected values indicate an increasing trend of sediment yield, while the opposite situation is observed for 2036;
- on climate change scenarios, we notice REMO4.5 and CLM4.5 generate values that are, in most cases, in the decreasing trend, while REMO8.5 and CLM8.5 indicate the increasing trend;
- scenario S3 leads, in all or almost all cases regardless of climate change scenario or year analysed, to the sediment yield increases;
- for scenarios S1 and S2 an overall decreasing trend is projected, particularly in REMO4.5 and CLM4.5.

In the second period (2040–2069), the frequency matrix of sediment yield (figure 4.46-b, Annex 4) highlights the following aspects:

- the prevalence of the decreasing trend (210/150) is more pronounced compared to the previous periods;
- for five of the 30 years of the studied period prevails the increasing trend of sediment yield; instead, the prevalence of the decreasing trend is projected for 19 of the total of 30 years; an equal frequency ratio (6/6) is projected for six years;
- the sharpest decreases of sediment yield are projected in scenarios S1 and S2, while the highest increases are projected in scenario S3;
- the decreasing trend prevails in all climate change scenarios; the sharpest decreases are projected in REMO8.5 and CLM8.5, while the highest increases are projected in REMO4.5 and CLM4.5.

The frequency matrix of the projected sediment yield for 2070–2100 (Figure 4.46-c, Annex 4) shows that:

- the frequency ratio of sediment yield shows an obvious decreasing trend (240/132) more pronounced compared to the previous periods; instead, the increasing trend is lower compared to the second period and more pronounced compared to the first;
- only for three of the 31 years of the analysed period prevails the increasing trend; instead, the prevalence of the decreasing trend is projected for 23 of 31 years; an equal frequency ratio was obtained for four years;
- on the land use change scenarios generate in the frequency matrix reveals a similar situation as in the previous period: insignificant differences in scenarios S1 and S2, while scenario S3 shows both the highest increases and decreases of sediment yield;
- the decreasing trend prevails in all climate change scenarios; the decreases can be observed mainly in REMO8.5 and CLM8.5, while the maximum increases are projected in REMO4.5 and CLM4.5.

4.6.3. The result of forecasts at the level of the entire period studied

If we analyse the three frequency matrices for the entire studied period (2020-2100) we distinguish that the increasing trend prevails for a certain number of years, but only for surface runoff and water discharge. Regarding the sediment yield, this exclusive prevalence is no longer highlighted.

To emphasize this, in Table 4.37 we listed the years of the entire studied period and we highlighted the exclusive prevalence of the increasing trend of the parameters analysed, in all climate and land use change scenarios. Thus, from the total of the 81 years of the entire period, were identified 28 years for surface runoff and 16 years for water discharge, for which the increasing trend prevails, in all 12 combinations of scenarios considered in the simulation. The simultaneously increases of surface runoff and water discharge are noticeable for a total of 14 years: 2021, 2022, 2023, 2026, 2040, 2042, 2044, 2047, 2048, 2064, 2071, 2073, 2078, 2090.

Table 4.37. Highlighting the years with an exclusive prevalence of increases tendency of the considered parameters within the entire studied period.

Period	Year	Considered parameters		
		Surface runoff	**Water discharge**	**Sediment yield**
2020-2039	2020	-	-	-
	2021			-
	2022			-
	2023			-
	2024		-	-
	2025		-	-
	2026			-
	2027	-	-	-
	2028		-	-
	2029		-	-
	2030	-	-	-
	2031			-
	2032	-	-	-
	2033	-	-	-
	2034	-	-	-
	2035	-	-	-
	2036	-	-	-
	2037	-	-	-
	2038	-	-	-
	2039		-	-
2040-2069	2040			-
	2041	-	-	-
	2042			-
	2043	-	-	-
	2044			-
	2045	-	-	-
	2046	-	-	-
	2047			-
	2048			-
	2049		-	-
	2050	-	-	-
	2051	-	-	-
	2052	-	-	-
	2053	-	-	-
	2054		-	-
	2055	-	-	-
	2056	-	-	-
	2057		-	-
	2058	-	-	-
	2059	-	-	-
	2060		-	-
	2061	-	-	-
	2062	-	-	-
	2063	-	-	-
	2064			-
	2065	-	-	-
	2066	-	-	-
	2067	-	-	-
	2068	-	-	-
	2069	-	-	-

Period	Year	Considered parameters		
		Surface runoff	**Water discharge**	**Sediment yield**
2070-2100	2070	-	-	-
	2071			-
	2072	-	-	-
	2073			-
	2074	-	-	-
	2075	-	-	-
	2076		-	-
	2077		-	-
	2078			-
	2079	-	-	-
	2080	-	-	-
	2081	-	-	-
	2082	-	-	-
	2083	-	-	-
	2084	-	-	-
	2085	-	-	-
	2086	-	-	-
	2087	-	-	-
	2088	-	-	-
	2089	-	-	-
	2090			-
	2091	-	-	-
	2092	-	-	-
	2093	-	-	-
	2094		-	-
	2095	-	-	-
	2096	-	-	-
	2097		-	-
	2098	-		-
	2099	-	-	-
	2100	-		-

On the other hand, if we centralize the frequency ratios obtained for each studied parameter, we can introduce in the analysis a new coefficient named "prevalence factor - Fp" (computed by dividing the numerator and the denominator value of the frequency ratio).

Thus, we can note the following:

1. For surface runoff (Table 4.38 and Figure 4.47-a):

- the prevalence factor for the total number of years is 3.76, which shows an obvious prevalence of the increasing trend compared to the decreasing one;

- on climate models, the prevalence factor varies from 2.47 to 5.75, the highest values being obtained in REMO4.5 and CLM4.5 and the lowest values in REMO and CLM8.5;

- on climate and land use change scenarios, the variation of the prevalence factor is much wider, from 1.89 to 7.10.

2. For water discharge (Table 4.39 and Figure 4.47-b):

- the value of the prevalence factor for the total years is 2.26, lower than the value obtained for surface runoff;

- on climate and land use change scenarios, the prevalence factor varies between 1.35 and 3.39, the values being smaller compared to the one obtained for surface runoff;

- on climate change scenarios, the prevalence factor varies between 1.37 and 3.29; the highest values being obtained in REMO4.5 and CLM8.5 and the lowest in CLM4.5 and REMO8.5.

Therefore, for water discharge, the differences of the prevalence factor in relation to the land use change scenarios are not as wide as in the case of surface runoff. The prevalence factor has the lowest values in scenario S1 excepting CLM8.5 where the lowest value was obtained in scenario S2. On the other hand, the highest values of the prevalence factor can be observed in scenario S3 coupled with REMO 4.5 and CLM4.5, while REMO8.5 and CLM8.5 shows quite similar prevalence factor values obtained for scenarios S2 and S3.

Table 4.38. The prevalence factor (Fp) of surface runoff obtained for the entire studied period, in all climate and land use change scenarios.

Period	Trend	REMO4.5			CLM4.5			REMO8.5			CLM8.5			TOTAL	F_p
		S1	S2	S3	S1	S2	S3	S1	S2	S3	S1	S2	S3		
2020–2039	+	16	18	18	17	17	19	19	19	19	15	15	16	208	6,50
	-	4	2	2	3	3	1	1	1	1	5	5	4	32	
2040–2069	+	26	27	28	24	24	24	20	23	24	23	27	27	297	4,71
	-	4	3	2	6	6	6	10	7	6	7	3	3	63	
2070–2100	+	24	25	25	23	25	28	14	17	18	18	21	24	263	2,41
	-	7	6	6	8	6	3	17	14	13	13	10	7	109	
Total	+	66	70	71	64	67	71	53	59	61	56	63	67	768	
	-	15	11	10	17	14	10	28	22	20	25	18	14	204	
	F_p	4,40	6,36	7,10	3,76	4,79	7,10	1,89	2,68	3,05	2,24	3,50	4,79		
Total	+	207			202			173			186			768	
	-	36			41			70			57			204	
	F_p	5,75			4,93			2,47			3,26			3,76	

Table 4.39. The prevalence factor (Fp) of water discharges obtained for the entire studied period, in all climate and land use change scenarios

Period	Trend	REMO4.5			CLM4.5			REMO8.5			CLM8.5			TOTAL	F_p
		S1	S2	S3	S1	S2	S3	S1	S2	S3	S1	S2	S3		
2020–2039	+	14	14	14	13	13	13	15	15	15	15	15	15	171	2,48
	-	6	6	6	7	7	7	5	5	5	5	5	5	69	
2040–2069	+	23	25	25	20	20	20	18	19	19	23	23	23	258	2,61
	-	6	5	5	10	10	9	11	11	11	7	7	7	99	
2070–2100	+	23	23	23	20	21	21	13	13	13	24	23	23	240	1,88
	-	8	8	8	11	10	9	18	18	18	7	7	6	128	
Total	+	60	62	62	53	54	54	46	47	47	62	61	61	669	
	-	20	19	19	28	27	25	34	34	34	19	19	8	296	
	F_p	3,00	3,26	3,26	1,89	2,00	2,16	1,35	1,38	1,38	3,26	3,21	3,39		
Total	+	184			161			140			184			669	
	-	58			80			102			56			296	
	F_p	3,17			2,01			1,37			3,29			2,26	

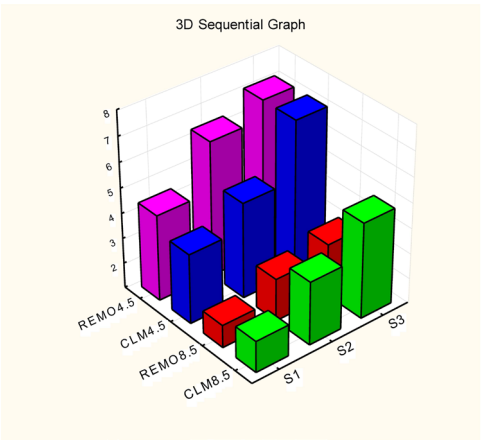

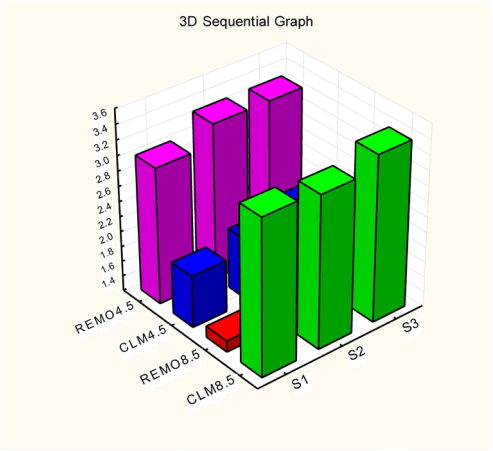

a) **b)**

Figure 4.47. The prevalence factor for surface runoff (a) and water discharges (b).

4.7. Brief summary and conclusions derived from the projected surface runoff, water discharge and sediment yield

4.7.1. Surface runoff

▪ Monthly surface runoff

In the short term (2020–2039), compared to baseline, both increases and decreases of the monthly surface runoff are projected. Decreases of up to 75% of this parameter are projected In June-August, the lowest values being obtained especially REMO4.5. The surface runoff increases are projected starting with September, the highest values of this parameter, 8.7 times fold compared to the baseline being projected for February under CLM4.5. The decreasing trend is more pronounced in scenario S1, while the highest increases of this parameter are projected in scenario S3.

In the medium term (2040–2069), the projected monthly surface runoff can register both increasing and decreasing trend compared to the baseline. The decreases up to 78% are projected for June, July and August in all climate scenarios, particularly in REMO4.5 and 8.5. The exception is July, when surface runoff is projected to increase by up to 26% in CLM4.5 and 8.5. The decreases by up to 68% are projected also for April, May and October in CLM scenarios, but also in September, in REMO8.5 coupled with scenario S1 when this parameter can decrease by 10%. A sharp increase is estimated for December-February, when the surface runoff can be up to 10 times higher due to the temperature and precipitation increments by 1–3 °C and 46% respectively. The decreasing trend is more pronounced in scenario S1, while the increasing one is more accentuated in scenario S3.

In the long term (2070–2100), the exclusive decreasing trend is also projected for June-August, when the monthly surface runoff can decrease by 1–69%, the lowest values being estimated with REMO4.5 and 8.5. The decrease by up to 58% is projected for April in all climate change scenarios, but also in March in the REMO8.5 and CLM8.5, when the surface runoff can decrease by 10–25%. The most important increases (8–11 times fold than the baseline) are projected for February, the highest values being obtained in CLM4.5 and 8.5. Scenario S1 generates the most significant decreases, while scenario S3 leads to the highest increase in the monthly surface runoff.

▪ **Seasonal surface runoff**

In the short term (2020–2039), during the spring, this parameter is projected to slightly decrease by 2% (CLM4.5), and also to increase between 4–86%, particularly in REMO8.5 and CLM8.5. In summer, the surface runoff can decrease by up to 69%, especially in REMO4.5 and 8.5. In autumn, is projected an increase of 70–248%, the highest values being obtained in REMO4.5 and CLM4.5. During winter, the surface runoff can register a sharp increase up to 319%, which can be attributed to the increments of temperature and precipitation by up to 1.5 °C and 35–60% respectively, but also to the land use change. The increasing trend is more pronounced in REMO4.5 and CLM4.5. The decreasing trend is more accentuated in scenario S1, while scenario S3 can lead to the most accentuated increases of this parameter.

In the medium term (2040–2069), the surface runoff during spring is projected to either decrease by 1% in CLM4.5, or to increase by 4–37%, particularly in REMO scenarios. In summer, the surface runoff can register a decrease of 15–57%, while in autumn this parameter will increase up to 194% particularly in REMO4.5 and CLM4.5. The most significant increases are projected in the winter months, when the surface runoff can increase by 2.5–4.6 times fold, due to the increments of temperature and precipitation of up to 2.6 °C and 70% respectively. The most pronounced increases and decreases are projected in REMO4.5 and CLM4.5. On land use change scenarios, scenario S1 generates the most significant decreases, while the increases are more pronounced in scenario S3.

In the long term (2070–2100), the projected surface runoff for spring can increase by 2–14% in the REMO4.5 and CLM4.5, can decrease by 1–28%, particularly in CLM8.5. In summer, is projected a decrease by 14–60%, the trend being more pronounced in REMO4.5 and 8.5. In autumn, surface runoff can increase two times fold compared to the baseline, especially in REMO4.5 and CLM4.5. In winter, the increases of this parameter by 3.4–4.7 times fold compared to the baseline are projected due to the increments of temperature and precipitation by 2–4 °C and 55% respectively. The decreasing is more accentuated in scenario S1, while the increases are more pronounced particularly in scenario S3.

▪ **Annual surface runoff**

In the short term (2020–2039), compared to the baseline, the annual surface runoff can register both decreases of up to 58% and increases between 1–226%. The decreasing trend is more pronounced in scenario S1, while in scenario S3 is projected the highest increases. Among climate change scenarios,

the most pronounced impact on surface runoff is projected in REMO8.5 and the most reduced in CLM4.5. The multiannual average surface runoff for this period is 27–87% higher than the baseline, the most pronounced increases being projected in REMO8.5, while the smallest in CLM4.5. For all scenarios, the highest values are projected in scenario S3.

In the medium term (2040–2069), the annual surface runoff can either decrease by up to 58% or increase two times fold than the baseline, the projected values being similar to the previous period. The most pronounced changes of this parameter are projected in REMO4.5 and CLM4.5, while less accentuated are projected in REMO8.5 and CLM8.5. The decreasing trend is more pronounced in scenario S1, while the increasing one is in scenario S3. The multiannual average of this period is 35–67% higher than the baseline, the largest increases being projected in REMO4.5 coupled with scenario S3, and the smallest increases in REMO8.5 coupled with scenario S1.

In the long term (2070–2100), it is projected that the annual surface runoff to decrease by up to 53%, but also increase by up to 192%, the value being slightly lower than the previous periods. The decreasing trend appears especially in REMO8.5 coupled with scenario S1, and the increasing trend in REMO4.5 coupled with scenario S1. Compared to the baseline, the multiannual average of this period is between 10–57%, the highest increases being projected in REMO4.5 coupled with scenario S3, and the smallest to the REMO8.5 coupled with scenario S1.**4.7.2. Water discharge**

- **Monthly water discharge**

In the short term (2020–2039), it is projected that the monthly water discharge can decrease by up to 53% in June-September (in all climate change scenarios), particularly in REMO8.5. Lower values, by up to 21%, are also projected for April-May, but only in CLM4.5. Starting with October, the monthly water discharge is projected to increase, the highest values being obtained for February, when, in CLM4.5 and 8.5, the projected flows are 7–8 times higher compared to the baseline. The decreasing trend of this parameter is quite similar on land use change scenarios, but the increasing trend is more pronounced particularly in scenario S3.

In the medium term (2040–2069), the monthly water discharge can decrease by up to 63% in June – September, the lowest values being projected in REMO8.5. A decrease by up to 10% compared to the baseline is projected for April in CLM4.5 and 8.5, but also for October when in REMO4.5 and 8.5 this parameter can decrease by 8–24%. The exclusive increasing trend is projected for November-March, the highest increases, eight times higher, being obtained

in February (CLM8.5). Scenario S1 generates the lowest water discharges, while the highest are projected under scenarios S2 and S3.

In the long term (2070–2100), a decrease between 10–63% of this parameter is projected for July-September, but also for April (up to 17%) in the CLM scenarios and October (up to 11%) in REMO8.5. During November–March, the water discharge is projected to increase compared to the baseline, particularly in February, when the increases 8–11 times fold are projected especially in CLM8.5. On land use change scenario, the increasing trend is more pronounced in scenario S3.

▪ **Seasonal water discharge**

In the short term (2020–2039), the water discharge is projected to decrease in spring by up to 75%, the sharpest decreases being obtained in REMO8.5 and CLM8.5. In summer, this parameter can decrease by up to 44%, particularly in REMO4.5. During autumn, the water discharge can register either a slight decrease of 3%, in REMO8.5 either an increase up to 73%, particularly in REMO4.5. In winter, the projected water discharge shows an increase by 2–3 times higher than the baseline, the highest values being noticed in REMO4.5 and CLM4.5. There are no significant differences between water discharge dynamics on land use change scenarios.

In the medium term (2040–2069), the projected water discharge for spring shows an increase of 14–41%, particularly in REMO4.5. In summer, this parameter can decrease by up to 38%, especially in REMO8.5. For autumn, both decreases (by 5–13% in REMO8.5 and CLM8.5) and increases (up to 20%, particularly in CLM4.5) are projected. Increases of 2.5–3.8 times fold compared to the baseline are projected for winter, the highest values being obtained in REMO4.5 and CLM4.5. Scenario S1 generates the most pronounced decreases of this parameter, while scenario S3 generates the most significant increases, but only in the winter season.

In the long term (2070–2100), this parameter is projected to increase in spring by up to 32% (particularly in REMO4.5). In summer, the water discharge is projected to decrease between 24–43%, especially in REMO8.5. In autumn, the projected trend shows both decreases by 13–15% in REMO8.5, and increases between 2–23%, more accentuated in REMO4.5. During winter, the water discharge is projected to reach values of 3–5 times higher than the baseline, the most pronounced increases being noticed in REMO8.5 and CLM8.5. The decreasing trend is slightly more pronounced in scenario S1, and the increasing trend is more accentuated in scenario S3.

▪ **Annual water discharge**

In the short term (2020–2039), the water discharge can either decrease by up to 35% or increase by up to 116%. The increasing trend is more frequent in REMO8.5, while decreasing appears especially in CLM4.5. On land use change scenarios, the decreases are more pronounced in scenario S1, while the increases are more accentuated in scenario S3. The multiannual projections show an increase of up to 13–33% of the annual water discharge.

In the medium term (2040–2069), the annual water discharge is projected to decrease by up to 49%, or to increase two times fold compared to the baseline. The increasing trend is more frequent in REMO4.5, while the most decreases are noticed especially in REMO8.5. On land use change scenarios, the decreases are more pronounced in scenario S1, while the increases are more accentuated in scenario S3. The multiannual average of water discharge is quite similar to the one from the previous period, the water discharge increases being between 14–29%.

In the long term (2070–2100), the water discharge can register both decreases up to 53% and increases between 1–101%. The decreasing trend is more frequent in REMO8.5 and the increasing one in CLM8.5. The decreases are more accentuated in scenario S1, while the increases are more pronounced in scenario S3. The multiannual water discharge is slightly lower compared to the previous period, increases between 5% and 26% compared to the baseline being projected.

4.7.3. Sediment yield

▪ **Monthly sediment yield**

In the short term (2020–2039), this parameter is projected either to decrease between 1–68% either to increase by up to approximately 11 times fold compared to the baseline. The decreasing trend is noticed mainly for June – August, particularly in REMO4.5, while the most pronounced increases are projected for February especially in CLM4.5. On land use change scenarios, the decreasing trend is more pronounced in scenario S1, and the increasing one in scenario S3.

In the medium term (2040–2069), a decrease between 5–70% of sediment yield is projected the lowest values were obtained for August in REMO8.5. The highest increase is projected for February, when, compared to the baseline, CLM8.5 shows an increase 13 times fold increase in scenario S3.

In the long term (2070–2100), during March – April, the monthly sediment yield is projected to decrease by up to 68%, the lowest values being obtained in REMO8.5. The exception is May, for which are projected increases between 5–194% of sediment yield (especially in REMO4.5 coupled with scenario S3). However, the sharpest increases are projected for February when increases of 3–14 times fold compared to the baseline are projected particularly in CLM4.5.

▪ **Seasonal sediment yield**

In the short term (2020–2039), both trends are projected for spring: decreases by up to 37% in CLM4.5 and increases by 47–120%, more accentuated in REMO8.5. In summer, the sediment yield is projected to decrease by 18–57% (more accentuated in REMO4.5) or can increase by 28–46% (in CLM scenarios). Both trends are projected for autumn, when sediment yield can either decrease up to 16% in REMO8.5 or increase by 13–201%, the maximum values being observed in REMO4.5. In winter, the sediment yield shows an exclusive increasing trend, the highest values being projected in REMO4.5. Among land use change scenarios, the sharpest decrease is projected in scenario S1, while the most pronounced in scenario S3.

In the medium term (2040–2069), during spring is projected both a decrease up to 45% of this parameter, more accentuated in REMO4.5 and CLM4.5, and also an increase up to 69% in REMO4.5 model coupled with scenario S3. In summer, sediment yield is projected to decrease up to 50%, excepting of CLM4.5 and 8.5 coupled with scenario S3 that shows an increase of 5–28%. In autumn, the sediment yield can either decrease up to 31%, in CLM8.5, or increase by 56–117% in all climate change scenarios coupled with scenario S3. During winter, this parameter is projected to increase by 32–476%, the higher values being observed in REMO4.5 and CLM4.5 coupled with scenario S3.

In the long term (2070–2100), the projected sediment yield for the spring months shows a decrease up to 59%, (especially in REMO8.5) and an increase by 30–58% (in REMO4.5 and CLM4.5 coupled with scenario S3. In the summer months, this parameter can either decrease up to 60% (REMO8.5) or increase by about 20% in CLM4.5 and 8.5 coupled with scenario S3. In autumn, this parameter can register a decrease of up to 33% (in REMO8.5) and an increase between 44–209%, (more accentuated in REMO4.5 and CLM4.5). In the winter months, a sharp increase in sediment yield is expected, the projected values being up to five times higher (REMO4.5 coupled with the scenario S3) compared to the baseline.

▪ **Annual sediment yield**

In the short term (2020–2039), the annual sediment yield can either decrease up to 70%, or increase up to 307% compared to the baseline. The most significant decreases can be noticed in CLM4.5, while the sharpest increases are projected in REMO8.5 coupled with scenario S3. Compared to the baseline, the multiannual average of sediment yield shows either the higher values (by 70–105%), but only in scenario S3 or slightly lower values (by 8–24%) in scenarios S1 and S2.

In the medium term (2040–2069), a decrease up to 82%, is projected in CLM4.5 model coupled with scenario S1, and an increase up to 258% is projected in REMO4.5 model coupled with scenario S3. The projected multiannual average is either higher by 64–94% (scenario S3), either lower by 17–32% (in scenarios S1 and S2) compared to the baseline.

In the long term (2070–2100), the annual sediment yield is projected to decrease up to 80% or to increase up to 288% compared to the baseline. Both the largest increases and decreases are projected in REMO4.5. The decreasing trend is more pronounced in scenario S1, while the increasing one is more accentuated in scenario S3. Regarding the multiannual average, the projections are similar to the previous periods, the increases by 29–97% and decreases by 22–46% being projected.

4.7.4. The frequency of projected trends in the annual dynamics of surface runoff, water discharge and sediment yield

▪ **Annual surface runoff**

The frequency ratio of the projected annual surface runoff highlights the prevalence of the increasing trend in all periods analysed. The frequency ratio of the increasing trend is obtained for all 20 years of the short-term period, for 27 of the 30 years of the medium-term and for 19 of the total of the 31 years of the long term period. On the other hand, the frequency ratio of the decreasing trend is noticeable only for long time period, which is obtained only for four years. Exclusive increasing trend is obtained for 10 of the total number of years that constituent the short- and medium-term periods, while in the long term it is observed for eight years. On land use change scenarios, we distinguish that, in all considered periods scenario S1 generates the lowest values of the frequency ratio, while the highest appear in scenario S3.

The analysis of the frequency matrices on climate change scenarios shows that, in the short term, the frequency ratio of the increasing trend reaches maximum values in REMO8.5, while, in the medium and long term, those are obtained in REMO4.5 and CLM4.5. The frequency ratio of the decreasing trend is more pronounced in REMO8.5 and CLM8.5, in all considered periods.

The prevalence of the increasing trend of the annual surface runoff is also highlighted by the value obtained for the prevalence factor (3.76). The highest values of this factor are obtained in the REMO4.5 and CLM4.5, and the lowest in REMO8.5 and CLM8.5. The variation of the prevalence factor on land use change scenarios highlights the fact that scenario S1 will generate the lowest values, while scenario S3 generates the maximum values of the annual surface runoff. In addition, the increasing trend of annual surface runoff is more pronounced in the short term, when the value of the prevalence factor is 6.50. Instead, is the long term, the prevalence factor has a value of 2.41, which means that the increased trend of surface runoff is lower in the third considered period.

- **Annual water discharge**

A prevalence of the frequency ratio of the increasing trend can be observed in all considered periods. If in the first period, the frequency ratio of the increasing trend prevails for 15 of the total of 20 years, on medium and long term, can be observed for 22 and 17 years respectively. In addition, on short term, an exclusive increasing trend of the frequency ratio is obtained for four years, while on medium and long term it is projected for five years. The frequency ratio of the decreasing trend prevails only for two years from the short-term period, for one year in the medium term and for four years on long term. Regarding the land use change scenarios, no noticeable differences can be observed between the frequency ratios of the two trends. Conversely, on climate change scenarios, on short and long term, REMO8.5 and CLM8.5 will generate the highest frequency ratios of the increasing trend, while, on medium term, the higher values of the frequency ratio are obtained in REMO4.5. The frequency ratio of the decreasing trend is higher in CLM4.5 but only on short term, while on medium and long term it is obtained in REMO8.5. Even if the value of the prevalence factor for water discharge (2.26) is slightly lower than the one obtained for surface runoff, the increasing trend prevails also for this parameter. Similar to the previous parameter, the lowest value of the prevalence factor for water discharge is projected in scenario S1 and the highest values in scenario S3. On climate change scenarios, both the lowest and the highest value of the prevalence factor are obtained in REMO8.5 and CLM8.5. On the three considered periods, the largest increases of water discharge (Fp = 2.61) are observed on medium term and the lowest (Fp = 1.88) on long term.

- **Annual sediment yield**

The frequency ratio of the sediment yield is quite balanced, but only on short term. On medium and long term, contrary to those obtained for surface runoff and water discharge, we observe that prevail the decreasing trend. The frequency ratio of the increasing trend is obtained for nine, five and three years respectively (short term, medium term, long term respectively). Instead, the frequency ratio of the decreasing trend is obtained for six years (short term), 19 years (medium term) and 23 years (long term). On land use change scenarios, the frequency ratio of the increasing trend reaches the highest values in scenario S3, while the decreasing trend reach the highest values of the frequency ratio in scenario S1. On climate change scenarios, the frequency ratio of increasing trends is higher in the CLM8.5 (short-term) but also in REMO4.5 (medium-term) and CLM4.5 (long-term). Conversely, the frequency ratio of the decreasing trend reaches the highest values in CLM4.5, but only on short term, while on medium and long term are observed in REMO8.5 and CLM8.5.

5. FINAL CONCLUSIONS, PERSONAL CONTRIBUTIONS, PRACTICAL RECOMMENDATIONS, DISEMINATION RESULTS, FUTURE EXTENSIONS

5.1. Final conclusions

After analysing the current state-of-the-art knowledge and based on the current research performed, partial conclusions at the end of each chapter were drawn. In the following, are summarized the general conclusions of this research, highlighting the methodological premises considered:

1. Given the vulnerability of forest ecosystems and water resources to climate change, forecasting the hydrological impact in watersheds with different afforestation percentages is widely investigated to find answers such as:

- in the climate and land use change context, how will be modified the hydrological balance until the end of this century?

- how must be adapted the watershed management solutions to climate change induces that influence the availability of water resources and their quantity and quality?

2. In such an approach, is essential to take into account the land use change and the forest must be included in the assessment of the hydrological impact of climate change, through hydrological models. The SWAT hydrological model - calibrated and validated in this paper - is one of the most used models in studies focused on estimating the hydrological impact of climate change.

3. To scientifically substantiate the solutions for alleviating the negative effects of the hydrological impact of climate change, first of all, must be acknowledged the dimension of this impact through case studies performed in various watersheds, as has been done in the current research. This documentation allowed a deepened knowledge especially on researches that were carried out in watersheds, with the afforestation percentage and area (up to 100 km^2) as close as possible to the studied one.

4. One of the important stages within the research was that the averages of the climatic parameters that characterize the two regional climate change models (REMO and CCLM) were locally downscaled and adjusted both in agreement with climatic data taken from EURO-CORDEX, and climatic records from the surrounding meteorological stations (Predeal, Întorsura Buzăului and Ghimbav).

5. The analysis performed for 2020–2100 period did not show major differences in precipitation dynamics compared to the baseline (1961-2013), the percentage difference being only ± 3-5% between the projected multiannual averages and the baseline value. However, the most pronounced changes were

projected in climate change scenarios derived from RCP8.5. Regarding the temperatures, for 2020–2100 are projected increases in air temperature of 2–3.2 °C, with more pronounced increments in climate change scenarios developed from RCP8.5.

6. The hydrological impact of climate and land use change in the Upper Tărlung watershed was highlighted using the SWAT hydrological model. The projections regarding the evolution of three hydrological parameters (surface runoff, water discharge and sediment yield) for 2020–2100 (divided into three periods), were made considering four levels of analysis (monthly, seasonal, annual and multiannual level), four local climate and land use change scenarios. The 1979-1988 period was adopted as baseline.

7. According to the conclusions given in 4.9 subchapter, the projected results have a wide range due to the considered three time periods, each with four levels of analysis. The three hydrological parameters were evaluated under four local climate change scenarios and three land use change scenarios.

8. Despite the large variability of the projections, the future dynamics of the studied parameters are somewhat similar, if we refer to one and the same level of analysis (monthly/seasonal/annual/multiannual).

Thus, for the monthly level, the surface runoff, water discharge and sediment yield projections are either increasing or decreasing in all time periods; the largest increase is projected for February, and the decrease for June-August/ September.

During the seasons, the average monthly dynamics varies from one season to another. In spring, the water discharge shows an increasing trend over the entire period (2020–2100); instead, for surface runoff and sediment yield, we noticed an alternative trend some scenarios forecasting exclusively increases or decreases. In summer, both surface runoff and water discharge will decrease over the entire period, while sediment yield presents an alternative variation: increases (particularly in the short term) and decreases (especially in the rest of the studied interval).

In autumn, although surface runoff is projected to increase, water discharge and sediment yield will present a short-term increasing trend and a long-term decreasing trend.

In winter, all studied parameters show only the increasing trend in all time periods considered.

And at the annual level, the projected trend is alternative, increases or decreases, depending on the scenarios used and time period considered.

The multiannual average projected shows an exclusively increasing trend for surface runoff and water discharge in all scenarios considered. However, the

surface runoff shows a much broader increase, especially in REMO and S3 scenarios. Conversely, for sediment yield, is projected an alternative trend: increases in all climate change scenarios coupled with S3, and decreases in scenarios S1 and S2 (more pronounced in REMO scenarios).

9. For all studied parameters, regardless of the analysis level (monthly/seasonal/annual/multiannual), in the climate change context, the S1 scenario shows a decrease of considered parameters, while scenarios S2 and S3 show their increase (particularly scenario S3). Therefore, this confirms the well-known hydrological role of the forest, namely the reduction of surface runoff, mitigating flash floods and reducing sediment yield.

10. To highlight the future dynamics of the studied parameters from such a wide range of projected results, the question remains: for the next eight decades, what will be the annual prevailed trend in the evolution of surface runoff, water discharge and sediment yield?

In this respect, we designed the "frequency matrix of projections" for each of the studied parameters. These matrixes were subsequently analysed according to two own criteria: the frequency ratio and the prevalence factor. The overall prevalence of the increasing trend was observed for a certain number of years, but only for surface runoff and water discharge.

If we consider the entire studied period (2020–2100), from the total of 81 years, 28 years were identified for surface runoff and 16 years for water discharge, for which was projected an overall increasing trend.

The increasing trend for both surface runoff and water discharge were simultaneously projected for a number of 14 years, namely: 2021, 2022, 2023, 2026, 2040, 2042, 2044, 2047, 2048, 2064, 2071, 2073, 2078, and 2090.

Instead, for sediment yield, the prevalence of the increasing trend has not been observed.

11. For the total number of years of the study period, the prevalence factor is 3.76 for surface runoff and 2.26 for water discharge. Therefore, for these parameters, the projected annual values indicate an increasing trend compared to the baseline, trend that is 2-4 times more frequent than the values that foresees decreases.

On climate change scenarios, the prevalence factor varies from 2.47 to 5.75 for surface runoff and from 1.37 to 3.29 for water discharge. The highest values are assigned to REMO4.5 for surface runoff and to CLM8.5 for water discharge, while the lowest values correspond to REMO8.5 for both analysed parameters.

On climate and land use change scenarios, although the variation of the prevalence factor is wider in the case of surface runoff (from 1.89, differentiation of these values can be observed depending on the land use change scenario.

Thus, the lowest values are generated by scenario S1 and the highest by scenario S3. This proves that the forested areas are one of the amplifying factors in the future evolution of the studied hydrological processes particularly in the climate change context.

In the analysis performed on time periods, we notice a pronounced imbalance in the evolution of surface runoff, for which the prevalence factor decreases over time from 6.50 (in the first time period) to 4.71 (in the second time period) and 2.41 (in the third time period). For water discharge, the evolution of the prevalence factor is quite balanced and with much lower values (2.48 in the first time period). 2.61 in the second time period; 1.88 in the third time period).

12. The baseline values are consistent both with the data published in the 'Râurile României monography and with the data from a hydrology handbook (Pisota and Buta, 1975). Regarding the projected results, those are in line, to a large extent, with other results reported by studies performed in watersheds with similar characteristics.

13. Finally, we anticipate that some of the projected results may provoke scientific controversy in response to the following questions:

- how the inconsistencies between the much more accentuated evolution of the studied parameters compared to the attenuated dynamics of the precipitation amount can be explained?

- how the inconsistencies between the prevailed increasing trend for surface runoff and water discharge and the prevailed decreasing one obtained for sediment yield can be explained?

Other studies also report these inconsistencies that are considered as some of the limits that the SWAT model in small forested watersheds. Therefore:

- this model operates only with the amount of precipitation, without taking into account their duration and intensity;

- in the simulation are considered only the land use types, not the structural characteristics of the vegetation; or, for a mainly forested watershed, as is the studied one, this deficiency leads to an overestimation of the surface runoff and water discharge;

- on the other hand, the vegetation characteristics are too little integrated in the simulation process while soil characteristics are more detailed, thus the sediment yield can be more accurately captured.

5.2. Original contributions

Analysing the present research, the following personal contributions can be underlined:

▪ Highlighting the projected trends, at national and international level, on

the hydrological processes in the small forested watersheds during the 21st century;

▪ Applying, for the first time, the modelling process within the Upper Tărlung watershed by adapting the SWAT model to the local specificity and by a detailed customization of databases required;

▪ The methodology designed and adapted to watershed with an area smaller than 100 km^2, allows its replication in other studies, thus harnessing the forest management plan data source in the hydrological and climate modelling field. These data are easy to be uptake in SWAT, and the algorithms applied to fill in the missing data are also usable in other small watersheds;

▪ Projecting the evolution of precipitations and air temperature for 2020–2100 period under four climate change scenarios and three land use change scenarios;

▪ Simulating, within studied watershed, the dynamics of three hydrological processes in the context of climate and land use change scenarios;

▪ Projecting future trends in the dynamics of surface runoff, water discharge and sediment yield by quantifying the monthly, seasonal, annual and multiannual evolution of these parameters;

▪ Analysing the frequency of the projections made for studied parameters in the 2020–2100 period, by introducing, calculating and assessing the significance of two own indicators: the frequency ratio and the prevalence factor;

▪ Appraising the extent to which the results of this research are in line with those obtained in previous international research;

▪ SWAT modelling provides useful information both in terms of water resource availability (in quantitative and qualitative terms) and in establishing sustainable development policies (rural / urban / tourism);

▪ Depending on the communities' priorities and in direct relation with watershed land use (e.g., pasture extension, urban development), this study allows to spot the trade-offs necessary for achieving sustainable management of land use;

▪ This research facilitates the substantiation of the strategy of flood risk management plans for small watershed located in mountainous areas and including them in the modelling process for assessing the small watersheds contribution to floods occurrence;

▪ Finally, through the applied methodology and the analysis level of the results obtained, this research has a modest contribution to substantiate the measures and actions contained in Romania's National Strategy on Climate Change, in line with the latest decisions of the European Union in this regard.

5.3. Practical recommendations

After analysing of the projected results, we can bring to the attention of the scientific community and the responsible institutions the following recommendations:

1. Although the reduction of the forest area within the Upper Tarlung watershed is possible but improbable over the next eight decades, this study has the role of highlighting the importance of forests in alleviating the negative effects of climate change. Therefore, the first and most important recommendation is addressed to all institutions responsible for managing the land use within studied watershed to preserve as much as possible the current land uses and promote an optimal management from the hydrological point of view. Moreover, in the climate change context, the decision-makers should advocate for increasing the forested areas within the studied watershed;

2. It is recommended that decision-makers take into account the results obtained at multiannual level, as well as the conclusions drawn in the short, medium and long term, which offer the possibility to spatially (at subwatersheds level) and temporally (depending on decades with hydrological or erosional risk) stagger the intervention with torrent control structures of the torrential hydrographic network.

3. The modelling performed allows establishing the limits of land exploitation considering the land uses categories (animal husbandry, forest production, clean water production, biodiversity).

4. To prevent (or at least mitigate) the climate change hydrological impact, forestry practitioners should consider the scientific basis for sustainable management of forests with hydrological and soil protection functions and the adaptation of these forests to future climate changes (Florescu și Nicolescu, 1998; Leahu, 2001; Carcea și Seceleanu, 2004; Giurgiu 2004, 2006, 2008; Târziu, 2006; Florescu și Clinciu, 2009; Seceleanu, 2013; Barbu et al., 2016; Constandache et al., 2018) through:

- establishing optimal proportion by land use categories so that the productive capacity of the lands within the watershed to be exploited in a sustainable manner;
- promoting a ‘close to nature’ biocenotic structures, able to ensure the maintenance of the optimal quality of water resources in the years for which is projected increased trend of sediment yield;
- increasing the proportion of mixed stands with local species that are less vulnerable to changing climatic conditions;
- adaptation of the stands structure and composition both from the climate

and land use change perspective, and from the perspective of the possible changes on the altitudinal scale of forests.

5. The projected simultaneous increase in surface runoff and water discharge, which has been shown to be prevalent for a significant number of years (14), draws attention to the likelihood of exceeding the evacuation capacity of minor riverbeds, especially in the winter months. In this context, the responsible authorities should consider:

- the design of specific torrent control works to ensure the protection of the objectives in the area and the directed management of the floodwaters;
- the design of specific torrent control works to ensure the retention of sediment yield in the case of reduction of the forested area within the watershed;
- the design of adjacent structures to store large amounts of water estimated either for the winter or for years in which the increasing trend prevails, and their future use during water scarcity periods (especially in summer), but also in the years for which is projected significant decreases in surface runoff and water discharge.

It is recommended that, in all the situations aforementioned, be paid increased attention the promotion of ecological, environmentally friendly solutions, such as those described in recently published research (Niță, 2013; Clinciu et al., 2012, 2014, 2015; Adorjani et al., 2015; Davidescu, 2015; Clinciu și Niță, 2019; Tudose et al., 2020).

6. In the years for which is projected an increase in sediment yield, the Water Company (which manages the Water Plant) should adopt either additional measures to treat water turbidity through professional filtration systems and solutions, treatment and purification simultaneously with their delivery from Sacele Reservoir to consumers, or to resort to alternative sources for this purpose.

7. To alleviate the hydrological impact projected for the next eight decades, we consider it appropriate for the Brașov Metropolitan Area to advocate a revision of studies regarding the development of the Upper Tarlung watershed and propose to the decision-makers the development and implementation of new projects focused on ensuring sustainable and integrated management of land, forests, soil and water resources.

8. To facilitate the comparative analysis of the results obtained it is recommended that instead of the runoff volume (in cm) the height of the runoff layer (in mm) should be used.

5.4. Results dissemination

A. Papers published in ISI indexed journals

1. Cremades, R., Mitter, H., Tudose, N.C., Sanchez-Plaza, A., Graves, A., Broekman, A., Bender, S., Giupponi, C., Koundouri, P., Bahri, M., Cheval, S., Cortekar, J., Moreno, Y., Melo, O., Karner, K., Ungurean, C., Davidescu, S.O., Kropf, B., Brouwer, F., Marin, M., 2019: Ten principles to integrate the water-energy-land nexus with climate services for co-producing local and regional integrated assessments. Science of The Total Environment, vol. 693, 133662, https://doi.org/10.1016/j.scitotenv.2019.133662

2. Mihalache, A.L., Marin, M., Davidescu, Ș.O., Ungurean, C., Adorjani, A., Tudose, N.C., Davidescu, A.A., Clinciu, I., 2020: Physical status of torrent control structures in Romania. Environmental Engineering and Management Journal, vol. 19, nr.5.

3. Tudose, N.C., Ungurean, C., Davidescu, Ș.O., Clinciu, I., Marin, M., Niță, M.D., Adorjani, A., Davidescu, A.A, 2020: Torrential flood risk assessment and environmentally friendly solutions for small catchments located in the Romania Natura 2000 sites Ciucas, Postavaru and Piatra Mare. Science of The Total Environment, vol. 698, 134271, https://doi.org/10.1016/j.scitotenv.2019.134271

4. Marin, M., Clinciu, I., Tudose, N.C., Ungurean, C., Adorjani, A., Mihalache, A.L., Davidescu, A.A., Davidescu, Ș.O., Dincă, L., Cacovean, H., 2020: Assessing the vulnerability of water resources in the context of climate changes in a small forested watershed using SWAT: A review. Environmental Research, vol.184, 109330, https://doi.org/10.1016/j.envres.2020.109330

5. Tudose, N.C., Cheval, S., Ungurean, C., Broekman, A., Sanchez-Plaza, A., Cremades, R., Mitter, H., Kropf, B., Davidescu, Ș.O., Dincă, L., Cacovean, H., Marin, M., Miska, K., Pereira, P., 2020: Climate services for sustainable management of the Water–Energy–Land nexus under climate change in the Tărlung river basin, Romania. Land Use Policy (în curs de recenzare).

B. In extenso papers published in Proceedings of journals indexed in international database (BDI)

1. Marin, M., Clinciu, I., Tudose, N.C., Davidescu, Ș.O., Constandache, C., 2019: Assessing the performance of the Soil and Water Assessment Tool hydrological model for a small mountain forested watershed in the central part of Romania, in: GEOLINKS 2019 Conference Proceedings Book 3, vol. 1. SAIMA CONSULT LTD, pp. 265–273, https://doi.org/10.32008/geolinks2019/b3/v1/30

C. Papers published in BDI indexed journals

1. Marin, M., Clinciu, I., Tudose, N.C., Cheval, S., Ungurean, C., Davidescu, Ș.O., Adorjani, A., Mihalache, A.L., Davidescu, A.A., Tudose, O.N., 2020: Analiza previziunilor privind regimul termic și pluvial din bazinul hidrografic Tărlungul Superior în contextul schimbărilor climatice. Revista de Silvicultură și Cinegetică, nr 45, pp. 15–21.

2. Marin, M., Clinciu, I., Tudose, N.C., Cheval, S., Ungurean, C., Davidescu, Ș.O., Adorjani, A., Mihalache, A.L., Davidescu, A.A., Tudose, O.N., 2020: Simularea impactului schimbărilor climatice și al modificării folosinței terenului asupra proceselor hidrologice din bazinul hidrografic Tărlungul Superior. Revista Pădurilor, 135(3), 26 p.

D. Papers published in international database

1. Tudose, N.C., Ungurean, C., Marin, M., Mihalache, A.L., Davidescu, Ș., 2019: Meteorological research datasets collected from the Tarlung river basin using research infrastructure installed within the CLISWELN project. În 4TU.Centre for Research Data – Science Engineering Design, https://doi.org/10.4121/uuid:8cdfd0c6-1976-417c-bc20-7397f6382e7f

E. Papers presented at international symposia and conferences

1. Tudose, N.C., Babătă (actual Marin), M., Ungurean, C., Davidescu, Ș.O., Cheval, S., Crivăț, M., Adorjani, A., Davidescu, A.A., Constandache, C., 2018: Hydrological modeling of stream flow through the SWAT model in the Tarlung river basin (upperstream Sacele Lake). International Conference „Forest Science for a Sustainable Forestry and Human Wellbeing in a Changing World", Institutul Național de Cercetare Dezvoltare în Silvicultură „Marin Drăcea", 18–21 septembrie, București

2. Crivăț, M., Ungurean, C., Davidescu, Ș.O., Adorjani, A., Tudose, N.C., Davidescu, A.A., Babătă (actual Marin), M., 2018: Assessment of logging trails erosion coupled with timber harvesting. International Conference „Forest Science for a Sustainable Forestry and Human Wellbeing in a Changing World", Institutul Național de Cercetare Dezvoltare în Silvicultură „Marin Drăcea", 18–21 septembrie, București

3. Marin, M., 2019: Forest management to decrease energy consumption for urban water supply in a mixed groundwater and surface water system. 4th European Climate Change Adaptation Conference - ECCA, 28-31 mai, Lisabona, Portugalia

4. Marin, M., Clinciu, I., Tudose, N.C., Ungurean, C., Davidescu, Ș.O., Mihalache, A.L., Tudose, O.N., 2020: The impact of forest and climate change on seasonal dynamics of hydrological processes in Upper Tarlung watershed. 9TH International Symposium Forest and Sustainable Development. 16-17 octombrie, Brașov

5. Tudose, N.C., Ungurean, C., Marin, M., Davidescu, Ș.O., Mihalache, A.L., 2020: Assessing the hydrological impact of land and forest management change under climate projections in the Tarlung river basin (upstream Sacele Reservoir). 9TH International Symposium Forest and Sustainable Development. 16-17 octombrie, Brașov

6. Mihalache, A.L., Marin, M., Davidescu, Ș., Ungurean, C., Tudose, N.C., Davidescu, A., Tudose, O., Clinciu, I., 2020: Assessment of the physical status of the torrent control structures in Romania. 9TH International Symposium Forest and Sustainable Development. 16-17 octombrie, Brașov

7. Davidescu, Ș.O., Marin, M., 2020: Water resources vulnerability under climate and land use change. Global Challenges of the 21st Century. 18-22 noiembrie, București

F. Papers presented at innational symposia and conferences

1. Babătă (actual Marin), M, Clinciu, I., Tudose, N.C., Ungurean, C., Davidescu, Ș.O., Adorjani, A., Davidescu, A.A., Mihalache, A.L., Chendeș, V., 2018: Aplicarea modelului SWAT în bazine hidrografice mici. Studiu de caz: bazinele hidrografice Tărlungul Mare și Chișag. Conferința Științifică Anuală a Institutului Național de Hidrologie și Gospodărire a Apelor, 20-21 noiembrie, București

2. Tudose, N.C., Ungurean, C., Marin, M., Clinciu, I., Mihalache, A.L., Davidescu, Ș.O., 2019: Proiecții ale debitelor lichide și solide în bazinul superior al râului Tărlung în contextul diverselor scenarii climatice și de gospodărire a terenurilor. Conferința Științifică Anuală a Institutului Național de Hidrologie și Gospodărire a Apelor, 19-20 noiembrie, București

G. Book and book chapter

1. Marin, M., Cremades, R., Tudose, N.C., Davidescu, Ș.O., Ungurean, C., Mitter, H., Sanchez-Plaza, A., 2020: Climate Services. Capitolul 10 în Handbook on the Water-Energy-Food Nexus, partea a II a – Concepts of the Nexus; the applications. Editura Edward Elgar, 23 p, capitol trimis spre publicare (în curs de recenzare).

2. Davidescu, Ș.O., Tudose, N.C., Adorjani, A., Ungurean, C., Păcurar, V.D., Davidescu, A.A., Crivăț, M., Clinciu, I., Niță, M.D., Gancz, C., Oprea,

V., Petrițan, I.C., Mihalache, A.L., Marin, M., 2020: Estimarea torențialității bazinelor hidrografice mici și monitorizarea lucrărilor de amenajare a albiilor torențiale, pe baza indicilor de risc și de stare. Seria II: Lucrări de cercetare. Editura Silvică, 210 p

H. Deliverables and research reports

1. Tudose, N., Davidescu, Ș.O., Cheval, S., Chendeș, V., Ungurean, C., Babătă (actual Marin), M., 2018. Integrated model of river basin, land use and urban water supply. Deliverable 3.4. CLISWELN project. Poate fi accesat la adresa: https://www.hzg.de/imperia/md/content/csc/projekte/projekte/clisweln_d3.4_romania_study_case_final-2.pdf.

2. Tudose, N., Ungurean, C., Davidescu, Ș.O., Cheval, S., Marin, M., 2019. Information tailored to the needs of stakeholders in the Romanian case study. Deliverable 4.3. CLISWELN project. [WWW Document]. Poate fi accesat la adresa: https://www.hzg.de/ms/clisweln/075105/index.php.en.

3. Tudose, N., Davidescu, Ș.O., Cheval, S., Chendeș, V., Ungurean, C., Babătă (actual Marin), M., 2018b. Engagement and Societal Impact Plan. Deliverable 5.1. CLISWELN project. [WWW Document]. Poate fi accesat la adresa: https://www.hzg.de/ms/clisweln/075105/index.php.en

4. Tudose, N., Davidescu, Ș.O., Cheval, S., Chendeș, V., Ungurean, C., Babătă (actual Marin), M., 2020. Academic working paper "Climate services for river basins: providing robust policy recommendations through the WELFN". Deliverable 5.3. CLISWELN project. Poate fi accesat la adresa: https://www.hzg.de/ms/clisweln/075105/index.php.en

5. Raport științific și tehnic (Etapa I) Proiectul "Servicii climatice pentru complexul Apă-EnergieTeren-Hrană", PN-III-CEI-H2020-ERA, aprobat prin contract Nr. 77/2017. Brașov, 2017, 21 p. Poate fi accesat la adresa: http://clisweln.info/wp-content/uploads/2017/12/raport_stiintific_tehnic_etapa_I.pdf

6. Raport științific și tehnic (Etapa II) Proiectul "Servicii climatice pentru complexul Apă-EnergieTeren-Hrană", PN-III-CEI-H2020-ERA, aprobat prin contract Nr. 77/2017. Brașov, 2018, 56 p. Poate fi accesat la adresa: http://clisweln.info/wp-content/uploads/2018/12/raport_stiintific_tehnic_etapa_II_2018_CLISWELN.pdf

7. Raport științific și tehnic (Etapa III) Proiectul "Servicii climatice pentru complexul Apă-EnergieTeren-Hrană", PN-III-CEI-H2020-ERA, aprobat prin contract Nr. 77/2017. Brașov, 2018, 56 p. Poate fi accesat la adresa: http://clisweln.info/wp-content/uploads/2019/12/raport_stiintific_tehnic_etapa_III_2019.pdf

5.5. Future works

Given the importance of hydrological modelling studied, we consider that the following future works would be appropriate:

▪ Design and embedding in SWAT of a subroutine to introduce in the modelling process the main characteristic data of the structure of the stands, as they are presented in the forest management plans;

▪ Developing new possible scenarios of land use change within the studied watershed;

▪ Extending the analysis to other hydrological processes that take place within the watershed;

▪ Expanding research by quantifying the hydrological and anti-erozional impact of climate and land use change at sub-watershed level;

▪ Designing and analysing the frequency matrices regarding the monthly and seasonal projected values of the studied parameters;

▪ Developing new research, similar to the present one, but that use as input instead of the daily precipitation, the maximum precipitations corresponding to the insurances of 1%, 0.1%, etc., to find out to which extent climate change (with or without land use change) can influence the impact of extreme events within small, torrential, forested watersheds. Based on this type of research will it be possible to provide a reasoned answer to the question we stated in chapter 1.4, namely: how should be adapted the torrent control solutions within mainly forested watershed to climate changes that influence the availability of water resources, respectively the quantity and quality of water?

▪ Development of research on the hydrological impact of climate change in small, forested watershed and their integration in the broader theme of climate services and the water–energy–land–food nexus (Cremades et al., 2019).

REFERENCES

1. Abbas, T., Nabi, G., Boota, M.W., Hussain, F., Azam, M.I., Jin, H., Faisal, M., 2016: Uncertainty analysis of runoff and sedimentation in a forested watershed using sequential uncertainty fitting method, Sciences in Cold and Arid regions, vol. 8, nr. 4, pp. 297-310.

2. Abbaspour, K.C., Yang, J., Maximov, I., Siber, R., Bogner, K., Mieleitner, J., Zobrist, J., Srinivasan, R., 2007: Modelling hydrology and water quality in the pre-alpine/alpine Thur watershed using SWAT. Journal of Hydrology, vol. 333, nr. 2-4, pp. 413–430, https://doi.org/10.1016/j.jhydrol.2006.09.014.

3. Abbaspour, K.C., Rouholahnejad, E., Vaghefi¸S., Srinivasan, R., Yang, H., Kløve, B., 2015: A continental-scale hydrology and water quality model for Europe: Calibration and uncertainty of a high-resolution large-scale SWAT model. Journal of Hydrology, vol. 524, pp. 733–752, http://dx.doi.org/10.1016/j.jhydrol.2015.03.027.

4. Abbaspour, K.C., 2015: SWAT-CUP. SWAT Calibration and Uncertainty Programs. Downloaded from: https://swat.tamu.edu/media/114860/usermanual_swatcup.pdf.

5. Adorjani, A., Clinciu, I., Davidescu, Ș.O., Gancz, C., 2015: Lucrări pe rețeaua hidrografică torențială. În: Fundamente și soluții privind proiectarea și monitorizarea lucrărilor de amenajare a bazinelor hidrografice torențiale, predominant forestiere. Etapa a II a, Raport științific final la tema de cercetare finanțată de Regia Națională a Pădurilor. Coordonator științific: Prof. dr. ing. Ioan Clinciu.

6. Adams, M., Markart, G., Stary, U., 2010: A comparison of hydrological models for forest management and climate change. How can existing models capture and reproduce hydrological effect of forest? Disponibil la adresa: https://www.researchgate.net/publication/273761385_A_comparison_of_hydrological_models_for_forest_management_and_climate_change_How_can_existing_models_capture_and_reproduce_hydrological_effects_of_forests.

7. Ahn, S.R., Park, G.A., Jang, C.H., Kim, S.J, 2013: Assessment of Climate Change Impact on Evapotranspiration and Soil Moisture in a Mixed Forest Catchment Using Spatially Calibrated SWAT Model. J. KOREA WATER RESOURCES ASSOCIATION, vol. 46, no. 6, pp. 569-583, http://dx.doi.org/10.3741/JKWRA.2013.46.6.569.

8. Alfieri, L., Feyen, L., Dottori, F., Bianchi, A. 2015: Ensemble flood risk assessment in Europe under high end climate scenarios. Global Environmental Change, vol. 35, pp 199–212.

9. Alvarenga, L.A., de Mello, C.R., Colombo, A., Cuartas, L.A., Chou, S.C., 2016: Hydrological responses to climate changes in a headwater watershed. Ciência e Agrotecnologia, vol. 40, no. 6, pp. 647-657, http://dx.doi.org/10.1590/1413-70542016406027716.

10. Alvarenga, L.A., de Mello, C.R., Colombo, A., Chou, S.C., Cuartas, L.A., Viola, M.R., 2018: Impacts of Climate Change on the Hydrology of a Small Brazilian Headwater Catchment Using the Distributed Hydrology-Soil-Vegetation Model. American Journal of Climate Change, vol. 7, pp. 355-366, https://doi.org/10.4236/ajcc.2018.72021.

11. Anders, I., Stagl, J., Auer, I., Pavlik, D., 2014: Chapter 2: Climate Change in Central and Eastern Europe. Advances in Global Change Research, vol. 58, DOI 10.1007/978-94-007-7960-0_2.

12. ANM, 2018: oficial site of the National Meteorological Agency. Accesed in november 2018: http://www.meteoromania.ro/clima/scenarii-climatice/

13. Arias, R., Rodríguez-Blanco, M.L., Taboada-Castro, M.M., Nunes, J.,P., Keizer, J.J., Taboada-Castro, M.T., 2014: Water Resources Response to Changes in Temperature, Rainfall and CO_2 Concentration: A First Approach in NW Spain. Water, vol. 6, pp. 3049-3067; doi:10.3390/w6103049.

14. Arnell, N.W., Livermore, M.J.L., Kovats, S., Levy, P.E., Nicholls, R., Parry, M.L., Gaffin, S.R., 2004: Climate and socio-economic scenarios for global-scale climate change impacts assessments: characterising the SRES storylines. Global Environmental Change, vol. 14, pp. 3–20, doi:10.1016/j.gloenvcha.2003.10.004.

15. Arnold, J.G., Srinivasan, R., Muttiah, R.S., Williams, J.R., 1998: Large area hydrologic modeling and assessment. Part I: Model development. Journal of the American Water Resources Association, vol. 34, no. 1, pp.73-89.

16. Arnold, J.G., Kiniry, J.R., Srinivasan, R., Williams, J.R., Haney, E.B., Neitsch, S.L., 2012: Soil and Water Assessment Tool. Input/Output Documentation, version 2012. Texas Water Institute. Technical

Raport no. 439, 650 pp.

17. Badea, O., Pătrășcoiu, N., Tănase, M., în Silvologie, vol. IV A. Pădurea și modificările de mediu. Editura Academiei Române, sub redacția Victor Giurgiu, 2005, 238p. Capitolul 8: Posibile corelații între starea de sănătate a pădurilor și modificările climatice, pp. 127-137.

18. Bajracharya, A.R., Bajracharya, S.R., Shrestha, A.B., Maharjan, S.B., 2018: Climate change impact assessment on the hydrological regime of the Kaligandaki Basin, Nepal. Science of the Total Environment, vol. 625, pp. 837–848, https://doi.org/10.1016/j.scitotenv.2017.12.332.

19. Barbu, I., Barbu, C., Curcă, M., Ichim, V., 2016: Adaptarea pădurilor României la schimbările climatice. Editura Silvică, 380 p.

20. Beaulieu, E., Lucas, Y., Viville, D., Chabaux, F., Ackerer, P., Goddéris, Y., Pierret, M-C., 2016: Hydrological and vegetation response to climate change in a forested mountainous catchment. Modeling Earth Systems and Environment, vol. 2, no. 191, pp. 1–15, DOI 10.1007/s40808-016-0244-1.

21. Beckers J., Smerdon B., Wilson M., 2009: Review of Hydrologic Models for Forest Management and Climate Change Applications in British Columbia and Alberta. Forrex Forum for Research and Extension in Natural Resources. Forrex series 25. ISSN 1495-9658; 25.

22. Bekele, D., Alamirew, T., Kebede, A., Zeleke, G., Melessea, M., 2018: Modeling Climate Change Impact on the Hydrology of Keleta Watershed in the Awash River Basin, Ethiopia. Environmental Modeling & Assessment, vol. 24, pp. 95–107, https://doi.org/10.1007/s10666-018-9619-1.

23. Belmar, O., Barquín, J., Álvarez-Martínez, J.M., Peñas, F.J., del Jesus, M., 2016: The role of forest maturity on catchment hydrologic stability. Hydrology and Earth System Science. Discussions, DOI:10.5194/hess-2016-471.

24. Benestad, R., Haensler, A., Hennemuth, B., Illy, T., Jacob, D., Keup-Thiel, E., Kotlarski, S., Nikulin, G., Otto, J., Rechid, D., Sieck, K., Sobolowski, S., Szabó, P., Szépszó, G., Teichmann, C., Vautard, R., Weber, T., Zsebeházi, G., 2017: EURO-CORDEX Guidelines Guidance for EURO-CORDEX climate projections data use, https://doi.org/10.1186/2193-2697-1-9

25. Benti Tolera, M., Chung, I.-M., Chang, S.W., 2018: Evaluation of the Climate Forecast System Reanalysis Weather Data for Watershed Modeling in Upper Awash Basin, Ethiopia. Water, vol. 10, nr. 725, doi:10.3390/w10060725.

26. Bîrsan, M.-V., Zaharia, L., Chendes, V., Brănescu, E., 2012: Recent trends in streamflow in Romania (1976–2005). Romanian Reports in Physics, vol. 64, nr. 1, pp. 275–280.

27. Bjørnæs, C. 2015: A guide to Representative Concentration Pathways. Disponibil la adresa: http://www.cicero.oslo.no/en/posts/news/a-guide-to-representative-concentration-pathways.

28. Blujdea, V., 2005: în Silvologie, vol. IV A. Pădurea și modificările de mediu. Editura Academiei Române, sub redacția Victor Giurgiu, 2005, 238p. Capitolul 12: Contribuția sectorului forestier la reducerea emisiilor de gaze cu efect de seră în contextul strategic al abordării schimbărilor climatice, pp. 185-200.

29. Briones, R.U., Ella, V.B., Bantayan, N.C., 2016: Hydrologic Impact Evaluation of Land Use and Land Cover Change in Palico Watershed, Batangas, Philippines Using the SWAT Model. Journal of Environmental Science and Management, vol 1, nr 1, pp. 96-107.

30. Brooks, R.T., 2009: Potential impacts of global climate change on the hydrology and ecology of ephemeral freshwater systems of the forests of the northeastern United States. Climatic Change, vol. 95, pp. 469–483, DOI 10.1007/s10584-008-9531-9.

31. Busuioc, A., Dumitrescu, A., Soare, E., Orzan, A., 2007: Summer anomalies in 2007 in the context of extremely hot and dry summers in Romania. Romanian Journal of Meteorology, vol. 9, nr. 1-2, pp. 1-7.

32. Busuioc, A., Caian, M., Cheval, S., Bojariu, R., Boroneanț, C., Baciu, M., Dumitrescu, A., 2010: Variabilitatea și schimbarea climei în România. Editura Pro Universitaria 2010, București, 266 pp.

33. Cai, Y., Bandara, S.-J., Newth, D. 2016: A framework for integrated assessment of food production economics in South Asia under climate change. Environmental Modelling & Software, vol. 75, pp. 459-497.

34. Carcea, F., Seceleanu, I., 2004: Amenajarea și gestionarea durabilă a pădurilor cu funcții hidrologice. Revista Pădurilor, nr. 1, anul 119, pp. 12-15.

35. Chambers, B.M., Pradhanang, S.M., Gold, A.J., 2017: Simulating Climate Change Induced

Thermal Stress in Coldwater Fish Habitat Using SWAT Model. Water, vol.9, nr. 10, pp. 1-24, DOI:10.3390/w9100732.

36. Chendeș V., Cheval S., Dumitru S., 2010: The assessment of some hydrometeorological drought indices in the bend subcarpathians and peripheral zones. Research Journal of Agricultural Science. Agroprint Editorial, Timişoara, ISSN: 2066-1843, vol. 42, nr. 3, pp. 60-70.

37. Cheval, S., Curk, B.C., Vrhovnik, P., Verbovšek, T., Herrnegger, M., Nachtnebel, H.P., Marjanović, P., 2014: CC-WARE Mitigating Vulnerability of Water Resources under Climate Change WP3 - Vulnerability of Water Resources in SEE, 82 pp.

38. Chong-yu Xu., 2002: Textbook of Hydrologic models (Lärobok i Avrinningsmodeller). Uppsala University Department of Earth Sciences Hydrology, edition 2002. Available at: http://www.soil.tu-bs.de/lehre/Master.Unsicherheiten/2012/Lit/Hydrology_textbook.pdf.

39. Clinciu, I., 2001: Corectarea torenților. Curs universitar, ediția a-II-a revizuită și adăugită. Tipărit la Reprografia Universității Transilvania, 249 p.

40. Clinciu, I., Niță, M.D., Davidescu, Ș., 2012: Starea amenajării bazinelor hidrografice torențiale și rolul acesteia în reconstrucția ecologică a țării. Revista Pădurilor, nr. 6, pp. 42-52.

41. Clinciu, I., Niță, M.D., Davidescu, Ș., Gancz, C., 2014: Să reconsiderăm avantajele și gradul utilizării lucrărilor din lemn sau bazate pe lemn ori alte materiale naturale ori artificiale, la amenajarea rețelei hidrografice torențiale. Revista Pădurilor, nr. 1-2, anul 129, pp. 87-95.

42. Clinciu, I., Davidescu, Ș., Niță, M.D., Gancz, C., Ciornei, I., 2015: Promovarea de soluții ecologice în amenajarea bazinelor hidrografice torențiale, problemă majoră a silviculturii românești contemporane. Revista Pădurilor, nr. 1-2 anul 130, pp. 41-54.

43. Clinciu, I., Niță, M.D., 2019: Corectarea torenților. Curs universitar. Ediția a III-a revizuită și adăugită. Editura Universității Transilvania, 268p.

44. Compania Apa, 2020. Captarea apei brute - Compania Apa Brașov [WWW Document]. URL https://www.apabrasov.ro/servicii/captarea-apei-brute/. Accesat în 29 august 2019.

45. Constandache, C., Dinca, L., Popovici, L., Braga, C., Blaga, T., 2018: The effect of climatic changes over some Romanian forest ecosystems. 18th International Multidisciplinary Scientific GeoConference: SGEM 2018, vol. 18, nr. 3.2, pp. 941-948, DOI: 10.5593/sgem2018/3.2/S14.121.

46. Corbuș C., Mic R-P, Mătreață M., Chendeș V., Preda A., 2017: Potential climate change impact on mean flow in Romania. Danube Conference 2017. Electronic book with full papers from XXVII Conference of the Danubian countries on hydrological forecasting and hydrological bases of water management. 26-28 septembrie 2017, Bulgaria.

47. Costache, R., Bao Pham, Q., Corodescu-Roșca, E., Cîmpianu, C., Hong, H., Thi Thuy Linh, N., Ming Fai, C., Najah Ahmed, A., Vojtek, M., Muhammed Pandhiani, S., Minea, G., Ciobotaru, N., Cristian Popa, M., Diaconu, D.C., Thai Pham, B., 2020: Using GIS, Remote Sensing, and Machine Learning to Highlight the Correlation between the Land-Use/Land-Cover Changes and Flash-Flood Potential. Remote Sensing, vol. 12, https://doi.org/10.3390/rs12091422.

48. Cremades, R., Mitter, H., Tudose, N.C., Sanchez-Plaza, A., Graves, A., Broekman, A., Bender, S., Giupponi, C., Koundouri, P., Bahri, M., Cheval, S., Cortekar, J., Moreno, Y., Melo, O., Karner, K., Ungurean, C., Davidescu, S.O., Kropf, B., Brouwer, F., Marin, M., 2019: Ten principles to integrate the water-energy-land nexus with climate services for co-producing local and regional integrated assessments. Science of The Total Environment, vol. 693, 133662, https://doi.org/10.1016/j.scitotenv.2019.133662.

49. Cuculeanu, V., Bălteanu, D., 2005: în Silvologie, vol. IV A. Pădurea și modificările de mediu. Editura Academiei Române, sub redacția Victor Giurgiu, 2005, 238p. Capitolul 3: Modificarea climei în România în context global, pp. 50-56.

50. Cuculeanu, V., Geicu, A., Pătrășcoiu, N., 2005: în Silvologie, vol. IV A. Pădurea și modificările de mediu. Editura Academiei Române, sub redacția Victor Giurgiu, 2005, 238p. Capitolul 4: Impactul potențial al modificărilor climatice asupra ecosistemelor forestiere în România, pp. 57-73.

51. Davidescu, Ș.O., 2015: Lucrări de refacere a mediului în zona șantierelor de amenajare a bazinelor hidrografice torențiale. În: Fundamente și soluții privind proiectarea și monitorizarea lucrărilor de amenajare a bazinelor hidrografice torențiale, predominant forestiere. Etapa a II a, Raport științific final la tema de cercetare finanțată de Regia Națională a Pădurilor. Coordonator științific: Prof. dr. ing. Ioan

Clinciu.

52. Diaconu, C., 1971: Râurile României, monografie hidrologică. Institutul de Meteorologie și Hidrologie, București, 751 p.

53. Drobot, R., 1996: Bazele statistice ale hidrologiei. Editura Didactică și Pedagogică R.A., București 1996, 187p.

54. Dumitrescu, A., Bojariu, R., Bîrsan, M.-V., Marin, L., Manea, A., 2014: Recent climatic changes in Romania from observational data (1961–2013). Theoretical and Applied Climatology, DOI 10.1007/s00704-014-1290-0.

55. Dumitrescu, A., Bîrsan, M.-V., 2015: ROCADA: A gridded daily climatic dataset over Romania (1961–2013) for nine meteorological variables. Natural Hazards, vol. 78, pp. 1045–1063, DOI 10.1007/s11069-015-1757-z.

56. Durło, G., Jagiełło-Leńczuk, K., Małek, S., Banach, J., Dudek,K., Kormanek, M. 2016: Hydrological responses to forest cover change in mountains under projected climate conditions. International Journal of Environmental & Agriculture Research (IJOEAR), vol-2, nr. 10, pp. 60-68.

57. Dwarakish G.S., Ganasri B.P., 2015: Impact of land use change on hydrological systems: A review of current modeling approaches. Cogent Geoscience, vol. 1. DOI: 10.1080/23312041.2015.1115691.

58. Džubáková K., 2010: Rainfall-runoff modelling: its developoment, clasification and possible applications. Acta Geographica Universitatis Comenianae, vol 54, nr 2, pp. 173-181.

59. Ekness, P., Randhir, T.O., 2015: Effect of climate and land cover changes on watershed runoff: A multivariate assessment for storm water management. Journal of Geophysical Research: Biogeosciences, pp. 1785-1796, DOI: 10.1002/2015JG002981.

60. Emam, A.R., Kappas, M., Linh, H.K.N., Renchin, T., 2016: Hydrological Modeling in an Ungauged Basin of Central Vietnam Using SWAT Model. Hydrology and Earth System Sciences Discussions, pp. 1-33, DOI: 10.5194/hess-2016-44.

61. Feser, F., Rrockel, B., Storch, H., Winterfeldt, J., Zahn, M., 2011: Regional climate models add value to global model data a review and selected examples. Bulletin of American Meteorological Society, vol. 92, nr. 9, pp. 1181–1192, https://doi.org/10.1175/2011BAMS3061.1.

62. Fekete, B.M., Vörösmarty, C.J., Roads, J.O., Willmott, C.J., 2004: Uncertainties in precipitation and their impacts on runoff estimates. Journal of. Climate, vol. 17, nr. 2, pp 294–304, DOI: https://doi.org/10.1175/1520-0442(2004)017<0294:UIPATI>2.0.CO;2.

63. Flato, G., J. Marotzke, B. Abiodun, P. Braconnot, S.C. Chou, W. Collins, P. Cox, F. Driouech, S. Emori, V. Eyring, C. Forest, P. Gleckler, E. Guilyardi, C. Jakob, V. Kattsov, C. Reason and M. Rummukainen, 2013: Evaluation of Climate Models. In: Climate Change 2013: The Physical Science Basis. Contribution of Working Group I to the Fifth Assessment Report of the Intergovernmental Panel on Climate Change [Stocker, T.F., D. Qin, G.-K. Plattner, M. Tignor, S.K. Allen, J. Boschung, A. Nauels, Y. Xia, V. Bex and P.M. Midgley (eds.)]. Cambridge University Press, Cambridge, United Kingdom and New York, NY, USA.

64. Florescu, I.I., Nicolescu, N.V., 1998: Silvicultură. Vol. II – Silvotehnică. Editura Universității Transilvania din Brașov.

65. Florescu, I.I., Clinciu, I., 2009: Măsuri silvotehnice pentru gestionarea durabilă a pădurilor cu funcții speciale de protecție hidrologică. Revista de Silvicultură și Cinegetică, nr. 25, anul XIV, pp. 9-17.

66. Galavi, H., Shui, L.T., 2012: Uncertainty Analysis of Climate Change Impacts on Runoff. International Conference on Future Environment and Energy, Singapore 2012, IPCBEE vol. 28, pp. 235-239.

67. Gan, T.Y., Dlamini, E.M., Biftu, G.F., 1997: Effects of model complexity and structure, data quality, and objective functions on hydrologic modeling. Journal of. Hydrology, vol. 192, nr, 1-4, pp. 81–103, https://doi.org/10.1016/S0022-1694(96)03114-9.

68. Gao, Y., Weiher, S., Markkanen, T., Pietikäinen, J.P., Gregow, H., Henttonen, H.M., Jacob, D., Laaksonen, A., 2015: Implementation of the CORINE land use classification in the regional climate model REMO. Boreal Environment Research, vol. 20, nr. 2, pp. 261–282.

69. Gaspar, R., 2004: Rolul pădurii în prevenirea și combaterea viiturilor torențiale din bazine hidrografice mici. Revista Pădurilor, anul 119, nr 1, pp. 16-22.

70. Gassman P.W., Reyes M.R., Green C.H., Arnold J.G., 2007: The Soil and Water Assessment

Tool: historical development, applications, and future research directions. American Society of Agricultural and Biological Engineers, vol 50, nr 4, pp. 1211-1250.

71. Gassman P.W., Sadeghi A.M., Srinivasan R., 2014: Applications of the SWAT Model Special Section: Overview and Insights. Journal of Environmental Quality, vol. 46, pp. 1-8, doi:10.2134/jeq2013.11.0466.

72. Gautam, B., 2012: Modelling Streamflow from Forested Watersheds on the Canadian Boreal Shield using The Soil And Water Assessment Tool (SWAT). Masters of Science thesis degree, University of Saskatchewan, 124 pp. Available at: https://harvest.usask.ca/handle/10388/ETD-2012-05-476.

73. Gautam, S., Costello, C., Baffaut, C., Thompson, A., Svoma, B.M., Phung, Q.A., Sadler, E.J., 2018: Assessing Long-Term Hydrological Impact of Climate Change Using an Ensemble Approach and Comparison with Global Gridded Model-A Case Study on Goodwater Creek Experimental Watershed. Water, vol. 10, 564, doi:10.3390/w10050564.

74. Gayathri K.D., Ganasri B.P., Dwarakish G.S., 2015: International conference on water resources, coastal and ocean engineering (ICWRCOE). Aquatic Procedia, nr 4, pp. 1001-1007.

75. GAESC, 2008: Ghidul privind Adaptarea la Efectele Schimbărilor Climatice din 29.09.2008, published by Ministerul Mediului şi Dezvoltării Durabile în Monitorul Oficial.

76. Girod, B., Wiek, A., Mieg, H., Hulme, M., 2009: The evolution of the IPCC's emissions scenarios. Environmental Science & Policy, vol. 12, pp. 103–118, doi:10.1016/j.envsci.2008.12.006.

77. Giurgiu, V., 1972: Metode ale statisticii matematice aplicate în silvicultură. Editura Ceres, București, 565p.

78. Giurgiu, V., 2004: Gestionarea durabilă a pădurilor României. Editura Academiei Române, 320 p.

79. Giurgiu, V., 2005: Silvologie, vol. IV A. Pădurea și modificările de mediu. Editura Academiei Române 238p. Capitolul 1: Cu privire la relația dintre pădure și modificările de mediu, pp. 11-42.

80. Giurgiu, V., 2006: Gestionarea durabilă a pădurilor și regimul apelor. Capitolul 1 în Silvologie, vol. V: Pădurea și regimul apelor. Sub redacția V. Giurgiu și I. Clinciu, Editura Academiei Române, pp. 17-106.

81. Giurgiu, V., 2008: Cu privire la gestionarea durabilă a pădurilor din bazinele hidrografice torențiale. Capitolul 15 în Silvologie, vol. VI: Amenajarea bazinelor hidrografice torențiale. Noi concepții și fundamente științifice. Sub redacția V. Giurgiu și I. Clinciu, Editura Academiei Române, pp. 353-371.

82. Golmohammadi G., Prasher S., Madani A., Rudra R., 2014: Evaluating Three Hydrological Distributed Watershed Models: MIKE-SHE, APEX, SWAT. Hydrology, vol. 1, pp. 20-39; DOI:10.3390/hydrology1010020.

83. Gudmundsson, L., Bremnes, J.B., Haugen, J.E., Engen Skaugen, T., 2012: Technical Note: Downscaling RCM precipitation to the station scale using quantile mapping – a comparison of methods. Hydrology and Earth System Sciences, vol. 16, pp. 3383-3390, https://doi.org/10.5194/hessd-9-6185-2012.

84. Guo, S., Ying, A. 1997: Uncertainty analysis of impact of climate change on hydrology and water resources. Sustainability of Water Resources under Increasing Uncertainty (Proceedings of the Rabat Symposium S1, IAHS Publ. nr. 240, pp. 331-338.

85. Gupta, S.K., Sharma, G., Jethoo, A.S., Tyagi, J., Gupta, K.N., 2015: A critical review of hydrological models. HYDRO 2015 INTERNATIONAL IIT Roorkee, India, 17-19 December, 2015 20th International Conference on Hydraulics, Water Resources and River Engineering.

86. Harmel, R. D., Cooper, R. J., Slade, R. M., Haney, R. L., Arnold, J. G., 2006: Cumulative uncertainty in measured streamflow and water quality data for small watersheds. Transactions of the ASABE, American Society of Agricultural and Biological Engineers, vol. 49, nr. 3, pp. 689−701.

87. Hartman, M.D., Baron, J.S., Lammers, R.B., Cline, D.W., Band, L.E., Liston, G.E., Tague, C., 1999: Simulations of snow distribution and hydrology in a mountain basin. Water Resources Research, vol. 35, nr. 5, pp. 1587-1603.

88. Houghton, J. T., Jenkins, G. J., Ephraums, J. J. IPCC, 1990: Climate Change. The IPCC Scientific Assessment.

89. Huang, M., Zhang, L., 2004: Hydrological responses to conservation practices in a catchment of the Loess Plateau, China. Hydrological Processes, vol. 18, pp. 1885-1898, DOI: 10.1002/hyp.1454.

90. Hughes, J.D., Langevin, C.D., and Banta, E.R., 2017: Documentation for the MODFLOW 6 framework: U.S. Geological Survey Techniques and Methods, book 6, chap. A57, 40 p., https://doi.org/10.3133/tm6A57.

91. Im, S., Lee, S., An, D., 2007: Hydrologic Effects of Climate Changes in a Forest Watershed. Available at: https://www.mssanz.org.au/MODSIM07/papers/10_s61/HydrologicEffects_s61_Sangjun_.pdf.

92. Im, S., Kim, H., Kim, C., Jang, C., 2009: Assessing the impacts of land use change on watershed hydrology using MiKE SHE. Environ Geol, vol. 57, pp. 231–239, DOI 10.1007/s00254-008-1303-3.

93. INHGA, 2009: Evaluarea impactului schimbăarilor climatice asupra resurselor de apă din România. Available at: https://www.green-report.ro/1011209-inhga-evaluarea-impactului-schimbarilor-climatice-asupra-resurselor-de-apa-din-ro/.

94. IPCC, 1992: Climate Change 1992: The supplementary Report to the IPCC Scientific Assessment. Houghton, J.T., Callander, B.A., Varney, S.K, 195p.

95. IPCC, 2000: Emissions Scenarios. A Special Report of Working Group III of the Intergovernmental Panel on Climate Change [Nakicenovic, N., J. Alcamo, G. Davis, B. de Vries, J. Fenhann, S. Gaffin, K. Gregory, A. Grübler, T.Y. Jung, T. Kram, E.L. La Rovere, L. Michaelis, S. Mori, T. Morita, W. Pepper, H. Pitcher, L. Price, K. Raihi, A. Roehrl, H.-H. Rogner, A. Sankovski, M. Schlesinger, P. Shukla, S. Smith, R. Swart, S. van Rooijen, N. Victor, and Z. Dadi (eds.)]. Cambridge University Press, Cambridge, United Kingdom and New York, NY, USA, 599 p.

96. IPCC, 2007: Climate Change 2007: Synthesis Report. Contribution of Working Groups I, II and III to the Fourth Assessment Report of the Intergovernmental Panel on Climate Change [Core Writing Team, Pachauri, R.K and Reisinger, A. (eds.)]. IPCC, Geneva, Switzerland, 104 p.

97. IPCC, 2014: Climate Change 2014: Synthesis Report. Contribution of Working Groups I, II and III to the Fifth Assessment Report of the Intergovernmental Panel on Climate Change [Core Writing Team, R.K. Pachauri and L.A. Meyer (eds.)]. IPCC, Geneva, Switzerland, 151 p.

98. IPCC 2018: Global warming of 1.5 °C. Summary for Policymakers. Allen, M., Babiker, M., Chen, Y., de Coninck, H., Connors, S., van Diemen,R., Dube, O.P., Ebi,K., Engelbrecht, F., Ferrat, M., Ford, J., Forster, P., Fuss, S., Guillen, T., Harold, J., Hoegh-Guldberg, O., Hourcade, J.-C., Huppmann, D., Jacob, D., Jiang, K., Johansen, T.G., Kainuma, M., de Kleijne, K., Kriegler, E., Ley, D., Liverman, D., Mahowald, N., Masson-Delmotte, V., Matthews, R., Melcher, R., Millar, R., Mintenbeck, K., Morelli, A., Moufouma-Okia,W., Mundaca, L., Nicolai, M., Okereke, C., Pathak, M., Payne, A., Pidcock, R., Pirani, A., Poloczanska, E., Pörtner, H.-O., Revi, A., Riahi, K., Roberts, D.C., Rogelj, J., Roy, J., Seneviratne, S., Shukla, P.R., Skea, J., Slade, R., Shindell, D., Singh, C., Solecki, W., Steg, L., Taylor, M., Tschakert, P., Waisman, H., Warren, R., Zhai, P., Zickfeld, K. This Summary for Policymakers was formally approved at the First Joint Session of Working Groups I, II and III of the IPCC and accepted by the 48th Session of the IPCC, Incheon, Republic of Korea, 6 October 2018.

99. Jacob, D., Elizalde, A., Haensler, A., Hagemann, S., Kumar, P., Podzun, R., Rechid, D., Remedio, A.R., Saeed, F., Sieck, K., Teichmann, C., Wilhelm, C., 2012: Assessing the Transferability of the Regional Climate Model REMO to Different COordinated Regional Climate Downscaling EXperiment (CORDEX) Regions. Atmosphere (Basel), vol. 3, pp. 181–199. https://doi.org/10.3390/atmos3010181

100. Jacob, D., Petersen, J., Eggert, B., Alias, A., Christensen, O.B., Bouwer, L.M., Braun, A., Colette, A., Déqué, M., Georgievski, G., Georgopoulou, E., Gobiet, A., Menut, L., Nikulin, G., Haensler, A., Hempelmann, N., Jones, C., Keuler, K., Kovats, S., Kröner, N., Kotlarski, S., Kriegsmann, A., Martin, E., van Meijgaard, E., Moseley, C., Pfeifer, S., Preuschmann, S., Radermacher, C., Radtke, K., Rechid, D., Rounsevell, M., Samuelsson, P., Somot, S., Soussana, J.F., Teichmann, C., Valentini, R., Vautard, R., Weber, B., Yiou, P., 2014: EURO-CORDEX: New high-resolution climate change projections for European impact research. Regional Environmental Change, vol. 14, pp. 563–578, https://doi.org/10.1007/s10113-013-0499-2.

101. Jain, S.K., Sudheer, K.P., 2008: Fitting of Hydrologic Models: A Close Look at the Nash–Sutcliffe Index. Technical Notes. Journal of Hydrologic Engineering, vol. 13, pp. 981-986, DOI: 10.1061/(ASCE)1084-0699(2008)13:10(981).

102. Joh, H.K., Lee, J.W., Park, M.J., Shin, H.J., Yi, J.E., Kim, G.S., Srinivasan, R., Kim, S.J., 2011:

Technical note: Assessing climate change impact on hydrological components of a small forest watershed through swat calibration of evapotranspiration and soil moisture. American Society of Agricultural and Biological Engineers, vol. 54, nr. 5, pp. 1773-1781.

103. Jones, J.A., Achterman, G.L., Augustine, L.A., Creed, I.F., Ffolliott, P.F., MacDonald, I., Wemple, B.C. 2009: Hydrologic effects of a changing forested landscape - challenges for the hydrological sciences. Hydrological Processes, vol. 23, pp. 2699-2704, DOl: 10.1002/hyp.7404.

104. Kalogeropoulos, K., Chalkias, C., 2013: Modelling the impacts of climate change on surface runoff in small Mediterranean catchments: empirical evidence from Greece. Water and Environment Journal, vol. 27, pp. 505–513, DOI:10.1111/j.1747-6593.2012.00369.x

105. Kelemen, A., Munch, W., Poelman, H., Gakova, Z., Dijkstra, L., Torighelli, B., 2009: Regions 2020. The Climate Change Challenge for European Regions. Brussels, March 2009. Directorate General for Regional Policy. Background Document to Commission Staff Working Document Sec(2008), 2868 Final Regions 2020, an Assessment of Future Challenges for EU Regions.

106. Kotlarski, S., Keuler, K., Christensen, O.B., Colette, A., Déqué, M., Gobiet, A., Goergen, K., Jacob, D., Lüthi, D., Van Meijgaard, E., Nikulin, G., Schär, C., Teichmann, C., Vautard, R., Warrach-Sagi, K., Wulfmeyer, V., 2014: Regional climate modeling on European scales: A joint standard evaluation of the EURO-CORDEX RCM ensemble. Geoscientific Model Development, vol. 7, nr. 4, pp. 1297–1333, https://doi.org/10.5194/gmd-7-1297-2014.

107. Kovats, R.S., R. Valentini, L.M. Bouwer, E. Georgopoulou, D. Jacob, E. Martin, M. Rounsevell, and J.-F. Soussana, 2014: Europe. In: Climate Change 2014: Impacts, Adaptation, and Vulnerability. Part B: Regional Aspects. Contribution of Working Group II to the Fifth Assessment Report of the Intergovernmental Panel on Climate Change [Barros, V.R., C.B. Field, D.J. Dokken, M.D. Mastrandrea, K.J. Mach, T.E. Bilir, M. Chatterjee, K.L. Ebi, Y.O. Estrada, R.C. Genova, B. Girma, E.S. Kissel, A.N. Levy, S. MacCracken, P.R. Mastrandrea, and L.L. White (eds.)]. Cambridge University Press, Cambridge, United Kingdom and New York, NY, USA, pp. 1267-1326.

108. Kvočka, D., Ahmadian, R., Falconer, R.A., 2018: Predicting Flood Hazard Indices in Torrential or Flashy River Basins and Catchments. Water Resour Manage, vol. 32, pp. 2335-2352, https://doi.org/10.1007/s11269-018-1932-6.

109. Leahu, I., 2001: Amenajarea pădurilor. Editura Didactică și Pedagogică, 616 p.

110. Lehmann, N., Finger, R., Klein, T., Calanca, P., Walter A., 2013: Adapting crop management practices to climate change: Modelling optimal solutions at the field scale. Agricultural Systems, vol. 117, pp. 55–65.

111. Lee, S., Yeo, I.-Y., Sadeghi, A.M., McCarty, G.W., Hively, W.D., Lang, M.W., Sharifi, A., 2018: Comparative analyses of hydrological responses of two adjacent watersheds to climate variability and change using the SWAT model. Hydrology and Earth System Sciences, vol. 22, pp. 689–708, 2018, https://doi.org/10.5194/hess-22-689-2018.

112. Leta, O.T., El-Kadi, A.I., Dulai, H., Ghazal, K.A., 2016: Assessment of climate change impacts on water balancecomponents of Heeia watershed in Hawaii. Journal of Hydrology: Regional Studies, vol. 8, pp. 182–197, http://dx.doi.org/10.1016/j.ejrh.2016.09.006.

113. Leta, O.T., El-Kadi, A.I., Dulai, H., 2018: Impact of Climate Change on Daily Streamflow and Its Extreme Values in Pacific Island Watersheds. Sustainability, vol. 10, nr. 6, pp. 1-22, doi:10.3390/su10062057.

114. Lull, W.H., Sopper, W.E. 1966: Factors that influence streamflow in the Northeast. Water Resources Research 1966, vol 2, nr 3, pp. 371-379. https://doi.org/10.1029/WR002i003p00371.

115. Luo, M., Liu, T., Meng, F., Duan, Y., Frankl, A., Bao, A., De Maeyer, P., 2018: Comparing Bias Correction Methods Used in Downscaling Precipitation and Temperature from Regional Climate Models: A Case Study from the Kaidu River Basin in Western China. Water, vol. 10, nr. 8, https://doi.org/10.3390/w10081046.

116. Marcu, M., 2005: în Silvologie, vol. IV A. Pădurea și modificările de mediu. Editura Academiei Române, sub redacția Victor Giurgiu, 2005, 238p. Capitolul 5: De la Ștefan Hepites la schimbările climatice. Atitudini și strategii de precauție în silvicultură, pp. 74-81.

117. Marin, M., Clinciu, I., Tudose, N.C., Davidescu, Șerban O., Constandache, C., 2019: Assessing

the performance of the Soil and Water Assessment Tool hydrological model for a small mountain forested watershed in the central part of Romania. În: GEOLINKS 2019 Conference Proceedings Book 3, Vol. 1. Saima Consult LTD, pp. 265–273. https://doi.org/10.32008/geolinks2019/b3/v1/30.

118. Marin, M., Clinciu, I., Tudose, N.C., Cheval, S., Ungurean, C., Davidescu, S.O., Adorjani, A., Mihalache, A.L., Davidescu, A.A., Tudose, O.N., 2020a: Analiza previziunilor privind regimul termic și pluvial din bazinul hidrografic Tărlungul Superior în contextul schimbărilor climatice. Revista de Silvicultură și Cinegetică, nr. 45, pp. 15-21.

119. Marin, M., Clinciu, I., Tudose, N.C., Cheval, S., Ungurean, C., Davidescu, S.O., Adorjani, A., Mihalache, A.L., Davidescu, A.A., Tudose, O.N., 2020b: Impactul schimbărilor climatice și al modificării folosinței terenului asupra proceselor hidrologice din bazinul hidrografic Tărlungul Superior. Revista Pădurilor, 135(3), 26 p.

120. Marin, M., Clinciu, I., Tudose, N.C., Ungurean, C., Adorjani, A., Mihalache, A.L., Davidescu, A.A., Davidescu, Șerban O., Dinca, L., Cacovean, H., 2020c: Assessing the vulnerability of water resources in the context of climate changes in a small forested watershed using SWAT: A review. Environmental Research, vol. 184, 109330, https://doi.org/10.1016/j.envres.2020.109330.

121. Meaurio, M., Zabaleta, A., Uriarte, J.A., Srinivasan, R., Antigüedad, I., 2015: Evaluation of SWAT model performance to simulate streamflow spatial origin. The case of a small forested watershed. Journal of Hydrology, vol. 525, pp. 326–334, http://dx.doi.org/10.1016/j.jhydrol.2015.03.050.

122. Meehl, G.A., T.F. Stocker, W.D. Collins, P. Friedlingstein, A.T. Gaye, J.M. Gregory, A. Kitoh, R. Knutti, J.M. Murphy, A. Noda, S.C.B. Raper, I.G. Watterson, A.J. Weaver and Z.-C. Zhao, 2007: Global Climate Projections. In: Climate Change 2007: The Physical Science Basis. Contribution of Working Group I to the Fourth Assessment Report of the Intergovernmental Panel on Climate Change [Solomon, S., D. Qin, M. Manning, Z. Chen, M. Marquis, K.B. Averyt, M. Tignor and H.L. Miller (eds.)]. Cambridge University Press, Cambridge, United Kingdom and New York, NY, USA.

123. Meinshausen, M., Smith, S. J., Calvin, K., Daniel, J. S., Kainuma, M. L. T., Lamarque, J-F., Matsumoto, K., Montzka, S. A., Raper, S. C. B., Riahi, K., Thomson, A., Velders, G. J. M., van Vuuren, D.P. P., 2011: The RCP greenhouse gas concentrations and their extensions from 1765 to 2300. Climatic Change, vol. 109, pp. 213–241, DOI 10.1007/s10584-011-0156-z.

124. Michelangeli, P.A., Vrac, M., Loukos, H., 2009: Probabilistic downscaling approaches: Application to wind cumulative distribution functions. Geophysical Research Letters, vol. 36,nr. 11, https://doi.org/10.1029/2009GL038401.

125. Miță, P., 2019: Coeficientul de scurgere a apei în râuri. Rolul în calculele hidrologice. Editura Academiei Române, București, 2019, 202 p.

126. Moriasi D.N., Arnold J.G., Van Liew M.W., Bingner R.L., Harmel R.D., Veith T.L., 2007: Model Evaluation Guidelines for Systematic Quantification of Accuracy in Watershed Simulations. American Society of Agricultural and Biological Engineers, vol. 50, nr. 3, pp 885-900.

127. Moriasi, D.N., Wilson, B.N., Douglas-Mankin, K. R., Arnold, J. G., Gowda, P. H., 2012: Hydrologic and water quality models: use, calibration, and validation. Transactions of the ASABE, American Society of Agricultural and Biological Engineers ISSN 2151-0032, vol. 55, nr.4, pp. 1241-1247.

128. Munteanu, S., 1970: Considérations preliminaries sur le passage de la classification quantitative des basins torrentiels. FAO/EFC/TORR, Munich.

129. Munteanu, S., 1975: Premise fundamentale în problema amenajării bazinelor hidrografice torențiale. Revista Pădurilor, nr 4, pp. 196-201. București.

130. Munteanu, S., 1976: Evoluția pe plan european, a preocupărilor și concepțiilor FAO în domeniul corectării torenților. Revista Pădurilor nr 3, pp. 145-150, București.

131. Munteanu, S., Clinciu, I., 1982: Amenajarea bazinelor hidrografice torențiale. Partea a II a. Studiul torenților și al amenajării lor. Universitatea din Brașov, 285 p.

132. Nakicenovic, N., J. Alcamo, G. Davis, B. de Vries, J. Fenhann, S. Gaffin, K. Gregory, A. Grübler, T.Y. Jung, T. Kram, E.L. La Rovere, L. Michaelis, S. Mori, T. Morita, W. Pepper, H. Pitcher, L. Price, K. Raihi, A. Roehrl, H.-H. Rogner, A. Sankovski, M. Schlesinger, P. Shukla, S. Smith, R. Swart, S. van Rooijen, N. Victor, and Z. Dadi. IPCC, 2000: Emissions Scenarios. A Special Report of Working Group III of the Intergovernmental Panel on Climate Change. Cambridge University Press, Cambridge, United

Kingdom and New York, NY, USA, 599 p.

133. Nash, J.E., Sutcliffe, J.V., 1970: River flow forecasting through conceptual models. Part I – A discussion of principles. Journal of Hydrology, vol. 10, pp 282-290.

134. Neitsch S.L., Arnold J.G., Kiniry J.R., Williams J.R., King K.W., 2005: Soil and Water Assessment Tool (SWAT) Theoretical Documentation. Grassland Soil and Water Research Laboratory, Blackland Research Center, Texas Agricultural Experiment Station, Texas Water Resources Institute, Texas Water Resources Institute, College Station, Texas. AgriLIFE Research & Extension. College of Agriculture and life Science.

135. Neitsch, S.L., Arnold, J.R., Kiniry, J.R., Williams, J.R., 2009: Soil and Water Assessment Tool. Teoretical Documentation, version 2009. Texas Water Resources Insitute, Technical Raport no. 406, 647 pp.

136. Nicolescu, V.N., 2006: Curs de Silvicultură, partea I (semestrul I). Suport de curs. Universitatea Transilvania din Brașov, 99 p.

137. Niță, M.D., 2013: Amenajarea bazinelor hidrografice montane situate în arii naturale protejate. Editura Lux Libris, Brașov, ISBN 978-973-131-236-1.

138. Pandey, K. B., Gosain, A. K., Paul, G., Khare, D., 2017: Climate change impact assessment on hydrology of a small watershed using semi-distributed model. Applied Water Science, vol. 7, pp. 2029–2041, DOI 10.1007/s13201-016-0383-6.

139. Păcurar, V.D., 2007: Influența posibilelor modificări climatice asupra proceselor de degradare şi ameliorării silvice a terenurilor degradate. În Lucrările sesiunii științifice Pădurea și dezvoltarea durabilă, Proocedings of the Symposium Forest and Sustainable Developmnet, Editura Universității Transilvania, Braşov, 2007, pp. 367-370.

140. Păcurar, V.D., 2008a: Consecințe posibile ale schimbărilor climatice asupra pădurilor și importanța stabilirii unor scenarii locale. Revista Pădurilor anul 123, nr. 4, pp. 20-23.

141. Păcurar, V.D., 2008b: Climate Change Local Scenarios for Braşov Area Established by Statistical Downscaling. Bulletin of the Transilvania University, Braşov, Series II Forestry • Wood Industry • Agricultural Food Engineering, vol. I, nr. 50, pp. 25-28.

142. Păcurar, V.D., 2008c: Modelarea și simularea proceselor hidrologice și erozionale în bazine hidrografice împădurite la începutul secolului XXI. În Silvologie vol. VI: Amenajarea bazinelor hidrografice torențiale. Noi concepții și fundamente științifice. Sub redacția Giurgiu, V., Clinciu, I. Editura Academiei Române, București, 2008, 334 p.

143. Păcurar, V.D., 2016: Air temperature digital maps for representative concentration pathways and possible impacts on Postavaru mountains forests. Bulletin of the Transilvania University of Braşov Series II: Forestry • Wood Industry • Agricultural Food Engineering, vol. 9 (58), nr.2, pp 31-36.

144. Perry, K.A., 2014: Application of the SWAT hydrological model in a small, mountainous catchmentt in South Africa. Master of Science in Water Resources Management, University of Pretoria, 79 p. Available at: https://pdfs.semanticscholar.org/33a8/35545648af18a7e88dcf1c76f44efcd076d1.pdf.

145. Peraza-Castro, M., Ruiz-Romera, E., Meaurio, M., Sauvage, S., Sánchez-Pérez, J.M., 2018: Modelling the impact of climate and land cover change on hydrology and water quality in a forest watershed in the Basque Country (Northern Spain). Ecological Engineering, vol. 122, pp. 315–326, https://doi.org/10.1016/j.ecoleng.2018.07.016.

146. Petrițan, C.I., 2008: Contribuții la studiul statistic al parametrilor morfometrici și morfohidrologici ai bazinelor hidrografice mici, predominant forestiere. Rezumatul tezei de doctorat, Universitatea Transilvania Brașov, 60 p.

147. Pișota, I., Buta, I., 1975: Hidrologie. Editura Didactică și Pedagogică, 460p.

148. Qiu, L.-J., Zheng, F.-L., Yin, R.-S., 2012: SWAT-based runoff and sediment simulation in a small watershed, the loessial hilly-gullied region of China: capabilities and challenges. International Journal of Sediment Research, vol. 27, nr. 2, pp. 226–234.

149. Reed, M.S., Podesta, G., Fazey, I., Geeson, N., Hessel, R., Hubacek, K., Letson, D., Nainggolan, D., Prell, C., Rickenbach, M.G., Ritsema, C., Schwilch, G., Stringer, L.C., Thomas, A.D. 2013: Combining analytical frameworks to assess livelihood vulnerability to climate change and analyses adaptation options. Ecological Economics, vol. 94, pp. 66–77.

150. Rodríguez-Blanco, M.L., Arias, R., Taboada-Castro, M.M., Nunes, J.P., Keizer, J.J., Taboada-

Castro, M.T., 2016: Potential Impact of Climate Change on Suspended Sediment Yield in NW Spain: A Case Study on the Corbeira Catchment. Water, vol. 8, nr. 444, Doi:10.3390/w8100444.

151. Rogelj, J., Meinshausen, M., Knutti, R., 2012: Global warming under old and new scenarios using IPCC climate sensitivity range estimates. Nature Climate Change, pp. 1-6, DOI: 10.1038/NCLIMATE1385.

152. Schewe J., Heiune J., Gerden D., Haddeland I., Arnell N.W., Clark D.B., Dankers R., Eisner S., Fekete B.M., Colón-Gonzáles F. J., Gosling S.N., Kim H., Liu X., Masaki Y., Portmann F. T., Satoh Y., Stacke T., Tang Q., Wada Y., Wisser D., Albrecht T., Frieler K., Piontek F., Warszawski L., Kabat P., 2014: Multimodel assessment of water scarcity under climate change. Proceedings of the National Academy of Sciences of the United States of America, vol. 111, nr .9, pp. 3245-3250.

153. Seceleanu, I., 2013: Amenajarea pădurilor. Organizare și conducere structurală. Editura Ceres, 505 p.

154. Serpa, D., Nunes, J.P., Santos, J., Sampaio, E., Jacinto, R., Veiga, S., Lima, J.C., Moreira, M., Corte-Real, J., Keizer, J.J., Abrantes, N., 2015: Impacts of climate and land use changes on the hydrological and erosion processes of two contrasting Mediterranean catchments. Science of the Total Environment, vol. 538, pp. 64–77, http://dx.doi.org/10.1016/j.scitotenv.2015.08.033.

155. Senent-Aparicio, J., Pérez-Sánchez, J., Carrillo-García, J., Soto, J., 2017: Using SWAT and Fuzzy TOPSIS to Assess the Impact of Climate Change in the Headwaters of the Segura River Basin (SE Spain) Water, vol. 9, nr. 2, doi:10.3390/w9020149.

156. Spârchez, G., Târziu, D., Dincă, L., 2011: Pedologie. Editura Lux Libris, Brașov, 291 p.

157. Stonefelt, M.D., Fontaine, T.A., Hotchkiss, R.H., 2007: Impacts of climate change on water yield in the upper wind river basin. Journal of the American Water Resources Association, vol 36, nr 2, pp. 321-336, https://doi.org/10.1111/j.1752-1688.2000.tb04271.x.

158. Târziu, D., 1997: Pedologie și stațiuni forestiere. Editura Ceres, București, 478 p.

159. Târziu, D., 2006: Solul, verigă de bază în circuitul apei în ecosferă și reglarea apelor din bazinele hidrografice montane. Capitolul 6 în Silvologie, vol. V: Pădurea și regimul apelor. Sub redacția V. Giurgiu, I. Clinciu, Editura Academiei Române, pp. 206-215.

160. Tegart, WJ. McG., Sheldon, G. W., Griffiths, D. C. IPCC, 1990: Climate Change. The IPCC Impact Assessment, 296 p. Available at: https://www.ipcc.ch/site/assets/uploads/2018/02/ipcc_far_wg_II_full_report.pdf.

161. Thompson, J. R., 2012: Modelling the impacts of climate change on upland catchments in southwest Scotland using MIKE SHE and the UKCP09 probabilistic projections. Hydrology Research, vol. 43, nr. 4, pp. 507-530, DOI: 10.2166/nh.2012.105.

162. Tudose N.C., Davidescu Ș., Cheval S., Chendeș V., Ungurean C., Babată M., 2018: Integrated model of river basin, land use and urban water supply. Deliverable 3.4. CLISWELN project. Available at: https://www.hzg.de/imperia/md/content/csc/projekte/projekte/clisweln_d3.4_romania_study_case_final-2.pdf.

163. Tudose, N.C., Ungurean, C., Davidescu, Șerban, Clinciu, I., Marin, M., Nita, M.D., Adorjani, A., Davidescu, A., 2020: Torrential flood risk assessment and environmentally friendly solutions for small catchments located in the Romania Natura 2000 sites Ciucas, Postavaru and Piatra Mare. Sci.ence of the Total Environment, 698, 134271, https://doi.org/10.1016/j.scitotenv.2019.134271.

164. van Vuuren, D. P.P., Edmonds, J., Kainuma, M., Riachi, K., Thompson, A., Hibbard, K., Hurtt, G. C., Kram, T., Krey, V., Lamarque, J.-F., Masui, T., Meinshausen, M., Nakicenovic, N., Smith, S. J., Rose, S. K. 2011: The representative concentration pathways: an overview. Climatic Change, vol. 109, pp 5–31, DOI 10.1007/s10584-011-0148-z.

165. Vasile, D., Scărlătescu, V., Stuparu, E., Petrițan, A.M., Turcu, D., Ciuvăț, L., Merce, O., 2015: Definirea conceptului de habitat forestier periclitat, vulnerabil și rar în vederea actualizării Listei roșii a habitatelor forestiere din România. Revista de Silvicultură și Cinegetică, anul XX, nr 36.

166. Vertessy, R.A. 2000: Impacts of plantation forestry on catchment runoff. Proceedings of a national workshop, Melbourne, 2000. Water and Salinity Issues in Agroforestry nr. 7.

167. Wang, H., Sun, F., Xia, J., Liu,W., 2017: Impact of LUCC on streamflow based on the SWAT model over the Wei River basin on the Loess Plateau in China. Hydrology and Earth System Science, vol.

21, pp. 1929–1945, DOI:10.5194/hess-21-1929-2017.

168. Wayne, G. 2013: The Beginner's Guide to Representative Concentration Pathways. Available at: https://www.skepticalscience.com/docs/RCP_Guide.pdf.

169. Weber, A., Fohrer, N., Möller, D., 2001: Long-term land use changes in a mesoscale watershed due to socio-economic factors-Effects on landscape structures and functions. Ecological Modelling, vol. 140, pp 125–140, DOI: https://doi.org/10.1016/S0304-3800(01)00261-7.

170. Wei, X., Li, Q., Zhang, M., Giles-Hansen, K., Liu, W., Fan, H., Wang, Y., Zhou, G., Piao, S., Liu, S., 2018: Vegetation cover—another dominant factor in determining global water resources in forested regions. Global Change Biology, vol. 24, pp. 786–795, DOI: 10.1111/gcb.13983.

171. Williams J.R., 1995. Chapter 25: The Epic model, 909-1000. In Singh V.P. (ed.) Computer models of Watershed hydrology. Water Resources Publication.

172. Winchell, M., Srinivasan, R., Di Luzio, M., Arnold, J., 2013: ArcSWAT interface for SWAT2012: user's guide. Blackland Research and Extension Center, Texas Agrilife Research. Grassland, Soil and Water Research Laboratory. USDA Agricultural Research Service, Texas.

173. Yang, J., Reichert, P., Abbaspour, K.C., Xia, J., Yang, H., 2008: Comparing uncertainty analysis techniques for a SWAT application to the Chaohe Basin in China. ournal of Hydrology, vol. 358, pp. 1– 23, doi:10.1016/j.jhydrol.2008.05.012.

174. Zabaleta, A., Meaurio, M., Ruiz, E., Antigüedad, I., 2014: Simulation Climate Change Impact on Runoff and Sediment Yield in a Small Watershed in the Basque Country, Northern Spain. Journal of Environmental Quality, vol. 43 nr. 1, pp. 235-245, DOI:10.2134/jeq2012.0209.

175. Zhang, M., Liu, N., Harper,R., Li, Q., Liu, K.,Wei, X., Ning, D., Hou, Y., Liu, S., 2017: A global review on hydrological responses to forest change across multiple spatial scales: Importance of scale, climate, forest type and .hydrological regime. Journal of Hydrology, vol. 546, pp. 44–59, http://dx.doi.org/10.1016/j.jhydrol.2016.12.040.

176. Zhang, H., Wang, B., Liu, D.L., Zhang, M., Leslie, L.M., Yu, Q., 2020: Using an improved SWAT model to simulate hydrological responses to land use change: A case study of a catchment in tropical Australia. Journal of Hydrology, vol. 585, https://doi.org/10.1016/j.jhydrol.2020.124822.

177. Zhou, Z., Ouyang, Y., Li, Y., Qiu, Z., Moran, M., 2017: Estimating impact of rainfall change on hydrological processes inJianfengling rainforest watershed, China using BASINS-HSPF-CATmodeling system. Ecological Engineering, vol. 105, pp. 87–94. http://dx.doi.org/10.1016/j.ecoleng.2017.04.051.

178. ***, 2009: Raportul privind Starea Mediului în România. Available at http://www.anpm.ro/anpm_resources/migrated_content/uploads/16100_3%20SCHIMBARI%20CLIMATICE%202009.pdf. Accesed on March 2018.

179. ***2013. Strategia Națională a României privind Schimbările Climatice. Adoptată prin HG nr. 529/2013 published in Monitorul Oficial în iulie, 2013. Available at: http://mmediu.ro/app/webroot/uploads/files/Strategia-Nationala-pe-Schimbari-Climatice-2013-2020.pdf

180. ***, 1978: Metodologia de determinare a debitului maxim probabil de viitură generat de ploi torențiale în bazine hidrografice mici, pentru studii și proiecte de corectare a torenților. Redactare Radu Gaspar, mai 1978.

181. ***, 2018a: IPCC official site: http://www.ipcc.ch/, accesată în august 2018.

182. ***, 2018b: Modeling Ground-Water Flow with Modeling Ground-Water Flow with MODFLOW and Related Programs. U.S. Department of the Interior U.S. Geological Survey. Available at: https://pubs.usgs.gov/fs/FS-121-97/fs-121-97.pdf . Accesed in December 2018.

183. ***,2016:https://issuu.com/metropolabrasov5/docs/vol_i_profilul_zmb_46361b5ccabd3d.

184. ***, 2019a:https://is-enes-data.github.io/CORDEX_RCMs_info.html. Accesat în 6 mai 2019.

185. ***, 2019b: https://www.hzg.de/ms/clm-community/076389/index.php.en. Accesat în 7 mai 2019.

186. ***, 2019c: https://www.euro-cordex.net/060374/index.php.en. Accesat în 7 mai 2019.

187. ***, 2019d: http://www.cordex.org/domains/. Accesat în 7 mai 2019.

188. doi.pangaea.de/10.1594/PANGAEA.833627.Baza de date ROCADA.

189.https://www.nrcs.usda.gov/wps/portal/nrcs/detailfull/national/?&cid=stelprdb1045331. Agricultural Research Service official site.

190. https://swat.tamu.edu/software/swat-cup/. USDA-ARS official site for SWAT-CUP download.
191. https://swat.tamu.edu/. USDA-ARS official site for ArcSWAT and QGis download.
192. https://web.ics.purdue.edu/~vmerwade/education/fao_soil_tutorial.pdf. Creating SWAT Soil Database using FAO Soil and Terrain Database of East Africa (SOTER) Data.
193. www.vremea.ro/gt/clima-brasov/
194. https://esgf-data.dkrz.de/search/cordex-dkrz/
195. STATISTICA 13.5.0.17 software.
196. Excel Microsoft Office

ANNEXES

Annex 1. Monthly, seasonal, and annual surface runoff projected for the 2020−2100 period

Table 4.1. Monthly surface runoff (thousand cm) projected for the 2020–2039 period.

		Climate change scenarios											
		REMO4.5			CLM4.5			REMO8.5			CLM8.5		
Month	Baseline	S1	S2	S3	S1	S2	S3	S1	S2	S3	S1	S2	S3
January	305	867	913	970	686	735	796	529	568	623	237	254	281
February	193	1113	1167	1243	1668	1762	1872	1221	1284	1364	1319	1378	1465
March	3290	3984	4139	4302	4187	4380	4606	4842	4993	5164	4171	4368	4592
April	1829	2255	2352	2451	868	944	1015	3545	3714	3886	2257	2388	2497
May	179	187	205	228	159	181	209	637	703	785	214	242	278
June	653	190	213	242	349	394	451	193	222	260	245	279	322
July	305	221	251	287	211	241	280	92	108	129	401	449	511
August	285	71	86	105	221	253	293	100	116	136	218	243	275
September	87	173	203	240	183	208	240	88	100	117	98	118	143
October	79	278	322	378	160	189	225	211	241	279	191	219	254
November	270	712	795	895	770	847	939	567	644	740	451	509	582
December	308	982	1063	1165	398	446	504	846	931	1040	640	694	762

Table 4.2. Seasonal surface runoff (thousand cm) projected for the 2020–2039 period.

		Climate change scenarios											
		REMO4.5			CLM4.5			REMO8.5			CLM8.5		
Season	Baseline	S1	S2	S3	S1	S2	S3	S1	S2	S3	S1	S2	S3
Spring	1766	2142	2232	2327	1738	1835	1943	3008	3137	3278	2214	2333	2456
Summer	414	161	183	211	260	296	341	128	149	175	288	324	369
Autumn	145	388	440	504	371	415	468	289	328	379	247	282	326
Winter	269	987	1048	1126	917	981	1057	865	928	1009	732	775	836

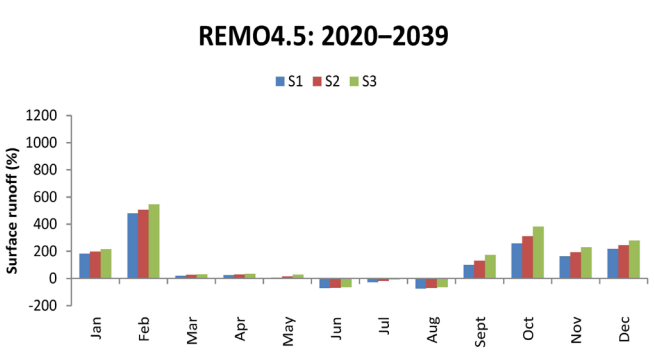

a)

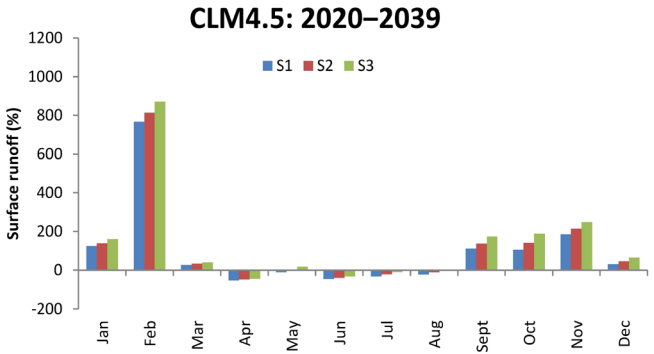

b)

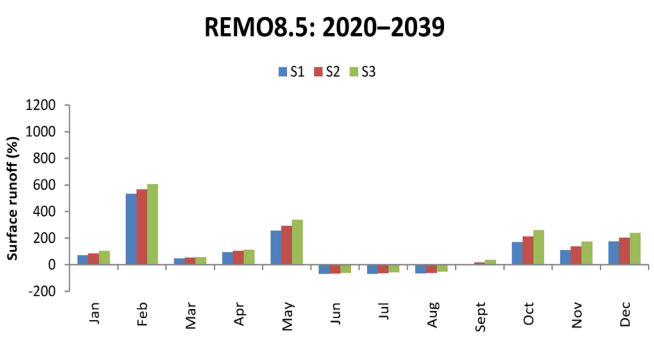

c)

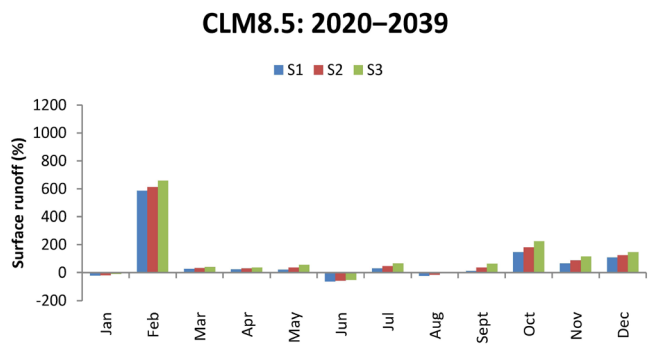

d)

Figure 4.1. Monthly surface runoff projected in all climate and land use change scenarios for the 2020–2039 period.

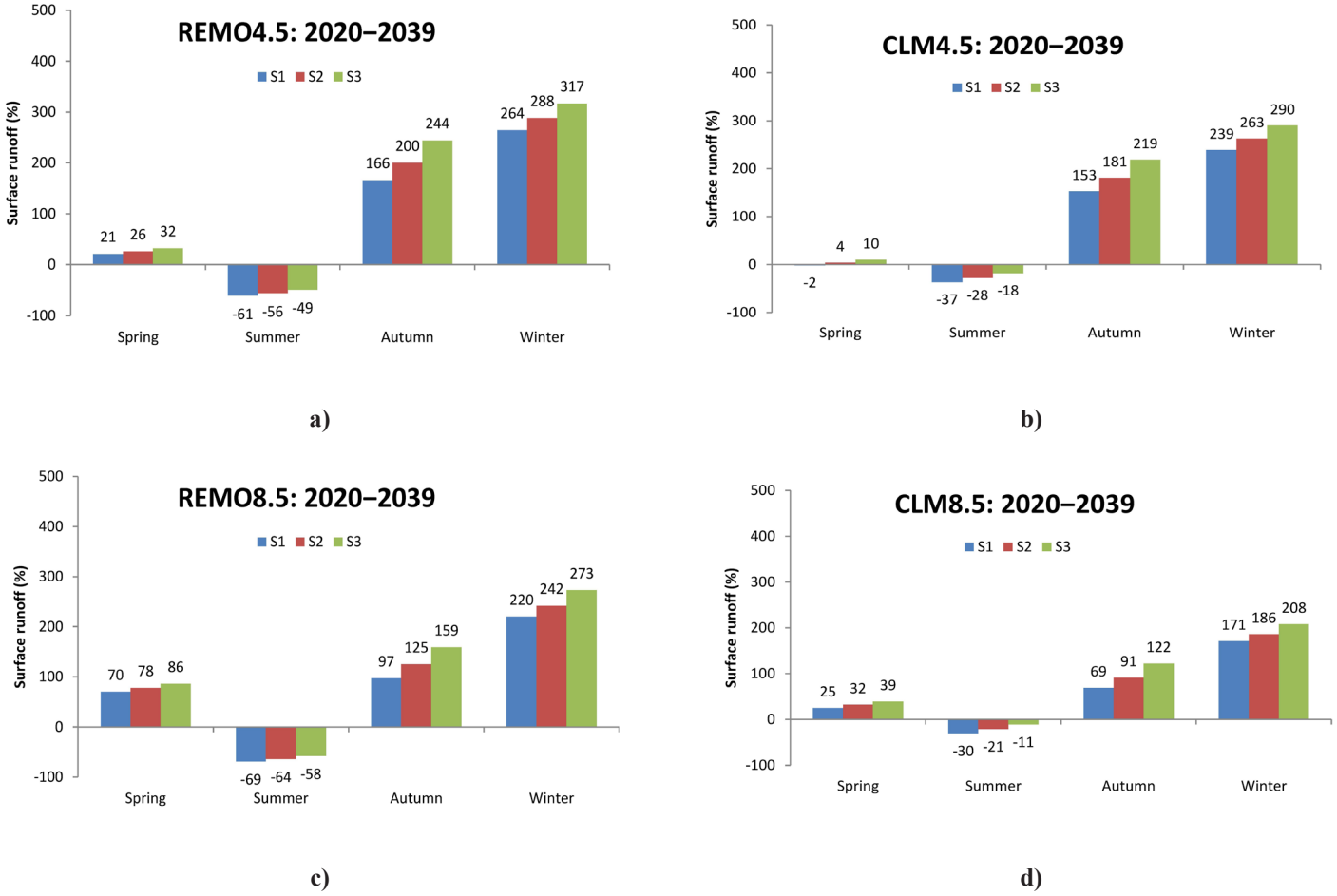

Figure 4.2. Seasonal surface runoff projected in all climate and land use change scenarios for the 2020–2039 period.

Table 4.3. Annual surface runoff (thousand cm) projected for the 2020–2039 period

		Climate change scenarios											
		REMO4.5			CLM4.5			REMO8.5			CLM8.5		
Baseline	Year	S1	S2	S3	S1	S2	S3	S1	S2	S3	S1	S2	S3
7782	2020	13334	13786	14324	11803	12558	13487	15970	16651	17446	7077	7773	8560
	2021	9939	10787	11786	10167	10849	11619	11480	12224	13051	9882	10584	11446
	2022	12509	13151	13845	10015	10943	12016	17550	18440	19526	12562	13325	14326
	2023	8123	8741	9468	9728	10491	11377	14881	15765	16793	13471	14245	15122
	2024	22954	24034	25357	7802	8471	9218	9993	10726	11568	10798	11547	12397
	2025	9125	9576	10027	12074	12812	13702	15751	16472	17362	16308	17108	18048
	2026	9064	9968	11038	13731	14719	15903	20020	21019	22179	11354	12028	12804
	2027	9886	10381	11001	6987	7515	8100	9315	9913	10630	8888	9487	10158
	2028	14301	15172	16202	8414	8986	9657	14434	15165	16058	7859	8553	9491
	2029	8803	9401	10122	14404	15283	16298	18198	19267	20637	13584	14258	14917
	2030	7673	8253	8961	4415	4814	5279	20302	21272	22389	14419	15266	16281
	2031	13433	14173	15065	11847	12429	13104	14027	14755	15617	9720	10403	11219
	2032	19156	20094	21289	8060	8815	9705	10682	11246	11903	6174	6554	7009
	2033	6133	6697	7370	12718	13314	14023	9099	9885	10796	15837	16726	17675
	2034	12252	12838	13476	8552	9113	9797	5530	6060	6713	10277	11172	12219
	2035	3285	3602	3961	7189	7811	8568	9672	10433	11363	11661	12438	13334
	2036	9649	10327	11085	10992	11956	13064	9750	10457	11400	5422	5930	6564
	2037	14060	14750	15528	8919	9893	11068	11706	12421	13244	6427	6983	7623
	2038	7579	8261	9099	9968	10761	11733	9348	9819	10349	5614	6213	6904
	2039	9402	10193	11102	9427	10083	10851	9690	10501	11438	11504	12236	13131

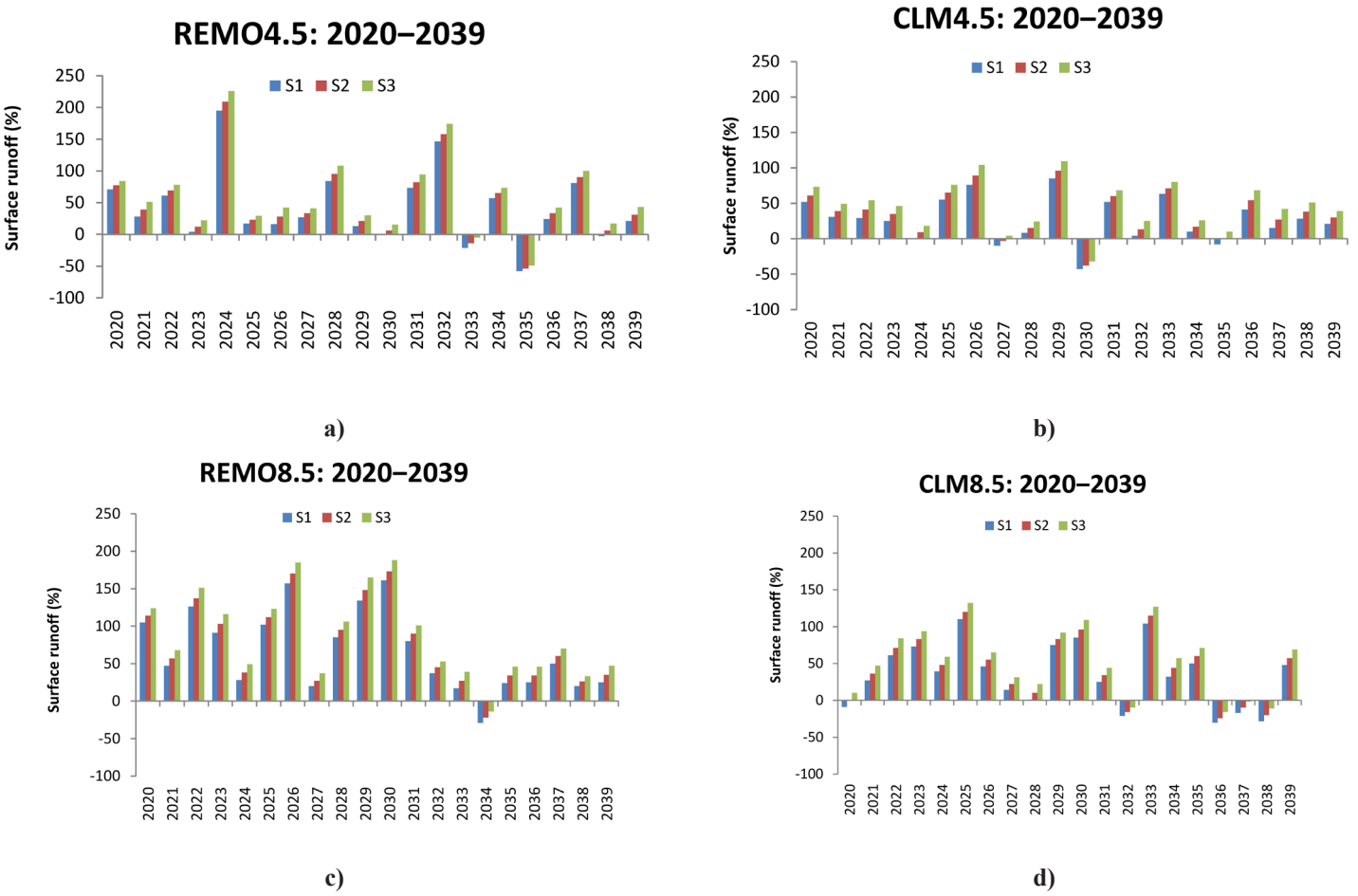

Figure 4.3. Annual surface runoff projected in all climate and land use change scenarios for the 2020–2039 period.

Table 4.4. Monthly surface runoff (thousand cm) projected for the 2040–2069 period

		Climate change scenarios											
		REMO4.5			CLM4.5			REMO8.5			CLM8.5		
Month	**Baseline**	**S1**	**S2**	**S3**	**S1**	**S2**	**S3**	**S1**	**S2**	**S3**	**S1**	**S2**	**S3**
January	305	1105	1188	1292	1291	1384	1494	691	754	836	466	506	557
February	193	1544	1621	1714	1502	1573	1653	1475	1583	1717	1920	2004	2120
March	3290	3597	3758	3934	3574	3730	3901	4416	4606	4829	5327	5593	5857
April	1829	2534	2680	2840	1355	1441	1526	1844	1953	2069	594	651	716
May	179	261	297	342	306	339	379	284	319	364	166	189	217
June	653	354	399	455	231	266	309	338	375	421	338	374	420
July	305	67	78	91	277	310	353	175	198	226	305	340	384
August	285	115	131	150	197	222	253	111	131	155	205	227	254
September	87	91	109	133	145	166	192	78	94	114	141	163	192
October	79	247	282	328	195	227	267	153	175	202	54	65	78
November	270	479	546	629	631	715	820	365	433	520	389	449	526
December	308	923	1004	1102	1138	1244	1373	589	661	749	708	783	881

Table 4.5. Seasonal surface runoff (thousand cm) projected for the 2040–2069 period.

		Climate change scenarios											
		REMO4.5			CLM4.5			REMO8.5			CLM8.5		
Season	**Baseline**	**S1**	**S2**	**S3**	**S1**	**S2**	**S3**	**S1**	**S2**	**S3**	**S1**	**S2**	**S3**
Spring	1766	2131	2245	2372	1745	1837	1935	2181	2293	2421	2029	2144	2263
Summer	414	179	203	232	235	266	305	208	235	267	283	314	353
Autumn	145	272	312	363	324	369	426	199	234	279	195	226	265
Winter	269	1191	1271	1369	1310	1400	1507	918	999	1101	1031	1098	1186

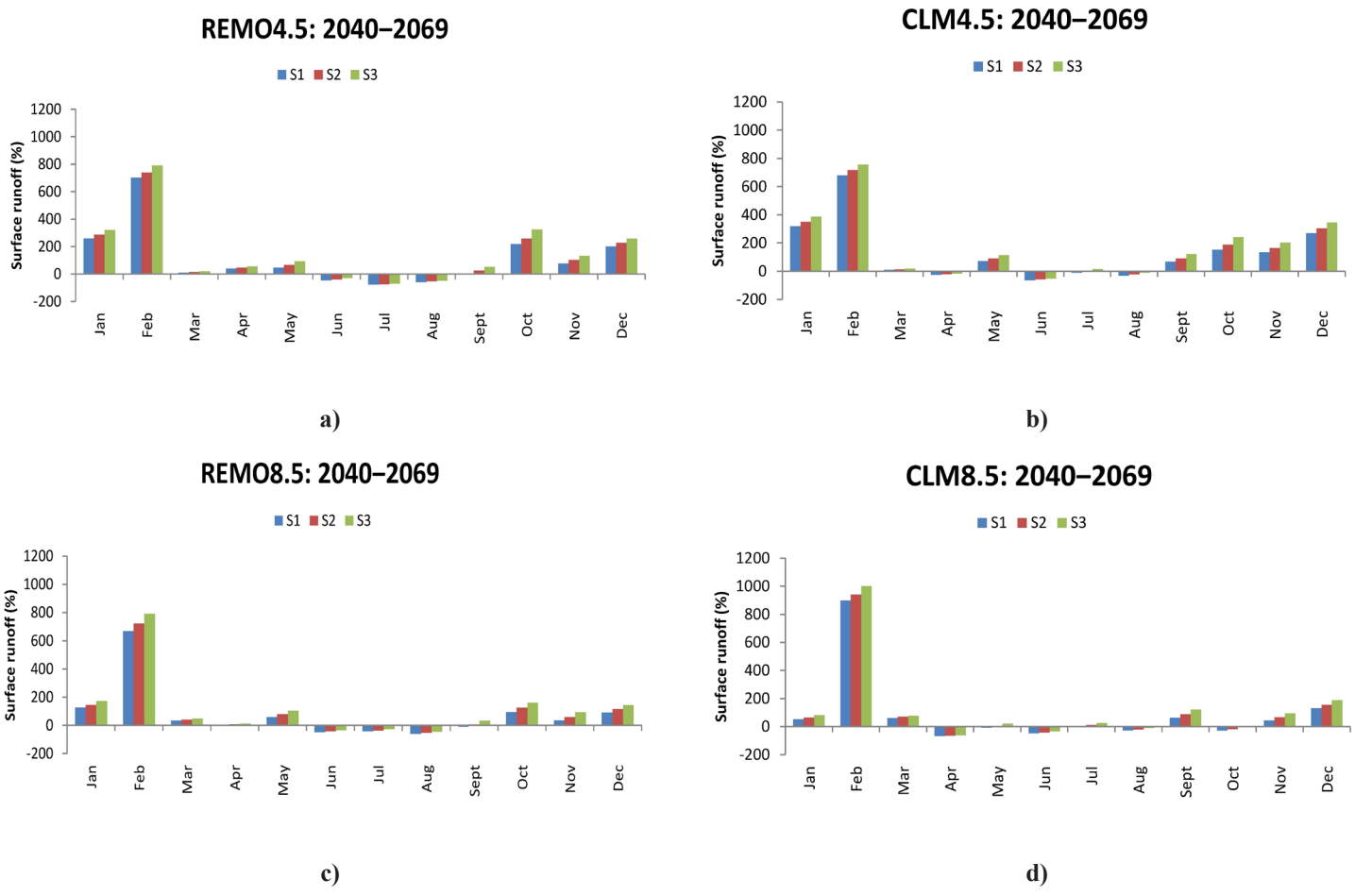

Figure 4.5. Monthly surface runoff projected in all climate and land use change scenarios for the 2040–2069 period.

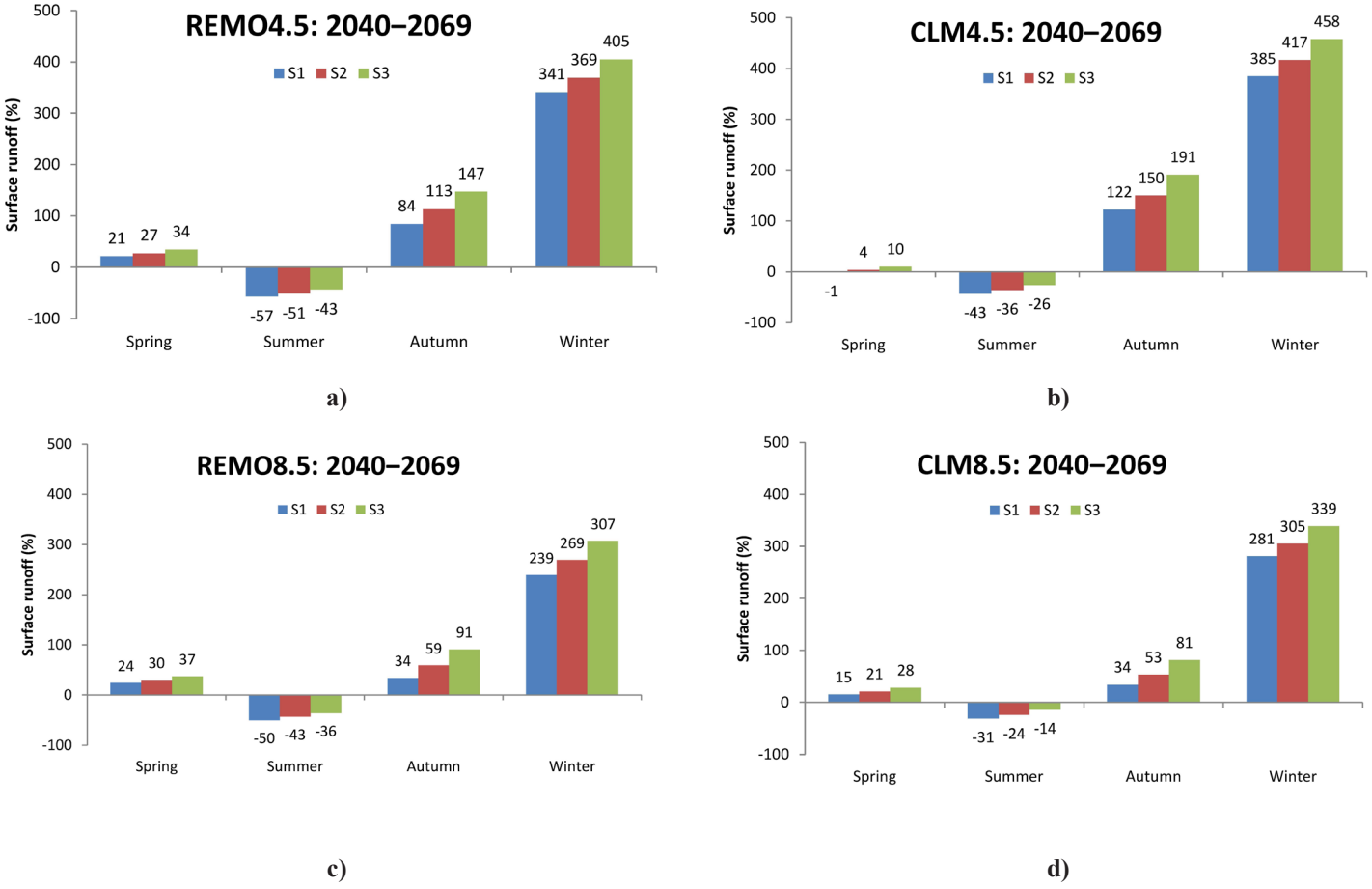

Figure 4.6. Seasonal surface runoff (expressed in percentage) projected in all climate and land use change scenarios for the 2040–2069 period.

Table 4.6. Annual surface runoff (thousand cm) projected for the 2040–2069 period.

		Climate change scenarios											
		REMO4.5			CLM4.5			REMO8.5			CLM8.5		
Baseline	Year	S1	S2	S3	S1	S2	S3	S1	S2	S3	S1	S2	S3
7782	2040	16530	17221	18032	14902	16057	17409	11715	12768	14030	11853	12689	13693
	2041	12733	13687	14793	13814	14507	15290	6426	6824	7296	13949	14673	15609
	2042	8414	9205	10141	11414	12172	13040	17777	18790	19986	13041	13687	14437
	2043	10545	11581	12834	9720	10513	11416	11370	12294	13413	7426	8086	8915
	2044	12824	13440	14169	8429	9248	10249	13163	13945	14862	18725	19581	20467
	2045	11148	11712	12337	5232	5682	6226	7395	8205	9150	9635	10362	11198
	2046	9604	10217	10926	10576	11369	12332	6479	7015	7613	10695	11273	11942
	2047	14184	15227	16443	11572	12355	13270	11803	12557	13483	12039	12801	13733
	2048	16947	17986	19255	20108	21106	22191	20041	21262	22799	9252	9923	10660
	2049	11862	12779	13872	8458	9032	9690	14025	14724	15532	9935	10714	11608
	2050	12341	13012	13727	11402	12168	13040	7617	8135	8733	10432	11267	12225
	2051	14566	15457	16481	15796	16875	18145	5451	6042	6749	7512	8063	8732
	2052	12952	13714	14618	10359	11060	11887	6308	7298	8503	4913	5494	6207
	2053	4138	4469	4866	9212	10023	10991	6899	7392	7967	9528	10370	11380
	2054	8351	9077	9995	10277	10826	11456	9138	9741	10475	8812	9471	10352
	2055	9269	10067	11027	6273	7021	7911	12960	13963	15159	14631	15555	16617
	2056	15598	16517	17576	5732	6286	6939	6450	7113	7928	7355	7878	8386
	2057	13275	13965	14707	18829	20128	21629	10030	11227	12758	9728	10545	11536
	2058	11914	12670	13581	9551	10130	10801	7647	8055	8537	10880	11747	12813
	2059	7674	8424	9329	3286	3805	4441	9443	9925	10503	13007	13744	14740
	2060	10764	11360	12080	9079	9965	11000	7887	8532	9302	7918	8550	9275
	2061	11525	12379	13380	6653	7283	7991	11595	12327	13155	15612	16630	17830
	2062	11105	11970	12996	5874	6624	7522	22695	23719	24964	13048	13893	14826
	2063	11372	12176	13096	10405	11354	12496	4644	5135	5729	7863	8549	9331
	2064	11860	12704	13728	16138	17033	18091	15553	16700	18153	13528	14185	14908
	2065	10288	11211	12297	10304	10961	11702	15372	16251	17336	5768	6221	6744
	2066	7258	7784	8339	17078	17953	18947	8633	9138	9749	13637	14389	15253
	2067	10506	11447	12636	13146	14078	15171	9762	10708	11865	6526	7244	8113
	2068	6200	6569	6950	12498	13028	13752	8830	9313	9927	13578	14361	15263
	2069	13762	14793	16122	9202	9846	10587	8500	9362	10360	7574	8368	9301

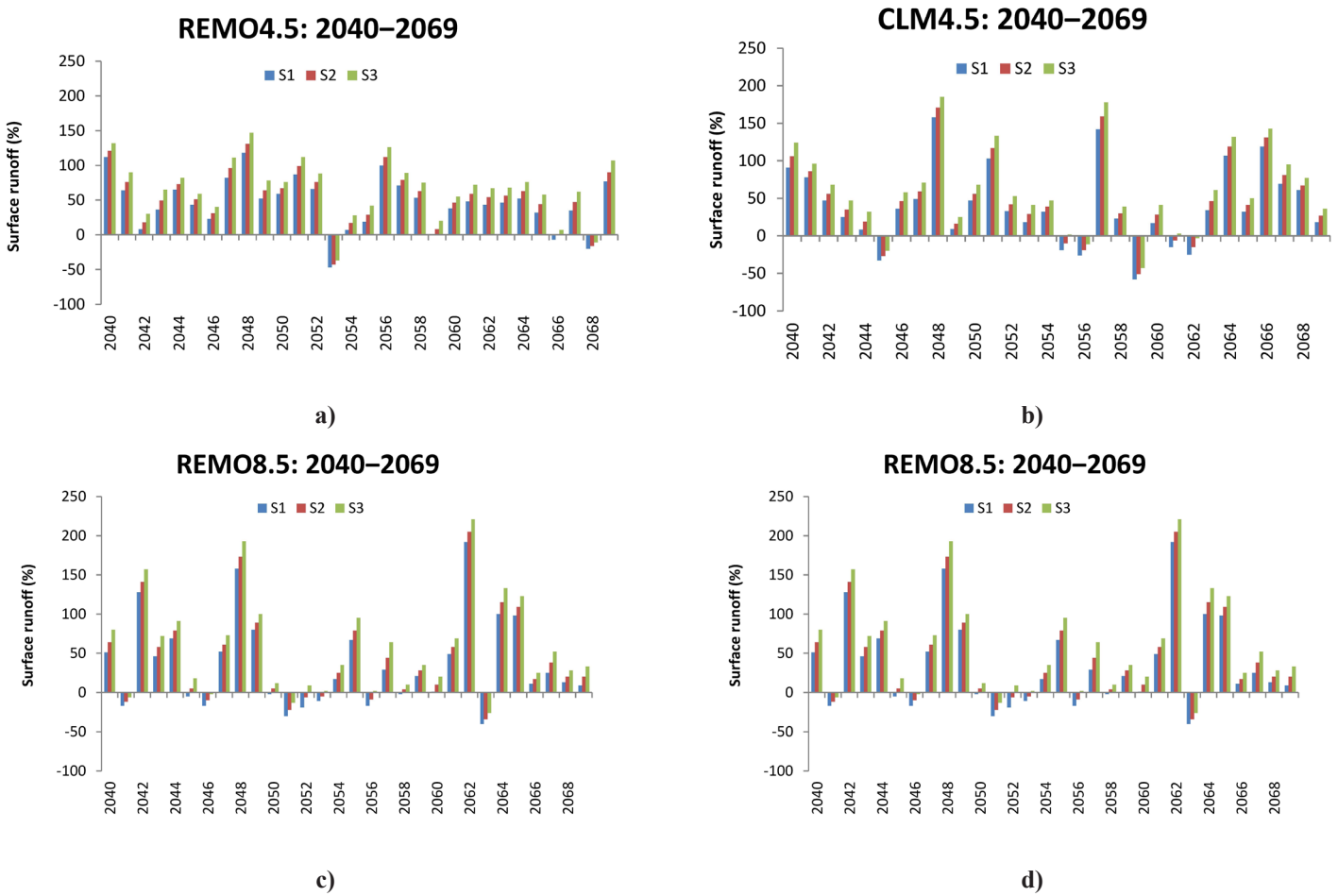

Figure 4.7. Annual surface runoff (expressed in percentage) projected in all climate and land use change scenarios for the 2040–2069 period.

Table 4.7. Monthly surface runoff (thousand cm) projected for the 2070–2100 period.

		Climate change scenarios											
		REMO4.5			CLM4.5			REMO8.5			CLM8.5		
Month	**Baseline**	**S1**	**S2**	**S3**	**S1**	**S2**	**S3**	**S1**	**S2**	**S3**	**S1**	**S2**	**S3**
January	305	912	986	1076	640	692	758	919	1008	1121	930	1005	1098
February	193	1715	1793	1889	2107	2237	2398	1697	1814	1956	2110	2236	2387
March	3290	3481	3654	3844	3755	3922	4108	2461	2592	2735	2710	2845	2971
April	1829	1574	1677	1787	1233	1311	1396	1072	1146	1231	765	816	867
May	179	340	381	433	250	285	329	312	352	403	325	360	405
June	653	250	280	318	280	319	369	229	264	309	421	477	549
July	305	161	184	213	288	323	368	115	132	154	266	301	344
August	285	88	99	114	180	201	228	211	228	250	137	154	175
September	87	208	236	272	131	148	168	63	79	99	146	170	200
October	79	153	173	198	172	201	239	176	209	253	245	282	330
November	270	741	814	904	483	549	632	400	453	518	385	438	503
December	308	950	1043	1155	788	877	984	917	1036	1183	855	959	1083

Table 4.8. Seasonal surface runoff (thousand cm) projected for the 2070–2100 period.

		Climate change scenarios											
		REMO4.5			CLM4.5			REMO8.5			CLM8.5		
Season	**Baseline**	**S1**	**S2**	**S3**	**S1**	**S2**	**S3**	**S1**	**S2**	**S3**	**S1**	**S2**	**S3**
Spring	1766	1798	1904	2021	1746	1839	1944	1282	1363	1456	1267	1340	1414
Summer	414	166	188	215	249	281	322	185	208	238	275	311	356
Autumn	145	367	408	458	262	299	346	213	247	290	259	297	344
Winter	269	1192	1274	1373	1178	1269	1380	1178	1286	1420	1298	1400	1523

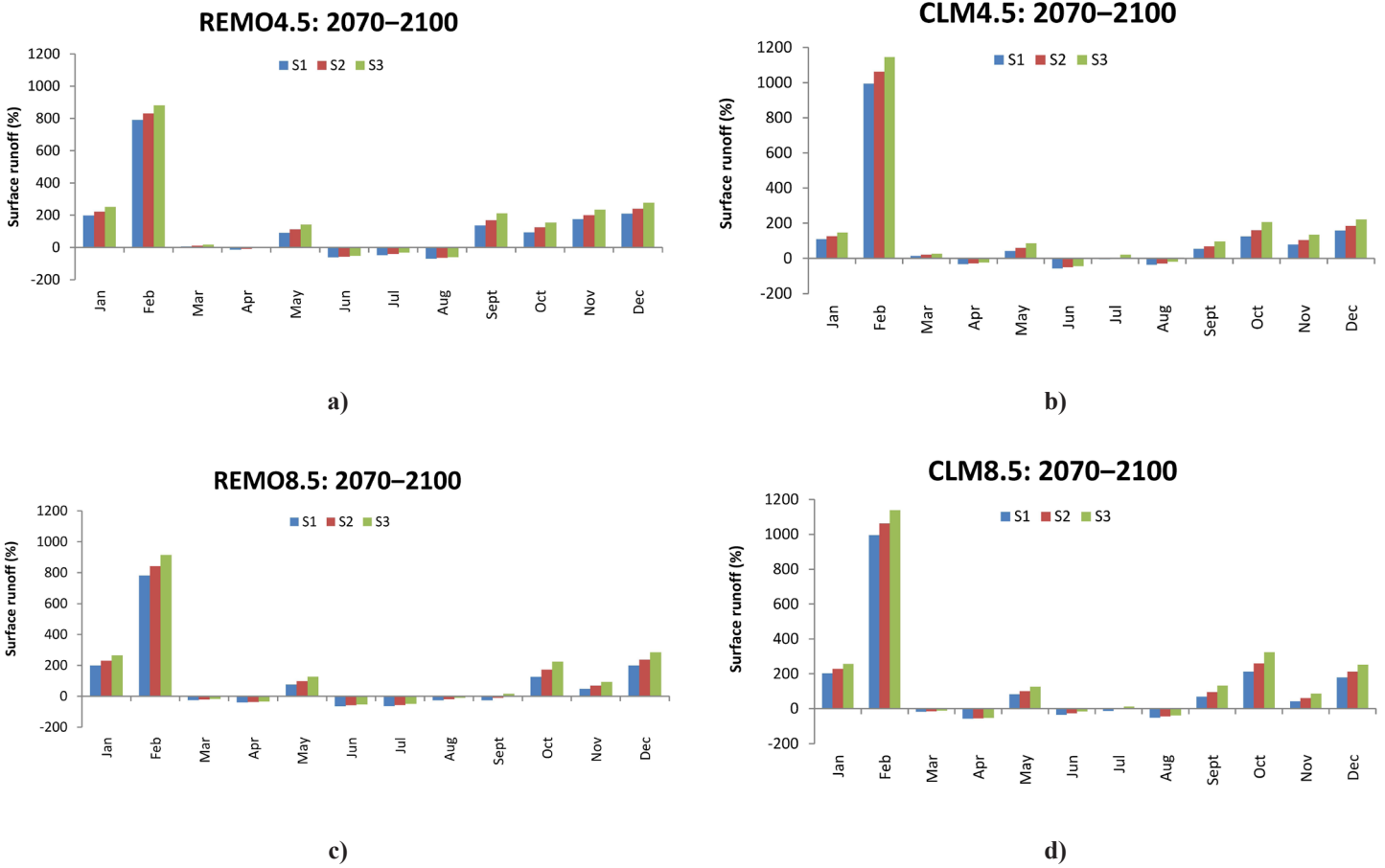

Figure 4.9. Monthly surface runoff (expressed in percentage) projected in all climate and land use change scenarios for 2070–2100 period.

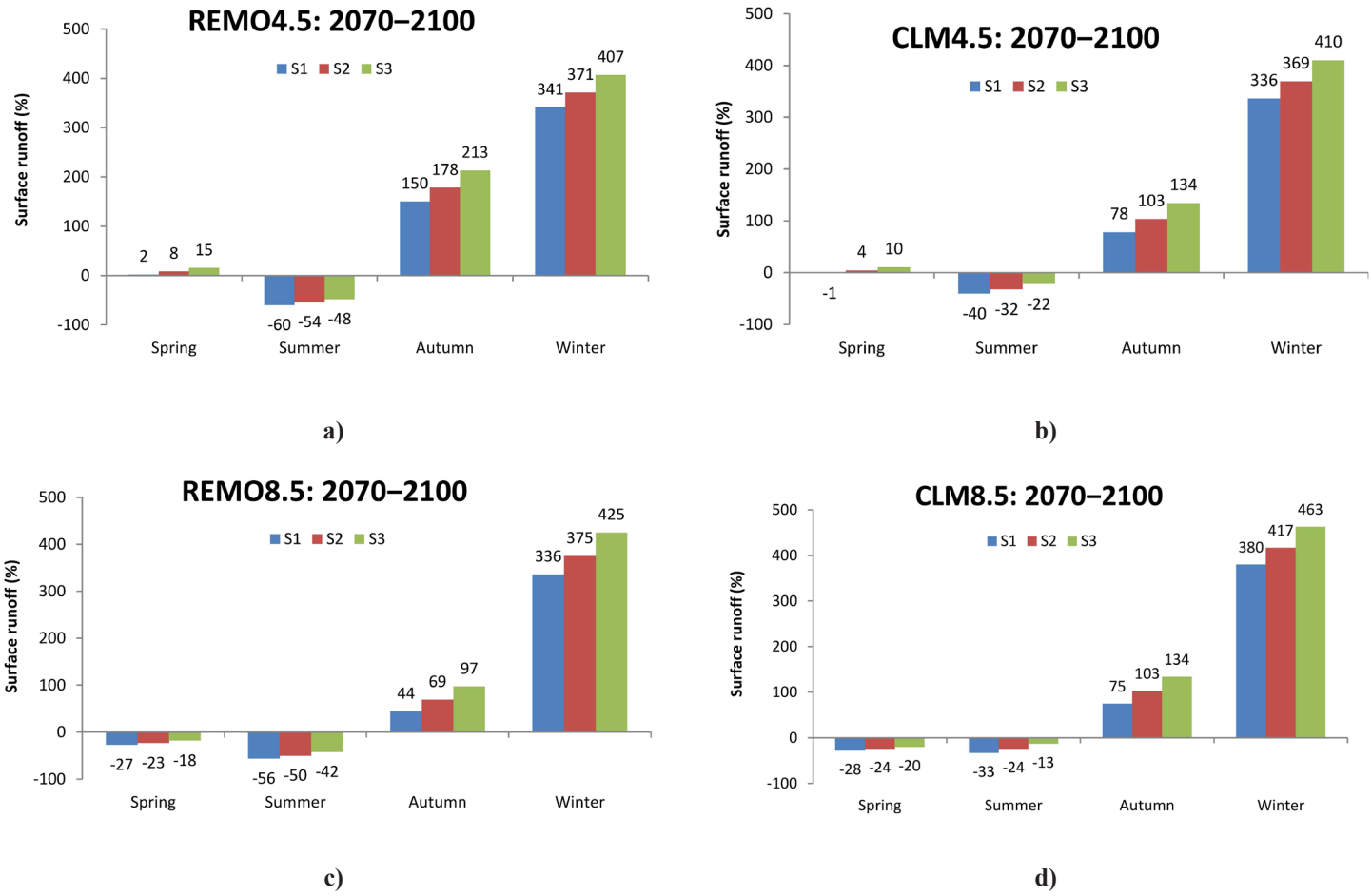

Figure 4.10. Seasonal surface runoff (expressed in percentage) projected in all climate and land use change scenarios for 2070–2100 period.

Table 4.9. Annual surface runoff (thousand cm) projected for the 2070–2100 period.

		Climate change scenarios											
		REMO4.5			CLM4.5			REMO8.5			CLM8.5		
Baseline	Year	S1	S2	S3	S1	S2	S3	S1	S2	S3	S1	S2	S3
7782	2070	5375	5857	6427	10814	11746	12868	6040	6787	7719	16777	17761	18811
	2071	12295	13047	13938	9902	10656	11560	11540	12269	13139	13914	14539	15235
	2072	11804	12617	13547	16557	17246	18079	15764	16675	17712	5958	6545	7230
	2073	12709	13564	14585	13017	14135	15490	11097	11807	12655	18759	19731	20924
	2074	14327	15138	16039	14161	15202	16456	6270	6908	7678	10215	11010	11897
	2075	20037	21274	22739	8633	9545	10620	4914	5443	6079	8995	9563	10198
	2076	7884	8414	9056	11487	12506	13705	8854	9424	10139	12850	13836	15052
	2077	17717	18487	19427	9012	9440	9938	8420	9357	10525	11365	12344	13504
	2078	15071	16019	17150	16489	17374	18428	11932	12687	13578	8828	9340	9916
	2079	4898	5324	5825	10497	11263	12153	12667	13467	14398	15388	16289	17356
	2080	12017	12815	13773	7461	8117	8858	17250	18502	20031	10654	11623	12759
	2081	6267	6877	7597	9903	10790	11823	6448	7015	7686	8321	9009	9785
	2082	5348	5938	6651	10324	10903	11586	13273	14292	15551	7610	8214	8928
	2083	10041	10707	11475	5624	6192	6851	5374	5810	6334	7531	8259	9161
	2084	12627	13244	13997	7162	7769	8517	9940	10563	11349	6756	7381	8045
	2085	8533	9104	9775	6797	7479	8312	5205	6011	6991	8845	9744	10778
	2086	3701	4183	4796	17481	18251	19174	7219	7999	8917	5931	6603	7382
	2087	10095	10732	11495	11247	12030	12956	4937	5526	6249	3646	4088	4650
	2088	4100	4739	5518	7942	8671	9533	7472	8137	8904	4179	4696	5316
	2089	9521	10272	11145	6139	6948	7934	4582	5291	6156	9506	10358	11370
	2090	12924	13912	15161	10655	11104	11696	12425	13247	14266	9479	10322	11326
	2091	9459	10290	11263	10395	11198	12155	6333	7041	7944	6008	6570	7200
	2092	7376	8136	9044	4637	5124	5728	6578	7228	8010	6300	6927	7674
	2093	9294	10064	10970	7512	8299	9237	11650	12368	13133	11130	12066	13100
	2094	13842	14884	16115	8697	9246	9893	9137	9834	10706	11279	12048	12901
	2095	14905	15861	16978	16489	17455	18711	6423	7247	8269	10523	11476	12594
	2096	7879	8497	9223	7449	7936	8448	7309	8102	9075	5257	5888	6628
	2097	10936	11948	13153	11336	12058	12891	8920	9672	10581	11238	11922	12724
	2098	12481	13139	13844	10696	11477	12490	5269	5877	6632	6570	7396	8351
	2099	14913	15692	16642	10076	10867	11771	6790	7681	8795	6930	7590	8353
	2100	9424	10120	10913	10910	12031	13388	5716	6483	7414	7369	8167	9148

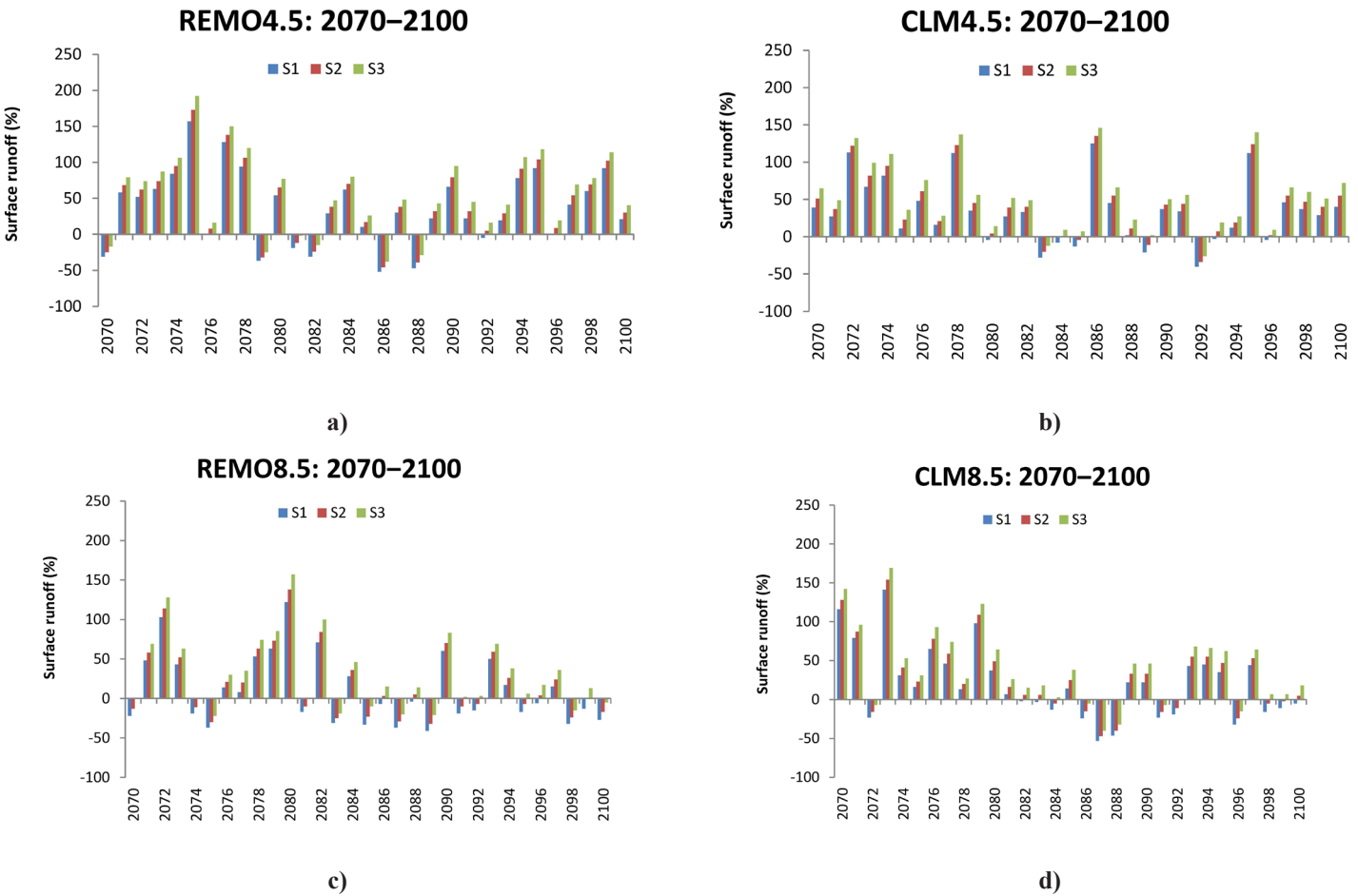

Figure 4.11. Annual surface runoff (expressed in percentage) projected in all climate and land use scenarios for the 2070–2100 period.

Annex 2. Monthly, seasonal and annual water discharges ($m^3 \cdot s^{-1}$) projected for the 2020–2100 period

Table 4.10. Monthly water discharges ($m^3 \cdot s^{-1}$) projected for the 2020–2039 period.

		Climate change scenarios											
		REMO4.5			CLM4.5			REMO8.5			CLM8.5		
Month	Baseline	S1	S2	S3	S1	S2	S3	S1	S2	S3	S1	S2	S3
January	0.15	0.55	0.56	0.57	0.36	0.37	0.39	0.27	0.28	0.30	0.19	0.19	0.19
February	0.10	0.59	0.61	0.63	0.81	0.83	0.87	0.55	0.57	0.60	0.61	0.63	0.66
March	1.31	1.83	1.85	1.88	1.84	1.88	1.94	2.09	2.12	2.16	1.87	1.92	1.97
April	1.26	1.68	1.66	1.64	1.05	1.03	0.99	2.25	2.26	2.25	1.80	1.79	1.76
May	0.78	0.84	0.81	0.78	0.77	0.74	0.71	1.51	1.48	1.44	1.04	1.01	0.98
June	1.20	0.72	0.71	0.70	0.93	0.93	0.93	1.08	1.06	1.05	0.95	0.95	0.94
July	1.04	0.60	0.60	0.61	0.82	0.82	0.83	0.70	0.70	0.70	0.98	0.99	1.00
August	0.88	0.41	0.42	0.42	0.64	0.65	0.66	0.42	0.43	0.43	0.73	0.74	0.74
September	0.55	0.54	0.55	0.57	0.50	0.51	0.51	0.31	0.31	0.32	0.48	0.48	0.49
October	0.37	0.62	0.64	0.66	0.43	0.44	0.44	0.4	0.41	0.42	0.51	0.52	0.52
November	0.28	0.79	0.82	0.85	0.58	0.60	0.63	0.46	0.49	0.52	0.58	0.59	0.61
December	0.19	0.69	0.72	0.75	0.32	0.33	0.35	0.46	0.49	0.53	0.45	0.46	0.48

Table 4.11. Seasonal water discharges ($m^3 \cdot s^{-1}$) projected for the 2020–2039 period.

		Climate change scenarios											
		REMO4.5			CLM4.5			REMO8.5			CLM8.5		
Season	Baseline	S1	S2	S3	S1	S2	S3	S1	S2	S3	S1	S2	S3
Spring	1.12	1.45	1.44	1.43	1.22	1.22	1.21	1.95	1.95	1.95	1.57	1.57	1.57
Summer	1.04	0.58	0.58	0.58	0.80	0.80	0.81	0.73	0.73	0.73	0.89	0.89	0.89
Autumn	0.40	0.65	0.67	0.69	0.50	0.52	0.53	0.39	0.4	0.42	0.52	0.53	0.54
Winter	0.15	0.61	0.63	0.65	0.50	0.51	0.54	0.43	0.45	0.48	0.42	0.43	0.44

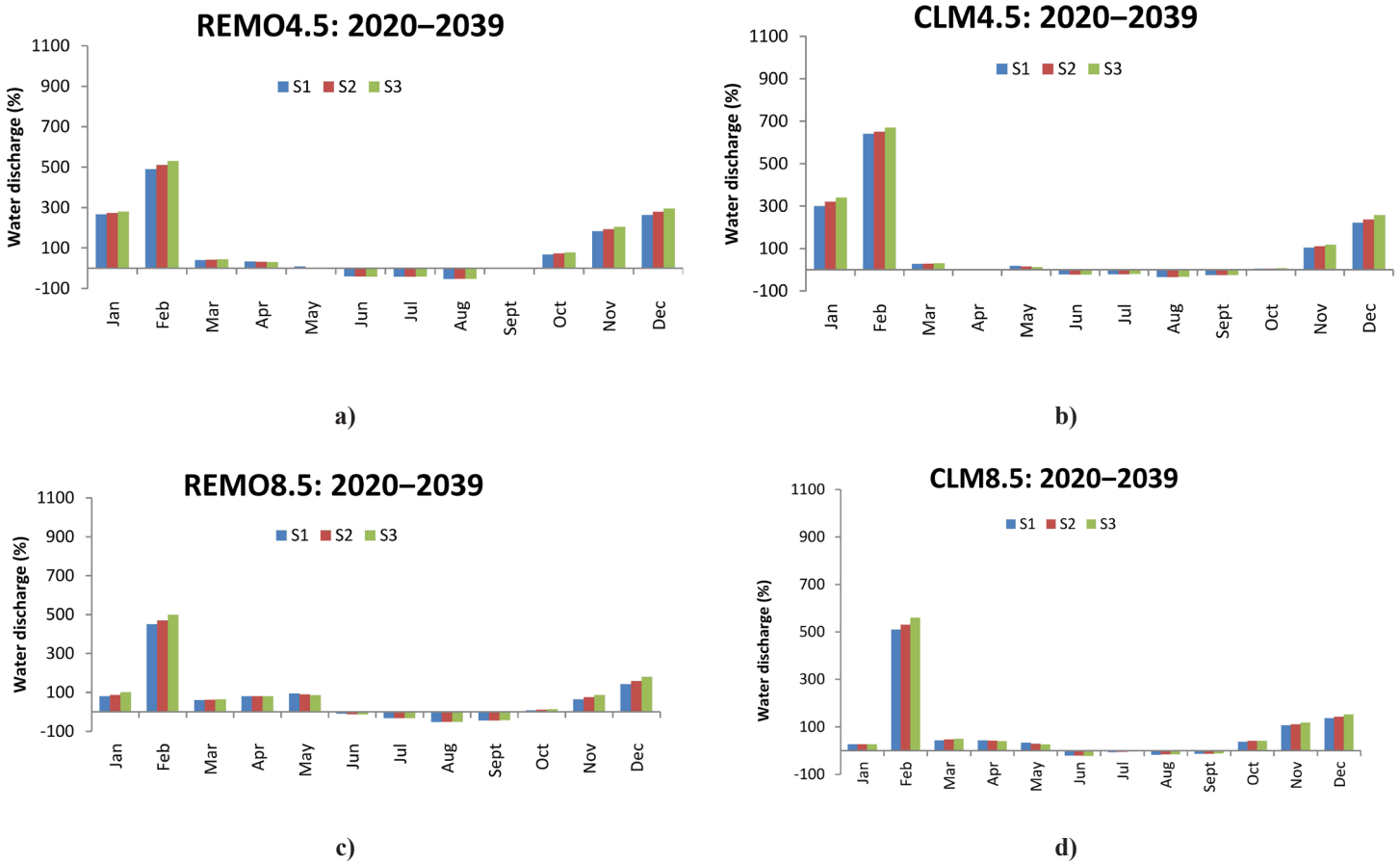

Figure 4.13. Monthly water discharges (expressed in percentage) projected in all climate and land use change scenarios for the 2020–2039 period.

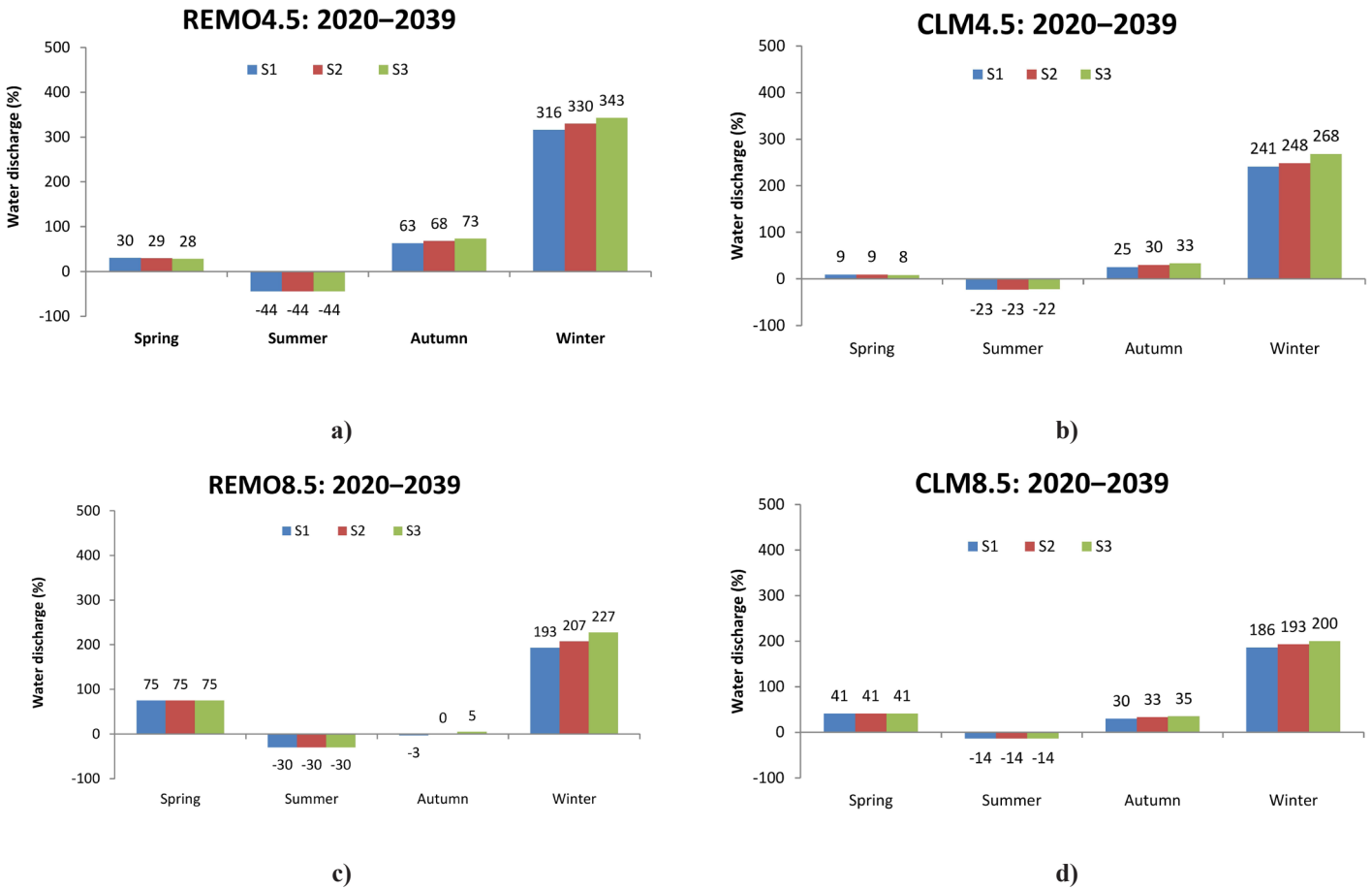

Figure 4.14. Seasonal water discharges (expressed in percentage) projected in all climate and land use change scenarios for the 2020–2039 period.

Table 4.12. Annual water discharges ($m^3 \cdot s^{-1}$) projected for the 2020–2039 period.

		Climate change scenarios											
		REMO4.5			CLM4.5			REMO8.5			CLM8.5		
Baseline	**Year**	**S1**	**S2**	**S3**	**S1**	**S2**	**S3**	**S1**	**S2**	**S3**	**S1**	**S2**	**S3**
0.67	2020	0.95	0.95	0.95	1.03	1.03	1.04	0.86	0.86	0.87	0.53	0.54	0.55
	2021	0.70	0.72	0.73	0.99	0.99	1.00	0.75	0.76	0.77	0.85	0.85	0.86
	2022	0.77	0.77	0.77	0.74	0.75	0.76	1.28	1.29	1.30	1.07	1.08	1.09
	2023	0.84	0.84	0.85	0.71	0.72	0.73	0.97	0.98	1.00	0.99	1.00	1.00
	2024	1.27	1.28	1.30	0.62	0.63	0.63	0.72	0.73	0.74	0.82	0.84	0.85
	2025	0.64	0.64	0.63	0.81	0.82	0.82	0.99	1.00	1.00	1.22	1.23	1.23
	2026	0.79	0.81	0.83	0.94	0.95	0.96	1.27	1.28	1.29	0.96	0.97	0.97
	2027	0.64	0.64	0.65	0.57	0.57	0.57	0.65	0.65	0.66	0.79	0.79	0.80
	2028	1.23	1.24	1.26	0.53	0.54	0.55	0.86	0.87	0.88	0.89	0.90	0.91
	2029	0.56	0.57	0.58	1.04	1.04	1.05	1.43	1.44	1.44	0.96	0.96	0.97
	2030	0.84	0.85	0.86	0.43	0.44	0.44	1.24	1.24	1.25	1.09	1.09	1.10
	2031	0.84	0.85	0.87	0.60	0.61	0.61	0.92	0.94	0.95	0.84	0.85	0.86
	2032	1.28	1.29	1.30	0.71	0.72	0.73	0.88	0.88	0.89	0.61	0.61	0.61
	2033	0.58	0.59	0.60	0.88	0.88	0.89	0.84	0.85	0.87	1.01	1.02	1.03
	2034	0.87	0.88	0.89	0.59	0.60	0.60	0.59	0.60	0.60	0.91	0.92	0.92
	2035	0.43	0.44	0.44	0.59	0.60	0.62	0.61	0.63	0.64	0.80	0.81	0.82
	2036	0.72	0.73	0.75	0.97	0.98	0.98	0.53	0.55	0.57	0.65	0.65	0.66
	2037	1.01	1.01	1.02	0.79	0.79	0.80	0.71	0.72	0.73	0.64	0.65	0.66
	2038	0.63	0.64	0.65	0.69	0.70	0.71	0.73	0.74	0.74	0.53	0.55	0.56
	2039	0.83	0.83	0.84	0.86	0.87	0.87	0.65	0.65	0.66	0.81	0.82	0.82

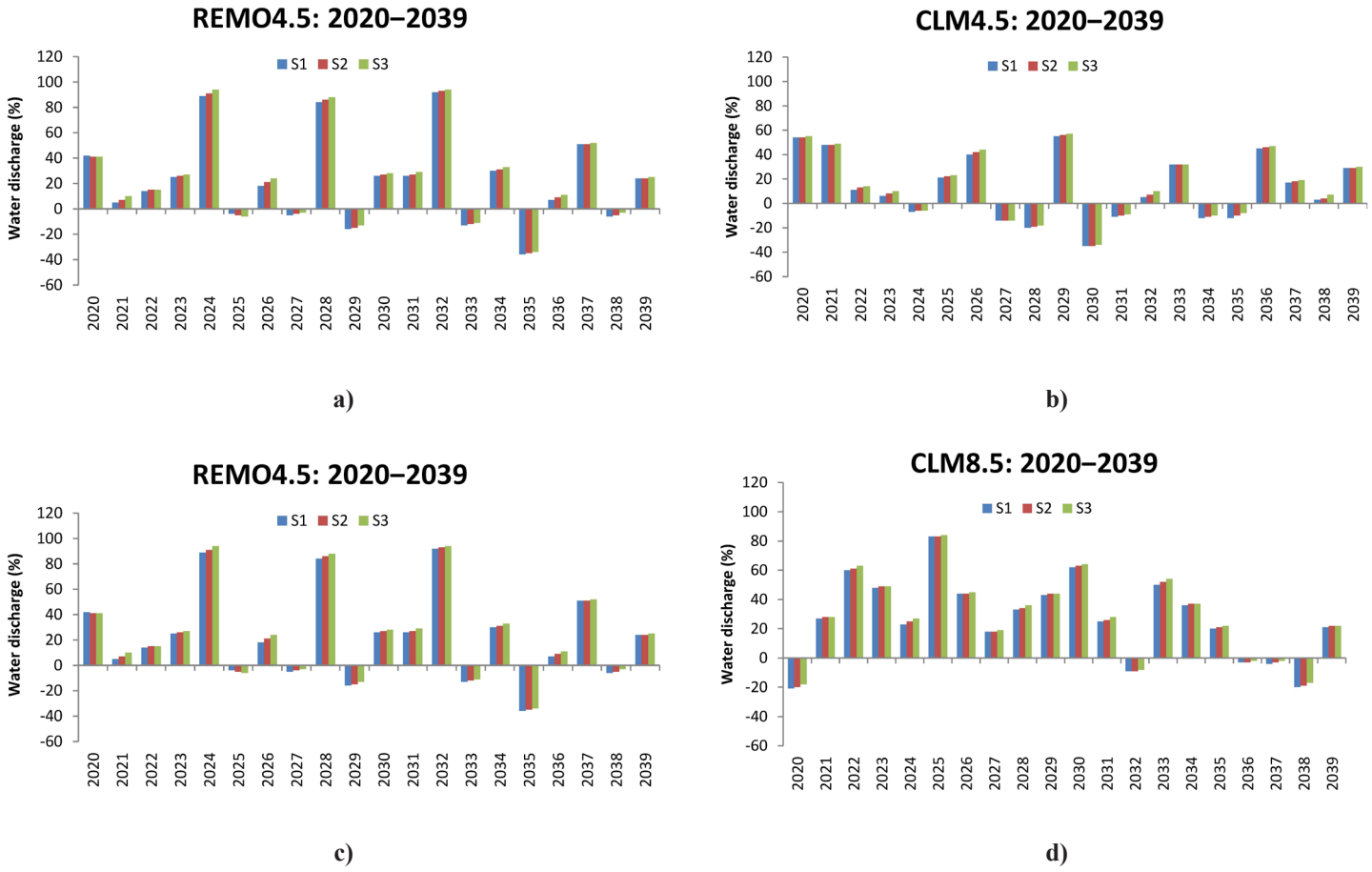

Figure 4.15. Annual water discharges (expressed in percentage) projected in all climate and land use change scenarios for the 2020–2039 period.

Table 4.13. Monthly water discharges ($m^3 \cdot s^{-1}$) projected for the2040–2069 period.

		Climate change scenarios											
		REMO4.5			CLM4.5			REMO8.5			CLM8.5		
Month	**Baseline**	**S1**	**S2**	**S3**	**S1**	**S2**	**S3**	**S1**	**S2**	**S3**	**S1**	**S2**	**S3**
January	0.15	0.55	0.57	0.61	0.60	0.63	0.66	0.39	0.40	0.43	0.26	0.27	0.29
February	0.10	0.79	0.81	0.84	0.74	0.75	0.77	0.74	0.77	0.82	0.87	0.90	0.94
March	1.31	1.69	1.72	1.75	1.66	1.68	1.71	2.03	2.07	2.12	2.46	2.52	2.58
April	1.26	1.88	1.88	1.87	1.27	1.25	1.23	1.52	1.51	1.05	1.20	1.17	1.13
May	0.78	1.17	1.14	1.11	0.93	0.90	0.87	1.09	1.07	1.04	0.98	0.95	0.92
June	1.20	1.16	1.15	1.15	0.94	0.93	0.93	0.99	0.99	0.98	0.99	0.98	0.98
July	1.04	0.68	0.68	0.67	0.82	0.82	0.83	0.61	0.61	0.61	0.83	0.83	0.84
August	0.88	0.42	0.42	0.43	0.58	0.58	0.59	0.33	0.33	0.34	0.54	0.55	0.55
September	0.55	0.29	0.30	0.31	0.42	0.42	0.42	0.29	0.30	0.30	0.37	0.37	0.37
October	0.37	0.41	0.43	0.44	0.39	0.39	0.40	0.33	0.33	0.34	0.29	0.28	0.28
November	0.28	0.52	0.54	0.57	0.57	0.59	0.61	0.44	0.46	0.48	0.46	0.48	0.50
December	0.19	0.57	0.59	0.63	0.61	0.64	0.68	0.43	0.45	0.48	0.44	0.46	0.50

Table 4.14 Seasonal water discharges ($m^3 \cdot s^{-1}$) projected for the 2040–2069 period

		Climate change scenarios											
		REMO4.5			CLM4.5			REMO8.5			CLM8.5		
Season	**Baseline**	**S1**	**S2**	**S3**	**S1**	**S2**	**S3**	**S1**	**S2**	**S3**	**S1**	**S2**	**S3**
Spring	1.12	1.58	1.58	1.58	1.29	1.28	1.27	1.55	1.55	1.55	1.55	1.55	1.54
Summer	1.04	0.75	0.75	0.75	0.78	0.78	0.78	0.64	0.64	0.64	0.79	0.79	0.79
Autumn	0.40	0.41	0.42	0.44	0.46	0.47	0.48	0.35	0.36	0.37	0.37	0.38	0.38
Winter	0.15	0.64	0.66	0.69	0.65	0.67	0.70	0.52	0.54	0.58	0.52	0.54	0.58

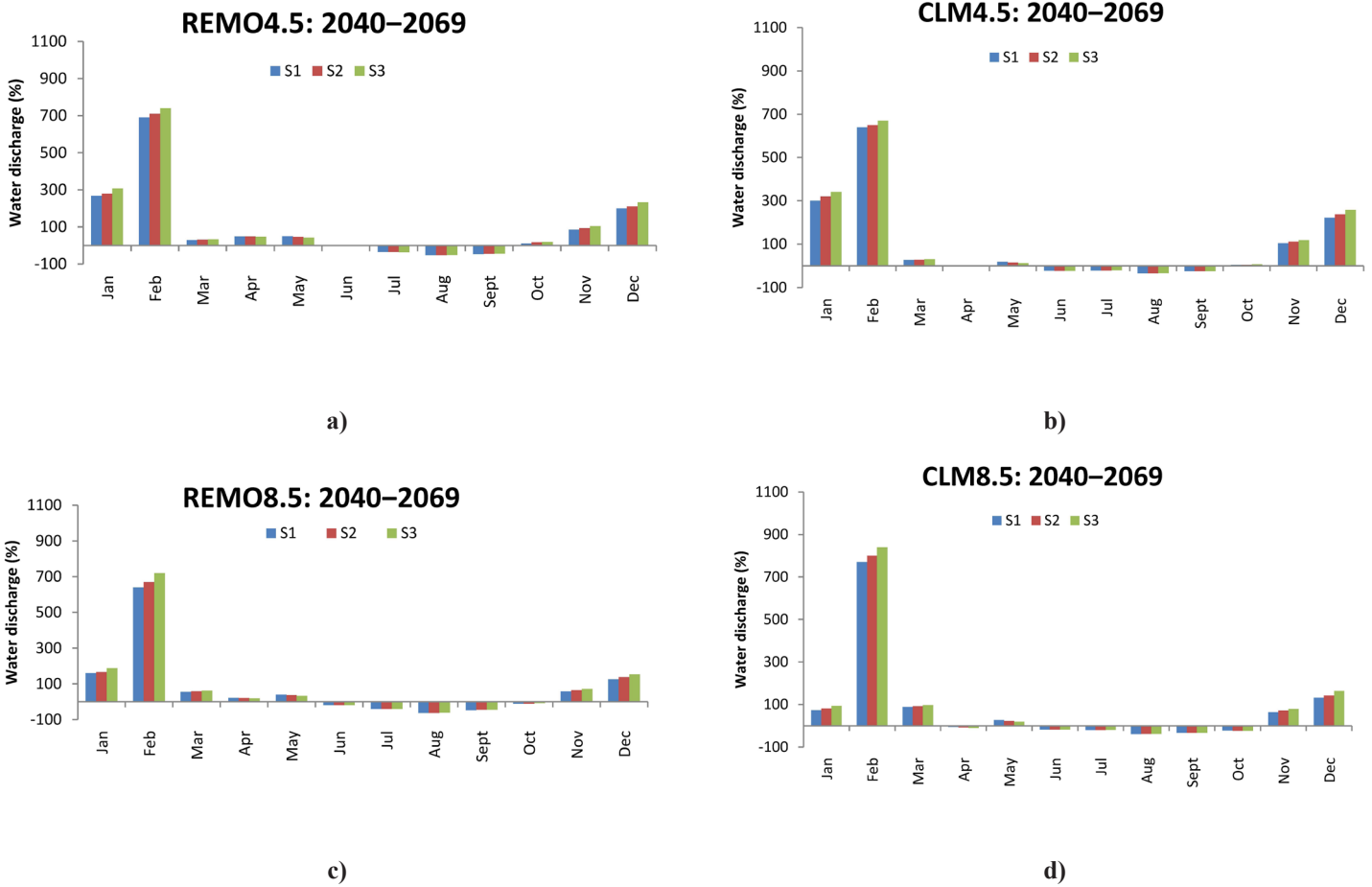

Figure 4.17. Monthly water discharges (expressed in percentage) projected in all climate and land use change scenarios for the 2040–2069 period.

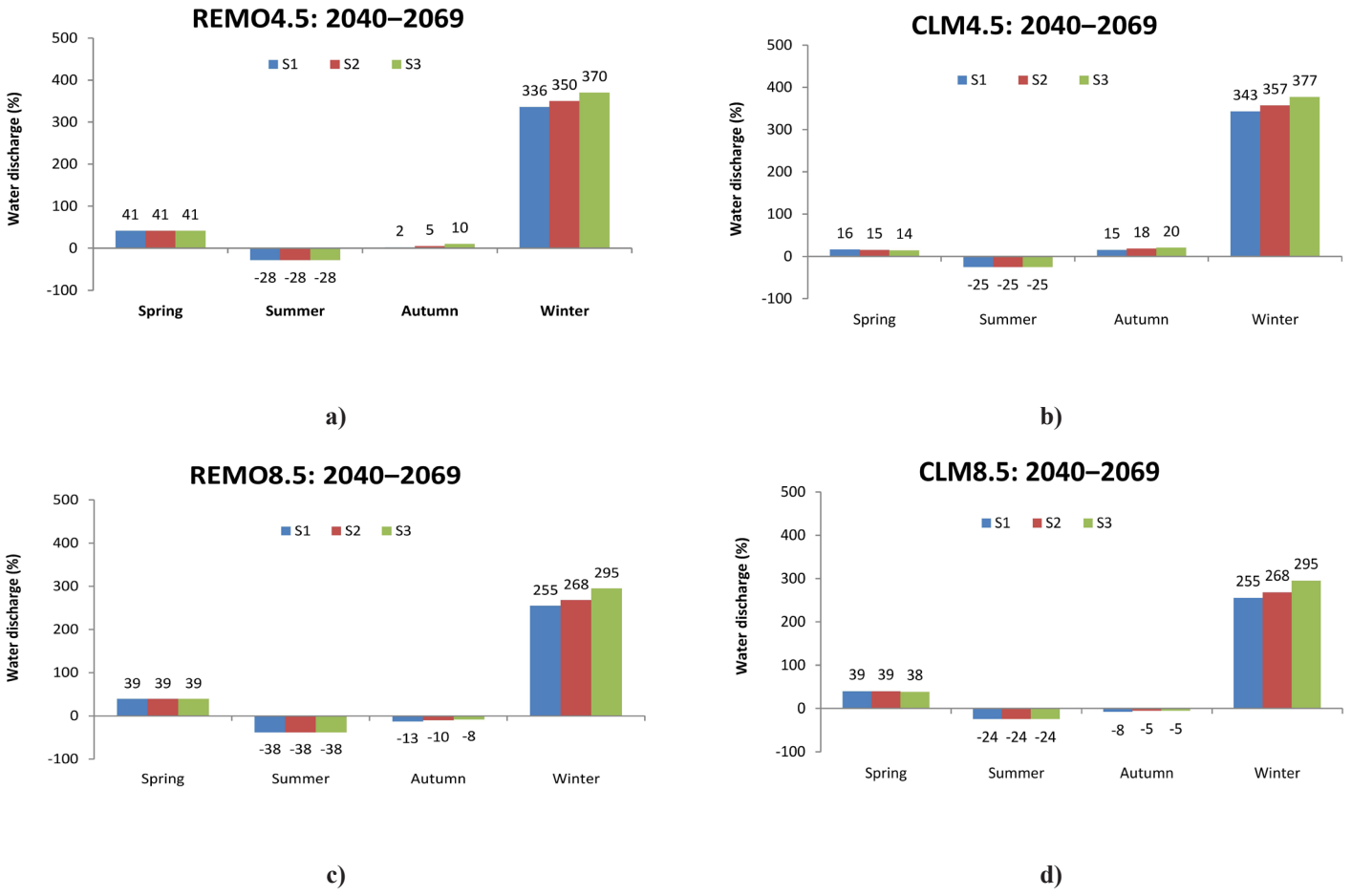

Figure 4.18. Seasonal water discharges (expressed in percentage) projected in all climate and land use change scenarios for the 2040–2069 period.

Table 4.15. Annual water discharges ($m^3 \cdot s^{-1}$) projected for the 2040–2069 period.

		Climate change scenarios											
		REMO4.5			CLM4.5			REMO8.5			CLM8.5		
Baseline	**Year**	**S1**	**S2**	**S3**	**S1**	**S2**	**S3**	**S1**	**S2**	**S3**	**S1**	**S2**	**S3**
0.67	2040	0.88	0.89	0.90	1.12	1.13	1.14	1.18	1.19	1.20	0.84	0.85	0.86
	2041	0.76	0.78	0.79	0.77	0.77	0.78	0.47	0.47	0.48	1.12	1.12	1.13
	2042	0.85	0.86	0.86	0.84	0.85	0.86	0.95	0.96	0.97	0.80	0.81	0.82
	2043	1.14	1.15	1.16	0.66	0.66	0.67	0.90	0.91	0.93	0.60	0.61	0.62
	2044	0.96	0.96	0.97	0.84	0.85	0.86	1.15	1.16	1.17	1.18	1.19	1.19
	2045	0.67	0.68	0.69	0.39	0.40	0.41	0.77	0.78	0.79	0.63	0.64	0.65
	2046	0.69	0.70	0.72	0.64	0.65	0.66	0.56	0.56	0.57	0.70	0.70	0.71
	2047	1.06	1.08	1.09	0.99	1.00	1.01	0.76	0.77	0.78	0.69	0.70	0.71
	2048	1.33	1.33	1.33	1.08	1.09	1.09	1.34	1.35	1.37	0.70	0.70	0.71
	2049	1.21	1.21	1.22	0.59	0.59	0.60	1.02	1.02	1.03	0.78	0.78	0.79
	2050	0.87	0.87	0.87	0.99	1.00	1.00	0.52	0.53	0.53	0.79	0.80	0.81
	2051	0.98	0.99	1.01	1.00	1.01	1.03	0.42	0.43	0.45	0.81	0.81	0.81
	2052	0.92	0.93	0.94	0.70	0.70	0.71	0.77	0.79	0.81	0.61	0.62	0.63
	2053	0.36	0.36	0.37	0.82	0.83	0.83	0.58	0.58	0.58	0.90	0.91	0.92
	2054	0.63	0.64	0.65	0.59	0.59	0.59	0.74	0.75	0.75	1.03	1.03	1.04
	2055	0.66	0.68	0.69	0.35	0.36	0.37	0.74	0.76	0.78	0.95	0.96	0.97
	2056	1.01	1.02	1.04	0.76	0.76	0.77	0.73	0.73	0.73	0.65	0.65	0.65
	2057	0.89	0.89	0.89	1.26	1.27	1.28	0.61	0.63	0.66	0.74	0.75	0.76
	2058	0.96	0.96	0.97	0.62	0.63	0.64	0.69	0.69	0.69	1.12	1.12	1.13
	2059	0.56	0.57	0.59	0.34	0.35	0.36	0.46	0.46	0.47	1.22	1.23	1.24
	2060	0.73	0.74	0.75	0.91	0.91	0.91	0.45	0.46	0.48	0.61	0.61	0.62
	2061	1.03	1.04	1.05	0.53	0.53	0.54	0.67	0.68	0.70	1.02	1.03	1.04
	2062	0.83	0.84	0.86	0.47	0.48	0.49	1.11	1.12	1.13	0.93	0.94	0.95
	2063	0.75	0.76	0.78	0.81	0.82	0.84	0.42	0.43	0.44	0.70	0.70	0.71
	2064	0.80	0.82	0.84	1.17	1.17	1.18	1.31	1.32	1.34	0.77	0.78	0.79
	2065	0.81	0.82	0.82	0.95	0.95	0.95	0.90	0.91	0.93	0.34	0.35	0.36
	2066	0.42	0.42	0.43	0.99	1.00	1.01	0.74	0.75	0.75	0.82	0.82	0.83
	2067	0.95	0.96	0.99	1.01	1.03	1.04	0.91	0.92	0.93	0.58	0.59	0.60
	2068	0.60	0.59	0.59	0.90	0.90	0.90	0.57	0.58	0.59	0.90	0.91	0.92
	2069	1.03	1.05	1.07	0.72	0.72	0.73	0.54	0.56	0.58	0.72	0.73	0.74

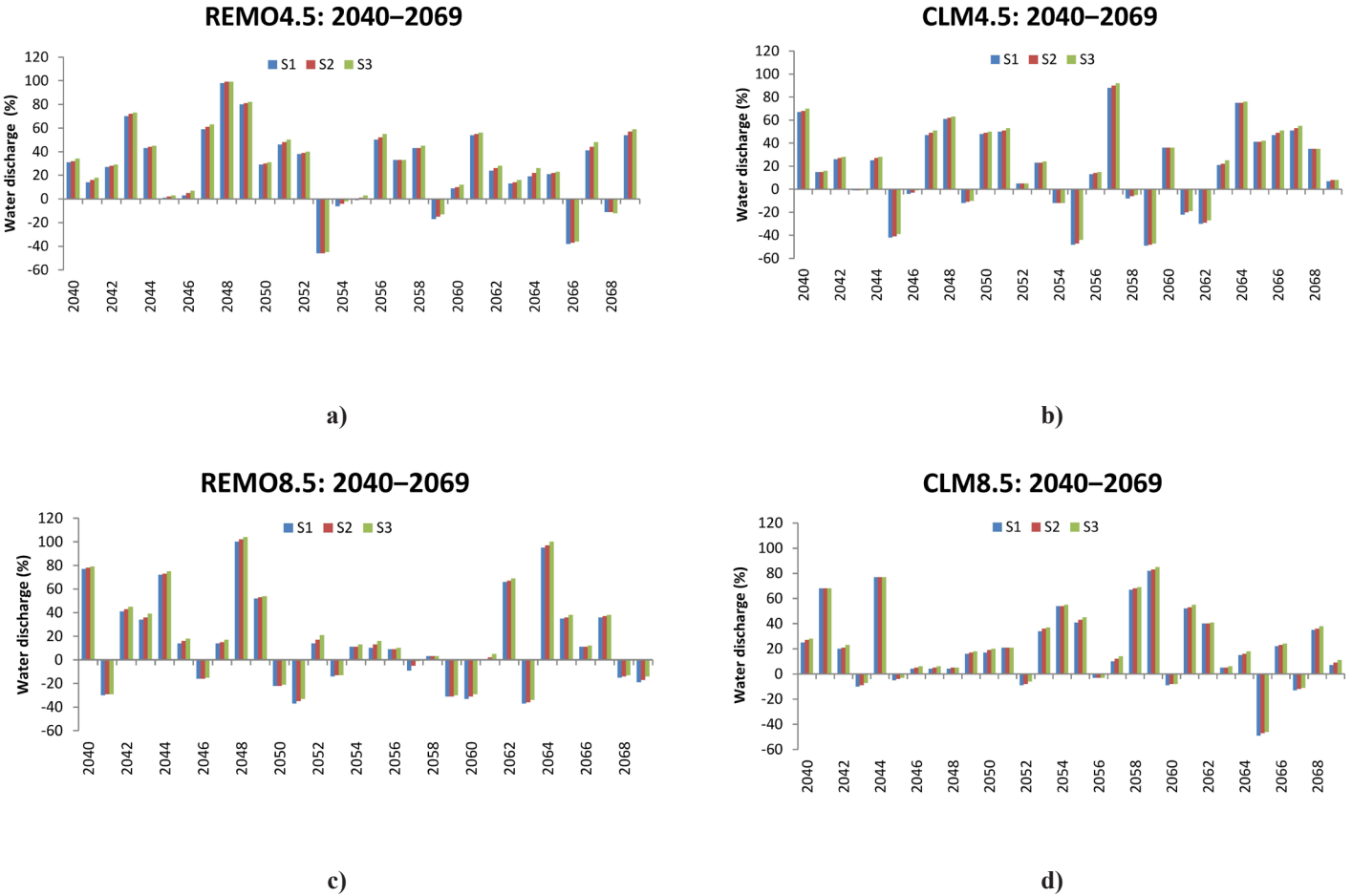

Figure 4.19. Annual water discharges (expressed in percentage) projected in all climate and land use change scenarios for the 2040–2069 period.

Table 4.16. Monthly water discharges ($m^3 \cdot s^{-1}$) projected for the 2070–2100 period.

		Climate change scenarios											
		REMO4.5			CLM4.5			REMO8.5			CLM8.5		
Month	**Baseline**	**S1**	**S2**	**S3**	**S1**	**S2**	**S3**	**S1**	**S2**	**S3**	**S1**	**S2**	**S3**
January	0.15	0.49	0.51	0.54	0.39	0.40	0.41	0.52	0.54	0.57	0.58	0.60	0.62
February	0.10	0.91	0.93	0.96	1.00	1.04	1.10	0.90	0.94	0.99	1.11	1.15	1.20
March	1.31	1.75	1.78	1.82	1.84	1.86	1.89	1.32	1.34	1.36	1.52	1.53	1.53
April	1.26	1.47	1.46	1.44	1.24	1.22	1.19	1.28	1.26	1.24	1.11	1.08	1.05
May	0.78	1.19	1.17	1.14	0.89	0.87	0.85	1.08	1.07	1.05	0.93	0.92	0.90
June	1.20	1.01	1.00	0.99	0.92	0.92	0.92	0.91	0.91	0.92	1.07	1.07	1.08
July	1.04	0.70	0.71	0.71	0.78	0.79	0.80	0.53	0.53	0.54	0.80	0.81	0.82
August	0.88	0.39	0.39	0.39	0.53	0.53	0.54	0.33	0.33	0.33	0.47	0.47	0.47
September	0.55	0.38	0.39	0.40	0.37	0.37	0.37	0.23	0.23	0.23	0.36	0.36	0.36
October	0.37	0.39	0.40	0.40	0.36	0.37	0.37	0.33	0.33	0.34	0.46	0.47	0.47
November	0.28	0.61	0.63	0.67	0.50	0.51	0.54	0.46	0.47	0.49	0.56	0.57	0.58
December	0.19	0.61	0.64	0.67	0.54	0.56	0.59	0.58	0.62	0.67	0.67	0.69	0.73

Table 4.17. Seasonal water discharges ($m^3 \cdot s^{-1}$) projected for the 2070–2100 period.

		Climate change scenarios											
		REMO4.5			CLM4.5			REMO8.5			CLM8.5		
Season	**Baseline**	**S1**	**S2**	**S3**	**S1**	**S2**	**S3**	**S1**	**S2**	**S3**	**S1**	**S2**	**S3**
Spring	1.12	1.47	1.47	1.47	1.32	1.32	1.31	1.23	1.22	1.22	1.19	1.18	1.16
Summer	1.04	0.70	0.70	0.70	0.74	0.75	0.75	0.59	0.59	0.60	0.78	0.78	0.79
Autumn	0.40	0.46	0.47	0.49	0.41	0.42	0.43	0.34	0.34	0.35	0.46	0.47	0.47
Winter	0.15	0.67	0.69	0.72	0.64	0.67	0.70	0.67	0.70	0.74	0.79	0.81	0.85

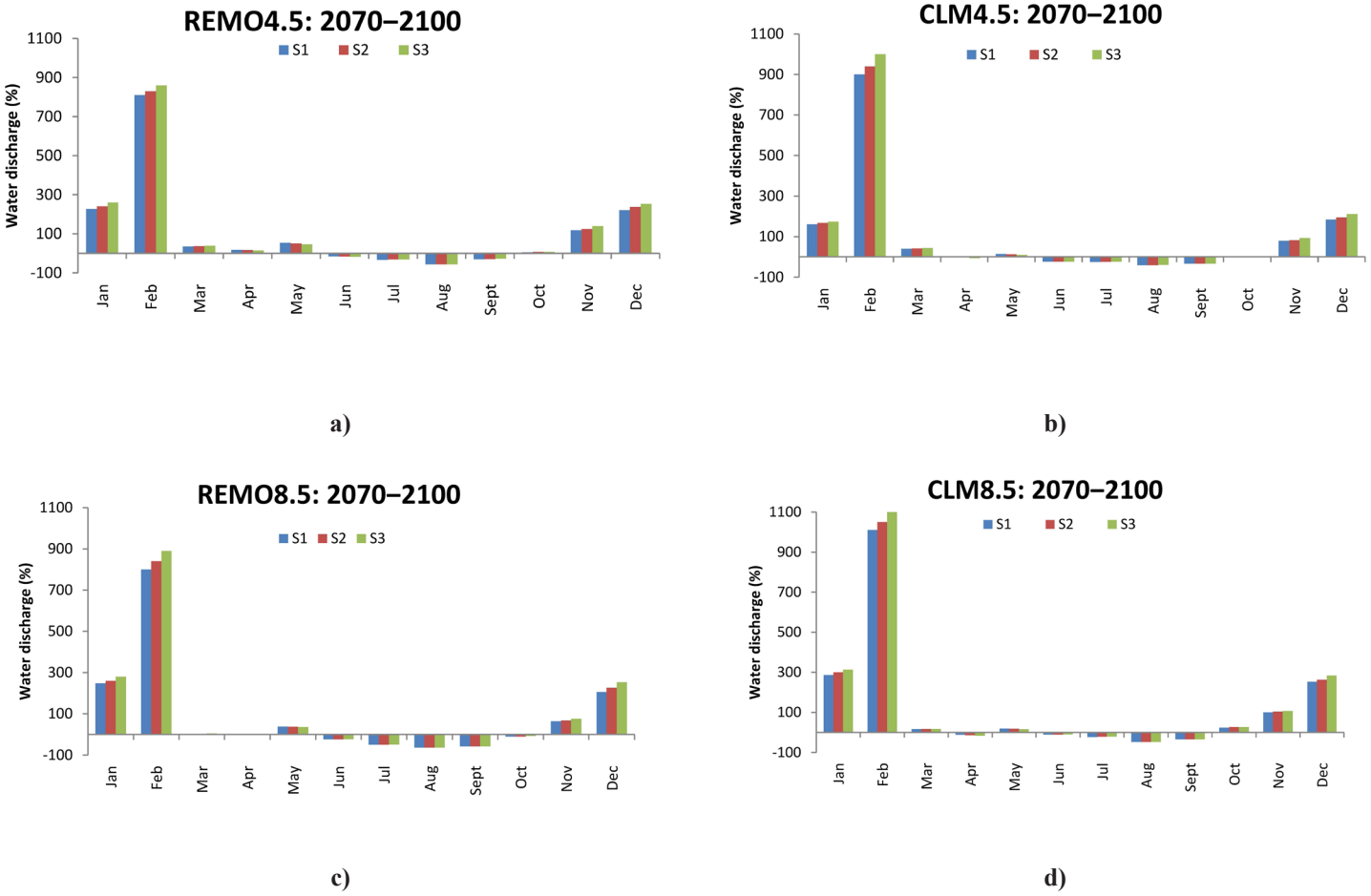

Figure 4.21. Monthly water discharges (expressed in percentage) projected in all climate and land use change scenarios for the 2070–2100 period.

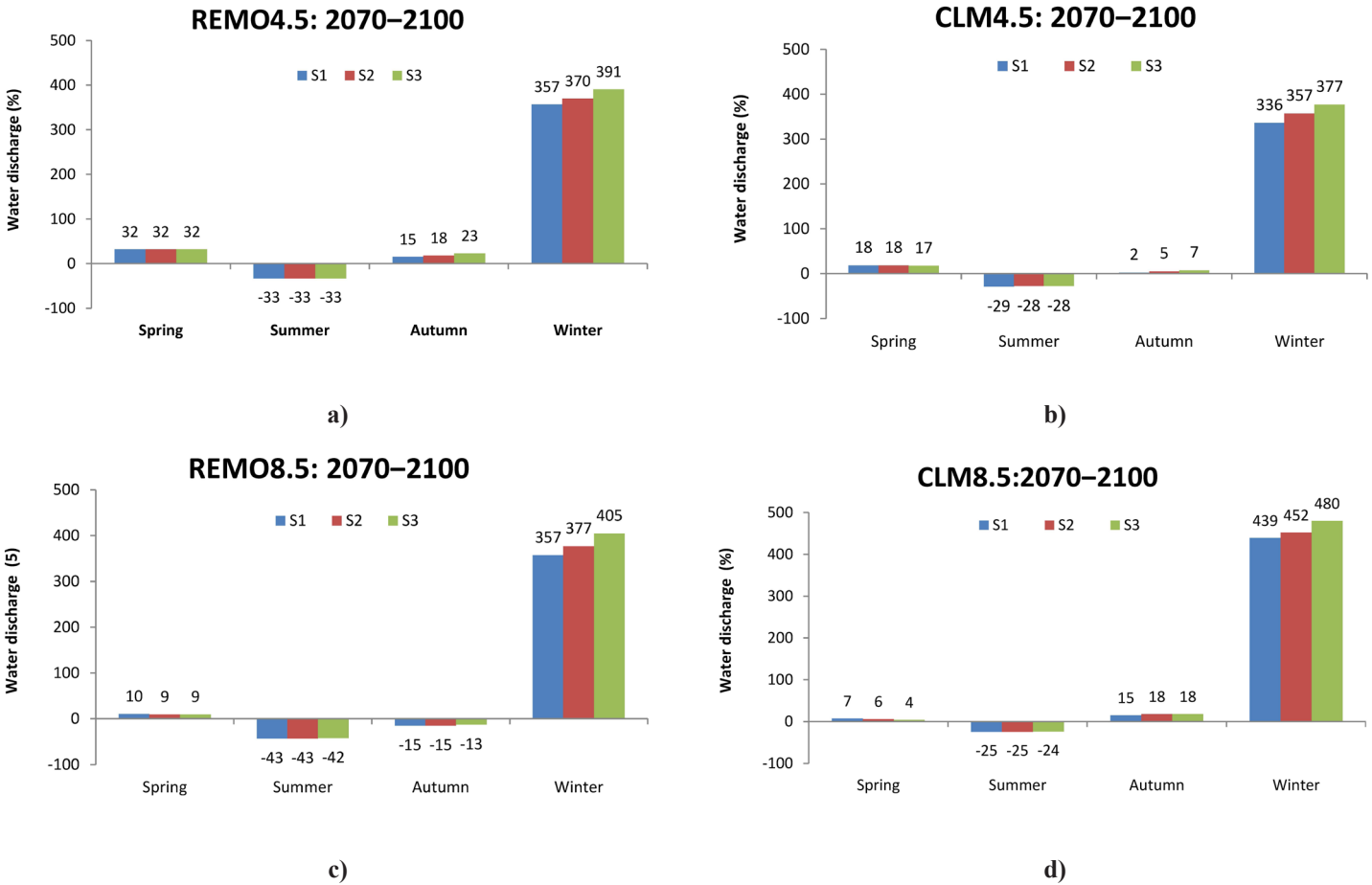

Figure 4.22. Seasonal water discharges (expressed in percentage) projected in all climate and land use change scenarios for the 2070–2100 period.

Table 4.18. Annual water discharges ($m^3 \cdot s^{-1}$) projected for the 2070–2100 period.

		Climate change scenarios											
		REMO4.5			CLM4.5			REMO8.5			CLM8.5		
Baseline	Year	S1	S2	S3	S1	S2	S3	S1	S2	S3	S1	S2	S3
	2070	0.63	0.64	0.65	0.75	0.77	0.79	0.49	0.51	0.53	1.23	1.24	1.24
	2071	0.90	0.91	0.93	0.78	0.78	0.79	0.95	0.96	0.97	0.94	0.94	0.95
	2072	0.98	0.99	1.00	0.85	0.86	0.87	1.10	1.11	1.12	0.48	0.48	0.49
	2073	0.98	0.99	0.99	1.21	1.22	1.23	0.88	0.89	0.90	1.16	1.17	1.18
	2074	1.00	1.01	1.02	1.09	1.09	1.10	0.39	0.40	0.42	0.74	0.75	0.76
	2075	1.31	1.32	1.34	0.91	0.92	0.93	0.59	0.59	0.60	0.70	0.70	0.70
	2076	0.80	0.80	0.81	0.99	1.00	1.01	0.46	0.47	0.48	0.96	0.97	0.99
	2077	1.02	1.03	1.04	0.63	0.63	0.64	0.92	0.94	0.96	0.88	0.90	0.91
	2078	1.18	1.20	1.21	1.16	1.17	1.18	0.83	0.83	0.84	0.74	0.75	0.75
	2079	0.56	0.56	0.56	0.58	0.59	0.60	0.79	0.80	0.81	1.32	1.32	1.33
	2080	0.79	0.80	0.81	0.45	0.46	0.47	1.31	1.33	1.35	1.20	1.21	1.22
	2081	0.50	0.51	0.53	0.73	0.75	0.77	0.58	0.58	0.58	0.81	0.82	0.82
	2082	0.58	0.58	0.59	0.93	0.94	0.94	0.99	1.01	1.03	0.66	0.66	0.67
	2083	0.80	0.81	0.82	0.39	0.40	0.41	0.66	0.65	0.65	0.63	0.64	0.66
	2084	0.84	0.85	0.86	0.62	0.63	0.64	0.58	0.58	0.60	0.71	0.72	0.72
0.67	2085	0.74	0.74	0.75	0.66	0.68	0.69	0.52	0.53	0.55	0.89	0.90	0.91
	2086	0.37	0.38	0.39	0.97	0.97	0.98	0.61	0.62	0.63	0.68	0.67	0.67
	2087	0.61	0.62	0.63	1.07	1.08	1.09	0.58	0.59	0.59	0.41	0.42	0.43
	2088	0.31	0.33	0.35	0.70	0.71	0.72	0.54	0.54	0.55	0.63	0.64	0.65
	2089	0.70	0.71	0.73	0.77	0.77	0.78	0.58	0.59	0.61	0.96	0.97	0.98
	2090	1.03	1.04	1.07	0.71	0.71	0.71	0.89	0.90	0.91	0.87	0.87	0.88
	2091	0.93	0.93	0.93	0.83	0.84	0.85	0.62	0.63	0.65	0.54	0.55	0.56
	2092	0.89	0.89	0.90	0.48	0.49	0.50	0.58	0.58	0.59	0.70	0.70	0.71
	2093	0.55	0.57	0.58	0.76	0.77	0.78	0.97	0.98	1.00	0.77	0.78	0.79
	2094	0.96	0.97	0.99	0.54	0.54	0.54	0.72	0.72	0.72	0.76	0.76	0.77
	2095	0.98	0.99	0.99	1.01	1.03	1.05	0.58	0.59	0.60	0.99	1.00	1.01
	2096	0.87	0.88	0.88	0.57	0.58	0.59	0.62	0.63	0.65	0.53	0.54	0.55
	2097	1.05	1.06	1.07	0.65	0.66	0.67	0.49	0.50	0.52	0.87	0.87	0.87
	2098	0.90	0.90	0.91	0.97	0.97	0.98	0.76	0.76	0.77	0.75	0.76	0.77
	2099	1.01	1.02	1.03	0.59	0.60	0.61	0.51	0.53	0.55	0.68	0.68	0.69
	2100	0.79	0.80	0.81	0.77	0.78	0.80	0.79	0.80	0.81	0.74	0.74	0.75

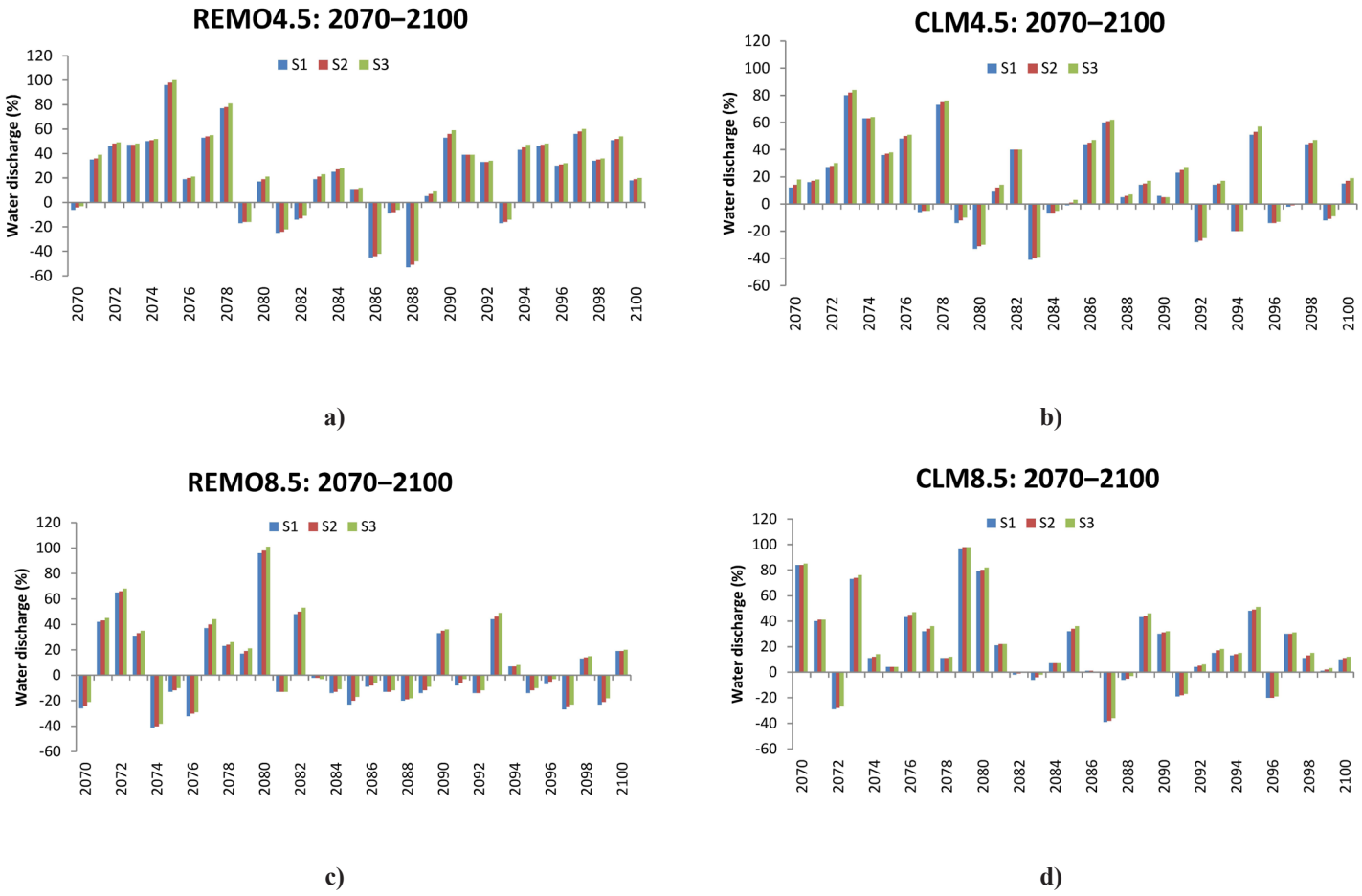

Figure 4.23. Annual water discharges (expressed in percentage) projected in all climate and land use change scenarios for the 2070–2100 period.

Annex 3. Monthly, seasonal, and annual sediment yield (tonnes) projected for the 2020−2100 period

Table 4.19. Monthly sediment yield (tonnes) projected for 2020–2039 period.

		Climate change scenarios											
		REMO4.5			CLM4.5			REMO8.5			CLM8.5		
Month	Baseline	S1	S2	S3	S1	S2	S3	S1	S2	S3	S1	S2	S3
January	315	412	435	1095	252	277	749	171	191	605	97	107	322
February	160	454	482	1185	692	740	1831	478	517	1443	625	663	1689
March	3030	1896	1979	4415	2201	2304	5696	2207	2296	5452	2210	2310	5369
April	1792	1366	1392	2622	769	777	1485	1843	1910	4430	1611	1657	3255
May	373	378	368	577	311	305	513	941	936	1576	521	511	779
June	767	313	316	527	458	470	908	457	451	709	457	460	773
July	535	293	304	532	395	404	742	261	262	399	579	597	1188
August	408	129	135	193	275	288	544	150	155	293	342	351	540
September	185	203	215	320	205	213	338	106	110	172	161	166	259
October	149	276	294	522	170	179	291	160	172	341	210	218	339
November	268	445	478	973	354	389	934	240	273	710	309	330	732
December	272	435	470	1074	153	170	419	296	331	799	314	338	809

Table 4.20. Seasonal sediment yield (tonnes) projected for the 2020–2039 period.

		Climate change scenarios											
		REMO4.5			CLM4.5			REMO8.5			CLM8.5		
Season	Baseline	S1	S2	S3	S1	S2	S3	S1	S2	S3	S1	S2	S3
Spring	1732	1213	1246	2538	1094	1129	2565	1664	1714	3819	1447	1492	3134
Summer	570	245	252	418	376	387	731	289	289	467	459	469	834
Autumn	201	308	329	605	243	260	521	168	185	408	227	238	443
Winter	249	433	462	1118	366	396	1000	315	346	949	346	369	940

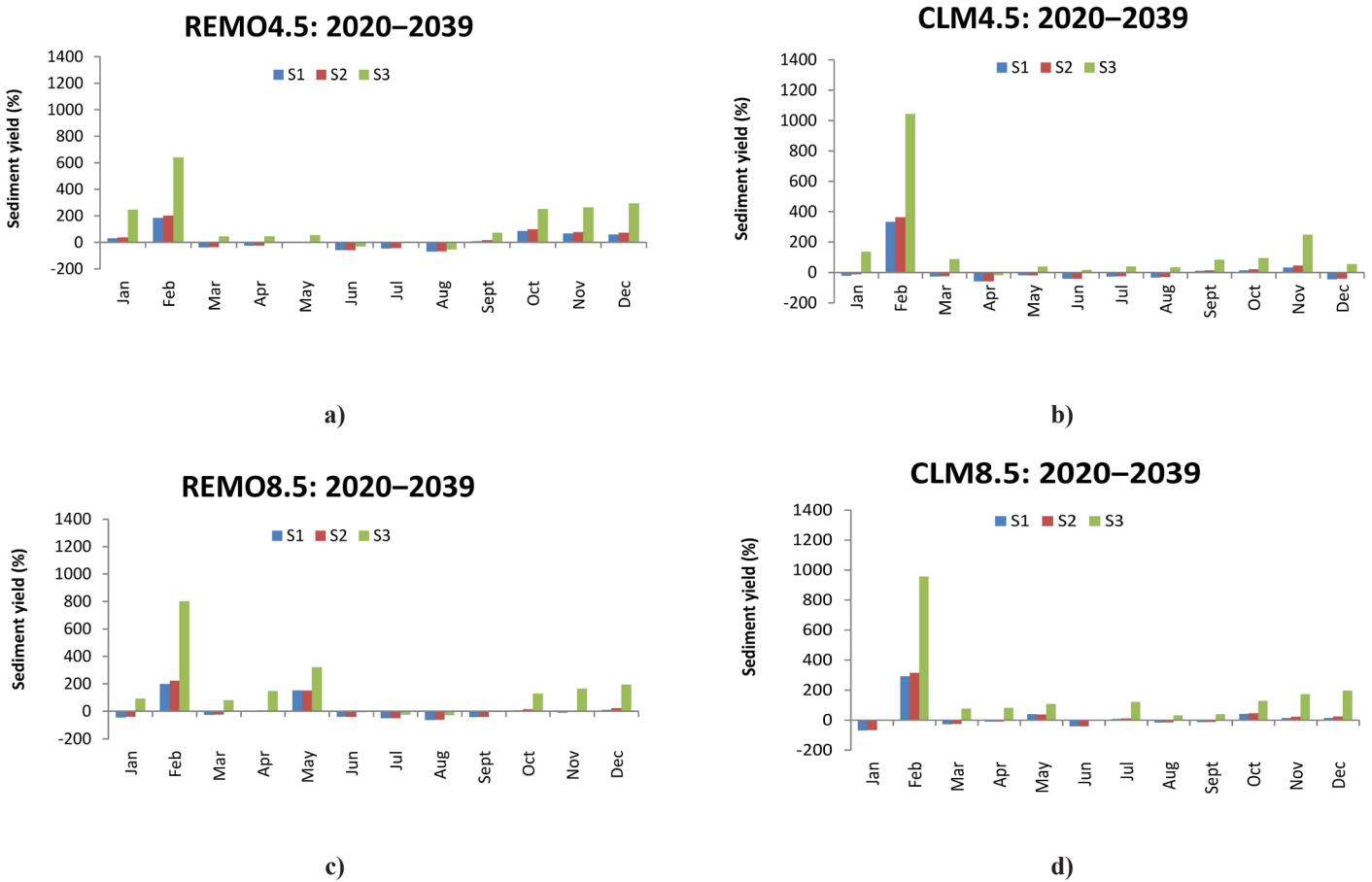

Figure 4.25. Monthly sediment yield (expressed in percentage) projected in all climate and land use change scenarios for the 2020–2039 period.

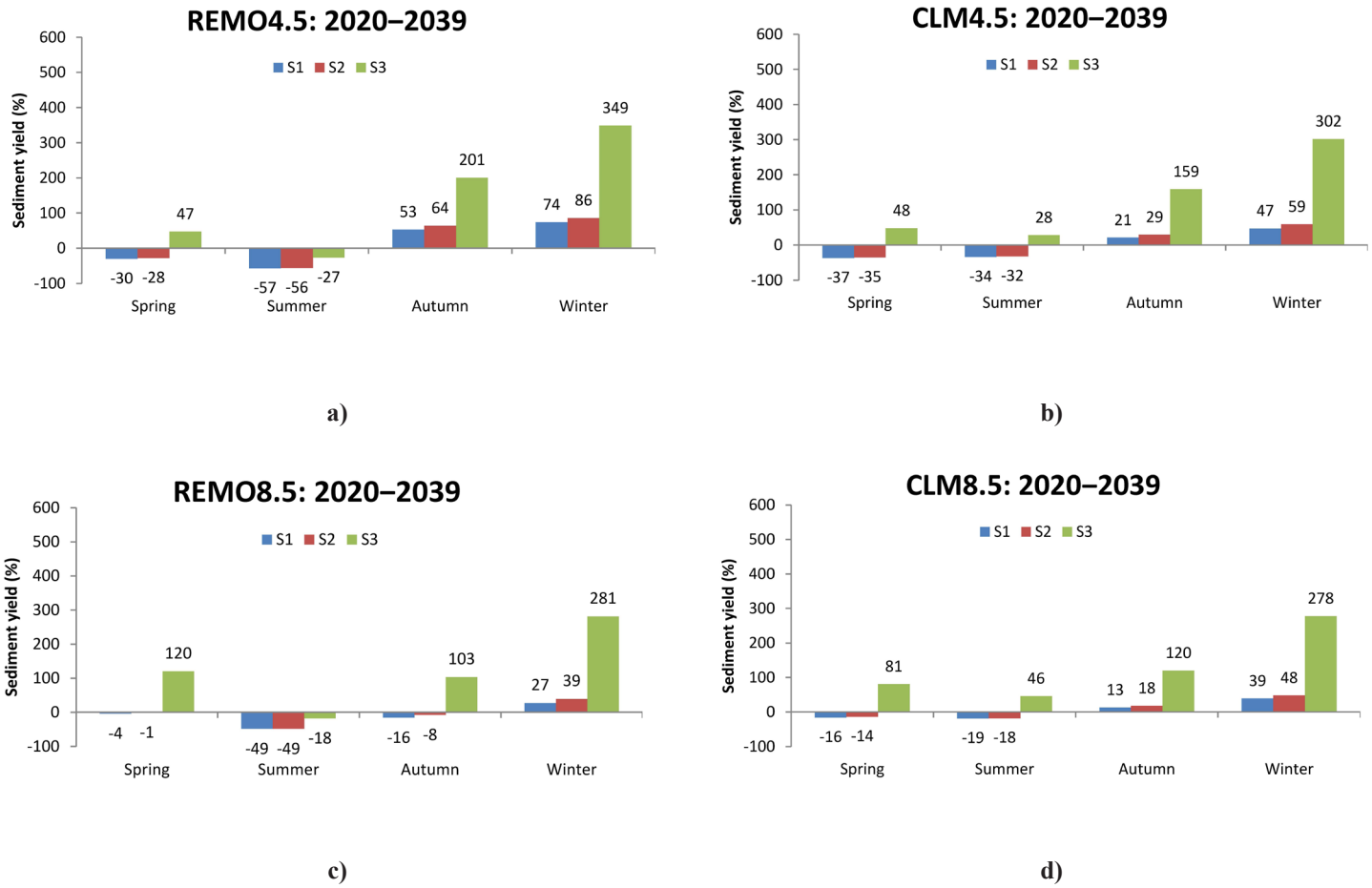

Figure 4.26. Seasonal sediment yield (expressed in percentage) projected in all climate and land use change scenarios for the 2020–2039 period.

Table 4.21. Annual sediment yield (tonnes) projected for the 2020–2039 period.

		Climate change scenarios											
		REMO4.5			CLM4.5			REMO8.5			CLM8.5		
Baseline	Year	S1	S2	S3	S1	S2	S3	S1	S2	S3	S1	S2	S3
8253	2020	8331	8502	16797	11519	11758	24258	7834	8168	18810	3609	3875	9806
	2021	5969	6339	14702	11907	12174	24644	5432	5735	12137	5679	5955	13278
	2022	6045	6288	14431	7983	8317	19200	10372	10720	20524	9542	9834	18319
	2023	5765	5968	11582	5182	5478	12611	10154	10513	23810	11705	12058	26047
	2024	15152	15626	32222	4438	4707	11381	4991	5308	13240	6963	7321	18259
	2025	6368	6509	14032	7003	7274	15729	8000	8271	17544	13158	13476	26853
	2026	5482	5857	12424	6923	7385	18152	10784	11193	25414	8859	9117	17969
	2027	5264	5501	9534	3647	3811	9649	5062	5277	12570	6556	6778	12372
	2028	10369	10733	20003	4698	4918	9648	6946	7279	16649	6115	6350	12658
	2029	4224	4452	10328	7249	7614	15541	12455	12574	23310	9225	9513	19900
	2030	4938	5183	9449	2457	2613	6634	12514	12903	33587	10191	10516	21060
	2031	6049	6314	12309	10735	11037	29894	8129	8374	17476	8083	8359	16497
	2032	11297	11635	23293	4082	4388	8780	10470	10703	20966	5361	5496	11096
	2033	4804	5030	10578	6374	6615	14034	5710	6056	15636	11049	11525	27011
	2034	7415	7714	15401	4306	4509	9528	3980	4235	11243	8529	8761	18516
	2035	2493	2601	4115	3653	3920	8914	4370	4676	10803	7982	8267	15501
	2036	5207	5515	10798	6607	6913	13171	4314	4655	9082	3508	3648	7605
	2037	7550	7781	15352	5458	5814	13904	5122	5411	12913	3816	4045	9472
	2038	4067	4354	10446	4988	5317	11956	5399	5607	11375	3194	3449	7152
	2039	5210	5473	12951	5527	5752	11373	4154	4423	11454	5591	5806	11681

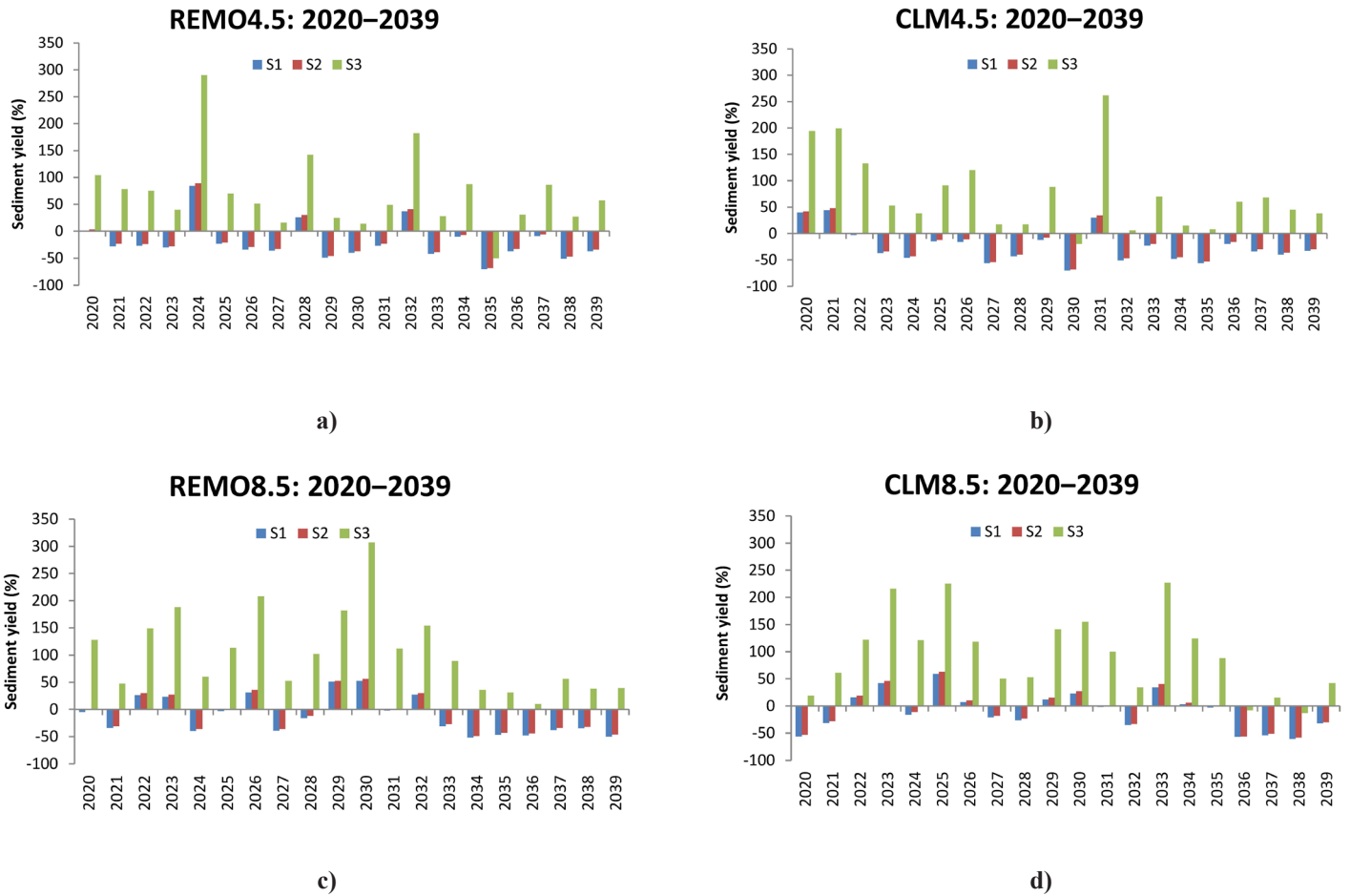

Figure 4.27. Annual sediment yield (expressed in percentage) projected in all climate and land use change scenarios for the 2020–2039 period.

Table 4.22. Monthly sediment yield (tonnes) projected for the 2040–2069 period.

		Climate change scenarios											
		REMO4.5			CLM4.5			REMO8.5			CLM8.5		
Month	**Baseline**	**S1**	**S2**	**S3**	**S1**	**S2**	**S3**	**S1**	**S2**	**S3**	**S1**	**S2**	**S3**
January	315	413	451	1352	478	521	1461	246	274	811	169	189	588
February	160	602	646	1781	560	598	1528	511	562	1586	726	784	2177
March	3030	1660	1748	4653	1593	1676	4108	1829	1917	4820	2308	2453	6120
April	1792	1439	1490	3267	844	866	1826	1028	1055	2342	625	622	1092
May	373	545	538	840	424	421	754	483	469	777	414	405	623
June	767	589	598	1116	396	402	651	469	468	895	505	516	972
July	535	251	252	309	394	405	697	254	256	453	406	421	857
August	408	150	157	233	253	262	452	121	125	238	226	233	368
September	185	95	101	170	157	163	244	95	97	155	128	136	264
October	149	179	193	394	160	169	309	136	141	298	82	84	121
November	268	256	285	757	292	323	758	199	220	521	203	226	553
December	272	374	413	1171	426	471	1146	228	252	647	242	276	764

Table 4.23. Seasonal sediment yield (tonnes) projected for the 2040–2069 period.

		Climate change scenarios											
		REMO4.5			CLM4.5			REMO8.5			CLM8.5		
Season	**Baseline**	**S1**	**S2**	**S3**	**S1**	**S2**	**S3**	**S1**	**S2**	**S3**	**S1**	**S2**	**S3**
Spring	1732	1215	1258	2920	954	987	2229	1113	1147	2646	1116	1160	2612
Summer	570	330	335	552	348	356	600	281	283	529	379	390	732
Autumn	201	177	193	440	203	218	437	143	153	325	138	149	313
Winter	249	463	503	1435	488	530	1378	328	363	1014	379	416	1176

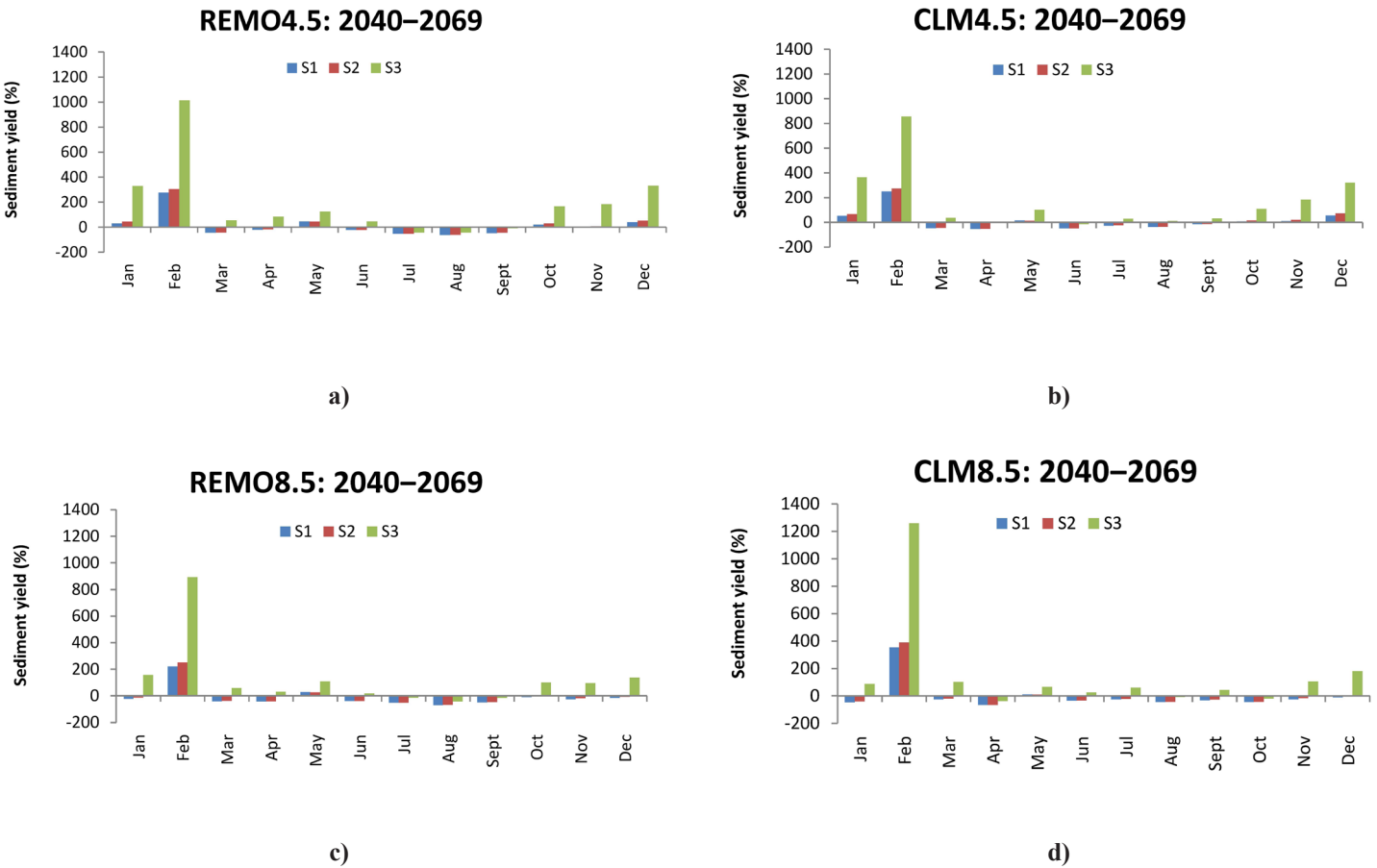

Figure 4.29. Monthly sediment yield (expressed in percentage) projected in all climate and land use change scenarios for the 2040–2069 period.

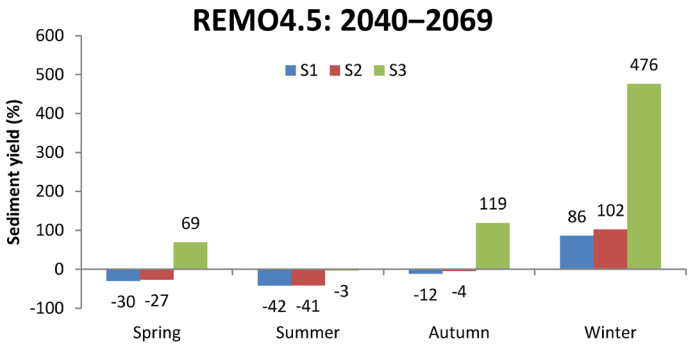

a)

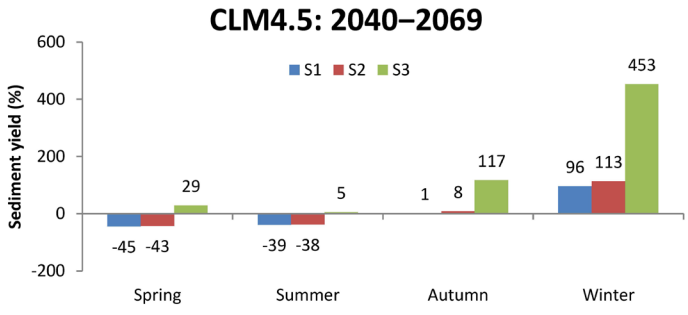

b)

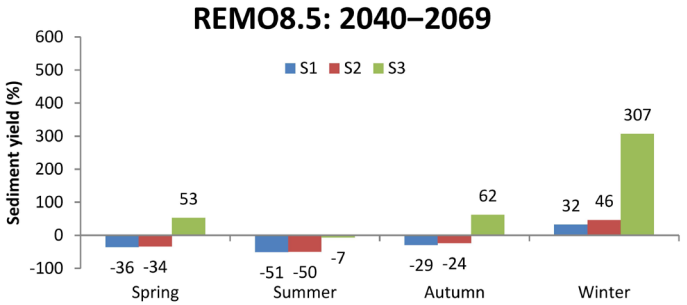

c)

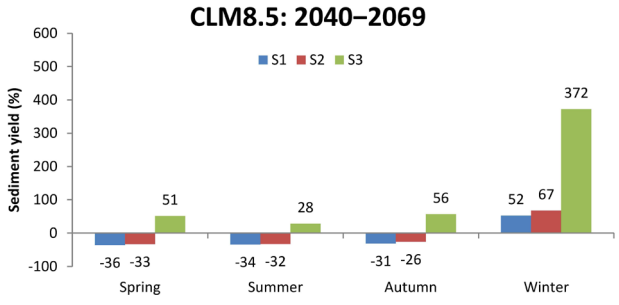

d)

Figure 4.30. Seasonal sediment yield (expressed in percentage) projected in all climate and land use change scenarios for the 2040–2069 period.

Table 4.24. Annual sediment yield (tonnes) projected for the 2040–2069 period.

		Climate change scenarios											
		REMO4.5			CLM4.5			REMO8.5			CLM8.5		
Baseline	Year	S1	S2	S3	S1	S2	S3	S1	S2	S3	S1	S2	S3
8253	2040	8440	8761	18155	9579	10029	22969	7427	7592	16731	5733	6138	22969
	2041	5744	6153	16881	9716	9986	22718	3089	3252	9218	9369	9613	22718
	2042	5495	5795	14552	6343	6649	15314	8406	8693	19174	6802	7096	15314
	2043	7733	8103	19171	7480	7770	18235	6701	6959	16032	4295	4585	18235
	2044	9007	9302	20727	5787	6044	13519	8689	8946	20690	13325	13706	13519
	2045	5295	5601	13994	2368	2610	7280	4892	5175	13319	6741	7007	7280
	2046	5204	5486	12878	4736	5029	11025	3339	3497	8832	4998	5277	11025
	2047	7394	7808	17815	6852	7175	14422	5963	6121	13134	5506	5821	14422
	2048	12774	13104	25754	10147	10501	23717	11743	12008	27092	4665	4948	23717
	2049	11549	11936	29561	3780	4030	8903	7524	7655	16590	5086	5382	8903
	2050	10654	10835	23452	6649	6925	13429	3444	3623	10152	5310	5659	13429
	2051	8021	8507	22970	7919	8356	18130	2397	2589	7671	4817	5018	18130
	2052	6840	7212	22330	5845	6076	12708	4240	4458	8963	3459	3629	12708
	2053	2466	2616	7734	4934	5206	11150	4032	4134	7980	6155	6503	11150
	2054	4178	4400	10874	4245	4441	10943	6191	6369	12476	7588	7790	10943
	2055	4465	4817	12853	2132	2422	6532	6334	6824	19254	7211	7657	6532
	2056	7395	7870	22447	4281	4532	9136	4289	4473	12952	4338	4575	9136
	2057	6923	7211	18325	11451	12007	28186	4005	4452	12224	4557	4902	28186
	2058	7438	7706	16251	4969	5263	11982	4556	4552	8989	8426	8685	11982
	2059	3602	3896	9634	1507	1656	3858	4211	4401	10897	9225	9578	3858
	2060	5609	5910	11936	5341	5637	10889	3501	3696	8770	3973	4221	10889
	2061	6706	7031	13780	3250	3455	8257	5094	5329	11609	7765	8235	8257
	2062	5481	5796	14718	2498	2755	6722	10730	11048	25802	7065	7477	6722
	2063	5666	5985	14839	5166	5538	12203	2264	2447	6503	4439	4729	12203
	2064	5583	5980	13920	8640	8975	18795	9785	10041	20343	6400	6792	18795
	2065	4970	5265	10619	5908	6133	12577	7244	7584	18115	2456	2665	12577
	2066	3256	3452	7604	8732	9152	22818	4455	4722	10443	7106	7495	22818
	2067	6135	6508	12827	7028	7460	16492	5635	6043	13426	3198	3435	16492
	2068	3693	3764	7445	6846	7052	13389	4526	4786	9513	6905	7256	13389
	2069	8902	9301	17246	5193	5427	11699	3259	3624	9339	4150	4459	11699

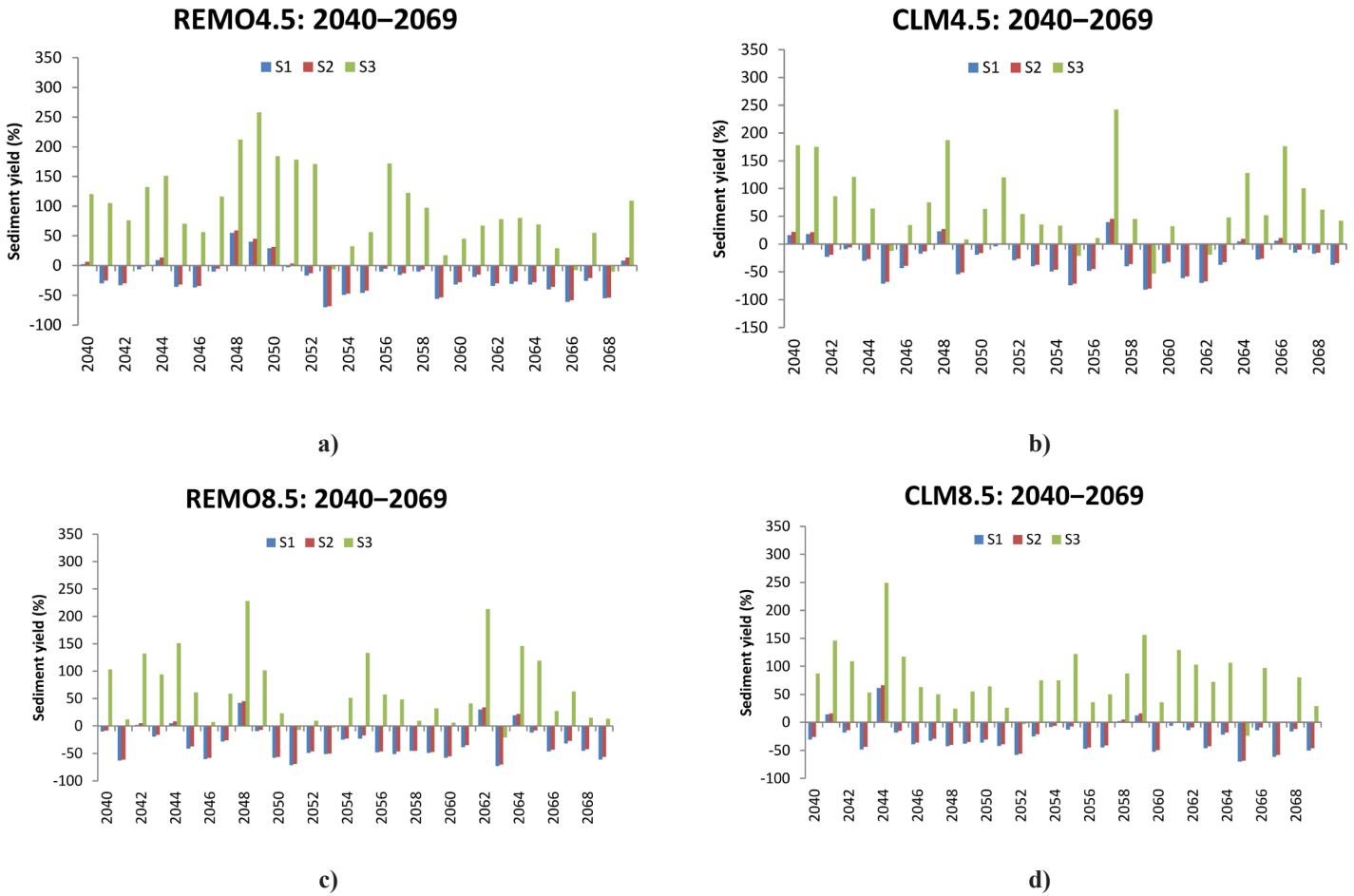

Figure 4.31. Annual sediment yield (expressed in percentage) projected in all climate and land use change scenarios for the 2040–2069 period.

Table 4.25. Monthly sediment yield (tonnes) projected for the 2070–2100 period.

		Climate change scenarios											
		REMO4.5			CLM4.5			REMO8.5			CLM8.5		
Month	**Baseline**	**S1**	**S2**	**S3**	**S1**	**S2**	**S3**	**S1**	**S2**	**S3**	**S1**	**S2**	**S3**
January	315	372	407	1316	233	257	758	302	345	980	330	364	987
February	160	724	769	2166	761	832	2387	589	656	1718	764	832	2193
March	3030	1550	1642	4715	1664	1740	4137	978	1056	2717	1161	1224	3105
April	1792	945	974	2402	768	782	1853	687	716	1437	592	592	1074
May	373	584	583	1095	394	391	774	461	474	871	423	421	932
June	767	458	465	816	397	405	848	348	363	627	482	496	1079
July	535	287	297	496	368	380	735	179	186	329	335	341	653
August	408	138	144	256	222	230	393	162	172	288	168	170	297
September	185	171	186	378	138	143	267	67	72	121	131	135	238
October	149	155	164	298	141	150	275	134	145	252	195	203	374
November	268	374	410	1188	234	260	596	203	226	496	236	249	471
December	272	376	419	1116	315	351	900	318	370	822	346	382	888

Table 4.26. Seasonal sediment yield (tonnes) projected for the 2070–2100 period.

		Climate change scenarios											
		REMO4.5			CLM4.5			REMO8.5			CLM8.5		
Season	**Baseline**	**S1**	**S2**	**S3**	**S1**	**S2**	**S3**	**S1**	**S2**	**S3**	**S1**	**S2**	**S3**
Spring	1732	1026	1066	2737	942	971	2255	709	749	1675	725	746	1704
Summer	570	294	302	523	329	338	659	230	240	415	328	335	676
Autumn	201	234	253	621	171	184	379	135	148	290	188	196	361
Winter	249	491	532	1533	436	480	1348	403	457	1173	480	526	1356

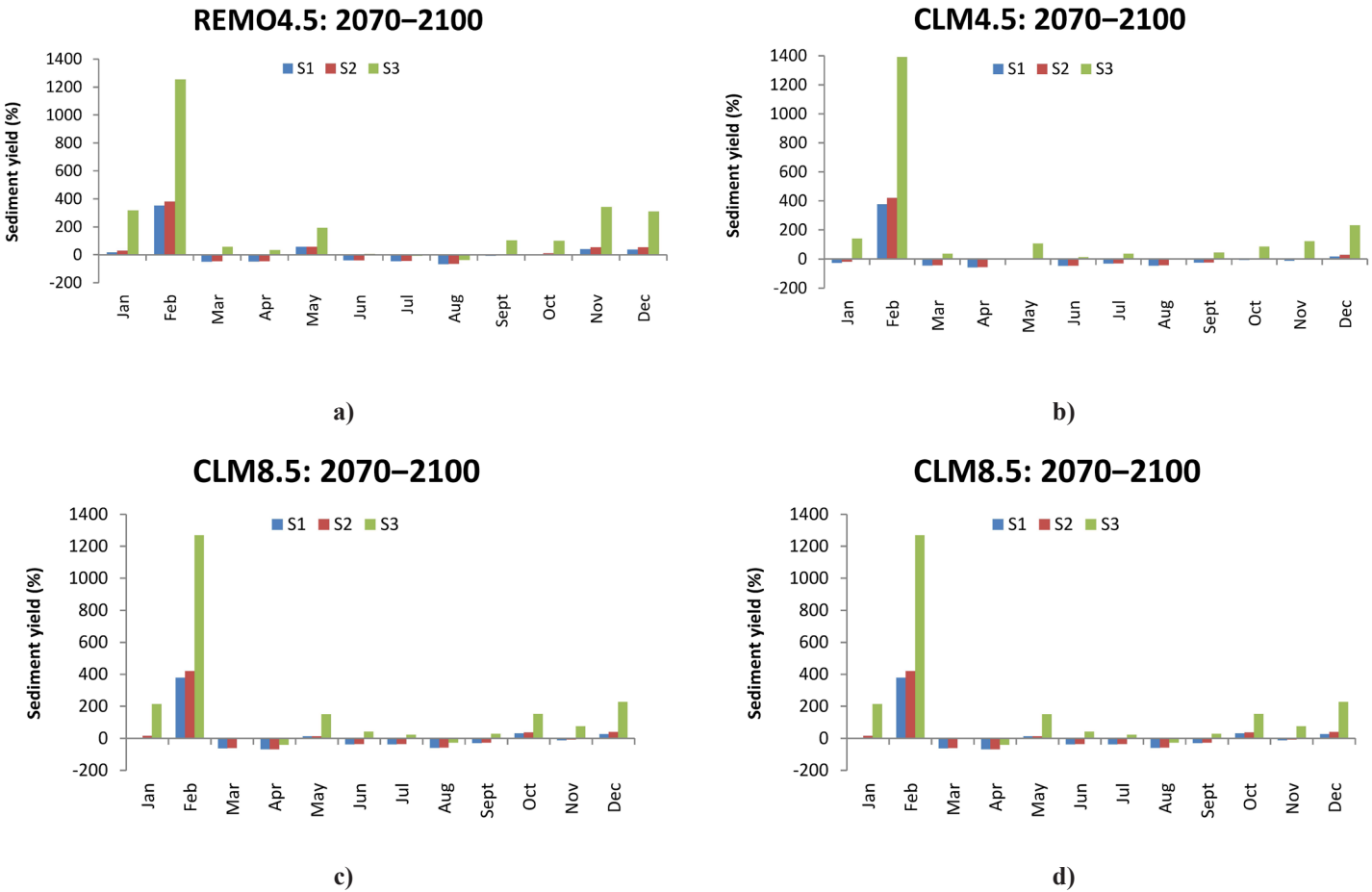

Figure 4.33. Monthly sediment yield (expressed in percentage) in all climate and land use change scenarios for the 2070–2100 period.

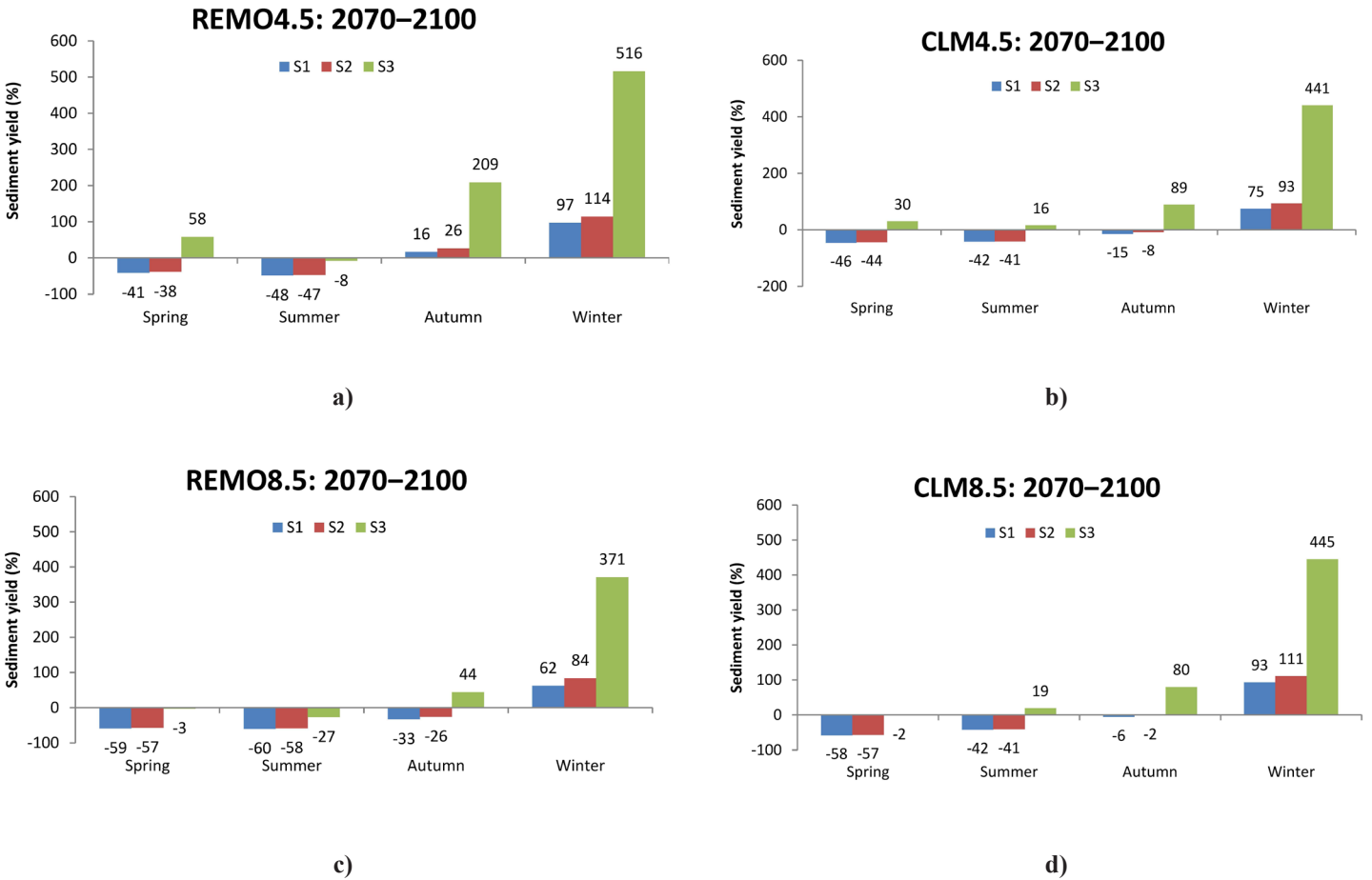

Figure 4.34. Seasonal sediment yield (expressed in percentage) projected in all climate and land use change scenarios for the 2070–2100 period.

Table 4.27. Annual sediment yield (tonnes) projected for the 2070–2100 period.

		Climate change scenarios											
		REMO4.5			CLM4.5			REMO8.5			CLM8.5		
Baseline	Year	S1	S2	S3	S1	S2	S3	S1	S2	S3	S1	S2	S3
	2070	3775	4005	11052	5473	5916	16143	2514	2815	6639	8895	9374	20432
	2071	6764	7157	19187	5570	5890	14116	6322	6674	12613	7237	7596	17046
	2072	6786	7126	16577	9746	10097	22402	8472	8875	18829	2845	3088	8901
	2073	8580	8876	19517	8094	8578	21122	5908	6260	15628	10058	10526	22912
	2074	7721	8138	21005	8666	9089	24485	2433	2676	6192	5043	5457	13399
	2075	11904	12446	32038	5698	6055	15757	3207	3405	6485	4467	4707	12287
	2076	5790	5954	17871	6704	7110	16696	3289	3590	7966	6779	7228	18776
	2077	9065	9518	26493	4279	4460	11643	5167	5627	11167	5993	6431	17234
	2078	9179	9629	23500	8872	9282	20946	5961	6377	13104	4888	5054	10620
	2079	3298	3492	12072	5151	5466	13929	5896	6337	14170	9852	10152	25287
	2080	6259	6608	16334	2903	3174	9182	9835	10508	23524	7588	7814	18150
	2081	2993	3259	7626	4839	5183	12176	3089	3331	7617	4665	4913	12981
	2082	2936	3115	6556	6392	6600	13982	7317	7822	16206	3907	4126	10189
	2083	5595	5905	12492	3171	3370	7866	3597	3706	7652	3698	3895	9290
	2084	6297	6575	15321	3651	3864	8571	4140	4408	9734	3821	3931	7479
8253	2085	5449	5697	12746	3686	3967	9056	2466	2798	7098	5011	5301	13120
	2086	1979	2171	6556	9108	9454	18859	3497	3860	9169	3602	3696	8607
	2087	4440	4728	10500	7268	7570	15239	2756	2983	6925	1935	2070	4394
	2088	1610	1863	5963	4450	4742	11840	3354	3688	8757	3090	3175	5504
	2089	4988	5335	11289	4442	4749	10866	2760	3075	5925	5703	5855	10242
	2090	7504	7937	16364	5791	5834	10970	6777	7181	15241	5582	5816	12264
	2091	5756	6061	16233	5743	6020	14404	3330	3678	7638	3101	3311	7426
	2092	6223	6501	15840	2690	2857	6769	3592	3935	12597	3775	3932	7928
	2093	4746	5086	14182	4768	5051	11652	6287	6822	15597	4869	5160	10923
	2094	7365	7847	20244	4144	4298	10137	4520	4870	11588	5696	5847	11041
	2095	7222	7620	20053	8440	8674	18955	3174	3530	8218	6760	6958	14591
	2096	5854	6117	13781	3468	3649	9199	3551	3892	8013	2644	2844	6704
	2097	9323	9754	24024	4758	4978	11552	3355	3749	9428	6290	6490	13604
	2098	6680	6957	18737	7186	7280	14604	3951	4220	9122	4271	4550	11843
	2099	8500	8850	22101	4632	4951	12408	2778	3146	7121	3778	3975	8785
	2100	5613	5919	17244	4904	5366	16097	4006	4346	10458	4212	4375	9026

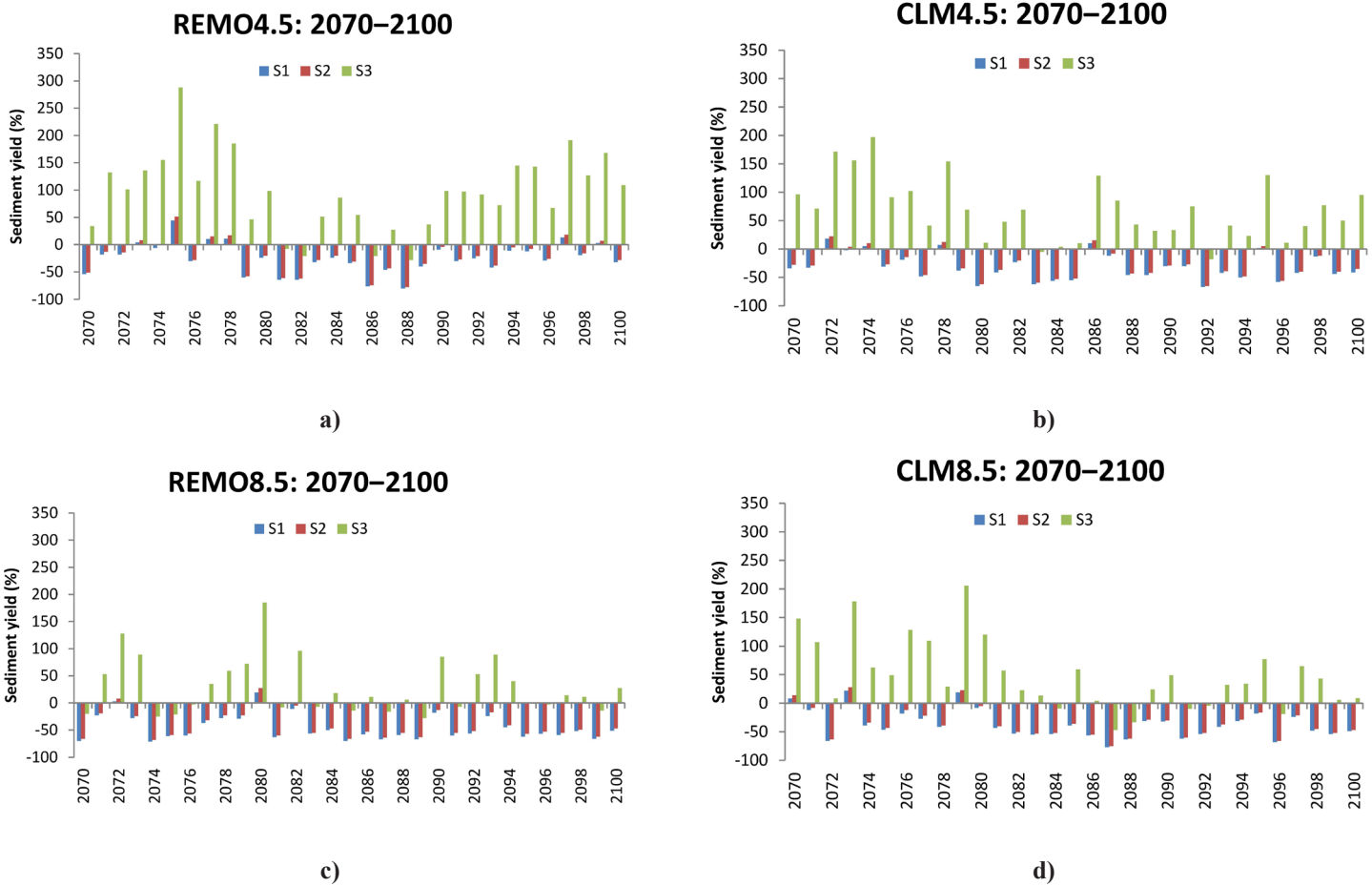

Figure 4.35. Annual sediment yield (expressed in percentage) projected in all climate and land use change scenarios for the 2070–2100 period.

Annex 4. The frequency matrix of annual surface runoff, water discharge and sediment yield for the 2020−2100 period

a) Short term

Year	REMO4.5			CLM4.5			REMO8.5			CLM8.5			Frequency ratio
	S1	S2	S3	S1	S2	S3	S1	S2	S3	S1	S2	S3	+ / -
2020													10 / 2
2021													12/0
2022													12/0
2023													12/0
2024													12/0
2025													12/0
2026													12/0
2027													10/2
2028													12/0
2029													12/0
2030													8/4
2031													12/0
2032													9/3
2033													9/3
2034													9/3
2035													7/5
2036													9/3
2037													9/3
2038													8/4
2039													12/0
LU +	16	18	18	17	17	19	19	19	19	15	15	16	208
LU -	4	2	2	3	3	1	1	1	1	5	5	4	32
CC +	52			53			57			46			208
CC -	8			7			3			14			32

b) Medium term

Year	REMO4.5			CLM4.5			REMO8.5			CLM8.5			Frequency ratio
	S1	S2	S3	S1	S2	S3	S1	S2	S3	S1	S2	S3	+ / -
2040													12/0
2041													9/3
2042													12/0
2043													11/1
2044													12/0
2045													8/4
2046													9/3
2047													12/0
2048													12/0
2049													12/0
2050													11/1
2051													8/4
2052													7/5
2053													6/6
2054													12/0
2055													9/3
2056													5/7
2057													12/0
2058													11/1
2059													8/4
2060													12/0
2061													9/3
2062													9/3
2063													9/3
2064													12/0
2065													9/3
2066													10/2
2067													9/3
2068													9/3
2069													11/1
Land +	26	27	28	24	24	24	20	23	24	23	27	27	297
Land -	4	3	2	6	6	6	10	7	6	7	3	3	63
Clim +	81			72			67			77			297
Clim -	9			18			23			13			63

c) Long term

Year	REMO4.5			CLM4.5			REMO8.5			CLM8.5			Frequency
	S1	S2	S3	S1	S2	S3	S1	S2	S3	S1	S2	S3	+ / -
2070													6/6
2071													12/0
2072													9/3
2073													12/0
2074													9/3
2075													9/3
2076													12/0
2077													12/0
2078													12/0
2079													9/3
2080													11/1
2081													6/6
2082													8/4
2083													5/7
2084													8/4
2085													7/5
2086													5/7
2087													6/6
2088													5/7
2089													6/6
2090													12/0
2091													6/6
2092													2/10
2093													11/1
2094													12/0
2095													9/3
2096													7/5
2097													12/0
2098													7/5
2099													8/4
2100													8/4
Land +	24	25	25	23	26	28	14	17	18	18	21	24	263
Land -	7	6	6	8	5	3	17	14	13	13	10	7	109
Clim +	74			77			49			7			263
Clim -	19			16			44			30			109

Figure 4.44. The frequency matrix of projections regarding the increase (red) or decrease (blue) tendency of annual surface runoff, projected in all climate and land use change scenarios

a) Short term

Year	REMO4.5			CLM4.5			REMO8.5			CLM8.5			Frequency
	S1	S2	S3	S1	S2	S3	S1	S2	S3	S1	S2	S3	+ / -
2020													9 / 3
2021													12/0
2022													12/0
2023													12/0
2024													9/3
2025													9/3
2026													12/0
2027													3/9
2028													9/3
2029													9/3
2030													9/3
2031													9/3
2032													9/3
2033													9/3
2034													6/6
2035													3/9
2036													6/6
2037													9/3
2038													6/6
2039													9/3
Land +	14	14	14	13	13	13	15	15	15	15	15	15	171
Land -	6	6	6	7	7	7	5	5	5	5	5	5	69
Clim +	42			39			45			45			171
Clim -	18			21			15			15			69

b) Medium term

Year	REMO4.5			CLM4.5			REMO8.5			CLM8.5			Frequency
	S1	S2	S3	S1	S2	S3	S1	S2	S3	S1	S2	S3	+ / -
2040													12/0
2041													9/3
2042													12/0
2043													6/5
2044													12/0
2045													5/6
2046													6/6
2047													12/0
2048													12/0
2049													9/3
2050													9/3
2051													9/3
2052													9/3
2053													6/6
2054													6/6
2055													8/4
2056													9/3
2057													9/3
2058													9/3
2059													3/9
2060													6/6
2061													8/3
2062													9/3
2063													9/3
2064													12/0
2065													9/3
2066													9/3
2067													9/3
2068													6/6
2069													9/3
Land +	23	25	25	20	20	20	18	19	19	23	23	23	258
Land -	6	5	5	10	10	9	11	11	11	7	7	7	99
Clim +	73			60			56			69			258
Clim -	16			29			33			21			99

c) Long term

Year	REMO4.5			CLM4.5			REMO8.5			CLM8.5			Frequency
	S1	S2	S3	S1	S2	S3	S1	S2	S3	S1	S2	S3	+ / -
2070													6/6
2071													12/0
2072													9/3
2073													12/0
2074													9/3
2075													9/3
2076													9/3
2077													9/3
2078													12/0
2079													6/6
2080													9/3
2081													6/6
2082													6/5
2083													3/9
2084													6/6
2085													8/4
2086													4/6
2087													3/9
2088													3/9
2089													9/3
2090													12/0
2091													6/6
2092													6/6
2093													9/3
2094													9/3
2095													9/3
2096													3/9
2097													6/5
2098													12/0
2099													6/6
2100													12/0
Land +	23	23	23	20	21	21	13	13	13	24	23	23	240
Land -	8	8	8	11	10	9	18	18	18	7	7	6	128
Clim +	69			62			39			70			240
Clim -	24			30			54			20			128

Figure 4.45.The frequency matrix of projections regarding the increase (red), decrease (blue) or similarity (yellow) tendency of annual water discharges, projected in all climate and land use change scenarios

a) Short term

Year	REMO4.5			CLM4.5			REMO8.5			CLM8.5			Frequency
	S1	S2	S3	S1	S2	S3	S1	S2	S3	S1	S2	S3	+ / -
2020													8/4
2021													6/6
2022													9/3
2023													8/4
2024													6/6
2025													7/5
2026													8/4
2027													4/8
2028													6/6
2029													8/4
2030													7/5
2031													8/4
2032													8/4
2033													6/6
2034													6/6
2035													4/8
2036													3/9
2037													4/8
2038													3/9
2039													4/8
Land +	4	4	19	3	4	19	6	8	20	8	10	18	123
Land -	16	16	1	17	16	1	14	12	0	12	10	2	117
Clim +	27			26			34			36			123
Clim -	33			34			26			24			117

b) Medium term

Year	REMO4.5			CLM4.5			REMO8.5			CLM8.5			Frequency
	S1	S2	S3	S1	S2	S3	S1	S2	S3	S1	S2	S3	+ / -
2040													8/4
2041													8/4
2042													6/6
2043													4/8
2044													10/2
2045													2/10
2046													4/8
2047													4/8
2048													10/2
2049													6/6
2050													6/6
2051													5/7
2052													4/8
2053													2/10
2054													4/8
2055													2/10
2056													4/8
2057													6/6
2058													6/6
2059													4/8
2060													4/8
2061													4/8
2062													4/8
2063													3/9
2064													8/4
2065													4/8
2066													5/7
2067													4/8
2068													3/9
2069													6/6
Land +	6	7	27	6	7	26	5	5	7	4	4	26	150
Land -	24	23	3	24	23	4	25	25	23	26	26	4	210
Clim +	40			39			37			34			150
Clim -	50			51			53			56			210

c) Long term

Year	REMO4.5			CLM4.5			REMO8.5			CLM8.5			Frequency
	S1	S2	S3	S1	S2	S3	S1	S2	S3	S1	S2	S3	+ / -
2070													5/7
2071													4/8
2072													8/4
2073													9/3
2074													5/7
2075													5/7
2076													3/9
2077													6/6
2078													8/4
2079													6/6
2080													6/6
2081													2/10
2082													3/9
2083													2/10
2084													3/9
2085													3/9
2086													5/7
2087													2/10
2088													2/10
2089													3/9
2090													4/8
2091													2/10
2092													2/10
2093													4/8
2094													4/8
2095													5/7
2096													2/10
2097													6/6
2098													4/8
2099													5/7
2100													4/8
Land +	6	6	27	5	5	29	2	2	18	3	3	25	132
Land -	25	25	4	26	26	2	29	29	13	28	28	6	240
Clim +	39			40			22			31			132
Clim -	54			53			71			62			240

Figure 4.46. The frequency matrix of projections regarding the increase (red) or decrease (blue) tendency of annual sediment yield, projected in all climate and land use change scenarios

Annex 5. Dynamics of monthly surface runoff (mm) for the 2020-2039 period

		Climate change scenarios											
		REMO4.5			CLM4.5			REMO8.5			CLM8.5		
Month	Baseline	S1	S2	S3	S1	S2	S3	S1	S2	S3	S1	S2	S3
January	6.7	18.9	19.9	21.1	15.0	16.0	17.4	11.5	12.4	13.6	5.2	5.5	6.1
February	4.2	24.3	25.4	27.1	36.4	38.4	40.8	26.6	28.0	29.7	28.8	30.0	31.9
March	71.7	86.9	90.2	93.8	91.3	95.5	100.4	105.6	108.9	112.6	90.9	95.2	100.1
April	39.9	49.2	51.3	53.4	18.9	20.6	22.1	77.3	81.0	84.7	49.2	52.1	54.4
May	3.9	4.1	4.5	5.0	3.5	3.9	4.6	13.9	15.3	17.1	4.7	5.3	6.1
June	14.2	4.1	4.6	5.3	7.6	8.6	9.8	4.2	4.8	5.7	5.3	6.1	7.0
July	6.7	4.8	5.5	6.3	4.6	5.3	6.1	2.0	2.4	2.8	8.7	9.8	11.1
August	6.2	1.5	1.9	2.3	4.8	5.5	6.4	2.2	2.5	3.0	4.8	5.3	6.0
September	1.9	3.8	4.4	5.2	4.0	4.5	5.2	1.9	2.2	2.6	2.1	2.6	3.1
October	1.7	6.1	7.0	8.2	3.5	4.1	4.9	4.6	5.3	6.1	4.2	4.8	5.5
November	5.9	15.5	17.3	19.5	16.8	18.5	20.5	12.4	14	16.1	9.8	11.1	12.7
December	6.7	21.4	23.2	25.4	8.7	9.7	11.0	18.4	20.3	22.7	14.0	15.1	16.6

Annex 6. Dynamics of seasonal surface runoff (mm) for the 2020-2039 period

		Climate change scenarios											
		REMO4.5			CLM4.5			REMO8.5			CLM8.5		
Season	Baseline	S1	S2	S3	S1	S2	S3	S1	S2	S3	S1	S2	S3
Spring	38.5	46.7	48.7	50.7	37.9	40.0	42.4	65.6	68.4	71.5	48.3	50.9	53.5
Summer	9.0	3.5	4.0	4.6	5.7	6.5	7.4	2.8	3.2	3.8	6.3	7.1	8.0
Autumn	3.2	8.5	9.6	11.0	8.1	9.0	10.2	6.3	7.2	8.3	5.4	6.1	7.1
Winter	5.9	21.5	24.6	29.8	20.0	21.4	23.0	18.9	20.2	22.0	16.0	16.9	18.2

Annex 7. Dynamics of annual surface runoff (mm) for the 2020-2039 period

		Climate change scenarios											
		REMO4.5			CLM4.5			REMO8.5			CLM8.5		
Baseline	Year	S1	S2	S3	S1	S2	S3	S1	S2	S3	S1	S2	S3
169.7	2020	290.7	300.6	312.3	257.3	273.8	294.1	348.2	363.1	380.4	154.3	169.5	186.6
	2021	216.7	235.2	257.0	221.7	236.5	253.3	250.3	266.5	284.6	215.5	230.8	249.6
	2022	272.7	286.7	301.9	218.4	238.6	262.0	382.7	402.1	425.7	273.9	290.5	312.4
	2023	177.1	190.6	206.4	212.1	228.7	248.1	324.5	343.7	366.1	293.7	310.6	329.7
	2024	500.5	524.0	552.9	170.1	184.7	201.0	217.9	233.9	252.2	235.4	251.8	270.3
	2025	199.0	208.8	218.6	263.3	279.3	298.8	343.4	359.1	378.6	355.6	373.0	393.5
	2026	197.6	217.3	240.7	299.4	320.9	346.7	436.5	458.3	483.6	247.6	262.3	279.2
	2027	215.5	226.3	239.9	152.3	163.9	176.6	203.1	216.1	231.8	193.8	206.9	221.5
	2028	311.8	330.8	353.3	183.5	195.9	210.6	314.7	330.7	350.1	171.4	186.5	206.9
	2029	191.9	205.0	220.7	314.1	333.2	355.4	396.8	420.1	450.0	296.2	310.9	325.2
	2030	167.3	179.9	195.4	96.3	105.0	115.1	442.7	463.8	488.2	314.4	332.9	355.0
	2031	292.9	309.0	328.5	258.3	271.0	285.7	305.8	321.7	340.5	211.9	226.8	244.6
	2032	417.7	438.1	464.2	175.7	192.2	211.6	232.9	245.2	259.5	134.6	142.9	152.8
	2033	133.7	146.0	160.7	277.3	290.3	305.8	198.4	215.5	235.4	345.3	364.7	385.4
	2034	267.1	279.9	293.8	186.5	198.7	213.6	120.6	132.1	146.4	224.1	243.6	266.4
	2035	71.6	78.5	86.4	156.7	170.3	186.8	210.9	227.5	247.8	254.3	271.2	290.7
	2036	210.4	225.2	241.7	239.7	260.7	284.8	212.6	228.0	248.6	118.2	129.3	143.1
	2037	306.6	321.6	338.6	194.5	215.7	241.3	255.2	270.8	288.8	140.1	152.3	166.2
	2038	165.2	180.1	198.4	217.3	234.6	255.8	203.8	214.1	225.6	122.4	135.5	150.5
	2039	205.0	222.2	242.1	205.5	219.8	236.6	211.3	229.0	249.4	250.8	266.8	286.3

Annex 8. Dynamics of monthly surface runoff (mm) for the 2040-2069 period

		Climate change scenarios											
		REMO4.5			CLM4.5			REMO8.5			CLM8.5		
Month	Baseline	S1	S2	S3	S1	S2	S3	S1	S2	S3	S1	S2	S3
January	6.7	24.1	25.9	28.2	28.1	30.2	32.6	15.1	16.4	18.2	10.2	11.0	12.1
February	4.2	33.7	35.3	37.4	32.7	34.3	36.0	32.2	34.5	37.4	41.9	43.7	46.2
March	71.7	78.4	81.9	85.8	77.9	81.3	85.1	96.3	100.4	105.3	116.1	121.9	127.7
April	39.9	55.3	58.4	61.9	29.5	31.4	33.3	40.2	42.6	45.1	13.0	14.2	15.6
May	3.9	5.7	6.5	7.5	6.7	7.4	8.3	6.2	7.0	7.9	3.6	4.1	4.7
June	14.2	7.7	8.7	9.9	5.0	5.8	6.7	7.4	8.2	9.2	7.4	8.2	9.2
July	6.7	1.5	1.7	2.0	6.0	6.8	7.7	3.8	4.3	4.9	6.7	7.4	8.4
August	6.2	2.5	2.9	3.3	4.3	4.8	5.5	2.4	2.9	3.4	4.5	4.9	5.5
September	1.9	2.0	2.4	2.9	3.2	3.6	4.2	1.7	2.0	2.5	3.1	3.6	4.2
October	1.7	5.4	6.1	7.2	4.3	4.9	5.8	3.3	3.8	4.4	1.2	1.4	1.7
November	5.9	10.4	11.9	13.7	13.8	15.6	17.9	8.0	9.4	11.3	8.5	9.8	11.5
December	6.7	20.1	21.9	24.0	24.8	27.1	29.9	12.8	14.4	16.3	15.4	17.1	19.2

Annex 9. Dynamics of seasonal surface runoff (mm) for the 2040-2069 period

		Climate change scenarios											
		REMO4.5			CLM4.5			REMO8.5			CLM8.5		
Season	Baseline	S1	S2	S3	S1	S2	S3	S1	S2	S3	S1	S2	S3
Spring	38.5	46.5	48.9	51.7	38.0	40.1	42.2	47.6	50.0	52.8	44.2	46.7	49.3
Summer	9.0	3.9	4.4	5.1	5.1	5.8	6.7	4.5	5.1	5.8	6.2	6.8	7.7
Autumn	3.2	5.9	6.8	7.9	7.1	8.0	9.3	4.3	5.1	6.1	4.3	4.9	5.8
Winter	5.9	26.0	27.7	29.8	28.6	30.5	32.9	20.0	21.8	24.0	22.5	23.9	25.9

Annex 10. Dynamics of annual surface runoff (mm) for the 2040-2069 period

		Climate change scenarios											
		REMO4.5			CLM4.5			REMO8.5			CLM8.5		
Baseline	Year	S1	S2	S3	S1	S2	S3	S1	S2	S3	S1	S2	S3
169.7	2040	360.4	375.5	393.2	324.9	350.1	379.6	255.4	278.4	305.9	258.4	276.7	298.6
	2041	277.6	298.4	322.5	301.2	316.3	333.4	140.1	148.8	159.1	304.1	319.9	340.3
	2042	183.5	200.7	221.1	248.9	265.4	284.3	387.6	409.7	435.8	284.3	298.4	314.8
	2043	229.9	252.5	279.8	211.9	229.2	248.9	247.9	268.1	292.5	161.9	176.3	194.4
	2044	279.6	293.0	308.9	183.8	201.6	223.5	287.0	304.1	324.0	408.3	426.9	446.3
	2045	243.1	255.4	269.0	114.1	123.9	135.7	161.2	178.9	199.5	210.1	225.9	244.2
	2046	209.4	222.8	238.2	230.6	247.9	268.9	141.3	153.0	166.0	233.2	245.8	260.4
	2047	309.3	332.0	358.5	252.3	269.4	289.3	257.3	273.8	294.0	262.5	279.1	299.4
	2048	369.5	392.2	419.8	438.4	460.2	483.8	437.0	463.6	497.1	201.7	216.4	232.4
	2049	258.6	278.6	302.5	184.4	196.9	211.3	305.8	321.0	338.7	216.6	233.6	253.1
	2050	269.1	283.7	299.3	248.6	265.3	284.3	166.1	177.4	190.4	227.5	245.7	266.5
	2051	317.6	337.0	359.3	344.4	367.9	395.6	118.9	131.7	147.2	163.8	175.8	190.4
	2052	282.4	299.0	318.7	225.9	241.1	259.2	137.5	159.1	185.4	107.1	119.8	135.3
	2053	90.2	97.4	106.1	200.9	218.5	239.6	150.4	161.2	173.7	207.7	226.1	248.1
	2054	182.1	197.9	217.9	224.1	236.0	249.8	199.2	212.4	228.4	192.1	206.5	225.7
	2055	202.1	219.5	240.4	136.8	153.1	172.5	282.6	304.4	330.5	319.0	339.2	362.3
	2056	340.1	360.1	383.2	125.0	137.1	151.3	140.6	155.1	172.9	160.4	171.8	182.8
	2057	289.4	304.5	320.7	410.5	438.9	471.6	218.7	244.8	278.2	212.1	229.9	251.5
	2058	259.8	276.3	296.1	208.2	220.9	235.5	166.7	175.6	186.1	237.2	256.1	279.4
	2059	167.3	183.7	203.4	71.6	83.0	96.8	205.9	216.4	229.0	283.6	299.7	321.4
	2060	234.7	247.7	263.4	198.0	217.3	239.8	172.0	186.0	202.8	172.6	186.4	202.2
	2061	251.3	269.9	291.7	145.1	158.8	174.2	252.8	268.8	286.8	340.4	362.6	388.8
	2062	242.1	261.0	283.4	128.1	144.4	164.0	494.8	517.2	544.3	284.5	302.9	323.3
	2063	247.9	265.5	285.5	226.9	247.6	272.5	101.3	112.0	124.9	171.4	186.4	203.4
	2064	258.6	277.0	299.3	351.9	371.4	394.4	339.1	364.1	395.8	295.0	309.3	325.0
	2065	224.3	244.4	268.1	224.7	239.0	255.1	335.2	354.3	378.0	125.8	135.6	147.0
	2066	158.3	169.7	181.8	372.4	391.4	413.1	188.2	199.2	212.6	297.3	313.7	332.6
	2067	229.1	249.6	275.5	286.6	307.0	330.8	212.8	233.5	258.7	142.3	157.9	176.9
	2068	135.2	143.2	151.5	272.5	284.1	299.8	192.5	203.1	216.4	296.0	313.1	332.8
	2069	300.1	322.5	351.5	200.6	214.7	230.8	185.3	204.1	225.9	165.1	182.5	202.8

Annex 11. Dynamics of monthly surface runoff (mm) for the 2070-2100 period

		Climate change scenarios											
		REMO4.5			CLM4.5			REMO8.5			CLM8.5		
Month	Baseline	S1	S2	S3	S1	S2	S3	S1	S2	S3	S1	S2	S3
January	6.7	19.9	21.5	23.5	14.0	15.1	16.5	20.0	22.0	24.4	20.3	21.9	23.9
February	4.2	37.4	39.1	41.2	45.9	48.8	52.3	37.0	39.6	42.6	46.0	48.8	52.0
March	71.7	75.9	79.7	83.8	81.9	85.5	89.6	53.7	56.5	59.6	59.1	62.0	64.8
April	39.9	34.3	36.6	39	26.9	28.6	30.4	23.4	25.0	26.8	16.7	17.8	18.9
May	3.9	7.4	8.3	9.4	5.5	6.2	7.2	6.8	7.7	8.8	7.1	7.8	8.8
June	14.2	5.5	6.1	6.9	6.1	7.0	8.0	5.0	5.8	6.7	9.2	10.4	12.0
July	6.7	3.5	4.0	4.6	6.3	7.0	8.0	2.5	2.9	3.4	5.8	6.6	7.5
August	6.2	1.9	2.2	2.5	3.9	4.4	5.0	4.6	5.0	5.5	3.0	3.4	3.8
September	1.9	4.5	5.1	5.9	2.9	3.2	3.7	1.4	1.7	2.2	3.2	3.7	4.4
October	1.7	3.3	3.8	4.3	3.8	4.4	5.2	3.8	4.6	5.5	5.3	6.1	7.2
November	5.9	16.2	17.7	19.7	10.5	12.0	13.8	8.7	9.9	11.3	8.4	9.5	11.0
December	6.7	20.7	22.7	25.2	17.2	19.1	21.5	20.0	22.6	25.8	18.6	20.9	23.6

Annex 12. Dynamics of seasonal surface runoff (mm) for the 2070-2100 period

		Climate change scenarios											
		REMO4.5			CLM4.5			REMO8.5			CLM8.5		
Month	Baseline	S1	S2	S3	S1	S2	S3	S1	S2	S3	S1	S2	S3
Spring	38.5	39.2	41.5	44.1	38.1	40.1	42.4	28.0	29.7	31.7	27.6	29.2	30.8
Summer	9.0	3.6	4.1	4.7	5.4	6.1	7.0	4.0	4.5	5.2	6.0	6.8	7.8
Autumn	3.2	8.0	8.9	10.0	5.7	6.5	7.5	4.6	5.4	6.3	5.6	6.5	7.5
Winter	5.9	26.0	27.8	29.9	25.7	27.7	30.1	25.7	28.0	31.0	28.3	30.5	33.2

Annex 13. Dynamics of annual surface runoff (mm) for the 2070-2100 period

		Climate change scenarios											
		REMO4.5			CLM4.5			REMO8.5			CLM8.5		
Baseline	Year	S1	S2	S3	S1	S2	S3	S1	S2	S3	S1	S2	S3
	2070	117.2	127.7	140.1	235.8	256.1	280.6	131.7	148.0	168.3	365.8	387.3	410.1
	2071	268.1	284.5	303.9	215.9	232.3	252.0	251.6	267.5	286.5	303.4	317.0	332.2
	2072	257.4	275.1	295.4	361.0	376.0	394.2	343.7	363.6	386.2	129.9	142.7	157.6
	2073	277.1	295.7	318.0	283.8	308.2	337.7	242.0	257.4	275.9	409.0	430.2	456.2
	2074	312.4	330.1	349.7	308.8	331.5	358.8	136.7	150.6	167.4	222.7	240.1	259.4
	2075	436.9	463.8	495.8	188.2	208.1	231.6	107.1	118.7	132.5	196.1	208.5	222.4
	2076	171.9	183.5	197.5	250.5	272.7	298.8	193.0	205.5	221.1	280.2	301.7	328.2
	2077	386.3	403.1	423.6	196.5	205.8	216.7	183.6	204.0	229.5	247.8	269.1	294.4
	2078	328.6	349.3	373.9	359.5	378.8	401.8	260.2	276.6	296.0	192.5	203.6	216.2
	2079	106.8	116.1	127.0	228.9	245.6	265.0	276.2	293.6	313.9	335.5	355.2	378.4
	2080	262.0	279.4	300.3	162.7	177.0	193.1	376.1	403.4	436.7	232.3	253.4	278.2
	2081	136.6	149.9	165.6	215.9	235.3	257.8	140.6	153.0	167.6	181.4	196.4	213.3
	2082	116.6	129.5	145.0	225.1	237.7	252.6	289.4	311.6	339.1	165.9	179.1	194.7
	2083	218.9	233.5	250.2	122.6	135.0	149.4	117.2	126.7	138.1	164.2	180.1	199.7
	2084	275.3	288.8	305.2	156.2	169.4	185.7	216.7	230.3	247.4	147.3	160.9	175.4
169.7	2085	186.0	198.5	213.1	148.2	163.1	181.2	113.5	131.1	152.4	192.9	212.5	235.0
	2086	80.7	91.2	104.6	381.1	397.9	418.1	157.4	174.4	194.4	129.3	144.0	161.0
	2087	220.1	234.0	250.6	245.2	262.3	282.5	107.6	120.5	136.3	79.5	89.1	101.4
	2088	89.4	103.3	120.3	173.2	189.1	207.9	162.9	177.4	194.1	91.1	102.4	115.9
	2089	207.6	224.0	243.0	133.9	151.5	173.0	99.9	115.4	134.2	207.3	225.8	247.9
	2090	281.8	303.3	330.6	232.3	242.1	255.0	270.9	288.8	311.0	206.7	225.1	246.9
	2091	206.2	224.4	245.6	226.6	244.2	265.0	138.1	153.5	173.2	131.0	143.2	157.0
	2092	160.8	177.4	197.2	101.1	111.7	124.9	143.4	157.6	174.6	137.4	151.0	167.3
	2093	202.6	219.4	239.2	163.8	180.9	201.4	254.0	269.7	286.3	242.7	263.1	285.6
	2094	301.8	324.5	351.4	189.6	201.6	215.7	199.2	214.4	233.4	245.9	262.7	281.3
	2095	325.0	345.8	370.2	359.5	380.6	408.0	140.0	158.0	180.3	229.4	250.2	274.6
	2096	171.8	185.3	201.1	162.4	173.0	184.2	159.4	176.7	197.9	114.6	128.4	144.5
	2097	238.4	260.5	286.8	247.2	262.9	281.1	194.5	210.9	230.7	245.0	259.9	277.4
	2098	272.1	286.5	301.8	233.2	250.2	272.3	114.9	128.1	144.6	143.2	161.3	182.1
	2099	325.2	342.1	362.9	219.7	236.9	256.6	148.0	167.5	191.8	151.1	165.5	182.1
	2100	205.5	220.7	237.9	237.9	262.3	291.9	124.6	141.4	161.7	160.7	178.1	199.5

The simulations performed with the SWAT hydrological model under four climate and land use change scenarios allowed us to foreseen the evolution of three hydrological processes (surface runoff, water discharge, and sediment yield) in the Upper Tarlung watershed, at monthly, seasonal, annual and multiannual level for 2020–2100 divided into three periods. Compared to the baseline (1979-1988), at the monthly level, the projections regarding the evolution of the surface runoff, water discharge, and sediment yield are either increasing or decreasing in all time periods. At the seasonal level, the projections show variations from season to season. At the annual level, the projected tendency is alternative, increasing or decreasing, depending on the climate change scenario and time interval. The multiannual average shows an exclusive increasing trend for surface runoff and water discharge in all climate and land use change scenarios, while for sediment yield an alternative trend is projected consisting of increments in all climate change scenarios coupled with land use scenario S3 and decreases in scenarios S1 and S2. Finally, the annual projections of surface runoff and water discharge frequency shows a prevalent increasing trend, highlighted also by the prevalence factor value, while for sediment yield a prevalent decreasing trend is projected, regardless of climate and use change scenario.

ISBN 978-606-8020-84-6